Series in BioEngineering

Xian Jun Loh *Editor*

In-Situ Gelling Polymers

For Biomedical Applications

Springer

Series in BioEngineering

More information about this series at http://www.springer.com/series/10358

Xian Jun Loh
Editor

In-Situ Gelling Polymers

For Biomedical Applications

Springer

Editor
Xian Jun Loh
Synthesis and Integration
Institute of Materials Research
and Engineering (IMRE), A*STAR
Singapore
Singapore

ISSN 2196-8861 ISSN 2196-887X (electronic)
ISBN 978-981-287-151-0 ISBN 978-981-287-152-7 (eBook)
DOI 10.1007/978-981-287-152-7

Library of Congress Control Number: 2014949491

Springer Singapore Heidelberg New York Dordrecht London

Printed on acid-free paper

Springer is part of Springer Science+Business Media (www.springer.com)

Preface

The bottom-up synthesis of highly complex functional materials from simple modular blocks is an intriguing area of research. Driven by the chemistry of supramolecular assembly, modules which self-assemble into intricate structures have been described. These hierarchically assembled systems extend beyond the individual molecule and relies on noncovalent interactions in a directed self-assembly process. The intrinsic properties of the materials can be modified by exploiting the dynamic and specific unidirectional interactions among the building. This also allows the building of novel supramolecular structures such as hydrogels, micelles, and vesicles. These aqueous supramolecular networks belong to a novel category of soft biomaterials exhibiting attractive properties such as stimuli-responsiveness and self-healing properties derived from their dynamic behavior. These are important for a wide variety of emerging applications. In this book, the latest literature describing the formation of dynamic polymeric networks through host–guest complex formation will be summarized. These approaches carried out in the aqueous medium has unlocked a versatile toolbox for the design and fine-tuning of supramolecular self-assembled materials.

Contents

Introduction

Xian Jun Loh

The rapid growth of supramolecular chemistry has led to the development of novel materials which are built based on the theory of self-assembly on the molecular level. Whitesides and Grzybowski [1] defined self-assembly as "the autonomous organization of components into patterns or structures without human intervention". The idea of building up an ordered structure from a mass of disordered individual subunits is immensely intriguing. From the building of order from disorder to the emergence of novel properties from self-assembled structures not observed in individual subunits, there are interesting scientific questions that draw researchers to this field. The science of supramolecular chemistry is intrinsically reliant on the connecting moieties, their specific association/dissociation and the thermodynamics of the process. The bulk properties can be greatly affected by the individual components, either having an environmental response, varied mechanical properties as well stability. Self-assembled built-up materials have been extensively reported for several years, these exist in the form of vesicles, micelles and hydrogels.

Vesicles are molecular containers made up of a thin membrane encasing a volume. Vesicles have attracted great research interest as they are important building blocks resembling the cellular units that make up most organisms and are useful in chemistry, biology, and material science [2–4]. They have wide applicability and can be used as drug/gene delivery systems, for the study of the function of ion channels and also light-harvesting systems. Synthetic vesicles are typically derived from amphiphiles with different polar or hydrophilic head groups and hydrophobic tails. Polymeric micelles are yet another type of encapsulating agents that are built up from the self-assembly of amphiphilic polymers [5]. Polymeric micelles have been used in a variety of applications including purification of wastewater [6], templating agents for materials synthesis, biologically relevant nanobioreactors

X.J. Loh (✉)
Synthesis and Integration, Institute of Materials Research and Engineering (IMRE), A*STAR, Singapore, Singapore
e-mail: lohxj@imre.a-star.edu.sg; XianJun_Loh@scholars.a-star.edu.sg

X.J. Loh (ed.), *In-Situ Gelling Polymers*, Series in BioEngineering,
DOI 10.1007/978-981-287-152-7_1

[7], and as phase-transfer catalysts [8]. They have been widely investigated for their potential biomedical applications, particularly in drug delivery [9]. Micelles with their hydrophobic cores and hydrophilic coronas solubilize hydrophobic compounds, encapsulating them within the micelle core. Bulkier materials such as hydrogels can also be assembled from small molecules. Hydrogels are crosslinked, three-dimensional macromolecular network of hydrophilic copolymers. Hydrogels are widely used as wound dressings, soft contact lenses and soft tissue substitutes. Physical or chemical crosslinking of hydrogels have been described. Chemical crosslinks can take place with the incorporation of functional crosslinkers with more than two reactive groups. Physical crosslinks can be formed via hydrophobic interactions between polymer chains, host-guest complexation, metallo-mediated binding or electrostatic approaches.

The delivery of drugs requires scientific and engineering manipulation of biologically active components into practically implementable therapeutic modalities. The most serious issue facing today's healthcare industry is the 'on-cue' release of therapeutics to their designated target site in a safe, repeatable and patient-friendly manner. Conventional therapy is fraught with obstacles, this happens regardless of the route of administration. For example, the drug molecule could be degraded by enzymes in the stomach, be absorbed drug molecules across intestinal epithelium, cleared by the liver, be overwhelmed by the body's natural immune system resulting in a short plasma half-life and nonspecific tissue distribution. These natural barriers are important for the upkeep of critical bodily functions and yet results in the dilution of the therapeutic efficacy of the injected drugs. It is therefore very important, in the field of drug delivery, to totally understand the limits of these barriers and develop new strategies to overcome them.

As a result, an alternative administration by daily intravenous infusion is usually used to increase the bioavailability of the drug. Nevertheless, intravenous injections raise the possibility of contamination at the localized site and systemic adverse reactions that might result from a sudden high dosage of drug, such as, in the instance of chemotherapeutic medications for the management of cancer. To eliminate this complication, regulated drug release systems such as emulsions, liposomes, biodegradable microspheres and micelles have been developed. Even though effective for the intake of hydrophobic medications, these types of products have a variety of shortcomings, for example poor stability in vivo, prerequisite of organic solvents for the loading of drugs and inferior drug encapsulation efficiencies. These limitations have restricted the utilization of these DDS for the delivery of delicate curative agents such as, peptides and proteins. The use of organic solvents denatures these beneficial peptides, removing these approaches as the preference delivery agents of beneficial peptides. The significance and development of the peptides as therapeutic agents cannot be ignored. For instance, glucagon-like peptide-1 (GLP-1) is utilized for the management of diabetes, ghrelin for the management of obesity, gastrin-releasing peptide used in cancer treatment options, defensin for antimicrobial use and growth factors used for wound healing applications. Nonetheless, peptide delivery in vivo continues to be complicated due to their brief residence half-life. An optimum peptide treatment requires

a peptide delivery system that retains the bioactivity of the peptides while discharging them at a regulated rate. Here, biodegradable injectable in situ gelling copolymers offer themselves as ideal peptide delivery agents.

1 Outlook and Perspectives

There are many types of hydrogels, ranging from chemically-, physically- and supramolecularly-crosslinked hydrogels [10–22]. Of the different types of crosslinking techniques, supramolecular chemistry is of particular interest for the formation of in-situ gelling polymers. Although the chemistry for the synthesis of the macrocycles has been discovered more than 100 years ago, the functionalization and application of these macrocycles is still at its infancy. In recent years, there has been intense research in this direction, including the establishment of standard protocols for the modification of these macrocycles. This has caught the interest of many researchers globally. The hydrophilic modifications of these macrocycles have led these materials to be utilized in the formation of supramolecular structures in the aqueous medium. These are inherently useful for biomedical targeted applications, particularly for drug and protein delivery. Indeed, a variety of hierarchical structures, such as hydrogels, micelles and vesicles, have emerged from the self-assembly of polymer chains brought about by host-guest interactions. Some of the studies have even made into the in vivo research settings, showing great promise for these materials. The development of biocompatible supramolecular materials remains a big challenge as most of these materials have not been assessed for long term toxicity effects. For applications in the biomedical area, interactions of these supramolecular materials with bodily fluids, ionic buffers and protein-containing solutions have to be further evaluated. The wide use of these materials requires a larger quantity of materials to be prepared. The scale up production of these materials remains a major challenge as most of the work is currently done at the intricate laboratory scale. Supramolecular host-guest polymeric materials have great potential to succeed at the biggest stage. Their ability to be manipulated by various stimuli, their ease of use by people of disparate technical backgrounds and potential wide applicability in different biomedical areas as sensors, drug delivery agents, cell supporting scaffolds and molecular switches make for exciting times for this unique class of materials in the coming few years.

References

1. Whitesides, G.M., Grzybowski, B.: Self-assembly at all scales. Science **295**(5564), 2418–2421 (2002). doi:10.1126/science.1070821
2. Discher, D.E., Eisenberg, A.: Polymer vesicles. Science **297**(5583), 967–973 (2002). doi:10.1126/science.1074972

3. Discher, B.M., Won, Y.Y., Ege, D.S., Lee, J.C.M., Bates, F.S., Discher, D.E., Hammer, D.A.: Polymersomes: tough vesicles made from diblock copolymers. Science **284**(5417), 1143–1146 (1999). doi:10.1126/science.284.5417.1143
4. Zhang, L.F., Eisenberg, A.: Multiple morphologies of crew-cut aggregates of polystyrene-B-poly(acrylic acid) block-copolymers. Science **268**(5218), 1728–1731 (1995). doi:10.1126/science.268.5218.1728
5. Riess, G.: Micellization of block copolymers. Prog. Polym. Sci. **28**(7), 1107–1170 (2003). doi:10.1016/s0079-6700(03)00015-7
6. Zhao, W., Su, Y.L., Li, C., Shi, Q., Ning, X., Jiang, Z.Y.: Fabrication of antifouling polyethersulfone ultrafiltration membranes using Pluronic F127 as both surface modifier and pore-forming agent. J. Membr. Sci. **318**(1–2), 405–412 (2008). doi:10.1016/j.memsci.2008.03.013
7. Kawamura, A., Harada, A., Kono, K., Kataoka, K.: Self-assembled nano-bioreactor from block ionomers with elevated and stabilized enzymatic function. Bioconjug. Chem. **18**(5), 1555–1559 (2007). doi:10.1021/bc070029t
8. Borde, C., Nardello, V., Wattebled, L., Laschewsky, A., Aubry, J.M.: A gemini amphiphilic phase transfer catalyst for dark singlet oxygenation. J. Phys. Org. Chem. **21**(7–8), 652–658 (2008). doi:10.1002/poc.1344
9. Torchilin, V.P.: Structure and design of polymeric surfactant-based drug delivery systems. J. Control. Release **73**(2–3), 137–172 (2001). doi:10.1016/s0168-3659(01)00299-1
10. Appel, E.A., del Barrio, J., Loh, X.J., Dyson, J., Scherman, O.A.: High molecular weight polyacrylamides by atom transfer radical polymerization: enabling advancements in water-based applications. J. Polym. Sci. Part A Polym. Chem. **50**(1), 181–186 (2012). doi:10.1002/pola.25041
11. Appel, E.A., del Barrio, J., Loh, X.J., Scherman, O.A.: Supramolecular polymeric hydrogels. Chem. Soc. Rev. **41**(18), 6195–6214 (2012). doi:10.1039/C2CS35264H
12. Appel, E.A., Loh, X.J., Jones, S.T., Biedermann, F., Dreiss, C.A., Scherman, O.A.: Ultrahigh-water-content supramolecular hydrogels exhibiting multistimuli responsiveness. J. Am. Chem. Soc. **134**(28), 11767–11773 (2012). doi:10.1021/ja3044568
13. Appel, E.A., Loh, X.J., Jones, S.T., Dreiss, C.A., Scherman, O.A.: Sustained release of proteins from high water content supramolecular polymer hydrogels. Biomaterials **33**(18), 4646–4652 (2012). doi:10.1016/j.biomaterials.2012.02.030
14. Jiao, D., Geng, J., Loh, X.J., Das, D., Lee, T.-C., Scherman, O.A.: Supramolecular peptide amphiphile vesicles through host-guest complexation. Angew. Chem. Int. Ed. **51**(38), 9633–9637 (2012). doi:10.1002/anie.201202947
15. Loh, X.J., Deen, G.R., Gan, Y.Y., Gan, L.H.: Water-sorption and metal-uptake behavior of pH-responsive poly (N-acryloyl-N′-methylpiperazine) gels. J. Appl. Polym. Sci. **80**(2), 268–273 (2001)
16. Loh, X.J., del Barrio, J., Toh, P.P.C., Lee, T.-C., Jiao, D., Rauwald, U., Appel, E.A., Scherman, O.A.: Triply triggered doxorubicin release from supramolecular nanocontainers. Biomacromolecules **13**(1), 84–91 (2011). doi:10.1021/bm201588m
17. Loh, X.J., Nguyen, V.P.N., Kuo, N., Li, J.: Encapsulation of basic fibroblast growth factor in thermogelling copolymers preserves its bioactivity. J. Mater. Chem. **21**(7), 2246–2254 (2011)
18. Loh, X.J., Tsai, M.-H., Barrio, Jd, Appel, E.A., Lee, T.-C., Scherman, O.A.: Triggered insulin release studies of triply responsive supramolecular micelles. Polym. Chem. **3**(11), 3180–3188 (2012). doi:10.1039/C2PY20380D
19. Nguyen, V.P.N., Kuo, N., Loh, X.J.: New biocompatible thermogelling copolymers containing ethylene-butylene segments exhibiting very low gelation concentrations. Soft Matter **7**(5), 2150–2159 (2011). doi:10.1039/C0SM00764A
20. Rauwald, U., Jd, Barrio, Loh, X.J., Scherman, O.A.: "On-demand" control of thermoresponsive properties of poly(N-isopropylacrylamide) with cucurbit [8] uril host-guest complexes. Chem. Commun. **47**(21), 6000–6002 (2011). doi:10.1039/C1CC11214G
21. Wu, D.-C., Loh, X.J., Wu, Y.-L., Lay, C.L., Liu, Y.: 'Living' controlled in situ gelling systems: thiol−disulfide exchange method toward tailor-made biodegradable hydrogels. J. Am. Chem. Soc. **132**(43), 15140–15143 (2010). doi:10.1021/ja106639c
22. Ye, E., Loh, X.J.: Polymeric hydrogels and nanoparticles: a merging and emerging field. Aust. J. Chem. (2013) doi:10.1071/CH13168. http://dx.doi.org/10.1071/CH13168

Introduction to In Situ Forming Hydrogels for Biomedical Applications

Bogyu Choi, Xian Jun Loh, Aloysius Tan, Chun Keat Loh, Enyi Ye, Min Kyung Joo and Byeongmoon Jeong

Abstract In situ gelling polymer aqueous solutions undergo sol-to-gel transition through chemical and/or physical crosslinking. The criterion on sol and gel is an important issue, therefore, rheology of hydrogel have been discussed in detail. The in situ gelling system has been investigated for minimally invasive drug delivery, injectable tissue engineering, gene delivery, and wound healing. In this chapter, in situ gelling systems and their various biomedical applications were briefly summarized.

Keywords Injectable · Rheology · Physical crosslinking · Thermogel · Tissue engineering

B. Choi
Division of Advanced Prosthodontics, University of California, Los Angeles, CA 90095, USA

X.J. Loh (✉) · A. Tan · C.K. Loh · E. Ye
Institute of Materials Research and Engineering (IMRE), A*STAR, 3 Research Link, Singapore 117602, Singapore
e-mail: lohxj@imre.a-star.edu.sg

X.J. Loh
Department of Materials Science and Engineering, National University of Singapore, 9 Engineering Drive 1, Singapore 117576, Singapore

X.J. Loh
Singapore Eye Research Institute, 11 Third Hospital Avenue, Singapore 168751, Singapore

M.K. Joo
Center for Theragnosis, Biomedical Research Institute, Korea Institute of Science and Technology, Seoul, South Korea

B. Jeong (✉)
Department of Chemistry and Nano Science, Ewha Womans University, 52 Ewhayeodae-Gil, Seodaemun-Gu, Seoul 120-750, South Korea
e-mail: bjeong@ewha.ac.kr

X.J. Loh (ed.), *In-Situ Gelling Polymers*, Series in BioEngineering,
DOI 10.1007/978-981-287-152-7_2

1 Introduction

Hydrogels are hydrophilic macromolecular networks swollen in water or biological fluids [1]. Wichterle and Lim [2] reported the pioneering work using hydrophilic 2-hydroxyethyl methacrylate (HEMA) hydrogels in 1960. Recently, in situ gelling systems based on various natural and synthetic polymers have been widely investigated for biomedical applications due to effective encapsulation of cells and bioactive molecules, minimally invasive injection, and easy formation in any desired shape of defects, in addition to several advantages of typical hydrogels including high water contents similar to extracellular matrix (ECM), controllable physicochemical properties, and efficient mass transfer [3–5]. When hydrogels are prepared by covalent-crosslinking, they form permanent or chemical gels. On the other hand, when physical intermolecular association induces hydrogels, the hydrogels form physical gels and their formations are usually reversible.

2 Chemical Hydrogels

Chemical hydrogels are 3D crosslinked networks that formed by new covalent bonds between water-soluble macromers. To use chemical hydrogels for biomedical application, chemical reactions should not damage incorporated biopharmaceuticals or cells. There are several chemical crosslinking methods such as redox-initiated polymerization, photopolymerization, classical organic reactions between functional groups, and enzymatic reactions.

Redox-initiated polymerization using ammonium persulfate (APS)/N,N,N′,N′-tetramethylethylenediamine (TEMED) or APS/ascorbic acid has been used to encapsulate cells in poly(ethylene glycol) (PEG), oligo(PEG fumarate) (OPF), poly (lactide-co-ethylene oxide-co-fumarate) (PLEOF), chitosan derivatives, or carboxybetaine hydrogels [6–11]. In these systems, an increase of initiator concentration led a decrease in the gelling time, however, it also affected the cell viability. Therefore, low cytotoxic free radical polymerization is needed to use this method for biomedical applications.

Photo polymerization of vinyl groups bearing polymers via ultraviolet (UV) or visible light irradiation with photoinitiators is one of most common and effective encapsulation methods for cell or bioactive molecules in biomedical applications. The hydrogel can be performed at physiological pH and temperature. Various photo initiators, such as 2-hydroxy-1-[4-(hydroxyethoxy)phenyl]-2-methyl 1-propanone (Irgacure 2959) [12–14], lithium acyl phosphinate (LAP) [15, 16], methyl benzoylformate (MBF) [17], or 2,2-dimethoxy-2-phenylacetophenone (DMPA) [18] have been used to produce UV sensitive hydrogels. UV-initiated free radical polymerization systems showed lower cytotoxicity then redox-initiated polymerization. However, UV-irradiation can damage cells, proteins, or tissues; therefore, visible light inducible hydrogel systems have been developed. Exposure to

visible light is less-thermogenic yet causes less cell damage. In addition, visible light penetrating through human skin provided greater depth of cure than UV [19]. Riboflavin (vitamin B2) [20], eosin-Y [21, 22], or ruthenium (Ru (II))/sodium persulphate (SPS) [23] have been used as a visible light initiator.

Crosslinking via reactions between functional groups present in the water-soluble monomers or macromers produce hydrogels. Classical organic reactions between functional groups such as the Michael addition, click reaction, Schiff base formation, epoxide coupling, genipin coupling, and disulfide exchange reaction have been used to prepare hydrogels. The Michael addition of nucleophiles (amine or thiol group) to α,β-unsaturated carbonyl compounds or α,β-unsaturated sulfones in water forms hydrogels. Various functionalized polymers, such as poly(ethylene glycol) (PEG) [24–26], poly(vinyl alcohol) (PVA) [27], N-isopropylacrylamide (NIPAAm) [28], and natural polymers [14, 29] have been crosslinked via Michael addition and formed hydrogels. The copper [Cu(I)] catalyzed azide-alkyne cycloaddition is one of the most popular click chemistry reactions. Macromolecular derivatives of PVA [30], PEG [31–33], NIPAAm [34], and polysaccharides [35] with Cu(I) as a catalyst have been used to prepare in situ forming hydrogels. However, cytotoxic problem of Cu(I) should be solved to use these click chemistry induced hydrogels for biomedical applications. Thus, Cu(I)-free click reactions have been developed to be used as a tissue engineering scaffolds [36, 37]. The Diels-Alder reaction, highly selective [4 + 2] cycloaddition between a diene and a dienophile without a catalyst, is also known as a click type reaction. Diels-Alder click crosslinked PEG [38], NIPAAm [39], or hyaluronic acid (HA) [40, 41] based hydrogels have been investigated for tissue engineering applications.1

There has been an increased interest in the enzymatically crosslinked hydrogels that shows few side reactions since their high specificity for substrates. Horseradish peroxidase (HRP)/hydrogen peroxide (H_2O_2), transglutaminase (TG), phosphatase (PP), tyrosinase, or thermolysin catalyzed crosslinking provides in situ hydrogel formation of hydroxyphenyl propionic acid (HPA) functionalized 8-arm PEG [42], thiol functionalized poly(glycidol) [43], Tetronic-tyramine (Tet-TA)/gelatin-HPA (GFPA) [44], dextran-tyramine (Dex-TA) [45], alginate-g-pyrrole [46], or protein polymers containing either lysine or glutamine [47]. These enzymatic crosslinks provide fast gelation.

3 Physical Hydrogels

Heat, ions, inclusion complex, stereocomplex, and/or complimentary binding can induce a hydrogel formation by forming physical junctions via molecular entanglement, crystalline order, or intermolecular interactions. Hydrogels formed by physical association are called physical, reversible, and stimuli responsive hydrogels. These hydrogel systems should be biocompatible with a host as well as the incorporated bioactive agents.

Polymers containing well balanced hydrophilic blocks and hydrophobic blocks can physically crosslink as temperature increases by forming associations of hydrophobic domains. PEG has been used as a hydrophilic block in most of the thermogelling systems. Thermogelling systems that show sol-to-gel transition at around physiological temperature have been widely developed for injectable biomedical applications. At low temperature, thermo-sensitive polymer aqueous solution is easy to mix with cells, drugs, and/or bioactive molecules, followed by an injection of the mixture to target site to form a hydrogel. The target site can be a subcutaneous layer for a protein drug delivery, a tumor tissue for an anticancer drug delivery, or a damaged defect for tissue regeneration. As thermogelling polymers, (1) polyacrylates: NIPAAm copolymers and mono and dilactate substitute poly(2-hydroxypropyl methacrylamide), (2) polyesters: PEG/PLGA, PEG/poly(ε-caprolactone) (PCL), and PEG/poly(ε-caprolactone-co-lactide) (PCLA) block copolymers, (3) poly(ester urethane) (poly(1,4-butylene adipate) (PBA)/PEG/PPG connected by hexamethylene disiocyanate, (4) natural polymer and its derivatives (chitosan/β-glycerol phosphate, chitosan-g-PEG, HA-g-PNIPAAm, (5) polyphosphazenes, (6) Pluronic® and its derivatives, (7) poly(trimethylene carbonate), and (8) polypeptides: elastin-like (VPGVG) polypeptide (ELP), silk-like (GAGAGS) polypeptides, polyalanine (PA), poly(alanine-co-phenylalanine) (PAF), poly(alanine-co-leucine) (PAL), etc. have been developed [48–61]. Polypeptide-based thermogelling systems have several advantages compared with polyester-based hydrogels. (1) During gel degradation, polypeptide thermogels maintain neutral pH since degradation products are neutral amino acids, while pH of polyester thermogels decreases due to their acidic degradation products. Decrease in pH can be a problem for biomedical applications, since it can decrease cell viability or protein drug stability. (2) Enzyme-sensitive degradation of the polypeptide-based hydrogel systems provides a storage stability of the encapsulated material in vitro [62]. (3) Polypeptides have unique secondary structures including α-helix, β-sheet, triple helix, and random coil, allowing various nano-assemblies followed by sol-to-gel transition. These nano-assemblies can give unique nanostructures in the hydrogels. Thus, polypeptide-based hydrogels can provide biomimetic ECMs with various nanostructures that can affect proliferation and/or differentiation of encapsulated cells [3, 63].

Crosslinking by addition of ions provides reversible hydrogels. Alginate hydrogel formation using calcium ions can be carried out at mild condition of room temperature and physiological pH. Therefore, alginate gels have been used for encapsulating cells and protein drugs [64]. Salts in media also triggered MAX8 ($VKVKVKVKV^{D}P^{L}PTKVEVKVKV\text{-}NH_2$) and HLT2 ($VLTKVKTKV^{D}P^{L}PTKVEVKVLV\text{-}NH_2$) peptides to fold into a β-hairpin conformation that induced hydrogel formation [65].

Inclusion complexes between cyclodextrins (CDs) and guest molecules induce physical associations to form physical hydrogels. There are three subtypes of α-, β-, γ-CDs consisting of 6, 7, and 8 glucopyranose units, where the internal diameter of the cavity are 5.7, 7.8, and 9.5 Å, respectively [66]. Different-sized guest molecules can selectively insert into the inner cavity of CD with proper diameter.

Sequential inclusion complexations were used to form an in situ hydrogel [67]. First, Pluronic®s were immobilized on the cellulose nanocrystal via interaction between PPG block of Pluronic® and β-CD on the nanocrystal surface, and then uncovered PEG blocks of Pluronic® were inserted into cavity of α-CD followed by in situ hydrogel formation.

Stereocomplexation between enantiomers by stereoselective van der Waals interaction have been used in the design of in situ hydrogel systems. Mixing two polymer aqueous solutions containing poly(L-lactide) (PLLA) block and poly(D-lactide) (PDLA) block induces a stereocomplexed hydrogel. Stereocomplex of PLLA-PEG-PLLA, PDLA-b-cationic poly(carbonate)-PDLA (PDLA-CPC-PDLA), and PDLA-PEG-PDLA triblock copolymers provided a thermosensitive antimicrobial hydrogel [68]. The 8-armed star block copolymers of PEG-(NHCO)-$(PDLA)_8$ and PEG-(NHCO)-$(PLLA)_8$ were mixed to form stereocomplexed spontaneous hydrogel [69].

Complementary binding such as antigen/antibody interactions, ligand/receptor interactions, and base-pairing interactions between oligonucleotides can also form in situ hydrogels. Acrylamides attached either an antigen (rabbit immunoglobulin G; rabbit IgG) or its specific antibody (goat anti-rabbit IgG) formed semi-interpenetrating network hydrogel [70]. Gyrase subunit B (GyrB) was dimerized by the addition of the aminocoumarin antibiotic coumermycin, resulting in hydrogel formation [71]. Addition of increasing concentrations of clinically validated novobiocin (Albamycin) dissociated the GyrB subunits, thereby resulting in gel-to-sol transition. Multi-arm star shaped PEG functionalized with thymine and adenine self-assembled via base pairing of thymine and adenine to form a hydrogel [72]. The potential of this biological hydrogel for targeted growth factor delivery and cell encapsulation was confirmed.

4 Combining Chemical and Physical Crosslinking

Generally, physical hydrogels have the limitation of weak mechanical properties, thus, a combination of chemical and physical crosslinking has been used to overcome this weakness. Thiolated chondroitin sulfate (CS-TGA)/PEG diacrylate (PEGDA)/β-glycerophosphate disodium salt (β-GP) mixture formed hydrogel by Michael addition, disulfide bond forming, and temperature increasing to 37 °C [73]. The PNIPAAm-co-glycidyl methacrylate (GMA)/polyamidoamine (PAMAM) mixed solution was formed hydrogel by a physical and chemical dual-gelation [74].

5 Hydrogel Rheology

The basic principles and different aspects of hydrogels have been covered in several reviews [4, 75–77]. The mechanical properties of a hydrogel are important considerations for specific biological applications [78]. The free-standing ability

of the gel is an important consideration for cell growth scaffolds. The stiffness of hydrogels has been reported to direct the differentiation of different cell types [79–81]. For drug delivery, hydrogels should preferentially reduce in viscosity upon injection and undergo rapid recovery upon removal of the stress to form the drug release gel depot. This design principle has been the basis of several in situ thermogelling polymeric networks [5, 82–84]. Finally, rheological measurements allow for the understanding of the different gelation mechanisms which can be utilized in the optimization of the properties of the hydrogels for tissue reconstruction and drug delivery applications.

The flow and strain properties of soft materials have been extensively investigated since the 17th century. In the 1830s, scientists discovered that many materials possess time-dependent mechanical properties under various conditions, which cannot be explained by the classical theory of Newtonian fluid. For example, in 1835, Weber observed the phenomenon of elastic hysteresis when he studied the uranium filament. In 1865, Lord Kelvin discovered the viscosity behavior of zinc, and that its inner impedance was not proportional to the strain rate. Two years later, Maxwell proposed a model for viscoelastic materials having properties both of viscosity and elasticity. The Maxwell model can be simply represented by the series connection of a purely elastic spring and a purely viscous damper. At the same time, scientists also found many fluids, which were all called non-Newtonian fluid later due to the nonlinear relationship between the shear stress and shear rate. Based on the known constitutive equation, people proposed the concept of stress relaxation time, suggesting the viscosity to be the product of the elastic modulus and the stress relaxation time. In 1874, Boltzmann developed the linear viscoelasticity theory, suggesting that the stress in a given time is not only related to the strain in the given time, but also dependent on its previous deformation. In 1940s, Reiner pointed out that in order to eliminate the Weissenberg effect (The Weissenberg effect is a phenomenon that occurs when a spinning rod is inserted into a solution of liquid polymer. Instead of being thrown outward, the solution is drawn towards the rod and rises up around it), a stress proportional to the square of the spinning speed needs to be applied [85]. Almost at the same time, Rivlin's study on the torsion of a rubber cylinder helped to solve the problem of Poynting effect [86]. The intrinsic significance of these two studies is to further apply the generalized approach regarding the nonlinear constitutive equation, which brought in flourishing progress in the field of rheology. With the advance in rational mechanics, from small deformation theory to finite deformation theory, from linear theory to nonlinear constitutive theory, from classical object model to microstructure theory, rheology rapidly advanced after 1965, moving from phenomenological theory, which describes phenomena only into the ontology, which considers the internal structure. The term "rheology" was first coined by Bingham and Reiner in 1929 when the American Society of Rheology was founded in Columbus, Ohio [87]. This term was inspired by a Greek quotation, "panta rei", "everything flows". In the same year, Journal of Rheology started its publication. In 1932, the Committee on Viscosity of the Academy of Sciences at Amsterdam was founded, which was later renamed The Dutch Rheological Society in 1951. The British Society of Rheology was founded

as an informal British Rheologists' Club in 1940. In the following years, Society of Rheology/Group of Rheology was founded in countries like Germany, Austria, Belgium, Sweden, Czech Republic, France, Italy, Israel, Japan and Australia. Many of these societies/groups became members of the European Society of Rheology later, greatly promoting the development of rheology. Basically, rheology is defined as the science of the deformation and flow of matter, thus it mainly focuses on the investigation of the time-dependent strain and flow properties of soft materials under conditions like stress, strain, temperature, humidity and radiation [88]. Rheological parameters include the physic-mechanical properties of liquids and solids which describe strain and flow behavior. When external forces are exerted on the materials, strain can be measured and experimentally studied.

The viscoelastic properties of hydrogels can be determined by rheometry. The basics and theories of rheology, its measurements and the types of equipment can be found in several seminal publications [89, 90].

In rheology, the variable shear stress, τ, is defined as the ratio of the force F applied on a sample area A to cause the disruption of the material between the two plates. The strain, γ, is defined as the ratio of the deviation of x of the sample to the height of the sample, h or more simply defined as tan α. The velocity of the movement at the applied force is controlled by the internal force acting within the material.

The mechanical properties of hydrogels are determined by small perturbation rheology experiments on hydrogels. When the hydrogel is subjected to a small perturbation, the material particles are displaced relative to each other resulting in strain. When external anisotropic forces are exerted on elastic bodies, they undergo elastic strain. A spontaneous full recovery of the original form of the material results when the external force is removed. On the contrary, the strain on viscous bodies is irreversible once external anisotropic forces are exerted. The input energy is transformed and this causes the material to flow. Hydrogel materials are neither completely viscous nor elastic; instead it exhibits a behavior known as viscoelasticity. These small perturbations of the hydrogels are meant to ensure that the rheology experiment is carried out within the linear viscoelastic region (LVR) of the material, hence ensuring the measured properties of the hydrogels are independent of the magnitude of imposed strain or stress. In addition, the linear viscoelasticity region is when the magnitude and stress are related linearly. When small deformation is applied sufficiently slowly, the molecular arrangements of the polymers are still close to equilibrium. The mechanical response is then just a reflection of dynamic processes at the molecular level, which go on constantly, even for a system at equilibrium (Fig. 1).

Small amplitude oscillatory shear measurements, creep and creep recovery tests are examples of small perturbation tests carried out on hydrogels. The principle of small amplitude oscillatory shear measurements is shown in Fig. 2.

By applying shear stress, a laminar shear flow is generated between the two plates. The uppermost layer moves at the maximum velocity V_{max}, while the lowermost layer remains at rest. The shear rates of typical actions are summarized in Table 1.

$$\text{Shear rate } \dot{\gamma} = \frac{dv}{dh}$$

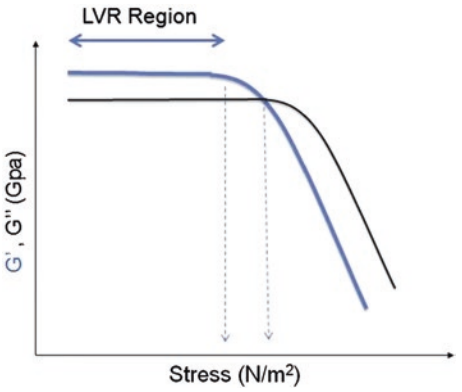

Fig. 1 Illustration of the linear viscoelastic region (LVR)

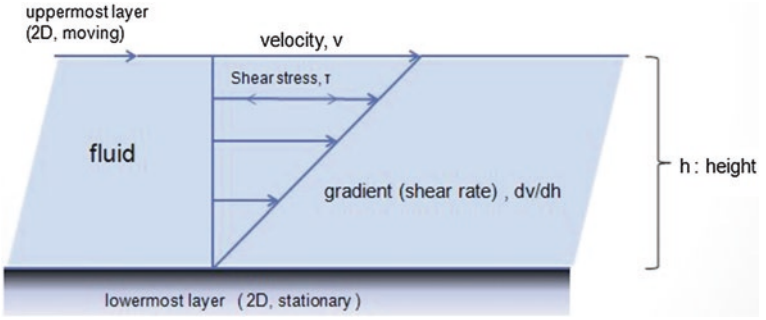

Fig. 2 Shear forces in rheology

Table 1 Examples of actions and the shear rate involved

Actions	Shear rate/s^{-1}
Spraying	10^4–10^5
Rubbing	10^4–10^5
Curtain coating	10^2–10^3
Mixing	10^1–10^3
Stirring	10^1–10^3
Brushing	10^1–10^2
Chewing	10^1–10^2
Pumping	10^0–10^3
Extruding	10^0–10^2
Levelling	10^{-1}–10^{-2}
Sagging	10^{-1}–10^{-2}
Sedimentation	10^{-1}–10^{-3}

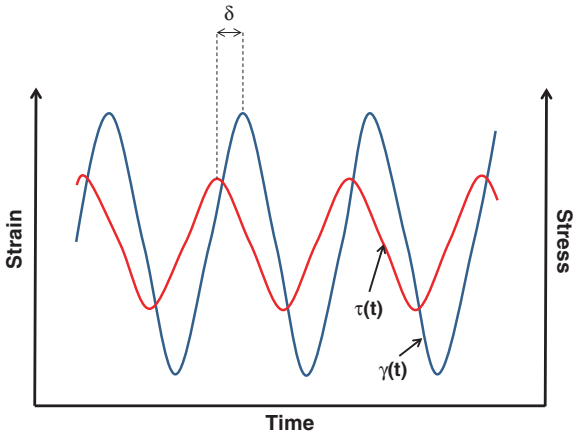

Fig. 3 Principle of a small amplitude oscillatory shear measurement

For controlled-strain rheometers, the shear strain that is a sinusoidal function of time, t, can be expressed as, $\gamma(t) = \gamma_0(\sin \omega t)$, where γ_0 is the amplitude of the applied strain and ω is the angular frequency of oscillation (in rad s^{-1}). The angular frequency is related to frequency, f, measured in cycles per second (Hz) whereby $\omega = 2\pi f$. The shear stress resulting from the applied sinusoidal strain will also be a sinusoidal function, which can be expressed as $\tau(t) = \tau_0(\sin \omega t + \delta)$ in which τ_0 is the amplitude of the stress response and δ is the phase difference between the two waves.

On the other hand, for stress-controlled rheometers, the shear stress is applied as $\tau(t) = \tau_0(\sin \omega t)$ and the resulting shear strain is measured as $\gamma(t) = \gamma_0(\sin \omega t + \delta)$. For a purely elastic material, it follows from Hooke's law that the strain and stress waves are always in phase ($\delta = 0°$). On the other hand, while a purely viscous response has the two waves out of phase by 90° ($\delta = 90°$). Viscoelastic materials give rise to a phase-angle somewhere in between (Fig. 3).

In small amplitude oscillatory shear measurements, the shear storage modulus, G′, loss modulus, G″, and loss factor, tan δ, are critical hydrogel properties monitored against time, frequency and strain. An alternative approach to discuss the dynamic response of a viscoelastic material is by using complex notation to describe an applied sinusoidal strain, $\gamma^* = \gamma_0 \exp(i\omega t)$, whereby $i = \sqrt{-1}$, the complex stress can be expressed as $\tau^* = \tau_0 \exp[i(\omega t + \delta)]$. From Hooke's law, the complex modulus of the tested material is $G^*(\omega) = \tau^*/\gamma^* = (\tau_0/\gamma_0) \exp(i\delta)$. This expression can be resolved into an in-phase component and an out-of-phase component by a substitution of the Euler's identity where $\exp(i\delta) = \cos \delta + i \sin \delta$. This gives $G^*(\omega) = G' + iG''$ with G′ and G″ as the real (i.e. elastic or in phase) and imaginary (i.e. viscous or loss or out-of-phase) components of G*, respectively. The loss factor, tan δ, is defined as G″/G′. To re-emphasize, G′ measures the deformation energy stored during shear process of a test material which is characteristic of the stiffness of the material and G″ is representative of the energy dissipated during shear which is characteristic of the flow response of the

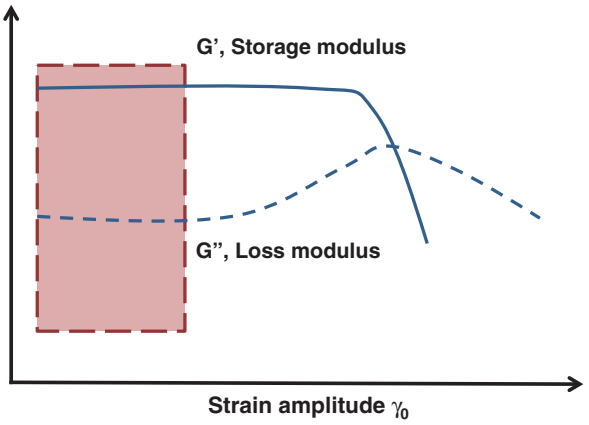

Fig. 4 Typical graph showing storage and loss modulus

material. If tan $\delta > 1$ ($G'' > G'$), the sample behaves more like a viscous liquid while, conversely, when tan $\delta < 1$ ($G' > G''$), the sample behaves more like an elastic solid (Fig. 4).

For gel samples, these parameters are often measured as a function of time, strain and frequency. Observation of the gelation process can be achieved by monitoring the temporal evolution of G' and G''. The linear viscoelastic region within which G' and G'' are independent of shear strain can be determined by monitoring the moduli of the material as a function of the strain.

The behavior of the hydrogel at short and long timescales can be studied by measurement of the moduli of the material as a function of frequency. The frequency dependence of the moduli is a critical hydrogel parameter since a single material can look quite solid-like ($G' \gg G''$) at a high frequency (short timescale) but behave much more liquid-like ($G'' > G'$) at low frequency (long timescale). Gelation kinetics and final gel stiffness are critical material properties that directly impact the application of the material.

Besides small perturbation measurements, creep and creep recovery tests are also employed to investigate the time-dependent evolution of compliance. This aids in the critical understanding of the long-term viscoelastic behavior of hydrogels. Different mammalian cells exert different stress levels on the hydrogel scaffolds and they behave differently in response to the compliance of the gel material. In typical experimental setups, creep and creep recovery tests are performed consecutively. For this experiment, there is an instantaneous increase in the stress from 0 to τ_1. This is kept constant from t_0 to t_1 in the creep phase to subject the material to a prolonged period of stress. Then the stress is completely removed in the subsequent recovery phase. The resulting strain is recorded as a function of time ($t_0 < t < t_2$) in both tests. The creep compliance is defined as $J(t) = \gamma(t)/\tau_0$ which has a unit of reciprocal modulus (Pa^{-1}). Within the linear viscoelastic region, the creep compliance is independent of applied stress and all J(t) curves obtained under various stresses should overlap with each other. Sometimes creep

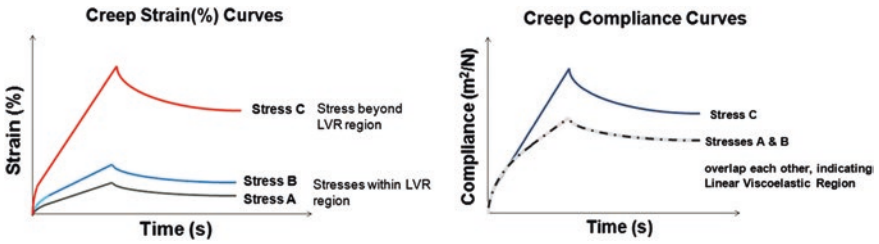

Fig. 5 Sample creep curves under different stresses

compliance is compared to reciprocal shear modulus measured in small amplitude oscillatory shear tests in order to judge if the sample displays pure elastic behavior. Figure 5 shows a typical example of creep strain curves and creep compliance curves of polystyrene at various stresses. In the linear viscoelasticity region, under different stresses of A and B, the creep compliance curves overlap each other. The curve induced by Stress C does not overlap as shown in Fig. 5, indicating that the linear viscoelasticity region has been exceeded.

In addition to the above-mentioned measurements, the flow properties of the hydrogels as well as their abilities to retain or recover their original form after experiencing shear flow or large strain are important factors to understand. Shear-thinning and self-healing hydrogels are excellent candidates for injectable therapeutic delivery vehicles. Monitoring rheological behavior and structural evolution of these gels during and after flow can help evaluate encapsulated therapy retention and delivery during syringe injection and the ability of the material to stay localized after injection against possible biological forces in vivo (Fig. 6).

Inspired by our bodies' ability to heal, self-healing materials have the ability to repair themselves when they are damaged. In the literature discussed in other chapters in this book, supramolecular chemistry as well as sample conditions were varied in order to examine whether gel rheological behavior is dependent on factors like polymer functionality sequence, polymer concentration, temperature and pH.

There could be situations where a test material has not been rheologically evaluated. This section focuses on the assessment of an unknown material. As a

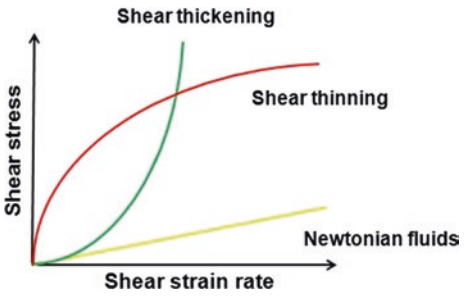

Fig. 6 Graph illustrating shear thickening and shear thinning

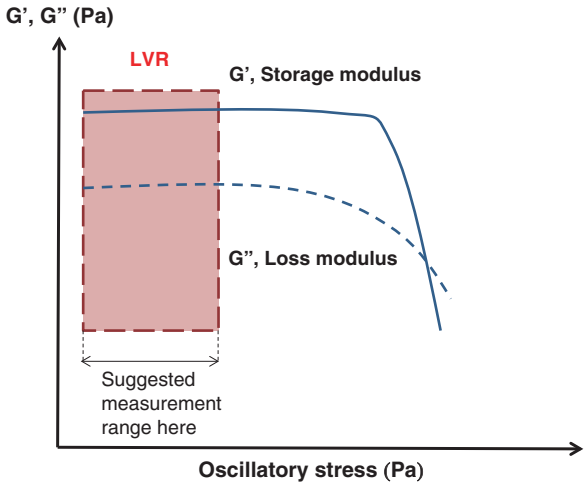

Fig. 7 Graph of an oscillatory stress sweep

general guide, this section should cover the general rheological characterization of the different unknown materials, however, it also requires certain amount of creativity on the part of the rheologist to design the most appropriate protocol. A point to note is that these recommended conditions could be independently used to further evaluate a materials' rheological response. In all the experiments, it is important that the sample is well conditioned to a particular temperature before proceeding with the measurements.

Most of the time, the rheological properties of a viscoelastic material are strain-independent up to a critical strain level. When the strain exceeds the critical level, the storage modulus of the material declines and a non-linear behavior is observed. The measurement of the strain amplitude dependence of the storage and loss moduli (G', G'') is a usually the first step taken to characterize a material's viscoelastic behavior and to determine the pseudo-linear viscoelastic region (LVR) of the material. An oscillatory stress sweep (OSS) will give a general range of where the LVR is located. The range of the stress sweep should be tested over the allowable shear stress (torque ~1–10,000 μN m) range of the instrument. In future experiments, the shear stress range can be adjusted appropriately to collect only reliable data. As the allowable shear stress range is dependent on the geometry used, torque will be used as the controlled variable. The frequency should be set to a value of about 1 Hz (Fig. 7).

After the material's LVR has been defined by a strain sweep, its structure can be further characterized using a frequency sweep at a strain below the critical strain. This experiment provides more information about the effect of colloidal forces and the interactions among particles.

In a frequency sweep, measurements are made over a range of oscillation frequencies at a constant oscillation amplitude and temperature. Below the critical strain, the elastic modulus G' is often nearly independent of frequency, which is a characteristic of a structured or solid-like material. On the other hand, frequency-dependent elastic modulus is a characteristic of a more fluid-like material.

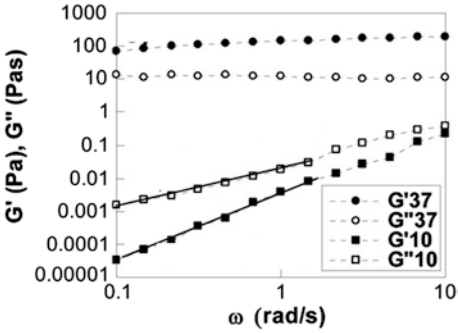

Fig. 8 Frequency sweep test in the sol (10 °C) and gel (37 °C) phases of the CS-g-(PAF-PEG) polymer aqueous solution (6.0 wt%). Reproduced with permission from [91]

These measurements have been used to determine the sol-gel properties of thermogelling polymers. Jeong et al. studied the sol gel behavior of thermogelling polymers with this approach [91]. The frequency sweep test showed that the sol and gel phases of the PEG-PAF grafted chitosan (CS-g-(PAF-PEG)) aqueous solution were characterized by fluid-like behavior and solid-like behavior (Fig. 8). At 10 °C, the elastic modulus and loss modulus of the aqueous polymer solution were proportional to $\omega^{2.1}$ and $\omega^{1.1}$, respectively, indicating a typical viscoelastic fluid-like phase of the sol [92–94]. In addition, the loss modulus was greater than elastic modulus at 10 °C. At 37 °C, the elastic modulus was greater than the loss modulus by an order of magnitude at 37 °C. The elastic modulus was nearly independent of frequency, whereas the loss modulus slightly decreased as the frequency increased in the investigated frequency range of 0.1–10 rad s^{-1}. In the solution state, the thermogelling system showed viscous fluid-like behavior with $G'' > G'$ and a frequency-dependent modulus, whereas in the gel state, $G' > G''$ and G' was independent of the frequency.

Next, it is important to determine if the material requires pre-treatment (such as pre-shearing) before measurements. This can be determined from the pseudo-viscosity profile of the material. Pre-shearing will determine a zero-time of shear, thereby eliminating any structure history prior to loading. This is done by performing a continuous flow test under the broad torque range. The data can be viewed as viscosity versus torque/stress and converted to viscosity versus shear rate.

Most food formulations, cosmetics, pharmaceuticals and paints are structured fluids, containing droplets of an immiscible fluid or particle suspended in a liquid matrix. The viscosity of the liquid matrix in the dispersions plays an important role on the flow properties of the material. When there are repulsive forces between particles they do not settle rapidly, forming a network structure, which stabilizes the suspension. The delicate network structure can be destroyed by shearing, resulting in decreased fluid viscosity.

Most structured fluids do not obey a simple linear relationship between applied stress and flow (Newtonian fluid behavior). Most of these materials have viscosities, which decrease with increasing stress. Such an observation is known as shear thinning which becomes progressively significant as the volume concentration of solid particles increases.

Another aspect that has to be ascertained is the stability of the material properties over the time of testing. For this experiment, an oscillatory time sweep of about 15 min, with oscillation shear stress/torque within the LVR and a frequency of 1 Hz can be carried out. The material can be pre-sheared at a shear rate beyond the 1st Newtonian plateau determined in the previous step. The experiment is allowed to run and a plot of modulus against time is obtained. The point where the modulus plateaus off is judged to be the minimum time required for the recovery of the material structure. This was applied by Moura et al. to understand the gelation kinetics and gel properties upon crosslinking the hydrogel. Both the components G′ and G″ moduli, was monitored. Figure 9 shows the time sweep profiles of elastic (G′) and viscous (G″) moduli near the gel point for pure chitosan solution (A) and for 0.10 % (B) and 0.15 % (C) genipin concentration networks. At the beginning, G″ was larger than G′, which was expected because the samples were still in a liquid state and, thus, viscous properties dominated. As the solutions began to turn into a gel-like state due to the formation of the cross-linked network, both moduli increased. However, the rate of increase of G′ ($\Delta G'/\Delta t$) was higher than that of G″ because the elastic properties started to dominate. This difference in the rates leads to a G′ and G″ crossover. The time required to achieve this crossover is, as mentioned above, the gelation time. From the figure, it is can be seen that higher genipin concentrations lead to lower gelation times. It should also be stressed that the gelation time decreases from about 8 min to about 2 min when the genipin concentration is increased from 0 to 0.15 %.

The creep test probes the time-dependent nature of a sample. Creep and recovery tests allow the differentiation between viscous and elastic responses when the viscoelastic material is subjected to a step constant stress (creep) and then the applied stress is removed (recovery). A standard creep experiment provides critical parameters such as zero shear viscosity (η_o) and equilibrium compliance (J_{eo}), which measures the elastic recoil of a material.

After a sample is allowed to creep under load, the material's elastic behavior can be obtained by abruptly relieving the imposed stress and measuring the extent the sample recovers. A creep/recovery test can be carried out as follows.

- First, standard temperature conditioning and pre-shearing beyond the 1st Newtonian plateau is performed.
- The sample is then equilibrated for a set time necessary to obtain a stable structure as determined earlier in the judgment of the material stability.
- Next, for the retardation step, a shear stress is again selected from within the 1st Newtonian plateau and performed for about 15 min or enough time for slope to be constant.
- Then the recovery of the sample is affected by setting the shear stress to zero and duration for the sample to recover is examined.

During the creep test, the stress causes a transient response, including the elastic and the viscous contributions. By following the recovery phase after the release of the applied stress, one can separate the total strain into the instantaneous elastic part, the recovered elastic part, and the permanently viscous part.

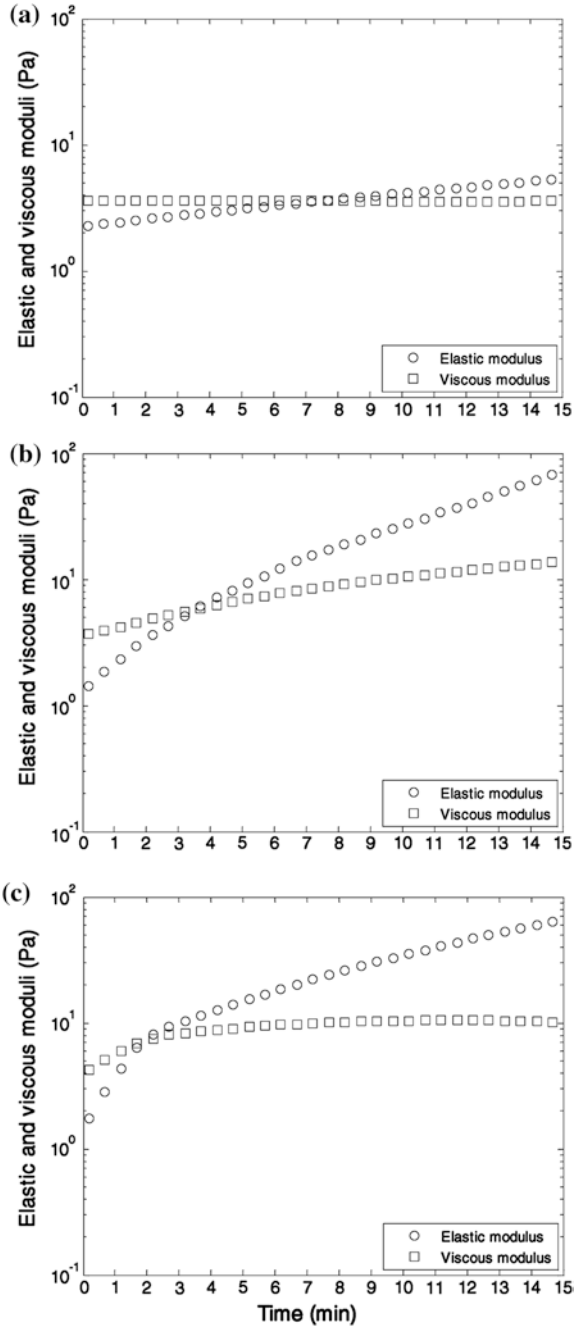

Fig. 9 Dynamics of elastic, G′, and viscous, G″, moduli near the gel point, at 1 Hz (**a**, pure chitosan; **b** and **c**, 0.10 % (w) and 0.15 % (w) genipin chitosan concentration network, respectively). The gelation time is determined as the time at which G′ and G″ intersect each other. Reproduced with permission from [95]

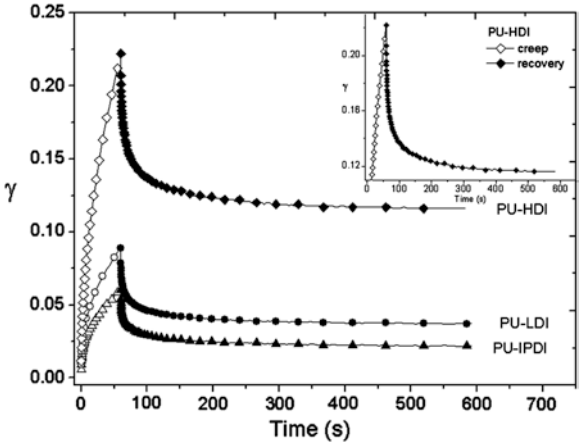

Fig. 10 Creep (*open symbols*) and recovery (*full symbols*) *curves* for the poly(isopropyl lactate diol)-based polyurethane hydrogels at 37 °C when a stress of 5 Pa was applied for 60 s. Reproduced with permission from [96]

Viscoelastic creep data can be presented by plotting the creep modulus (constant applied stress divided by total strain at a particular time) or the strain, as a function of time. Gradinaru et al. studied the creep response of thermogelling poly(isopropyl lactate diol)-based polyurethane hydrogels [96].

Figure 10 shows the curves that represent the viscoelastic response at an applied stress of 5 Pa for the three hydrogels obtained at 37 °C, in a creep test followed by recovery. The creep curves comprise three parts: the instantaneous strain, the retardation strain, and the viscous strain. When the applied stress is removed, the recovery process starts, and first the instantaneous strain is recovered, then the retardation one, and finally remains the viscous part. The high elasticity of the hydrogels can be observed, where the reached strain after the stress of 5 Pa was applied for 60 s is very high, and the recovered strain represents 52 % from the maximum value reached by the strain in the creep test.

Changes in modulus of thermogelling polymer aqueous solutions can be determined by dynamic rheometry (Fig. 11).

- First, standard temperature conditioning at the lower solution temperature and pre-shearing beyond the 1st Newtonian plateau is performed.
- The sample is then equilibrated for a set time necessary to obtain a stable structure at the lower temperature as determined earlier in the judgment of the material stability.
- Next, the material is subjected to a temperature ramp at a fixed stress and a fixed frequency rate.
- The point at which the elastic and loss modulus intersects is defined as the gel transition temperature.

Jeong et al. reported poly(alanine-co-leucine)-poloxamer-poly(alanine-co-leucine) (PAL-PLX-PAL) aqueous solution [62]. As the temperature increased, the polymer aqueous solution underwent sol-to-gel transition at 20−40 °C in a polymer concentration range of 3.0−10.0 wt%. The sol-gel transition of the polymer aqueous

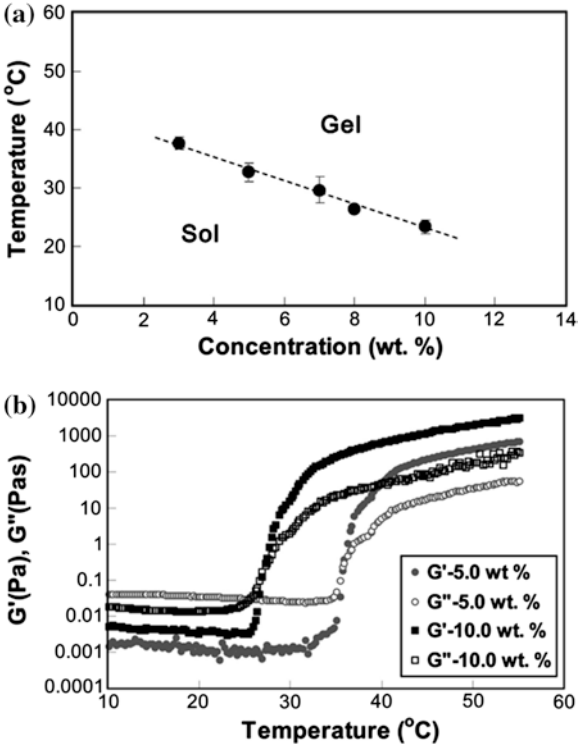

Fig. 11 **a** Phase diagram of the poly(alanine-co-leucine)-poloxamer-poly(alanine-co-leucine) aqueous thermogelling solutions determined by the test tube inverting method. **b** Storage modulus (G′) and loss modulus (G″) of the poly(alanine-co-leucine)-poloxamer-poly(alanine-co-leucine) aqueous thermogelling solutions as a function of temperature and concentration. The legends are the concentrations of the polymers in water. Reproduced with permission from [62]

solution was investigated by the test tube inverting method. The aqueous polymer solution (1.0 mL) was put in the test tube with an inner diameter of 11 mm. The transition temperatures were determined by a flow (sol)-no flow (gel) criterion with a temperature increment of 1 °C per step. Each data point is an average of three measurements. Changes in modulus of the polymer aqueous solutions were investigated by dynamic rheometry. The aqueous polymer solution was placed between parallel plates of 25 mm diameter and a gap of 0.5 mm. To minimize the water evaporation during the experiment, the plates were enclosed in a water-saturated chamber. The data were collected under a controlled stress (4.0 dyn/cm^2) and a frequency of 1.0 rad s^{-1}. The heating rate was 0.5 °C/min.

The phase diagram of PAL-PLX-PAL aqueous solutions determined by the test tube inverting method is shown in Fig. 11. Aqueous solutions of PAL-PLX-PAL undergo sol-to-gel transition as the temperature increases in a concentration range of 3.0–10.0 wt%. The sol-to-gel transition temperature decreased from 38 to 23 °C as the concentration increased from 3.0 to 10.0 wt%. At concentrations lower than 3.0 wt%, the viscosity of the polymer aqueous solution increased as the temperature increased; however, it was not large enough to resist the flow when the test tube was inverted, and thus they were regarded as a sol state. At polymer concentrations higher than 10.0 wt%, the polymer aqueous system formed a gel in a temperature range of 0–60 °C.

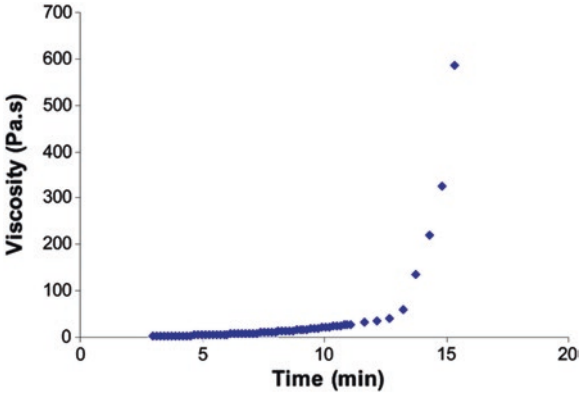

Fig. 12 Variation of viscosity of chitosan-ammonium hydrogen phosphate solution with time as measured using an oscillatory rheometer at a fixed frequency of 1 Hz and fixed temperature of 37 °C. Reproduced with permission from [97]

Sharp increases in both the storage modulus (G′) and loss modulus (G″) of PAL-PLX-PAL aqueous solutions were observed as the temperature increased (Fig. 11). G′ and G″ are an elastic component and a viscous component of the complex modulus of a system, respectively. When G′ is greater than G″, the system is considered to be a gel, and the crossover point was defined as the sol-to-gel transition temperature. The sol-to-gel transition temperatures defined by the test tube inverting method coincided with those defined by dynamic mechanical analysis of G′ and G″ within 2 to 3 °C. By varying the polymer concentration, not only sol-to-gel transition temperature but also modulus of the gel could be controlled. The control of gel modulus (G′) has a significant effect on 3D cell culture as well as the differentiation of the stem cell. In the case of chondrocytes, the modulus of 300–2,500 Pa showed a cytocompatible microenvironment for proliferation of the cells. The gel prepared from 10.0 wt% aqueous solution of PAL-PLX-PAL formed a gel with a G′ of 380 Pa at 37 °C, thus being recommendable as a 3D culture matrix for chondrocytes.

By raising the temperature above the gelation temperature, the time required for the gelation can be determined. Nair et al. demonstrates the thermogelation of chitosan-ammonium hydrogen phosphate solution determined as a function of time using oscillatory rheometers [97]. The viscosity of the chitosan–ammonium hydrogen phosphate solution was found to increase after 8 min and showed a significant increase within 15 min of incubation at 37 °C, demonstrating the sol-gel transition (Fig. 12).

6 Biomedical Applications

In situ forming hydrogels have been increasingly studied for various biomedical applications such as drug delivery, gene delivery, wound healing, tissue engineering, and microfluidics [83, 98–105]. To use hydrogel systems as drug or gene delivery systems or tissue regeneration matrices, (1) drugs, genes, and/or cells

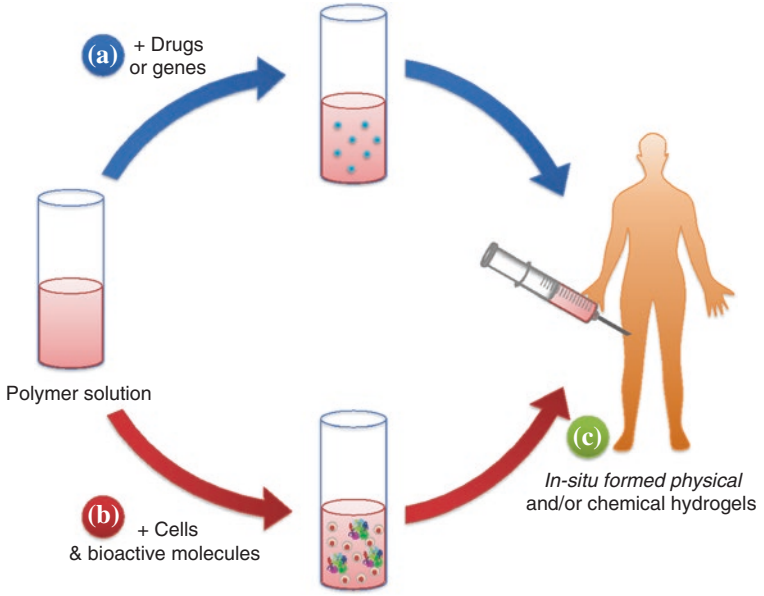

Fig. 13 **a** As injectable drug or gene delivery systems, drugs or genes were dispersed in the polymer solution and then injected to form in situ hydrogel depots. **b** As injectable tissue regeneration matrices, cells and bioactive molecules were mixed with polymer solutions and then injected to the defect area. **c** Injected solutions to the target sites form in situ hydrogels via physical and/or chemical crosslinking

were dispersed in the polymer solution, (2) injected subcutaneously or directly to the defect area, (3) then polymer solutions turn into hydrogels via chemical and/or physical crosslinks (Fig. 13).

"Tetrazole-alkene" photo-click chemistry induced hydrogel of 4-arm PEG-methacrylate (PEG-4-MA) and PEG-4-tetrazole (PEG-4-Tet) showed sustained release of proteins (cytochrome c, γ-globuline, and recombinant human interleukin-2) without losing their bioactivities [37]. PLGA-PEG-PLGA thermosensitive hydrogel with PEG/sucrose and a zinc acetate-exenatide complex (Zn-EXT) showed decreased initial burst and promoted late stage of release of EXT, a glucoregulatory peptide drug for type II diabetes [106]. Nanoscale liposomal polymeric gels (nanolipogels; nLGs) showed sustained delivery of both IL-2 and TGF-β inhibitor and this system enhanced anti-tumor activity against subcutaneous and metastatic melanomas (Fig. 14) [107]. Therapeutic contact lenses of poly[HEMA-co-acrylic acid-co-acrylamide-co-N-vinyl 2-pyrrolidone-co-PEG (200) dimethacrylate] [poly(HEMA-co-AA-co-AM-co-NVP-co-PEG200DMA)] loaded with ketotifen fumarate, a drug that relieves and prevents eye itching, irritation, and discomfort associated with seasonal allergies, showed a dramatic increase in ketotifen mean residence time and bioavailability up to 26 h [108]. A poly(HEMA) based hydrogel containing the ocular drug (DMSA) loaded micelles

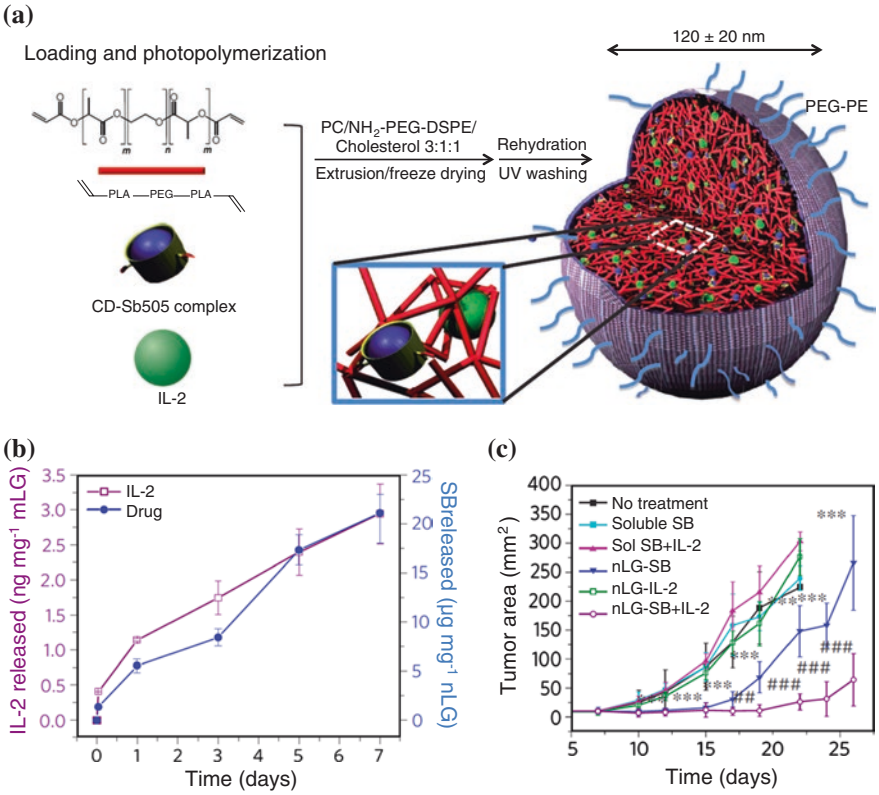

Fig. 14 **a** nLGs were formulated from lyophilized liposomes loaded with biodegradable PLA-PEG-PLA diacrylate, acrylated-CD-TGF-β inhibitor complex, and IL-2 cytokine. After loading, photopolymerization of the polymer and acrylated-CD induced gel formation. **b** Simultaneous release of IL-2 and TGF-β inhibitor released from co-loaded nLGs. **c** Tumor area growth versus time. Reproduced from [107]

(silica shell crosslinked methoxy micelles; SSCMs) was developed as a potential therapeutic contact lens material for long term treatment of ocular disease [109]. In vitro release of DMSA from SSCM embedded hydrogel system was observed over a month. Multiple model drugs of low steric hindrance molecules (LSH) and high steric hindrance molecules (HSH) loaded in the Agarose and Carbomer 974P based hydrogel was suggested as a promising spinal cord injury repair system [110]. LSH released almost completely in 1 day, whereas HSH released only 40 % at day 1 and sustained released during 7 days in vitro. In vivo release was more rapid than in vitro but release pattern was similar with in vitro. LSH can be drugs for short-term neuroprotection purposes, while HSH can be drugs for long-term neuroregeneration approaches. Anticancer drug of Paclitaxel (PTX) loaded PEG-PCL-PEG (PECE) hydrogel showed steady release of PTX for up to 20 days in vitro and prevented recurrence of breast cancer [111]. Another anticancer drug of

Doxorubicin release-profile from the hexamethylene diisocyanate-Pluronic® F127/HA composite hydrogel was almost zero-order release during 28 days [73]. This system also showed antitumor efficacy and therapeutic effects in animal study.

HA and fibrin hydrogels with plasmid DNA (pDNA)/PEI polyplexes loaded through the caged nanoparticle encapsulation were able to deliver genes in vivo without aggregation [112]. Oxidized alginate hydrogels loaded with DNA/PEI nDNA were shown to achieve sustained release in vitro and achieve enhanced revascularization in vivo [113]. Alginate hydrogels conjugated with various RGD densities for siRNA-mediated knockdown of eGFP demonstrated that increasing RGD density resulted in significantly higher knockdown of the targeted protein [114]. Nanostructured micelles-containing PEG based hydrogels that encapsulated cationic bolaamphiphile/DNA complexes and human mesenchymal stem cells (hMSCs) showed higher gene expression efficiency in hMSCs than the PEI/DNA complexes [24]. A CD-based supramolecular hydrogel system with supramolecularly anchored active cationic copolymer/pDNA polyplexes was able to sustain release of pDNA up to 6 days [115]. Hydrogel stiffness can also be used to modulate migration and gene delivery rates; stiffer gels result in slower release rates of encapsulated polyplexes and decreased cell populations, spreading, and transfection [116].

Hydrogels have been used for wound healing as moist wound dressing materials. Hydrogels not only keep the wound moist, but also help proliferation of fibroblasts to recover defects. Rutin-conjugated chitosan-PEG-tyramine hydrogels showed enhanced dermal wound healing efficacy and tissue-adhesive property [117]. Fibroblasts encapsulated PEG-L-PA hydrogels significantly improved in vivo wound healing rate than controls of PBS treated or cell-free PEG-L-PA hydrogel treated group [118]. Treatment of dextran based hydrogels on burn wound promoted neovascularization and skin regeneration [119]. The PECE hydrogel was treated to the full-thickness skin incision wounds and accelerated wound healing compared to untreated controls [111]. In situ forming hydrogels also can be used for prevention of postoperarive adhesion [120]. When biodegradable and thermoreversible PCLA-PEG-PCLA hydrogel treated onto the peritoneal wall defect, postoperative adhesion significantly reduced.

In situ hydrogel systems have been used for tissue engineering. For tissue engineering, usually patient-derived healthy cells are expanded in vitro, mixed with polymer solutions and bioactive molecules, and then inject into a defect area to form a hydrogel in situ. Fibronectin- and NT-3-functionalized silk hydrogels that triggered axonal bundling [121] and self-assembling peptide hydrogel of $RADA_{16}$-IKVAV (AcN-RADARADARADARADAIKVAV-$CONH_2$) that accelerated central nervous system brain tissue regeneration [122] were developed as neural tissue engineering systems. Thermosensitive PNIPAAm-O-phosphoethanolamine grafted poly(acrylic acid)-PNIPAAm hydrogel showed potential as an osteogenic matrix [123]. Mixture of chondroitin sulfate succinimidyl succinate (CS-NHS) and freeze-thawed bone marrow aspirate formed hydrogels and showed potentials as a meniscus repair system [124] or an articular cartilage regenerative matrix when rhBMP-2 localized within the hydrogel [125]. Thermoresponsive and various

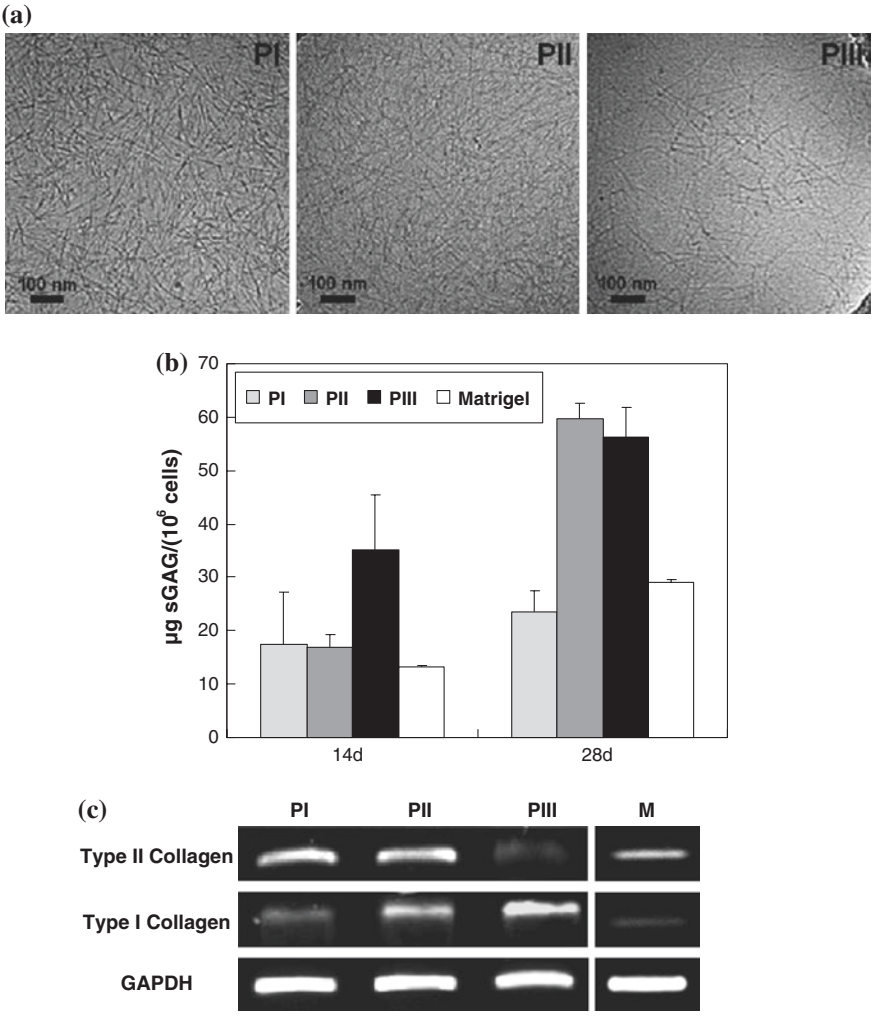

Fig. 15 **a** Nanofibrous interior morphology of (L/DL)-PA-Pluronic®-(L/DL)-PA thermogel. Expression of chondrogenic markers of (**b**) sulfated glycosaminoglycan (sGAG) and (**c**) type II collagen. Matrigel™ was used as a control for 3D chondrocytes culture. Glyceraldehyde 3-phosphate dehydrogenase (GAPDH) is compared as a house-keeping gene. Reproduced from [3]

terminal groups modified PNIPAAm brushes were fabricated for improving cell adhesion and cell sheet harvest [126]. Specifically, carboxyl-terminated PNIPAAm brush surface most enhanced cell adhesion and cell sheet harvesting. (L/DL)-PA-Pluronic®-(L/DL)-PA thermogel showed a higher population of nanofibrous structures as the L-Ala content increased and chondrocytes cultured in these thermogels expressed higher chondrogenic markers compared to commercially available Matrigel™ (Fig. 15) [3].

For the successful tissue regeneration, we need to better understand cell-matrix interactions. Stem cells can be differentiated into specific lineages through the interaction between cell and biological cues or between cell and physical cues [127]. Physicochemical properties of photodegradable PEG based hydrogels could be dynamically controlled by light [9]. Crosslinking density of hydrogel decreased via photodegradation and facilitated spreading or migration of embedded cells. In addition, MSCs showed enhanced chondrogenesis when cell adhesive sequence of Arg-Gly-Asp-Ser (RGDS) was photocleaved from hydrogels. Neurogenesis, myogenesis, and osteogenesis of stem cells on 2D gel surface were controlled by varying stiffness of the hydrogel surface from 0.1–1 kPa, 8–17 kPa, and 25–40 kPa, respectively [128]. Three-dimensional culture of mesenchymal stem cells in RGD-modified alginate hydrogels also showed stem cell differentiation is correlated to the hydrogel stiffness [129]. Briefly, adipogenesis or osteogenesis was predominantly occurred in 2.5–5 kPa or 11–30 kPa microenvironments, respectively. However, cell morphology remained spherical regardless of modulus. MSCs cultured in matrix metalloproteinase (MMP) degradable hydrogels showed high degrees of cell spreading followed by osteogenic differentiation, while remained spherical and underwent adipogenesis in non-degradable hydrogels [14]. MSCs can be induced various differentiation through the interactions between cells and small functional groups in hydrogels [130]. Specifically, phosphate or alkyl groups in PEG hydrogel induced osteogenesis or adipogenesis, respectively. Human adipose derived stem cells (hADSCs) encapsulated in PEG hydrogels with multifunctionalized α-CD nanobeads regulated stem cell fate [131]. Ultimately, the alcohol, hydrophobic methyl group, and phosphate-substituted α-CD nanobeads stimulated chondrogenic, adipogenic, and osteogenic differentiation, respectively.

7 Conclusions and Prospectives

In situ forming chemically and/or physically crosslinked hydrogels under mild conditions have been developed for various biomedical applications. Injectable hydrogel systems are minimally invasive and patient friendly. We can decrease injection frequency for better patient compliance by developing novel sustained drug delivery systems. Cells or bioactive molecules are easy to mix with polymer solutions and these mixtures are in situ and easy to form the 3D microenvironments into any desired defect shapes. For successful designing of an in situ gelling system for a specific biomedical application, several points should be carefully understood. (1) Different crosslinking type gives different degradation products and release-profiles of incorporated drugs. (2) Porosity and pore size of hydrogels can affect to cell viability, proliferation, and/or drug release profile. (3) Initiators, catalysts, or residual monomers can lead cytotoxicity. During radical polymerization, produced radicals not only can react with the vinyl group in monomer but also can damage cellular macromolecules. (4) Reactive functional groups of polymers can give side reactions with incorporated bioactive molecules

or cells. These side reactions might induce immunogenicity and damage cells or the efficacy of drugs. (5) Residual enzyme after enzymatic crosslinking also can provide unexpected reactions with incorporated protein drugs. (6) Development of various hydrogel-based drug delivery systems with non-modified original drug is one of the best ways to produce the improved versions of biologics. Biobetters can advance the efficacy, pharmacokinetic parameters, and safety profile of drugs than original biologics or Biosimilars (subsequent versions of off-patent biologics with demonstrated physicochemical similarity). In addition, Biobetters can also improve patient compliance due to a reduced rate of side effects and enhanced convenience. (7) Sustained-release systems without initial burst release should be considered. The charge interaction or the inclusion complex formation between polymer and drug can improve these problems. (8) Incorporated drugs or cells should be stable during the implantation period. Acidic degradation-products released from polyester-based hydrogels raise the local acidity inside and around the hydrogels, which lead an inflammatory response and a decrease of cell viability or drug stability. (9) For tissue regeneration application, ECM mimicking design of the hydrogel system is a key factor. Polypeptides have unique secondary structures of α-helix, triple helix, β-sheet, or random coil, etc. Different combinations of polypeptide-based hydrogel systems allow various nanostructures in the hydrogels that affect proliferation and/or differentiation of encapsulated cells. (10) Duration of in situ formed hydrogels should be adjusted to match with drug release profile or tissue regeneration rate. (11) Macromers should be selected based on application route. NIPAAm copolymer has been used for “cell sheet” (a tissue-like cellular monolayer) development that already showed successful applications to human clinical studies. However, in vivo application of PNIPAAm hydrogel still has limitation on the toxicity of the residual monomer. (12) Gel modulus, degradability, functional groups can affect stem cell fate. Soft gel improves neurogenesis or adipogenesis, while stiff gel enhances osteogenesis. Degradable or non-degradable hydrogels induces osteogenesis or adipogenesis, respectively. Phosphate groups or alkyl groups can stimulate osteogenesis or adipogenesis, respectively.

Challenging design of hydrogels with these understands and considerations about various hydrogel systems will advance the development of smart bioactive in situ gelling hydrogels for specific biomedical applications.

Also, study of flow properties of liquids is important for pharmacists working in the manufacture of several dosage forms, such as simple liquids, ointments, creams and pastes. The flow behavior of liquids under applied stress is of great relevance in the field of pharmacy. Flow properties are used as important quality control tools to maintain the superiority of the product and reduce batch-to-batch variations.

The clinically approved systems by using Pluronics/alginate (Guardix-SG) and chitosan/glycerol phosphate (BST-CarGel) based thermal gels are interesting examples. Alginate and Pluronics form interpenetrating network (IPN) by adding calcium salt, where it forms a temperature sensitive gelling system. The system was successfully applied as an antiadhesive agent after the surgery. BST-CarGel was applied for articular cartilage repair on the microfractured treatment.

Compared with current microfracture treatment, the BST-CarGel system improved the repair by successfully holding the cells/stem cells released from the microfractured site. Both systems are already on the market. Another system is Regel®, which was a pionieering system of biodegradable thermogelling system. The biocompatibility was good as evidenced by passing phase I clinical trial. However, the paclitaxel loaded Regel® (Oncogel) was stopped for further investigation [132]. When a patient is diagnosed as a solid tumor, he/she immediately wants surgery instead of waiting till the tumor size decreases by using the sustained release of the anticancer drug from the in situ formed gel. Therefore, the treatment was narrowed down for inoperable tumor such as inoperable esophageal cancer. However, compared with current treatment of anticancer drug combined with radiotherapy, the additional treatment by using Oncogel did not significantly improve the patient. Above cases studies suggest that the patient-oriented development of an in situ gelling system is very important.

References

1. Berger, J., Reist, M., Mayer, J.M., Felt, O., Peppas, N.A., Gurny, R.: Structure and interactions in covalently and ionically crosslinked chitosan hydrogels for biomedical applications. Eur. J. Pharm. Biopharm. **57**, 19–34 (2004)
2. Wichterle, O., Lim, D.: Hydrophilic gels for biological use. Nature **185**, 117–118 (1960)
3. Choi, B.G., Park, M.H., Cho, S.-H., Joo, M.K., Oh, H.J., Kim, E.H., et al.: In situ thermal gelling polypeptide for chondrocytes 3D culture. Biomaterials **31**, 9266–9272 (2010)
4. Hoffman, A.S.: Hydrogels for biomedical applications. Adv. Drug Deliv. Rev. **54**, 3–12 (2002)
5. Ko, D.Y., Shinde, U.P., Yeon, B., Jeong, B.: Recent progress of in situ formed gels for biomedical applications. Prog. Polym. Sci. **38**, 672–701 (2013)
6. Chien, H.W., Tsai, W.B., Jiang, S.Y.: Direct cell encapsulation in biodegradable and functionalizable carboxybetaine hydrogels. Biomaterials **33**, 5706–5712 (2012)
7. He, X., Ma, J., Jabbari, E.: Effect of grafting RGD and BMP-2 protein-derived peptides to a hydrogel substrate on osteogenic differentiation of marrow stromal cells. Langmuir **24**, 12508–12516 (2008)
8. Hong, Y., Song, H., Gong, Y., Mao, Z., Gao, C., Shen, J.: Covalently crosslinked chitosan hydrogel: properties of in vitro degradation and chondrocyte encapsulation. Acta Biomater. **3**, 23–31 (2007)
9. Kloxin, A.M., Kasko, A.M., Salinas, C.N., Anseth, K.S.: Photodegradable hydrogels for dynamic tuning of physical and chemical properties. Science **324**, 59–63 (2009)
10. Shin, H., Temenoff, J.S., Mikos, A.G.: In vitro cytotoxicity of unsaturated oligo[poly(ethylene glycol) fumarate] macromers and their cross-linked hydrogels. Biomacromolecules **4**, 552–560 (2003)
11. Temenoff, J.S., Park, H., Jabbari, E., Sheffield, T.L., LeBaron, R.G., Ambrose, C.G., et al.: In vitro osteogenic differentiation of marrow stromal cells encapsulated in biodegradable hydrogels. J. Biomed. Mater. Res., Prat A **70**, 235–244 (2004)
12. Chen, Y.C., Lin, R.Z., Qi, H., Yang, Y., Bae, H., Melero-Martin, J.M., et al.: Functional human vascular network generated in photocrosslinkable gelatin methacrylate hydrogels. Adv. Funct. Mater. **22**, 2027–2039 (2012)
13. Geng, X.H., Mo, X.M., Fan, L.P., Yin, A.L., Fang, J.: Hierarchically designed injectable hydrogel from oxidized dextran, amino gelatin and 4-arm poly(ethylene glycol)-acrylate for tissue engineering application. J. Mater. Chem. **22**, 25130–25139 (2012)

14. Khetan, S., Guvendiren, M., Legant, W.R., Cohen, D.M., Chen, C.S., Burdick, J.A.: Degradation-mediated cellular traction directs stem cell fate in covalently crosslinked three-dimensional hydrogels. Nat. Mater. **12**, 458–465 (2013)
15. Fairbanks, B.D., Singh, S.P., Bowman, C.N., Anseth, K.S.: Photodegradable, photoadaptable hydrogels via radical-mediated disulfide fragmentation reaction. Macromolecules **44**, 2444–2450 (2011)
16. McCall, J.D., Luoma, J.E., Anseth, K.S.: Covalently tethered transforming growth factor beta in PEG hydrogels promotes chondrogenic differentiation of encapsulated human mesenchymal stem cells. Drug Deliv. Transl. Res. **2**, 305–312 (2012)
17. Silva-Correia, J., Zavan, B., Vindigni, V., Silva, T.H., Oliveira, J.M., Abatangelo, G., et al.: Biocompatibility evaluation of ionic- and photo-crosslinked methacrylated gellan gum hydrogels: in vitro and in vivo study. Adv Healthc Mater. **2**, 568–575 (2013)
18. Barrow, M., Zhang, H.F.: Aligned porous stimuli-responsive hydrogels via directional freezing and frozen UV initiated polymerization. Soft Matter **9**, 2723–2729 (2013)
19. Elisseeff, J., Anseth, K., Sims, D., McIntosh, W., Randolph, M., Langer, R.: Transdermal photopolymerization for minimally invasive implantation. Proc. Natl. Acad. Sci. U. S. A. **96**, 3104–3107 (1999)
20. Park, H., Choi, B., Hu, J.L., Lee, M.: Injectable chitosan hyaluronic acid hydrogels for cartilage tissue engineering. Acta Biomater. **9**, 4779–4786 (2013)
21. Purcell, B.P., Elser, J.A., Mu, A., Margulies, K.B., Burdick, J.A.: Synergistic effects of SDF-1alpha chemokine and hyaluronic acid release from degradable hydrogels on directing bone marrow derived cell homing to the myocardium. Biomaterials **33**, 7849–7857 (2012)
22. Shih, H., Lin, C.C.: Visible-light-mediated thiol-ene hydrogelation using eosin-Y as the only photoinitiator. Macromol. Rapid Commun. **34**, 269–273 (2013)
23. Lim, K.S., Alves, M.H., Poole-Warren, L.A., Martens, P.J.: Covalent incorporation of non-chemically modified gelatin into degradable PVA-tyramine hydrogels. Biomaterials **34**, 7097–7105 (2013)
24. Li, Y., Yang, C., Khan, M., Liu, S., Hedrick, J.L., Yang, Y.Y., et al.: Nanostructured PEG-based hydrogels with tunable physical properties for gene delivery to human mesenchymal stem cells. Biomaterials **33**, 6533–6541 (2012)
25. Phelps, E.A., Enemchukwu, N.O., Fiore, V.F., Sy, J.C., Murthy, N., Sulchek, T.A., et al.: Maleimide cross-linked bioactive PEG hydrogel exhibits improved reaction kinetics and cross-linking for cell encapsulation and in situ delivery. Adv. Mater. **24**(64–70), 2 (2012)
26. Wang, H., Han, A., Cai, Y., Xie, Y., Zhou, H., Long, J., et al.: Multifunctional biohybrid hydrogels for cell culture and controlled drug release. Chem. Commun. **49**, 7448–7450 (2013)
27. Tortora, M., Cavalieri, F., Chiessi, E., Paradossi, G.: Michael-type addition reactions for the in situ formation of poly(vinyl alcohol)-based hydrogels. Biomacromolecules **8**, 209–214 (2007)
28. Wang, Z.C., Xu, X.D., Chen, C.S., Yun, L., Song, J.C., Zhang, X.Z., et al.: In situ formation of thermosensitive PNIPAAm-based hydrogels by Michael-type addition reaction. ACS Appl. Mater. Interfaces **2**, 1009–1018 (2010)
29. Chawla, K., Yu, T.B., Liao, S.W., Guan, Z.: Biodegradable and biocompatible synthetic saccharide-Peptide hydrogels for three-dimensional stem cell culture. Biomacromolecules **12**, 560–567 (2011)
30. Kupal, S.G., Cerroni, B., Ghugare, S.V., Chiessi, E., Paradossi, G.: Biointerface properties of core-shell poly(vinyl alcohol)-hyaluronic acid microgels based on chemoselective chemistry. Biomacromolecules **13**, 3592–3601 (2012)
31. Adzima, B.J., Tao, Y., Kloxin, C.J., DeForest, C.A., Anseth, K.S., Bowman, C.N.: Spatial and temporal control of the alkyne-azide cycloaddition by photoinitiated Cu(II) reduction. Nat. Chem. **3**, 256–259 (2011)
32. Chen, R.T., Marchesan, S., Evans, R.A., Styan, K.E., Such, G.K., Postma, A., et al.: Photoinitiated alkyne-azide click and radical cross-linking reactions for the patterning of PEG hydrogels. Biomacromolecules **13**, 889–895 (2012)

33. van Dijk, M., van Nostrum, C.F., Hennink, W.E., Rijkers, D.T., Liskamp, R.M.: Synthesis and characterization of enzymatically biodegradable PEG and peptide-based hydrogels prepared by click chemistry. Biomacromolecules **11**, 1608–1614 (2010)
34. Xu, X.D., Chen, C.S., Lu, B., Wang, Z.C., Cheng, S.X., Zhang, X.Z., et al.: Modular synthesis of thermosensitive P(NIPAAm-co-HEMA)/beta-CD based hydrogels via click chemistry. Macromol. Rapid Commun. **30**, 157–164 (2009)
35. Hu, X., Li, D., Zhou, F., Gao, C.: Biological hydrogel synthesized from hyaluronic acid, gelatin and chondroitin sulfate by click chemistry. Acta Biomater. **7**, 1618–1626 (2011)
36. Deforest, C.A., Sims, E.A., Anseth, K.S.: Peptide-functionalized click hydrogels with independently tunable mechanics and chemical functionality for 3D cell culture. Chem. Mater. **22**, 4783–4790 (2010)
37. Fan, Y., Deng, C., Cheng, R., Meng, F., Zhong, Z.: In situ forming hydrogels via catalyst-free and bioorthogonal "tetrazole-alkene" photo-click chemistry. Biomacromolecules **14**, 2814–2821 (2013)
38. Alge, D.L., Azagarsamy, M.A., Donohue, D.F., Anseth, K.S.: Synthetically tractable click hydrogels for three-dimensional cell culture formed using tetrazine-norbornene chemistry. Biomacromolecules **14**, 949–953 (2013)
39. Wei, H.-L., Yang, Z., Chu, H.-J., Zhu, J., Li, Z.-C., Cui, J.-S.: Facile preparation of poly(N-isopropylacrylamide)-based hydrogels via aqueous Diels-Alder click reaction. Polymer **51**, 1694–1702 (2010)
40. Nimmo, C.M., Owen, S.C., Shoichet, M.S.: Diels-Alder Click cross-linked hyaluronic acid hydrogels for tissue engineering. Biomacromolecules **12**, 824–830 (2011)
41. Tan, H.P., Rubin, J.P., Marra, K.G.: Direct Synthesis of Biodegradable Polysaccharide Derivative Hydrogels Through Aqueous Diels-Alder Chemistry. Macromol. Rapid Commun. **32**, 905–911 (2011)
42. Menzies, D.J., Cameron, A., Munro, T., Wolvetang, E., Grondahl, L., Cooper-White, J.J.: Tailorable cell culture platforms from enzymatically cross-linked multifunctional poly(ethylene glycol)-based hydrogels. Biomacromolecules **14**, 413–423 (2013)
43. Singh, S., Topuz, F., Hahn, K., Albrecht, K., Groll, J.: Embedding of active proteins and living cells in redox-sensitive hydrogels and nanogels through enzymatic cross-linking. Angewandte Chemie-International Edition **52**, 3000–3003 (2013)
44. Park, K.M., Lee, Y., Son, J.Y., Oh, D.H., Lee, J.S., Park, K.D.: Synthesis and characterizations of in situ cross-linkable gelatin and 4-arm-PPO-PEO hybrid hydrogels via enzymatic reaction for tissue regenerative medicine. Biomacromolecules **13**, 604–611 (2012)
45. Teixeira, L.S.M., Leijten, J.C.H., Wennink, J.W.H., Chatterjea, A.G., Feijen, J., van Blitterswijk, C.A., et al.: The effect of platelet lysate supplementation of a dextran-based hydrogel on cartilage formation. Biomaterials **33**, 3651–3661 (2012)
46. Devolder, R., Antoniadou, E., Kong, H.: Enzymatically cross-linked injectable alginate-g-pyrrole hydrogels for neovascularization. J. Controlled Release **172**, 30–37 (2013)
47. Davis, N.E., Ding, S., Forster, R.E., Pinkas, D.M., Barron, A.E.: Modular enzymatically crosslinked protein polymer hydrogels for in situ gelation. Biomaterials **31**, 7288–7297 (2010)
48. Vermonden, T., Besseling, N.A.M., van Steenbergen, M.J., Hennink, W.E.: Rheological studies of thermosensitive triblock copolymer hydrogels. Langmuir **22**, 10180–10184 (2006)
49. Jeong, B., Bae, Y.H., Kim, S.W.: Thermoreversible gelation of PEG-PLGA-PEG triblock copolymer aqueous solutions. Macromolecules **32**, 7064–7069 (1999)
50. Hwang, M.J., Suh, J.M., Bae, Y.H., Kim, S.W., Jeong, B.: Caprolactonic poloxamer analog: PEG-PCL-PEG. Biomacromolecules **6**, 885–890 (2005)
51. Yu, L., Zhang, H., Ding, J.: A subtle end-group effect on macroscopic physical gelation of triblock copolymer aqueous solutions. Angew. Chem. Int. Ed. **45**, 2232–2235 (2006)
52. Loh, X.J., Goh, S.H., Li, J.: New biodegradable thermogelling copolymers having very low gelation concentrations. Biomacromolecules **8**, 585–593 (2007)

53. Chenite, A., Chaput, C., Wang, D., Combes, C., Buschmann, M.D., Hoemann, C.D., Leroux, J.C., Atkinson, B.L., Binette, F., Selmani, : Novel injectable neutral solutions of chitosan form biodegradable gels in situ. Biomaterials **21**, 2155–2161 (2000)
54. Choi, Y.Y., Joo, M.K., Sohn, Y.S., Jeong, B.: Significance of secondary structure in nanostructure formation and thermosensitivity of polypeptide block copolymers. Soft Matter **4**, 2383–2387 (2008)
55. Jeong, Y., Joo, M.K., Bahk, K.H., Choi, Y.Y., Kim, H.T., Kim, W.K., Lee, H.J., Sohn, Y.S., Jeong, B.: Enzymatic degradable temperature-sensitive polypeptide as a new in situ gelling biomaterial. J. Controlled Release **137**, 25–30 (2009)
56. Kim, S.Y., Kim, H.J., Lee, K.E., Han, S.S., Sohn, Y.S., Jeong, B.: Reverse thermal gelling PEG-PTMC diblock copolymer aqueous solution. Macromolecules **40**, 5519–5525 (2007)
57. Lee, B.H., Lee, Y.M., Sohn, Y.S., Song, S.C.: A thermosensitive poly(organophosphazene) gel. Macromolecules **35**, 3876–3879 (2002)
58. Liu, C.D., Zhang, Z.X., Liu, K.L., Ni, X.P., Li, J.: Biodegradable thermogelling poly(ester urethane)s consisting of poly(1,4-butylene adipate), poly(ethylene glycol), and poly(propylene glycol). Soft Matter **9**, 787–794 (2013)
59. Megged, Z., Haider, M., Li, D., O'Malley Jr, B.W., Cappello, J., Ghandehari, H.: In vitro and in vivo evaluation of recombinant silk-elastinlike hydrogels for cancer gene therapy. J. Controlled Release **94**, 433–435 (2004)
60. Sosnik, A., Cohn, D.: Ethoxysilane-capped PEG-PPO-PEO triblocks:a new family of reverse thermo-responsive polymers. Biomaterials **25**, 2851–2858 (2004)
61. Wright, E.R., Conticello, V.P.: Self-assembly of block copolymers derived from elastin-mimetic polypeptide sequences. Adv. Drug Delivery Rev. **54**, 1057–1073 (2002)
62. Moon, H.J., Choi, B.G., Park, M.H., Joo, M.K., Jeong, B.: Enzymatically degradable thermogelling poly(alanine-co-leucine)-poloxamer-poly(alanine-co-leucine). Biomacromolecules **12**, 1234–1242 (2011)
63. Yeon, B., Park, M.H., Moon, H.J., Kim, S.J., Cheon, Y.W., Jeong, B.: 3D culture of adipose-tissue-derived stem cells mainly leads to chondrogenesis in poly(ethylene glycol)-poly(l-alanine) diblock copolymer thermogel. Biomacromolecules **14**, 3256–3266 (2013)
64. Kim, W.S., Mooney, D.J., Arany, P.R., Lee, K., Huebsch, N., Kim, J.: Adipose tissue engineering using injectable, oxidized alginate hydrogels. Tissue Eng., Part A **18**, 737–743 (2012)
65. Sinthuvanich, C., Haines-Butterick, L.A., Nagy, K.J., Schneider, J.P.: Iterative design of peptide-based hydrogels and the effect of network electrostatics on primary chondrocyte behavior. Biomaterials **33**, 7478–7488 (2012)
66. Appel, E.A., del Barrio, J., Loh, X.J., Scherman, O.A.: Supramolecular polymeric hydrogels. Chem. Soc. Rev. **41**, 6195–6214 (2012)
67. Lin, N., Dufresne, A.: Supramolecular hydrogels from in situ host-guest inclusion between chemically modified cellulose nanocrystals and cyclodextrin. Biomacromolecules **14**, 871–880 (2013)
68. Li, Y., Fukushima, K., Coady, D.J., Engler, A.C., Liu, S., Huang, Y., et al.: Broad-spectrum antimicrobial and biofilm-disrupting hydrogels: stereocomplex-driven supramolecular assemblies. Angew. Chem. Int. Ed. Engl. **52**, 674–678 (2013)
69. Buwalda, S.J., Calucci, L., Forte, C., Dijkstra, P.J., Feijen, J.: Stereocomplexed 8-armed poly(ethylene glycol)–poly(lactide) star block copolymer hydrogels: gelation mechanism, mechanical properties and degradation behavior. Polymer **53**, 2809–2817 (2012)
70. Miyata, T., Asami, N., Uragami, T.: A reversibly antigen-responsive hydrogel. Nature **399**, 766–769 (1999)
71. Ehrbar, M., Schoenmakers, R., Christen, E.H., Fussenegger, M., Weber, W.: Drug-sensing hydrogels for the inducible release of biopharmaceuticals. Nat. Mater. **7**, 800–804 (2008)
72. Tan, H.P., Xiao, C., Sun, J.C., Xiong, D.S., Hu, X.H.: Biological self-assembly of injectable hydrogel as cell scaffold via specific nucleobase pairing. Chem. Commun. **48**, 10289–10291 (2012)
73. Chen, C., Wang, L., Deng, L., Hu, R., Dong, A.: Performance optimization of injectable chitosan hydrogel by combining physical and chemical triple crosslinking structure. J. Biomed. Mater. Res., Part A **101**, 684–693 (2013)

74. Ekenseair, A.K., Boere, K.W., Tzouanas, S.N., Vo, T.N., Kasper, F.K., Mikos, A.G.: Synthesis and characterization of thermally and chemically gelling injectable hydrogels for tissue engineering. Biomacromolecules **13**, 1908–1915 (2012)
75. Gil, E.S., Hudson, S.M.: Stimuli-reponsive polymers and their bioconjugates. Prog. Polym. Sci. **29**, 1173–1222 (2004)
76. Peppas, N.A., Hilt, J.Z., Khademhosseini, A., Langer, R.: Hydrogels in biology and medicine: From molecular principles to bionanotechnology. Adv. Mater. **18**, 1345–1360 (2006)
77. Qiu, Y., Park, K.: Environment-sensitive hydrogels for drug delivery. Adv. Drug Deliv. Rev. **53**, 321–339 (2001)
78. Gunn, J.W., Turner, S.D., Mann, B.K.: Adhesive and mechanical properties of hydrogels influence neurite extension. J. Biomed. Mater. Res., Part A. **72A**, 91–97 (2005)
79. Discher, D.E., Janmey, P., Wang, Y.L.: Tissue cells feel and respond to the stiffness of their substrate. Science **310**, 1139–1143 (2005)
80. Lozoya, O.A., Wauthier, E., Turner, R.A., Barbier, C., Prestwich, G.D., Guilak, F., Superfine, R., Lubkin, S.R., Reid, L.M.: Regulation of hepatic stem/progenitor phenotype by microenvironment stiffness in hydrogel models of the human liver stem cell niche. Biomaterials **32**, 7389–7402 (2011)
81. Wang, L.S., Boulaire, J., Chan, P.P.Y., Chung, J.E., Kurisawa, M.: The role of stiffness of gelatin-hydroxyphenylpropionic acid hydrogels formed by enzyme-mediated crosslinking on the differentiation of human mesenchymal stem cell. Biomaterials **31**, 8608–8616 (2010)
82. Jeong, B., Kim, S.W., Bae, Y.H.: Thermosensitive sol-gel reversible hydrogels. Adv. Drug Deliv. Rev. **64**, 154–162 (2012)
83. Moon, H.J., Ko, D.Y., Park, M.H., Joo, M.K., Jeong, B.: Temperature-responsive compounds as in situ gelling biomedical materials. Chem. Soc. Rev. **41**, 4860–4883 (2012)
84. Park, M.H., Joo, M.K., Choi, B.G., Jeong, B.: Biodegradable thermogels. Acc. Chem. Res. **45**, 424–433 (2012)
85. Reiner, M., Blair, G.W.S., Hawley, H.B.: The Weissenberg effect in sweetened condensed milk. J. Soc. Chem. Ind. (London) **68**, 327–328 (1949)
86. Rivlin, R.S.: Torsion of a rubber cylinder. J. Appl. Phys. **18**, 444–449 (1947)
87. Barnes, H.A., Hutton, J.F., Walters, K.: An Introduction to Rheology. Elsevier, Amsterdam (1989)
88. Larson, R.G.: The rheology of dilute solutions of flexible polymers: progress and problems. J. Rheol. **49**, 1–70 (2005)
89. Mezger, T.G.: The Rheology Handbook. Vincentz, Hannover (2006)
90. Miller, D.R., Macosko, C.W.: New derivation of post gel properties of network polymers. Macromolecules **9**, 206–211 (1976)
91. Kang, E.Y., Moon, H.J., Joo, M.K., Jeong, B.: Thermogelling chitosan-g-(PAF-PEG) aqueous solution as an injectable scaffold. Biomacromolecules **13**, 1750–1757 (2012)
92. Jin, N., Woodcock, J.W., Xue, C., O'Lenick, T.G., Jiang, X., Jin, S., Dadmun, M.D., Zhao, B.: Tuning of thermo-triggered gel-to-sol transition of aqueous solution of multi-responsive diblock copolymer poly(methoxytri(ethylene glycol) acrylate-co-acrylic acid)-b-poly(ethoxydi(ethylene glycol) acrylate). Macromolecules **44**, 3556–3566 (2011)
93. Noro, A., Matsushita, Y., Lodge, T.P.: Gelation mechanism of thermoreversible supramacromolecular ion gels via hydrogen bonding. Macromolecules **42**, 5802–5810 (2009)
94. O'Lenick, T.G., Jiang, X., Zhao, B.: Thermosensitive aqueous gels with tunable sol gel transition temperatures from thermo- and pH-responsive hydrophilic ABA triblock copolymer. Langmuir **26**, 8787–8796 (2010)
95. Moura, M.J., Figueiredo, M.M., Gil, M.H.: Rheological study of genipin cross-linked chitosan hydrogels. Biomacromolecules **8**, 3823–3829 (2007)
96. Gradinaru, L.M., Ciobanu, C., Vlad, S., Bercea, M., Popa, M.: Thermoreversible poly(isopropyl lactate diol)-based polyurethane hydrogels: effect of isocyanate on some physical properties. Ind. Eng. Chem. Res. **51**, 12344–12354 (2012)
97. Nair, L.S., Starnes, T., Ko, J.W.K., Laurencin, C.T.: Development of injectable thermogelling chitosan-inorganic phosphate solutions for biomedical applications. Biomacromolecules **8**, 3779–3785 (2007)

98. Drury, J.L., Mooney, D.J.: Hydrogels for tissue engineering: scaffold design variables and applications. Biomaterials **24**, 4337–4351 (2003)
99. Gong, C., Qi, T., Wei, X., Qu, Y., Wu, Q., Luo, F., et al.: Thermosensitive polymeric hydrogels as drug delivery systems. Curr. Med. Chem. **20**, 79–94 (2013)
100. Langer, R., Tirrell, D.A.: Designing materials for biology and medicine. Nature **428**, 487–492 (2004)
101. Lee, K.Y., Mooney, D.J.: Hydrogels for tissue engineering. Chem. Rev. **101**, 1869–1879 (2001)
102. Matricardi, P., Di Meo, C., Coviello, T., Hennink, W.E., Alhaique, F.: Interpenetrating polymer networks polysaccharide hydrogels for drug delivery and tissue engineering. Adv. Drug Deliv. Rev. **65**(9), 1172–1187 (2013)
103. Peppas, N.A., Bures, P., Leobandung, W., Ichikawa, H.: Hydrogels in pharmaceutical formulations. Eur. J. Pharm. Biopharm. **50**, 27–46 (2000)
104. Vermonden, T., Censi, R., Hennink, W.E.: Hydrogels for protein delivery. Chem. Rev. **112**, 2853–2888 (2012)
105. Ziaie, B., Baldi, A., Lei, M., Gu, Y.D., Siegel, R.A.: Hard and soft micromachining for BioMEMS: review of techniques and examples of applications in microfluidics and drug delivery. Adv. Drug Deliv. Rev. **56**, 145–172 (2004)
106. Li, K., Yu, L., Liu, X.J., Chen, C., Chen, Q.H., Ding, J.D.: A long-acting formulation of a polypeptide drug exenatide in treatment of diabetes using an injectable block copolymer hydrogel. Biomaterials **34**, 2834–2842 (2013)
107. Park, J., Wrzesinski, S.H., Stern, E., Look, M., Criscione, J., Ragheb, R., et al.: Combination delivery of TGF-beta inhibitor and IL-2 by nanoscale liposomal polymeric gels enhances tumour immunotherapy. Nat. Mater. **11**, 895–905 (2012)
108. Tieppo, A., White, C.J., Paine, A.C., Voyles, M.L., McBride, M.K., Byrne, M.E.: Sustained in vivo release from imprinted therapeutic contact lenses. J. Controlled Release **157**, 391–397 (2012)
109. Lu, C., Yoganathan, R.B., Kociolek, M., Allen, C.: Hydrogel containing silica shell crosslinked micelles for ocular drug delivery. J. Pharm. Sci. **102**, 627–637 (2013)
110. Perale, G., Rossi, F., Santoro, M., Peviani, M., Papa, S., Llupi, D., et al.: Multiple drug delivery hydrogel system for spinal cord injury repair strategies. J. Controlled Release **159**, 271–280 (2012)
111. Lei, N., Gong, C.Y., Qian, Z.Y., Luo, F., Wang, C., Wang, H.L., et al.: Therapeutic application of injectable thermosensitive hydrogel in preventing local breast cancer recurrence and improving incision wound healing in a mouse model. Nanoscale **4**, 5686–5693 (2012)
112. Lei, Y., Rahim, M., Ng, Q., Segura, T.: Hyaluronic acid and fibrin hydrogels with concentrated DNA/PEI polyplexes for local gene delivery. J. Controlled Release **153**, 255–261 (2011)
113. Kong, H.J., Kim, E.S., Huang, Y.C., Mooney, D.J.: Design of biodegradable hydrogel for the local and sustained delivery of angiogenic plasmid DNA. Pharm. Res. **25**, 1230–1238 (2008)
114. Khormaee, S., Ali, O.A., Chodosh, J., Mooney, D.J.: Optimizing siRNA efficacy through alteration in the target cell-adhesion substrate interaction. J. Biomed. Mater. Res., Part A **100A**, 2637–2643 (2012)
115. Li, Z.B., Yin, H., Zhang, Z.X., Liu, K.L., Li, J.: Supramolecular anchoring of dna polyplexes in cyclodextrin-based polypseudorotaxane hydrogels for sustained gene delivery. Biomacromolecules **13**, 3162–3172 (2012)
116. Gojgini, S., Tokatlian, T., Segura, T.: Utilizing cell-matrix interactions to modulate gene transfer to stem cells inside hyaluronic acid hydrogels. Mol. Pharm. **8**, 1582–1591 (2011)
117. Tran, N.Q., Joung, Y.K., Lih, E., Park, K.D.: In situ forming and rutin-releasing chitosan hydrogels as injectable dressings for dermal wound healing. Biomacromolecules **12**, 2872–2880 (2011)

118. Yun, E.J., Yon, B., Joo, M.K., Jeong, B.: Cell therapy for skin wound using fibroblast encapsulated poly(ethylene glycol)-poly(l-alanine) thermogel. Biomacromolecules **13**, 1106–1111 (2012)
119. Sun, G., Zhang, X., Shen, Y.I., Sebastian, R., Dickinson, L.E., Fox-Talbot, K., et al.: Dextran hydrogel scaffolds enhance angiogenic responses and promote complete skin regeneration during burn wound healing. Proc. Natl. Acad. Sci. U. S. A. **108**, 20976–20981 (2011)
120. Zhang, Z., Ni, J., Chen, L., Yu, L., Xu, J.W., Ding, J.D.: Biodegradable and thermoreversible PCLA-PEG-PCLA hydrogel as a barrier for prevention of post-operative adhesion. Biomaterials **32**, 4725–4736 (2011)
121. Hopkins, A.M., De Laporte, L., Tortelli, F., Spedden, E., Staii, C., Atherton, T.J., et al.: Silk hydrogels as soft substrates for neural tissue engineering. Adv. Funct. Mater. **23**, 5140–5149 (2013)
122. Cheng, T.-Y., Chen, M.-H., Chang, W.-H., Huang, M.-Y., Wang, T.-W.: Neural stem cells encapsulated in a functionalized self-assembling peptide hydrogel for brain tissue engineering. Biomaterials **34**, 2005–2016 (2013)
123. Lin, Z., Cao, S., Chen, X., Wu, W., Li, J.: Thermoresponsive hydrogels from phosphorylated aba triblock copolymers: a potential scaffold for bone tissue engineering. Biomacromolecules **14**, 2206–2214 (2013)
124. Simson, J.A., Strehin, I.A., Allen, B.W., Elisseeff, J.H.: Bonding and fusion of meniscus fibrocartilage using a novel chondroitin sulfate bone marrow tissue adhesive. Tissue Eng. Part A **19**, 1843–1851 (2013)
125. Simson, J.A., Strehin, I.A., Lu, Q., Uy, M.O., Elisseeff, J.H.: An adhesive bone marrow scaffold and bone morphogenetic-2 protein carrier for cartilage tissue engineering. Biomacromolecules **14**, 637–643 (2013)
126. Takahashi, H., Matsuzaka, N., Nakayama, M., Kikuchi, A., Yamato, M., Okano, T.: Terminally functionalized thermoresponsive polymer brushes for simultaneously promoting cell adhesion and cell sheet harvest. Biomacromolecules **13**, 253–260 (2012)
127. Higuchi, A., Ling, Q.-D., Chang, Y., Hsu, S.-T., Umezawa, A.: Physical cues of biomaterials guide stem cell differentiation fate. Chem. Rev. **113**, 3297–3328 (2013)
128. Engler, A.J., Sen, S., Sweeney, H.L., Discher, D.E.: Matrix elasticity directs stem cell lineage specification. Cell **126**, 677–689 (2006)
129. Huebsch, N., Arany, P.R., Mao, A.S., Shvartsman, D., Ali, O.A., Bencherif, S.A., et al.: Harnessing traction-mediated manipulation of the cell/matrix interface to control stem-cell fate. Nat. Mater. **9**, 518–526 (2010)
130. Benoit, D.S., Schwartz, M.P., Durney, A.R., Anseth, K.S.: Small functional groups for controlled differentiation of hydrogel-encapsulated human mesenchymal stem cells. Nat. Mater. **7**, 816–823 (2008)
131. Singh, A., Zhan, J., Ye, Z., Elisseeff, J.H.: Modular multifunctional poly(ethylene glycol) hydrogels for stem cell differentiation. Adv. Funct. Mater. **23**, 575–582 (2013)
132. Mckee, S.: Pharma Times, UK News April 7 (2011)

Biodegradable Thermogelling Poly(Organophosphazenes) and Their Potential Biomedical Applications

Xiao Liu

Abstract Poly(organophosphazenes) as a new type of biodegradable polymers have been exploited as carriers for various drug delivery systems due to versatility of molecular structures and easily modulated physico-chemical properties. Thus, biodegradable thermogelling poly(organophosphazenes) are expected to be very promising biomaterials as injectable systems with minimal surgical intervention for drug delivery and tissue engineering applications. The key advantage of thermosensitive hydrogels based on poly(organophosphazenes) over other thermosensitive polymers is the ease of tuning the hydrogel properties by use of different compositions of side groups or through variations in co-substituent ratios. A variety of poly(organophosphazene) thermogels have been developed with desirable hydrophobic-hydrophilic balance, controllable degradation rate and suitable mechanical properties with respect to different applications. This chapter covers a comprehensive summary of the recent developments in this field of study, including polymer design, property assessment and potential biomedical applications.

Keywords Poly(organophosphazene) · Thermogels · Drug delivery · Biodegradable · In vivo

1 Introduction

Hydrogels as a potential controlled drug delivery system and biomedical device has been extensively studied over the past decade [1]. One of the more recent trends is the in situ formation of stimuli-sensitive hydrogels, which can undergo a simple reversible phase transition (sol-gel transition) with response to the external

X. Liu (✉)
Penn State Department of Chemistry, 104 Chemistry Building, University Park, PA 16802, USA
e-mail: liuxiaochem@gmail.com

X.J. Loh (ed.), *In-Situ Gelling Polymers*, Series in BioEngineering,
DOI 10.1007/978-981-287-152-7_3

stimuli such as temperature, pH, light, electromagnetic radiation and biomolecules [2–6]. Among the stimuli-sensitive hydrogels, the in situ forming hydrogels from reverse thermogelling biodegradable polymer aqueous solutions have attracted considerable interest, because pharmaceutical agents or cells can be premixed with specific thermogelling polymers as an aqueous solution (sol state) before administration but immediately transform to standing gels as a sustained drug delivery depot after injecting into a target site.

Reverse thermogelling polymers used to act as an effective injectable thermogel usually possess block architectures and a balanced structure of hydrophobicity and hydrophilicity. As temperature increases, the association of the polymers occurs due to increased hydrophobic interactions to show a temperature-sensitive sol-to-gel transition at a critical temperature, namely, lower critical solution temperature (LCST). Typical reverse thermogelling polymers include poly(N-substituted acrylamide)-based block copolymers [7–11], poly(vinyl ether)-based block copolymers, poly(ethylene oxide) (PEO)/poly(propylene oxide) (PPO)-based block copolymers [12–17] and PEG/polyester block copolymers [18–23]. The representative structures of each class are shown in Fig. 1. In most cases, PEG was used as a hydrophilic block. All the themogelling hydrogels formed from the amphiphilic block copolymers mentioned above exhibit a sol-gel phase-transition in the physiological conditions in a tunable manner and have been intensively studied in recent years.

Although thermosensitive hydrogels formed from aqueous solution of poly(N-isopropylacrylamide) (PNIPAM), poly(2-ethoxyethyl vinyl ether)-*b*-poly(2-methoxyethyl vinyl ether) (PEOVE-*b*-PMOVE) and poly(ethylene oxide)-*b*-poly(propylene oxide)-*b*-poly(ethylene oxide) (PEO-*b*-PPO-*b*-PEO)

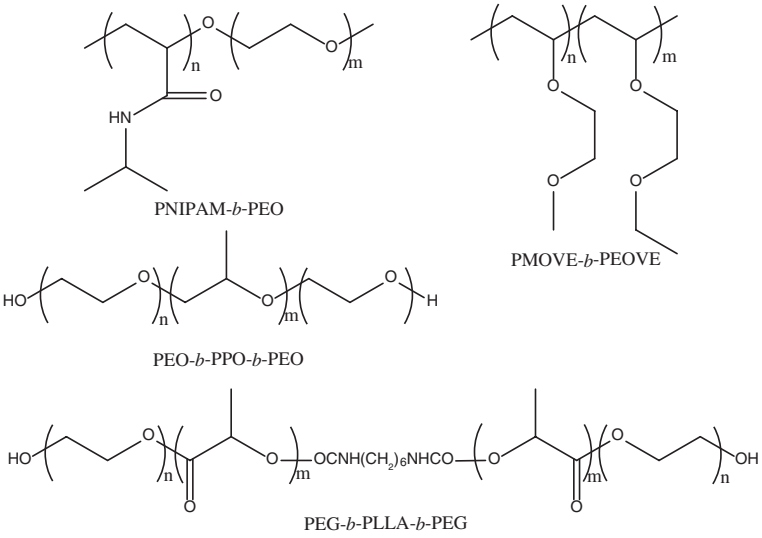

Fig. 1 Chemical structures of some temperature-sensitive block copolymers

(Pluronic^{TM}), have been reported to use for drug delivery and tissue engineering, most of these materials suffer from non-biodegradability, non-biocompatibility, toxicity, and poor mechanical properties [4, 20, 24, 25]. To address this issue, biodegradable reverse thermogelling polymers based on polyester and PEG, such as poly(ethylene glycol)-*b*-poly(L-lactic acid)-*b*-poly(ethylene glycol) (PEG-*b*-PLLA-*b*-PEG), were developed. [18, 20–23]. These novel thermogelling polymers exhibit multiple desired functionalities as ideal materials for injectable in situ forming hydrogels, including good biocompatibility, tunable drug release and degradation rate, improved mechanical properties and capability of encapsulating various drugs. However, the acidic degradation products from the polyester may cause tissue necrosis or irritation around the implant site as well as denaturation of the incorporated biopharmaceuticals. Therefore, there is still room for improving the current block copolymer hydrogels to meet the physiological and practical requirements.

As an alternative, poly(organophosphazenes) have been gaining significant attention in the biomedical field, because they can offer a number of crucial advantages for biological research and biomedical applications [26–28]. High molecular weight poly(organophosphazenes) are inorganic backbone polymers with an essentially linear backbone of alternating phosphorus and nitrogen atoms and two organic or organometallic side groups linked to each phosphorus atom [29–31]. Therefore, the polymer properties can be precisely tailored through changes in the side groups to optimize properties for specific biomedical applications. For example, hydrophobic poly(organophosphazenes) with fluoroalkoxy or aryloxy side groups have been evaluated as bioinert biomaterials for use in prosthetic blood vessels, artificial heart membranes, artificial heart valves, dental filling materials and soft denture liners [32–34]. On the other hand, a growing number of poly(organophosphazenes) have been designed specifically to be hydrolytically sensitive as biodegradable materials. Unlike polyesters, poly(organophosphazenes) can hydrolyze into nontoxic products, like phosphate, ammonium ion and free organic side groups, with near-neutral pH values [35]. The organic side groups of the hydrolytically sensitive poly(organophosphazenes) range from amino acid ester (**1**) [36–40], dipeptides (**2**) [41–44], depsipeptides (**3**) [45–47], to other benign or physiologically essential molecules (**4–6**) [48–54]. Several examples are shown in Fig. 2.

The objective of this chapter is to provide a comprehensive summary of the preparation and application of biodegradable reverse themogelling poly(organophosphazenes), including polymer design, property assessment and potential biomedical applications.

2 Design of Biodegradable Thermogelling Poly(Organophosphazenes)

By far the largest effort to construct biodegradable thermogelling poly(organophosphazenes) has been reported by Song and coworkers. The general molecular structures of these poly(organophosphazenes) consist of a short

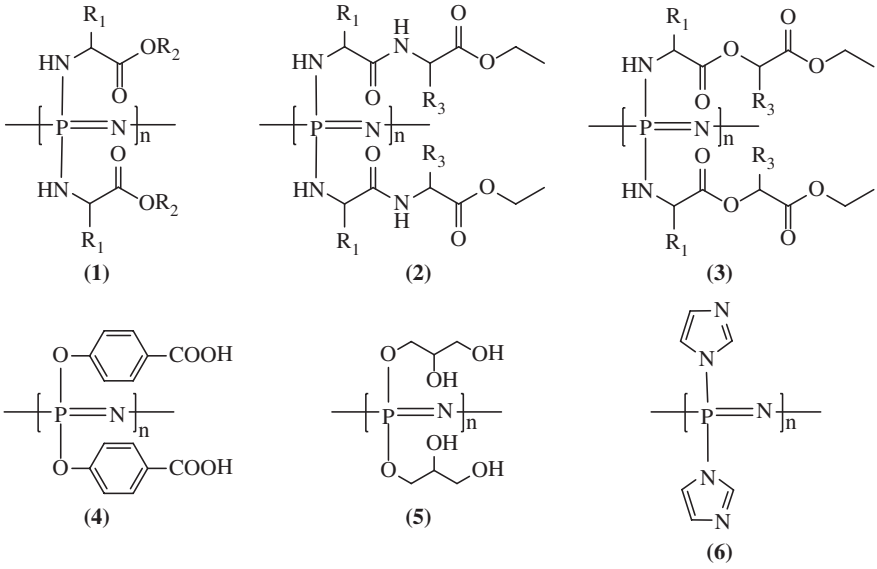

Fig. 2 Examples of biodegradable poly(organophosphazenes)

hydrophilic α-amino-ω-methoxy-poly(ethylene glycol) (AMPEG) segment with a molecular weight range of 350–750 Da and amino acid esters (such as Isoleucine ethyl ester [IleOEt] and leucine ethyl ester [LeuOEt]) [55–62], dipeptides (glycylglycine and glycylglycine ally ester) [63–67], depsipeptide (ethyl-2-(*O*-glycyl)glycolate and ethyl-2-(*O*-glycyl)lactate) [57, 60, 66–69] and oligopeptides (such as GlyPheLeuEt and GlyPheIleEt) [70] as both hydrophobic and hydrolysis-sensitive moieties. Examples of the molecular structures of biodegradable thermogelling poly(organophosphazenes) are shown in Table 1.

2.1 Synthetic Procedures

Several different synthetic routes are available for the synthesis of poly(organophosphazenes) [91–96], but the major method for the biodegradable thermogelling poly(organophosphzenes) involves a ring-opening polymerization followed by macromolecular substitution reactions as shown in Scheme 1 [55–63, 65, 66, 97, 98]. The thermal ring-opening polymerization of a commercially available cyclic trimer, hexachlorophosphazene (**7**), gives a high molecular weight poly(dichlorophosphazene) (**8**), which is an organic-soluble, reactive macromolecular intermediate with chlorine atoms that can be replaced with various organic nucleophiles (**9–11**).

Table 1 Biodegradable Thermogelling Poly(organophosphazenes)

Two cosubstituents: Amino Acid/PEG $[NP(NHCHR_1COOEt)(R_2)]_n$

Hydrophobic substituents	(R_1)	Hydrophilic substituents (R_2)	T_{LCST} (°C)	T_{max} (°C)	References
Isoleucine (IleuOEt)	$CH(CH_3)CH_2CH_3$	$NH(CH_2CH_2O)_7CH_3$ (AMPEG350)	37.0–74.0	29.0, 38.0	[61, 68]
		$NH(CH_2CH_2O)_{11}CH_3$ (AMPEG 550)	75.0	31.0–61.0	[55–57, 61, 66, 71–74]
		$NH(CH_2CH_2O)_{16}CH_3$ (AMPEG 750)	84.0	44.0–56.0	[56, 68, 71, 74]
Leucine (LeuOEt)	$CH_2CH(CH_3)_2$	$NH(CH_2CH_2O)_7CH_3$	40.0	34.0	[68]
		$NH(CH_2CH_2O)_{11}CH_3$	–	35.0, 40.0	[71, 75]
Valine	$CH(CH_3)_2$	$NH(CH_2CH_2O)_7CH_3$	54.0, 57.0	–	[55, 68]
		$NH(CH_2CH_2O)_{11}CH_3$	–	51.0–54.0	[56, 71, 75]

Two cosubstituents: Oligopeptide/PEG $[NP(NHCHR_1CONHCHR_3CONHCHR_4CONHCHR_5COOEt)(O(CH_2CH_2O)_7CH_3)]_n$

Hydrophobic substituent	(R_1)	(R_3)	(R_4)	(R_5)	T_{LCST} (°C)	T_{max} (°C)	References
Glycyl-phenylalanyl-leucine (GlyPheLeuEt)	H	$CH_2(C_5H_6)$	$CH_2CH(CH_3)_2$	–	30.0	25.0	[70]
Glycyl-phenylalanyl-isoleucine (GlyPheIleuEt)	H	$CH_2(C_5H_6)$	$CH(CH_3)CH_2CH_3$	–	39.0–50.0	28.0, 37.0	[70]
Glycyl-leucyl-phenylalanine (GlyLeuPheEt)	H	$CH_2CH(CH_3)_2$	$CH_2(C_5H_6)$	–	35.0, 42.0	30.0, 32.0	[70]
Glycyl-phenylalanyl-leucyl-glycine (GlyPheLeuGlyEt)	H	$CH_2(C_5H_6)$	$CH_2CH(CH_3)_2$	H	70.0	58.0	[70]

Three cosubstituents: Amino Acid/Depsipeptide/PEG $[NP(NHCHR_1COOEt)(NHCH_2COOCHR_3COOEt)(R_2)]_n$

Hydrophobic substituents	(R_1)	(R_3)	Hydrophilic substituents (R_2)	T_{LCST} (°C)	T_{max} (°C)	References
Isoleucine/ Ethyl-2-(*O*-glycyl)glycolate	$CH(CH_3)CH_2CH_3$	H	$NH(CH_2CH_2O)_7CH_3$	54.0	39.0	[68]
			$NH(CH_2CH_2O)_{11}CH_3$	75.0	48.0	[68]
			$NH(CH_2CH_2O)_{16}CH_3$	51.0, 87.0	28.0, 62.0	[68]
Isoleucine/ Ethyl-2-(*O*-glycyl)lactate (GlyLacOEt)	$CH(CH_3)CH_2CH_3$	CH_3	$NH(CH_2CH_2O)_7CH_3$	–	31.0–42.0	[57, 66, 67, 69, 74–87]
			$NH(CH_2CH_2O)_{11}CH_3$	–	41.0–57.0	[74, 86]

(continued)

Table 1 (continued)

Three cosubstituents: Amino Acid/Dipeptide/PGE [NP(NHCHR$_1$COOEt)(NHCH$_2$CONHCH$_2$COOR$_3$)(R$_2$)]$_n$

Hydrophobic substituents	(R_1)	(R_3)	Hydrophilic substituents (R_2)	T_{LCST} (°C)	T_{max} (°C)	References
Isoleucine/ Glycylglycine (GlyglyOH)	$CH(CH_3)CH_2CH_3$	H	$NH(CH_2CH_2O)_{11}CH_3$	31.0–64.0	21.8–59.0	[63–67, 74, 85, 88, 89]
			$NH(CH_2CH_2O)_{16}CH_3$	–	55.9	[89]
Isoleucine/Glycylglycine ally ester	$CH(CH_3)CH_2CH_3$	$CH_2CH{=}CH_2$	$NH(CH_2CH_2O)_{11}CH_3$	20.0–48.0	21.8–46.9	[88, 89]
			$NH(CH_2CH_2O)_{16}CH_3$	–	42.9, 52.9	[89]

Three cosubstituents: Amino Acid/Amino Acid/PEG [NP(NHCHR$_1$COOEt)(NHCHR$_3$COOR$_4$)(R$_2$)]$_n$

Hydrophobic substituents	(R_1)	(R_3)	(R_4)	Hydrophilic substituents (R_2)	T_{LCST} (°C)	T_{max} (°C)	References
Isoleucine/Glycine	$CH(CH_3)CH_2CH_3$	H	H	$NH(CH_2CH_2O)_{11}CH_3$	–	36.8	[74]
Leucine/Lysine	$CH_2CH(CH_3)_2$	$(CH_2)_4NH_2$	Et	$NH(CH_2CH_2O)_7CH_3$	65.0	48.0	[90]
Phenylalanine/Lysine	$CH_2(C_5H_6)$	$(CH_2)_4NH_2$	Et	$NH(CH_2CH_2O)_7CH_3$	55.0	31.0	[90]
Isoleucine/Lysine	$CH(CH_3)CH_2CH_3$	$(CH_2)_4NH_2$	Et	$NH(CH_2CH_2O)_7CH_3$	60.0	45.0	[90]
				$NH(CH_2CH_2O)_{11}CH_3$	85.0	64.0	[90]
				$NH(CH_2CH_2O)_{16}CH_3$	>100	78.0	[90]

Four cosubstituents: Amino Acid/Amino Acid/Depsipeptide/PEG [NP(NHCHR$_1$COOEt))(NHCHR$_3$COOR$_4$) (NHCH$_2$COOCH$_2$COOEt)(R$_2$)]$_n$

Hydrophobic substituents	(R_1)	(R_3)	(R_4)	Hydrophilic substituents (R_2)	T_{LCST} (°C)	T_{max} (°C)	Reference
Isoleucine/Lysine	$CH(CH_3)CH_2CH_3$	$(CH_2)_4NH_2$	Et	$NH(CH_2CH_2O)_{11}CH_3$	43.0	35.0	[90]

Notes Et Ethyl, T_{LCST} Phase transition temperature, T_{max} The temperature at which the polymer solution reach their maximum viscosity

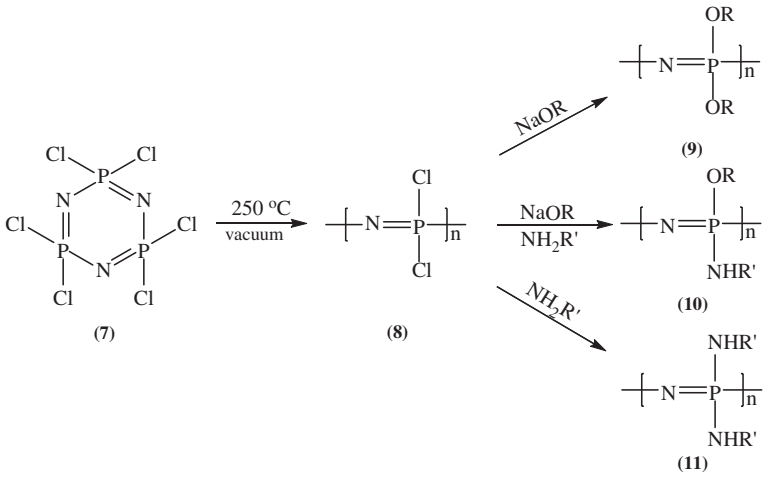

Scheme 1 Synthetic route of poly(organophosphazenes)

The significant difference between poly(organophosphazenes) and other polymers from the synthetic point of view lies in the introduction of side groups after the polymer backbone is assembled. Thus, this macromolecular substitution allows the introduction of side groups that may not survive a polymerization reaction. Also, properties can be controlled by use of different compositions of side groups or through variations in co-substituent ratios [99]. For example, poly(organophosphazenes) bearing isoleucine ethyl ester (IleOEt) and α-amino-ω-methoxy-poly(ethylene glycol) with molecular weight of 350 (AMPEG350), $NP[(IleOEt)_x(AMPEG350)_{2-x}]_n$, one of the typical structures of the biodegradable thermogelling poly(organophosphazenes) [61, 68], are synthesized by introducing the first nucleophile (IleOEt) while the progress of the reaction is being monitored by NMR techniques. After complete reaction of the first nucleophile, an excess of the second nucleophile (AMPEG350) is added to complete the halogen replacement. The composition of the final products can be easily and precisely controlled by using different feeding ratio of IleOEt and AMPEG350, leading to a series of $NP[(IleOEt)_x(AMPEG350)_{2-x}]_n$ with x from 0.87 to 1.45. In addition, three or four co-substituents can be introduced into the same poly(organophosphazene) in order to finely tune the properties as shown in Table 1. Therefore, the mechanical properties, biodegradability, and LCST can be controlled by varying the co-substituents, which will be discussed in the following sections.

The biodegradable thermogelling poly(organophosphazenes) have a molecular weight of about several 10^4 kDa, much lower than the molecular weight of poly(alkoxy or aryloxyphosphazenes) which are usually above a million kDa [100, 101]. The reason is that the introduction of amino side groups involves the release of hydrogen chloride. Although a strong base such as triethylamine is used in order to remove the hydrogen chloride generated, the released hydrogen

Table 2 Thermosensitive cyclotriphosphazenes $N_3P_3(NHCHR_1COOR_3)_3(R_2)_3$

Hydrophobic substituent	(R_1)	(R_3)	Hydrophilic substituent (R_2)	T_{LCST} (°C)	References
Glycine	H	Et	$O(CH_2CH_2O)_2CH_3$	>100	[59]
		Bz	$O(CH_2CH_2O)_2CH_3$	10.5	[59, 105]
			$O(CH_2CH_2O)_7CH_3$	65.5	[59, 105]
Aminomalonic acid	COOEt	Et	$O(CH_2CH_2O)_7CH_3$	95.0	[59]
L-Aspartic acid	CH_2COOEt	Et	$O(CH_2CH_2O)_2CH_3$	47.5	[59, 105]
			$O(CH_2CH_2O)_7CH_2CH_3$	21.5	[59]
			$O(CH_2CH_2O)_7CH_3$	83.0	[59, 105]
		Bz	$O(CH_2CH_2O)_7CH_3$	42.5	[59, 105]
			$O(CH_2CH_2O)_{11}CH_3$	69.0	[59, 105]
			$O(CH_2CH_2O)_{16}CH_3$	78.5	[59, 105]
L-Glutamic Acid	$(CH_2)_2COOEt$	Et	$O(CH_2CH_2O)_2CH_3$	30.0	[59]
			$O(CH_2CH_2O)_7CH_3$	73.0	[59]

Notes Bz Benzyl

chloride may still be able to coordinate to the backbone nitrogen atom and decompose the polymer backbone, leading to a decreased molecular weight [50, 52]. Nevertheless, the biodegradable thermogelling poly(organophosphazenes) still have much higher molecular weight than most of currently used biodegradable thermogelling block copolymers, which will give poly(organophosphazenes) more flexibility in molecular structure design over other polymer systems.

Another interesting and unique feature of the synthesis of poly(organophosphazenes) is that reaction conditions on polymers can be studied and optimized by using small molecules, cyclotriphosphazenes, as model compounds, due to its structural similarity with polyphosphazene, but more well-defined molecular structures [44, 49, 53, 102]. This model study will provide better understanding of more complicated and challenging reactions carried out later on polymer side groups. Therefore, a series of thermosensitive cyclotriphosphazenes bearing various amino acid and PEG segments were synthesized and their properties, such as LCST, degradation rate and ability as drug release carriers, were studied [59, 103–106]. However, no thermogelling behaviour was observed for all of the thermosensitive trimers. Examples of thermosensitive cyclotriphosphazenes are shown in Table 2.

2.2 Thermosensitivity and Thermogelling Behaviour

The temperature-based responsive behavior of poly(organophosphazenes) were found by using several different functional side groups as shown in Fig. 3. The first thermosensitive poly(organophosphazene) exhibiting LCST in aqueous

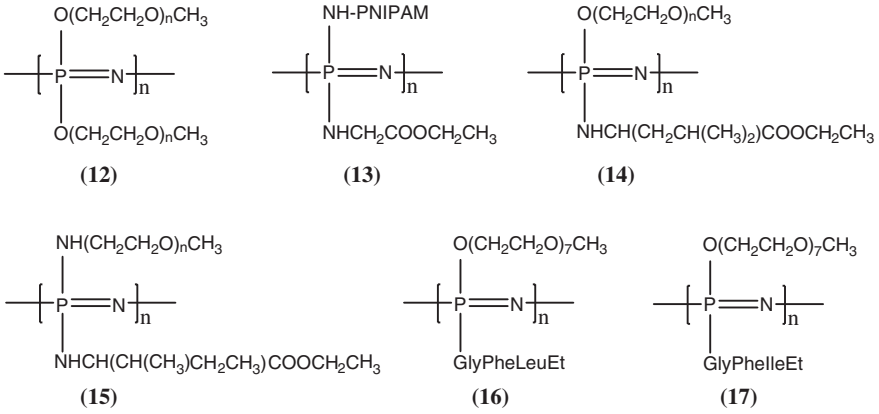

Fig. 3 Examples of thermosensitive poly(organophosphazenes)

media derived from polymers containing alkyl ether with varying chain length (**12**) [107–109]. However, chemical crosslinking by gamma radiation or ultraviolet irradiation was necessary in order to form thermo-responsive hydrogels. Later, an amphiphilic graft poly(organophosphazene) containing PNIPAM as hydrophilic segments and amino acid ester as hydrophobic parts with LCST 32.6 ºC was synthesized (**13**) [110–112]. Above its LCST, nanoparticles from the aggregation of self-assembled micelles were formed, which showed the potential as injectable carriers for the delivery of hydrophobic compounds. Furthermore, the authors report that the poly(organophosphazenes) do not degrade significantly during the time-frame of the release experiments, which may limit their biomedical applications in human body [112]. Continued efforts to develop thermosensitive poly(organophosphazenes) led to the discovery of a series of cyclic trimers [59, 103–106] and polymers [55, 58, 62, 113, 114], a) bearing mono-methoxy-poly(ethylene glycol) (MPEG) and amino acid (**14**) or depsipeptide ester as shown in Tables 2 and 3. All the cyclic trimers and polymers showed a LCST in range of 21.5–98.5 ºC, depending on the kinds of amino acid, length of MPEG and the mole ratio of the two substituents. The effect of salts, solvents, and surfactants on the LCST was studied in detail [15, 58, 114]. Nevertheless, no formation of reverse thermogelling hydrogels was reported from both cyclic trimers and polymers mentioned above, which exhibited sol-precipitation behavior upon exposure to an increased temperature.

The ability to impart a reverse themosensitive response sol-gel transition as a function of temperature in poly(organophosphazenes) was first developed by Song and coworkers with a typical structure of **15**, $NP[(IleOEt)_x(AMPEG350)_{2-x}]_n$ [61]. Typically, an aqueous solution of **15** with a concentration of 10 wt% exhibited four-phase transitions with temperature gradually increasing: a transparent sol, a transparent gel, an opaque gel, and a turbid sol as illustration in Fig. 4. As x increased from 0.55 to 1.13, the LCST of **15** decreased from 74 to 37 ºC,

Table 3 Thermosensitive Poly(organophosphazenes)

Two cosubstituents: Amino Acid/PEG $[NP(NHCHR_1COOR_3)(R_2)]_n$					
Hydrophobic substituent	(R_1)	(R_3)	Hydrophilic substituent (R_2)	T_{LCST} (°C)	References
Glycine (GlyOEt)	H	Me	$O(CH_2CH_2O)_7CH_3$	88.5	[58, 62, 114, 115]
		Bz	$O(CH_2CH_2O)_7CH_3$	49.5	[58, 62, 114, 115]
		Et	$O(CH_2CH_2O)_7CH_3$	35.0–93.2	[58, 62, 114, 115]
			$O(CH_2CH_2O)_{16}CH_3$	98.5	[62, 114, 115]
			$NH(CH_2CH_2O)_7CH_3$	62.0, >100	[113]
Alanine	CH_3	Et	$O(CH_2CH_2O)_7CH_3$	67.0	[58, 62]
			$NH(CH_2CH_2O)_7CH_3$	58.0, >100	[113]
Aminomalonic acid	COOEt	Et	$O(CH_2CH_2O)_7CH_3$	65.5	[58, 62]
Aspartic acid	CH_2COOEt	Me	$O(CH_2CH_2O)_7CH_3$	84.3	[62]
		Bz	$O(CH_2CH_2O)_7CH_3$	33.8	[62]
		Et	$O(CH_2CH_2O)_7CH_3$	38.5–60.2	[58, 62, 114]
			$O(CH_2CH_2O)_{16}CH_3$	60.2–75	[62, 115]
			$NH(CH_2CH_2O)_7CH_3$	38.5,61.5	[113]
Glutamic Acid	$(CH_2)_2COOEt$	Et	$O(CH_2CH_2O)_7CH_3$	25.2–66.5	[62]
			$NH(CH_2CH_2O)_7CH_3$	32.0,43.0	[113]
			$NH(CH_2CH_2O)_{16}CH_3$	79.0	[113]
β-Alanine	CH_3	Et	$O(CH_2CH_2O)_7CH_3$	70.3	[58, 114]
			$NH(CH_2CH_2O)_7CH_3$	65.0, >100	[113]

Three cosubstituents: Amino Acid/Amino Acid/PEG $[NP(NHCHR_1COOEt)(NHCHR_3COOR_4)(R_2)]_n$						
Hydrophobic substituents	(R_1)	(R_3)	(R_4)	Hydrophilic substituent (R_2)	T_{LCST} (°C)	Reference
Glycine/Glutamic acid	H	$(CH_2)_2COOEt$	Et	$O(CH_2CH_2O)_7CH_3$	53.6	[62]

Three cosubstituents: Amino Acid/Depsipeptide/PEG $[NP(NHCHR_1COOEt)(NHCH_2COOCHR_3COOEt)(R_2)]_n$					
Hydrophobic substituents	(R_1)	(R_3)	Hydrophilic substituent (R_2)	T_{LCST} (°C)	References
Glycine/Ethyl-2-(*O*-glycyl)glycolate	H	H	$O(CH_2CH_2O)_7CH_3$	64–70	[60]
Glycine/Ethyl-2-(*O*-glycyl)lactate	H	CH_3	$O(CH_2CH_2O)_7CH_3$	66	[60]

Note Me Methyl

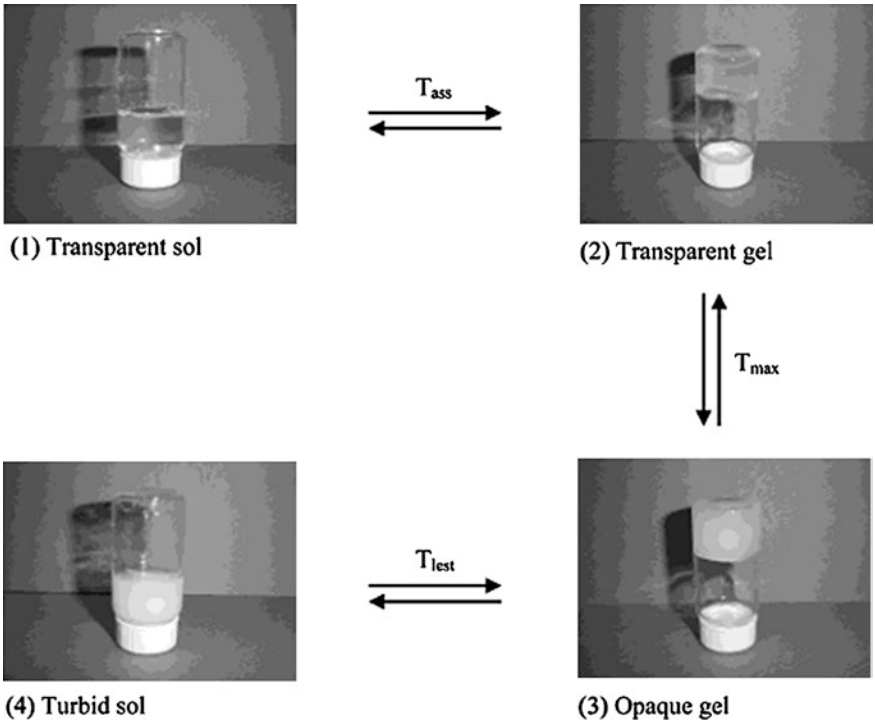

Fig. 4 Demonstration photograph of the sol-gel transition of polymer 15 in aqueous solution observed as temperature gradually increased. Reproduced with permission from Ref. [51]

indicating that the more hydrophobic composition of the polymers offers the lower LCST. In addition, it was found that polymers with more hydrophobic amino acid esters side groups exhibited stronger gelation properties [68]. It is interesting and noteworthy that a small change in the structure can develop a large change in the transition temperature. For example, the only difference between **16** and **17** is the terminal amino acid, leucine and isoleucine. However, they showed remarkable difference both in gelation temperature (15 and 32 ºC) and viscosity (56.1 and 73.5 Pas) [70]. Therefore, the gelation properties of the gels can be easily controlled by changing the composition of substituents, the chain length of AMPEG and the type of amino acid esters. The authors proposed that the formation of hydrogel is due to the hydrophobic interaction between the side chain fragments of amino acid esters, acting as a physical junction in the aqueous solution [68].

Besides the molecular structure, the sol-to-gel transition properties are also affected by several other factors, such as salts, pH, and blending. For example, the association temperature (T_{ass}) and the temperature at the maximum viscosity (T_{max}) of poly(organophosphazene) thermogels shifted to lower temperature in the presence of inorganic salts, such as NaCl, KCl, NaBr, and LiCl, while the gel strength was greatly augmented as well by increasing the density of physical junctions. In contrast, organic salts dramatically increased the gelation temperature,

which is attributed to hydrophobic interactions between the tetralkyl groups of organic salts and the non-polar side groups of the polymers, leading to ionization of the side groups [56, 71, 88]. Furthermore, the gelation property of poly(organophosphazenes) also depends greatly on pH. As the pH decreased from 7.4 to 3.9, the V_{max} (the viscosity of the polymer solutions at T_{max}) of a neutral polymer significantly decreased and the T_{max} of the polymer increased [68, 89]. This is due to a change in hydrophilic-hydrophobic balance by protonation in amine groups. On the other hand, the opposite trend was observed when carboxylic acid groups were present in a thermogelling poly(organophosphazene). This is due to the fact that the acidic polymer becomes almost completely neutral at lower pH due to the protonation of carboxylic acid groups [88, 89]. Moreover, gelation behavior, as well as the physical properties of thermogelling poly(organophosphazenes), can be also controlled by adjusting the hydrophobic-hydrophilic balance after polymerization through the blending of polymers [57, 75, 86]. By blending polymer **15** and [NP(Ile OEt)$_{1.07}$(GlyLacOEt)$_{0.02}$(AMPEG550)$_{0.91}$]$_n$ with a blend ratio of 3 to 1, a transparent hydrogel with T_{max} at 37 ºC and good gel strength (V_{max} > 200 Pas) was achieved, which could be effectively utilized as a locally injectable hydrogel. On the contrary, none of each component exhibited efficient viscosity at 37 ºC individually [57].

2.3 Biodegradability and Hydrolysis Mechanism

Poly(organophosphazenes) have long been found to be sensitive to hydrolysis by incorporating hydrolytically sensitive side groups as illustrated in Fig. 2, of which amino acid containing poly(organophosphazenes) resulted in many biodegradable materials for various biomedical applications [36, 45, 116–125]. Thus, one of the main reasons for understanding the mechanisms of hydrolysis of biodegradable poly(organophosphazenes) is to study the possible toxic intermediates or end products formed during hydrolysis.

Studies have shown that degradation rate of thermosensitive poly(organophosphazenes) can be controlled over periods of days to months by using different hydrophobic moieties, such as amino acid, depsipeptide and dipeptide, adjusting length of PEG segments and varying the co-substituent composition. Poly(organophosphazenes) containing glycine ester and MPEG, for an instance, showed a decreased degradation rate in the order of methyl > ethyl > benzyl esters [58]. Polymers substituted with α-amino acid esters hydrolyzed faster than that with β-amino acid ester. Also, a more rapid hydrolysis occurred in both acidic and basic buffer solutions than in the neutral solution [58]. Additionally, degradation rate can be accelerated significantly by either incorporating depsipeptide ethyl esters or switching from MPEG to AMPEG segments [60, 68, 90, 113]. The polymers with depsipeptide ethyl esters had half-lives of less than 10 days at pH 7 and 37 ºC, while the polymers without depsipeptide ethyl ester, had a half-life over 40 days [60]. On other hand, the half-lives of [NP(GlyOEt)$_{0.94}$(AMPEG350)$_{1.06}$]$_n$ at pH 5, 7.4 and 10 were 9, 16 and 5 days,

respectively, which are almost 2.5 to 4 times faster than that of the MPEG-based polymers [113].

Therefore, the hydrolytic degradation of these thermosensitive poly(organophosphazenes) has been explained in terms of carboxylic acid-catalyzed degradation mechanism as shown in Scheme 2 [58, 68, 74, 89, 90]. Initially, free carboxylic acid groups are generated by hydrolysis of amino acid ester or depsipeptide ester. Then, these resultant carboxylic acid groups can attack the same or an adjacent phosphazene chain to induce phosphorus-nitrogen skeletal cleavage. This mechanism explains the faster degradation rate of depsipeptide ester bearing poly(organophosphazenes), because it has been reported that depsipeptide ethyl ester is more hydrolytically labile than amino acid ethyl ester [37, 38], resulting in more rapid release of free carboxylic acid. This mechanism was also proved by the comparison of the degradation behavior of neutral and acidic poly(organophosphazene) gels bearing carboxylic acid group [74, 89]. The accelerated hydrolysis rate of the thermogelling poly(organophosphazenes) was observed in the order of without carboxylic acid and depsipeptide < depsipeptide < carboxylic acid both in vitro and in vivo [74], indicating the carboxylic acid-facilitated degradation. The poly(organophosphazene) bearing only IleOEt and AMPEG550, $[NP(IleOEt)_{1.16}(AMPEG550)_{0.84}]_n$, maintained 89 % of its original molecular weight after 45 days in the physiological conditions. In contrast, the molecular weight of the polymer containing carboxylic acid, $[NP(IleOEt)_{1.25}(GlyGlyOH)_{0.30}(AMPEG550)_{0.45}]_n$, was rapidly decreased to 38 % of the original molecular weight after 3 days. Hence, these biodegradable thermogelling poly(organophosphazenes) hold great potential as an injectable biodegradable hydrogel for biomedical application with controllable degradation rate.

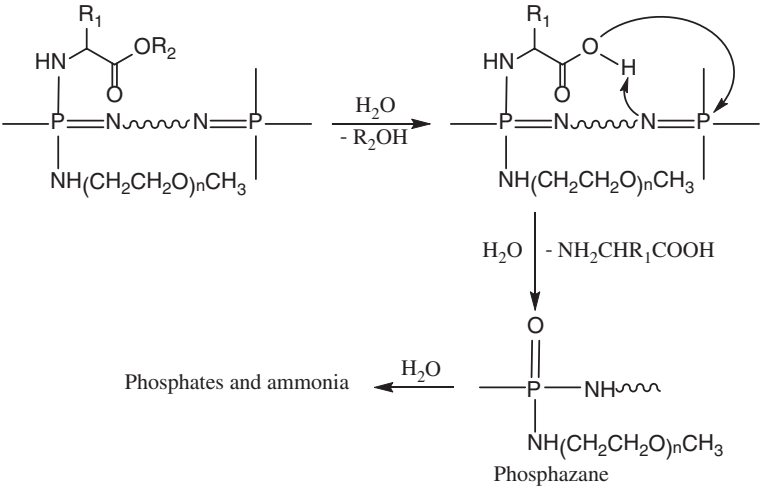

Scheme 2 Hydrolysis mechanism for thermosensitive poly(organophosphazenes)

3 Applications of Biodegradable Thermogelling Poly(Organophosphazenes)

Biodegradable thermogelling poly(organophosphazenes) have been widely used in various biomedical applications. According to the discussion in the previous sections, one of the advantages of this system over other currently used thermogelling polymers as injectable in situ forming hydrogels lies on their convenient tunability of properties depending on different applications by adjusting the type of hydrophobic moieties, the length of hydrophilic segments and the composition of substituents. Also, post modification of poly(organophosphazenes) backbone is possible by introducing additional functional groups during the macromolecular substitution, which will render the biodegradable thermogelling poly(organophosphazenes) more flexibility in designing multifunctional thermosensitive hydrogel. In this section, applications of the reverse thermogelling system based on poly(organophosphazenes) for drug delivery, bioimaging and tissue engineering will be reviewed.

3.1 Delivery of Antitumor Drugs

A new drug delivery system (DDS) based on biodegradable thermogelling poly(organophosphazenes) was developed for intratumoral delivery of chemotherapeutic agents in order to provide drug localization within the tumor and divert the drug from non-target organs to reduce toxicity and increase efficacy (Fig. 5). Hydrogels formed from poly(organophosphazenes) bearing hydrophobic IleOEt and hydrophilic AMPEG550 along with hydrolysis-sensitive GlyLacOEt (**18**) were found to be excellent solubilisers of hydrophobic antitumor drug, doxorubicin, compared with that in phosphate buffered saline (PBS, 0.01 M, pH 7.4) [80]. The aqueous polymer solution with doxorubicin showed a sol-gel transition at physiological conditions. The release of doxorubicin from the hydrogel system was significantly sustained over 20 days. The anticancer efficacy of the released doxorubicin was constant over a prolonged period of times for more than 30 days, when the P388D1 mouse lymphoblast cell line was evaluated. In another study, the doxorubicin-loaded hydrogels based on the same poly(organophosphazenes) (**18**) was evaluated on the human gastric cancer cell line, SNU-601 for their anticancer efficacy [76]. A sustained release was observed from the formulation of 10 % w/w of hydrgel and 0.6 % w/w of doxorubicin with 40 and 90 % released over 5 weeks in vitro and in vivo. The hydrogel mass was well retained over 7 weeks and exhibited excellent local tumor control with a slight initial burst when used intratumorally. In addition, the anticancer efficacy of doxorubicin load in the same hydrogels was also evaluated using the human gastric cancer cell line, HSC44Luc within Balb/c female nude mice [84]. The suppressive effects of doxorubicin-loaded hydrogels on tumor growth were evaluated by means of in vivo

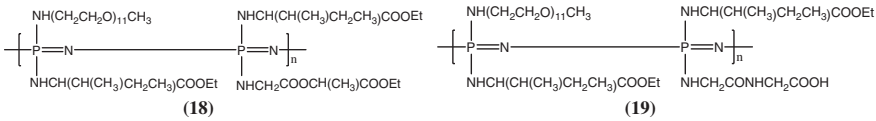

Fig. 5 Chemical structures of thermogelling poly(organophosphazenes) for drug delivery

bioluminescence, a more sensitive method for measuring tumor load. The study showed tumor growth was suppressed much more effectively among mice treated with polymer gel loaded with a dose of doxorubicin (30 mg/kg) compared with those given intravenous doxorubicin (15 mg/kg). The results indicated that local intratumoral delivery of doxorubicin with a large dose can be performed by using poly(organophosaphazenes) thermogels, while restricting its biodistribution to tumor tissue and reducing systemic exposure and toxicity.

Another widely used antineoplastic drug is paclitaxel. It has been shown to exhibit a significant activity against various solid tumors. However, due to its hydrophobicity, paclitaxel shows very poor solubility in water and has hypersensitivity reactions associated with its formulation, containing Chremophor^{TM} EL and ethanol [126]. Therefore, an injectable DDS based on poly(organophosphazenes) thermgels was developed for the local delivery of paclitaxel. Paclitaxel-loaded hydrogel based on polymer **18** was injected into six-week-old female Balb/c nude mice with the HSC44Luc human gastric cancer cell line [87]. The study showed that a hydrogel combined with paclitaxel (15 mg/kg) was a more effective treatment for peritoneal carcinomatosis than PBS or hydrogel alone in a mouse model. Although a paclitaxel solution had a similar antitumor effect, sever side effects were observed with a higher drug load (30 mg/kg). Furthermore, both human colorectal cancer cell line, DLD-1, and humane gastric cancer cell line, SNU-601 were also used to evaluate the antitumor efficacy of paclitaxel-loaded hydrogel (**18**). The in vitro and in vivo release of the formulation with 0.6 % w/w drug and 10 % w/w hydrgel were found to be 40 and 90 % of the dose over 4 weeks with a sustained manner [83]. The local tumor was well controlled for 42 days with a slight initial burst when used intratumorally. Therefore, a poly(organophosphazene) hydrogel mixed with anticancer drug, paclitaxel may be a safe and effective treatment for patients with peritoneal carcinomatosis.

Several other anticancer drugs were also evaluated for their effect on the properties of thermogels, release profile, antitumor efficacy in both in vitro and in vivo. The polymer solution of **18** can dramatically enhance the solubility of anticancer drug, 5-fluorouracil from 3.39 mg/ml in PBS (pH 7.4, 4 ºC) up to 34.26 mg/ml [66]. An increased T_{max} and a decreased V_{max} were observed for the 5-fluorouracil loaded hydrogel. According to the study, the release mechanism of 5-fluororacil from poly(organophosphazene) hydrogels was only a diffusion-controlled drug release. Besides, a prolonged release profile can be achieved by using poly(organophosphazenes) with higher content of AMPEG, due to the hydrophilic interaction between 5-fluorouracil and AMPEG segments. Additionally, polymer **18** was also used to enhance the bioavailability of the antitumor drug,

2-methoxyestradiol [77]. A 10 % polymer solution significantly increased the solubility of 2-methoxyestradiol by about 10^4 times compared to that of PBS solution. In the in vitro release study, the release mechanism of 2-methoxyestradiol was mainly dominated by diffusion, hydrophobic interaction, and surface erosion of the matrix. The in vivo antitumor activity of 2-methoxyestradiol-loaded hydrogels was evaluated by using MDA-MB-231 cell in six-week-old Balb/c nude female mice. It was found that the hydrogel loaded with 15 mg/kg 2-methoxyestradiol showed the improved antitumor over 4 weeks and antiangiogenic activity relatively to the original formulation. Similar studies were also conducted on another anticancer drug, silibinin, using thermosensitive hydrogels based on polymer **18** as matrix [78]. The aqueous solution of polymer **18** enhanced the solubility of silibinin (0.0415 g/ml) up to 2,000 times, compared with that of PBS (84.55 mg/ml). In the in vitro degradation study, about 80 % of the hydrogel was degraded in pH 6.8 media in a month, which was faster than the hydrogel in pH 7.4 with 40 % degradation over 4 weeks. In the in vivo anticancer activity evaluation, the silibinin-loaded hydrogel with a drug concentration of 10 mg/kg showed the inhibition effect of cancer growth for 40 days just with a single intratumoral injection. Hence, thermosensitive hydrogel based on poly(organophosphazenes) exhibit the diversity and feasibility on several different anticancer drugs as an efficient injectable local DDS.

In contrast to the drug release formulation formed by physical mixture between polymer solution and drugs, a poly(organophosphazene)-drug conjugate hydrogel has been developed as an improvement for locally controlled delivery of cancer therapeutics [63, 64, 84]. An additional functional group, through which a target anticancer drug can be conjugated in the post modification onto polymer, can be easily introduced on poly(organophosphazene) backbones during macromolecular substitution reaction. In this way, improved solubility of hydrophobic drugs, desirable pharmacokinetics, and enhanced antitumor activity can be achieved. Also, multidrug resistance (MDR) will be overcome through slow drug release and an enhanced permeation and retention (EPR) effect because of the accumulation of the polymer-drug conjugate within solid tumors [127, 128]. For example, the doxorubicin-poly(organophosphazene) conjugates were synthesized through the conjugation of doxorubicin with free carboxylic acid on polyphosphazene backbone (**19**) [63]. The resultant conjugates aqueous solution exhibited a sol-gel transition at body temperature by tuning the hydrophilic-hydrophobic balance through the composition of co-substituents. Based on the in vivo antitumor activities of the locally injected conjugate, the conjugate hydrogel (44.5 mg/kg) showed effective tumor growth inhibition for a prolonged period over 28 days, indicating the active doxorubicin was released slowly and effectively accumulated locally in the tumor sites. In addition, polymer **19** was also utilized to form poly(organophosphazene)-paclitaxel conjugate by a covalent ester linkages between paclitaxel and carboxylic acid on polymer backbone [64]. The conjugates showed a faster degradation and release profile in acidic condition (pH 6.8) than in neutral condiction (pH 7.4). The internalized poly(organophosphazene)-paclitaxel conjugate by tumor cells will be released intracellularly after exposure to lysosomal enzymes or lower pH (4.0–6.5)

in the endosomes and lysosomes. From the in vivo antitumor activity studies, the conjugate hydrogels were shown to inhibit tumor growth over 20 days, which was more effectively and longer than paclitaxel and saline alone.

3.2 Human Growth Hormone Delivery

Human growth hormone (hGH) used for growth stimulation and cell reproduction is one of the major protein drugs for treatment of short stature caused by growth hormone deficiency and growth failure due to Turner syndrome or chronic renal failure [129]. However, due to its poor absorbability in the gastrointestinal tract and short half-life in vivo, a daily administration by injection is necessary, leading to poor patient compliance and renal toxicity [130]. In order to solve the problems associated with the current hGH release systems, such as low loading efficiency, high initial burst release, protein aggregation, denaturation and inflammation [131], an injectable and biodegradable thermogel based on poly(organophosphazenes) loaded with polyelectrolyte drug complex has been developed and investigated for its controlled and sustained delivery of hGH to improve patient compliance [69]. The aqueous solution of polymer **18** containing polyelectrolyte complex formed between poly-L-arginine (PLA) and hGH showed a sol-gel transition at 37 ºC. In the in vitro release study, all polyelectrolyte complex loaded hydrogels exhibited a slower release rate than the hydrogels with hGH alone. Zinc increased the released amount of hGH from hydrogels for both in vitro and in vivo studies. The single administration of the hydrogel loaded with polyelectrolyte complex in male Sprague-Dawley rats with a dose of 1.1 mg/kg, resulted in sustained release of hGH for 5 days. For the purpose of more prolonged hGH release profile in human body, a dual ionic interaction system was developed by introducing carboxylic acid groups in poly(oganophosphazene) side groups (structure **19**) [85]. A positively charged polyelectrolyte complex was formed between hGH and protamine sulfate, the size of which can be adjusted by using varying ratio of each component. Later, an additional ionic interaction between the positively charge polyelectrolyte complex and anionic poly(organophosphazenes) was induced in the thermosensitive hydrogels. The resultant hydrogels suppressed the initial burst release of hGH and extended the release period in vitro and in vivo. In the in vivo efficacy study, a significantly increased growth rate for 7 days was observed by single injection of polyelectrolyte complex loaded anionic hydrogel, compared to daily injection of hGH solution. The results showed that the introduction of additional ionic interaction between polyelectrolyte complex and polymer matrix highly improved the bioavailability of hGH and an increased released manner.

As an alternative method, the release period of hGH can be efficiently increased by forming polyelectrolyte complex with cationic poly(organophosphazene) hydrogels. The positive charge can be introduced by modification of carboxylic

acid groups on poly(organophosphazene) backbone through covalent linkage. Protamine was conjugated to polymer **19** by an amide linkage [67]. The aqueous solution of the cationic polymer conjugates formed a gel at 37 ºC regardless of hGH presence. The release studies showed that the hGH loaded hydrogel based on poly(organophosphazene)-protamine conjugate had a prolonged release period and the initial burst release was significantly suppressed. In the in vivo pharmacokinetic and pharmacodynamic studies, an elevated plasma level of hGH was induced by a single administration of hGH-loaded hydrogel until 5 days as well as an increased plasma level of insulin-like growth factor-1 until 13 days. With the same concept, polyethylenimine (PEI) was also conjugated on polymer **19** to form cationic poly(organophosphazene)-PEI conjugates [86]. However, it was reported that a single administration showed equivalent efficacy with only four days' daily administration of hGH solution alone.

3.3 Long-Term Magnetic Resonance Contrast Platform

Poly(organophosphazene) thermogels have been utilized as a novel platform for a long-term imaging system, such as magnetic resonance imaging (MRI) due to their injectability, biodegradability, localizability, and sustainability [79, 81, 82]. Thus, it is not compulsory for the intravenous administration of the contrast agents every time due to the short half-life of the agents in vivo when a medical imaging diagnosis or a theragnosis is performed. A thermosensitive and magnetic hydrogel comprising cobalt ferrite ($CoFe_2O_4$) nanoparticles as contrast agents and hydrogels based on polymer **18** was designed for long-term magnetic resonance imaging [81]. The magnetic hydrogel showed extremely low cytotoxicity and adequate magnetic properties for use in long-term MRI. Approximately 70 % weight loss of the magnetic hydrogel was observed over 28 days in vitro. In the in vivo study, the applicable potentiality as a long-term MR contrast platform was successfully estimated over 4–5 weeks. Later, a long-term theranostic hydrogel based on polymer **18**, but with longer AMPEG segment, specifically designed for solid tumors was developed by cooperating both cobalt ferrite nanoparticles and paclitaxel [82]. The resultant hydrogel had an approximately 70 % weight loss at the twenty-eight day. About 71.16 ± 13.34 % of paclitaxel and 93.68 ± 1.06 % of iron in the theranostic hydrogel were released in vitro. In the in vivo test of the theramostic hydrogel in solid tumor-bearing nude mice, the increase of tumor volume was suppressed between the second and third week. Simultaneously, the long-term MR imaging was also accomplished for the same periods. In addition, the same magnetic hydrogel but with a different anticancer drug, 7-ethyl-10-hydroxycamptothecin, was used as MRI-monitored long-term therapeutic hydrogel for brain tumors [79]. The hydrogel can be injected into the area of brain tumor stereotactically within a very small-sized pin hole to minimize the drawbacks of surgical treatments.

3.4 Gene Delivery

Localized release of plasmid DNA or polymer/DNA complexes was performed by using biodegradable thermogelling hydrogels of poly(organophosphazenes) as release matrices. The complexes between galactosylated chitosan-graft-polyethylenimine (GC-*g*-PEI) were loaded within the thermosensitive hydrogels based on polymer **18** as a hepatocyte targeting gene delivery system [72]. The hydrogel loaded with GC-*g*-PEI/DNA complexes showed low cytotoxicity and higher transfection efficiency than PEI/DNA complexes only. The in vivo distribution study showed the specific accumulation of the released GC-*g*-PEI/DNA complexes in the liver, indicating better hepatocyte targeting and gene delivery. On the other hand, a low molecular weight PEI grafted poly(organophosphazenes) with a cleavable ester linkage formed a polyplex with siRNA of cyclin B1 with the size of 100 nm [132]. The polyplex aqueous solution underwent a sol-gel transition at physiological conditions. The polyplex-protected siRNA exhibited the enhanced stability up to 30 days in the presence of serum, compared with naked siRNAs, which showed degradation after 1 h. The release mechanism of the polyplexes was dominated by both dissolution and degradation of the polyplex hydrogel. The results showed an in vivo antitumor effect via cyclin B1 gene silencing for 4 weeks with only a single injection, indicating the polyplex hydrogel as an alternative siRNA carrier for many diseases that require localized and long-term therapy [132].

3.5 Tissue Engineering

Biodegradable thermogel formed from polymer **15** was employed to entrap islets of Langerhans in an artificial pancreas [73]. A prolonged insulin secretion in response to basal glucose concentration was observed from the rat islets entrapped in the hydrogel compared to free rat islets and islets entrapped in other types of polymer gels. The rat islets in the hydrogel showed higher cell viability and insulin production over a 28-day culture. The studies indicated that the thermosensitive injectable, biodegradable matrix from poly(organophosphazenes) can be used with several cell types as culture matrix. In addition, the hydrogels based on polymer **15** was also employed to entrap primary rat hepatocytes, cultivated as spheroids in order to examine differentiation morphology and enhanced liver-specific functions [133]. In a 28-day culture period, the spheroidal hepatocytes entrapped in the gel maintained a higher viability and produced albumin and urea at constant rates, indicating the potential application of poly(organophosphazene) hydrogel as a three-dimensional cell system for bioartifical liver devices and bioreactors. Furthermore, an injectable, thermogelling poly(organophosphazene)-RGD conjugate was developed for the enhancement of mesenchymal stem cell osteogenic differentiation [65]. The conjugate was synthesized by attaching RGD on

the carboxylic acid groups on polymer **19** through an amide linkage. The rabbit mesenchymal stem cells (rMSCs) on the conjugate hydrogels were shown to express markers for all stages towards osteogenesis, indicating the beginning of the maturation process. Both significantly high mineralization level for calcium contents and high expression of collagen type I were detected after 4th week. Thus the authors suggested that the poly(organophosphazene)-RGD conjugate holds a promise for cell delivery material to induce osteogenic differentiation for bone tissue engineering.

4 Dual Crosslinkable Biodegradable Poly(Organophosphazenes) Thermogels

One of the important aspects of poly(organophosphazenes) over other polymers lies on the ease of control of final properties by either introducing additional functionalities during macromolecular substitution reactions or secondary modification of side groups on the backbone. Thus, properties can be finely tuned with respect to different applications. Examples of biodegradable thermogelling poly(organophosphazenes) with additional functionality are shown in Table 4.

Chemically crosslinkable thermogelling poly(organophosphazenes) containing multiple thiol groups (**20**) shown in Fig. 6 were synthesized as injectable materials for biomedical applications [134]. In addition to the thermogelling behaviour of the polymer aqueous solution at body temperature, the gel strength can be further improved by the crosslinking of thiol groups with crosslinkers, such as divinyl sulfone and PEG divinyl sulfone under physiological conditions to form dual crosslinked hydrogels. The chemically crosslinked thermogel exhibited both enhanced storage modulus and decreased swelling ratio due to the increased crosslinking density. In the in vivo degradation study, the physically crosslinked gel degraded faster, compared to the dual crosslinked gels. Also, the gel strength can be controlled through the crosslinking degree. As a result, this chemically crosslinkable thermogel system has a unique advantage on degradability adjustment, tunable gelation properties, and controllable chemical and physical hydrogel network. Another dual crosslinkable poly(organophosphazene) hydrogel, containing acrylate groups (**21**) with improved structural properties was developed by the use of star-shaped multi-thiol crosslinkers, such as eight arm PEG thiol, compared with linear dithiol, PEG dithiol [139]. From FE-SEM, dual crosslinked hydrogel showed a sponge-like microporous structure with a relatively non-uniform pore size distribution in the matrix. The gels obtained by the physical and chemical crosslinking with star-shaped eight-arm thiols showed superior gel properties compared to gels with linear thiols. Through the nature of the crosslinking molecule and crosslinking density, the mechanical properties, swelling behaviors, three-dimensional inner networks and degradation rates can be controlled. Based on the similar concept, self-crosslinkable polymer blending system between polymer

Table 4 Functional biodegradable thermogelling poly(organophosphazenes)

Functional Group	Cosubstituents	T_{max} (ºC)	Category	Functionality	References
GlyGlyDOX	IleOEt/GlyGlyOH/AMPEG550	39,46	Polymer-drug conjugate	Locally controlled delivery of cancer therapeutics	[63, 84]
GlyGlyGRGDS	IleOEt/GlyGlyOH/AMPEG550	36.8–41.8	Polymer-drug conjugate	Enhancement of mesenchymal stem cell osteogenic differentiation	[65]
GlyGlyPTX	IleOEt/GlyGlyOH/AMPEG500	35.8–39.8	Polymer-drug conjugate	Controlled local release of antitumor drug	[64]
GlyGlyPro	IleOEt/GlyGlyOH/AMPEG500	49.8, 51.8	Polymer-drug complex	Enhanced sustained human growth hormone delivery	[67]
PEI	IleOEt/AMPEG550/Succinic acid	32.0,36.0	Polymer-drug complex	Increased biological efficiency and bioavailability of human growth hormone and siRNA	[86, 132]
Cysteamine	IleOEt/AMPEG550	37.8–43.8	Chemically crosslinkable hydrogel	Improvement of mechanical gel strength and controlled inner network and degradation rate	[134, 135]
2-Aminoethyl methacrylate	IleOEt/AMPEG550	23.9–57.9	Chemically crosslinkable hydrogel	Tunable mechanical gel property and the degradation rate	[135–137]
	IleOEt/AMPEG750	39.0			
	IleOEt/GlyLacOEt/AMPEG550	37.0, 39.0			
	IleOEt/GlyLacOEt/AMPEG750	39.0, 41.0			
2-Aminoethyl acrylate	IleOEt/AMPEG550	20.0–42.0	Chemically crosslinkable hydrogel	Rapid photocrosslinking hydrogel with enhanced mechanical strength	[138]
				Blending with cyseamine containing polyphosphazene to form self-crosslinkable hydrogel with improved mechanical strength	[135, 139]

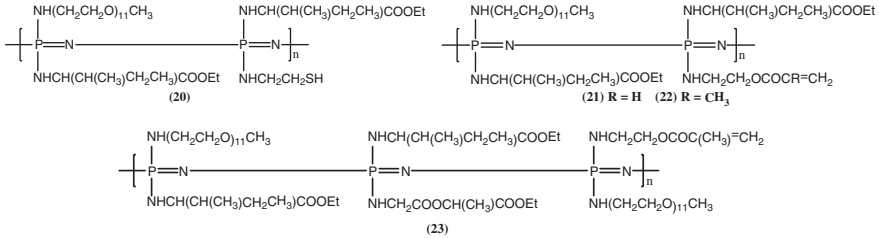

Fig. 6 Functional biodegradable thermogelling poly(organophosphazenes)

20 and **21** was investigated [135]. Thus, the leaching problems caused by the use of crosslinkers with low molecular weight can be avoided. However, a prolonged crosslinking time up to 4 h was observed for the polymer blending system, compared with the use of small crosslinkers (40 min).

Beside the further crosslinking with multi-thiol containing crosslinkers, the thermosensitive hydrogel bearing acrylate or methacrylate side groups can be crosslinked upon UV radiation under mild conditions, resulting in the formation of compact three-dimensional networks with properties of mechanically suitable strength and controllable biodegradation for injectable biomedical applications [136]. The hydrophobic interaction developed between the hydrophobic IleOEt and methacrylate in polymer **22** facilitated the rapid dual crosslinking accomplishment of the photo-crosslinking at 37 ℃, leading to a fully crosslinked gel in 5 min of exposure. The resultant dual crosslinked hydrogels showed improved mechanical properties with several folds from the in vivo degradation studies. The reported methacrylate-based system is more attractive compared to the thiol-based system because of its long-term stability and no crosslinker needed. Furthermore, the amount of photoinitiator, intensity of UV light, and time of exposure used were much less compared to the other reported photo-crosslinking systems. Later, another rapid photo-crosslinkable thermoresponsive injectable poly(organophosphazene) hydrogels were investigated by the presence of acrylate functional groups on the polymer backbone (**21**) [138]. Photocrosslinking was accomplished with even shorter UV exposure time, which was 120 and 180 s for in vitro and in vivo studies, compared with methacrylate-based system (5 min) owning to the higher reactivity of the acrylate double bond. Thus, the rapid photocrosslinking in the acrylate containing hydrogel enabled this system to be suitable for developing the carrier material for biomedical applications to avoid the possible damage of loaded cells or bioactive components from long UV exposure. The in vivo degradation study showed that the degradation rate of the dual crosslinked hydrogels was mainly affected by the type and degree substitutions of the side groups [137]. The incorporation of depsipeptide and long PEG chains as in polymer **23** accelerated the polymer degradation. The rate of polymer degradation in the initial period was depended on the degree of crosslinking, and later on the amount of depsipeptide and PEG chain lengths in the polymer networks. These results suggested that the mechanical property and degradation rate of the

dual crosslinked hydrogels can be tuned to the desired extent and may find wide application, where the gel property and degradation rate are needed to tightly regulated [137].

5 Summary

Poly(organophosphazenes) with the ability of sol-gel transition at body temperature in aqueous solution have been reviewed. The general molecular structures of these poly(organophosphazenes) consist of a short hydrophilic poly(ethyleneglycol) segment and amino acid esters, such as isoleucine ethyl ester and leucine ethyl ester. The properties of the resultant hydrogels can be simply controlled by adjusting the composition of cosubstituents or incorporating other functional side groups. These biodegradable thermosensitive hydrogels with controlled biodegradability, suitable mechanical strength, and biocompatibility exhibit tremendous potential as drug delivery carriers or tissue engineering matrices in bon in vitro and in vivo applications. While poly(organophosphazenes) lag behind many more established polymers for drug delivery application in terms of on-the-market applications, but most of other thermogelling copolymers are also at developmental research stage. Therefore, poly(organophosphazenes) are still competitive in this field, but a practical reality of this biomaterial require the close cooperation of chemists, chemical engineers, and medical experts on both long-range fundamental research and workable medical device investigation.

References

1. Hoffman, A.S.: Hydrogels for biomedical applications. Adv. Drug Deliv. Rev. **54**(1), 3–12 (2002). doi:10.1016/s0169-409x(01)00239-3
2. Bromberg, L.E., Ron, E.S.: Temperature-responsive gels and thermogelling polymer matrices for protein and peptide delivery. Adv. Drug Deliv. Rev. **31**(3), 197–221 (1998). doi:10.1016/s0169-409x(97)00121-x
3. Gil, E.S., Hudson, S.M.: Stimuli-reponsive polymers and their bioconjugates. Prog. Polym. Sci. **29**(12), 1173–1222 (2004). doi:10.1016/j.progpolymsci.2004.08.003
4. Jeong, B., Kim, S.W., Bae, Y.H.: Thermosensitive sol-gel reversible hydrogels. Adv. Drug Deliv. Rev. **54**(1), 37–51 (2002). doi:10.1016/s0169-409x(01)00242-3
5. Miyata, T., Uragami, T., Nakamae, K.: Biomolecule-sensitive hydrogels. Adv. Drug Deliv. Rev. **54**(1), 79–98 (2002). doi:10.1016/s0169-409x(01)00241-1
6. Schmaljohann, D.: Thermo- and pH-responsive polymers in drug delivery. Adv. Drug Deliv. Rev. **58**(15), 1655–1670 (2006). doi:10.1016/j.addr.2006.09.020
7. Kwon, I.K., Matsuda, T.: Photo-iniferter-based thermoresponsive block copolymers composed of poly(ethylene glycol) and poly(N-isopropylacrylamide) and chondrocyte immobilization. Biomaterials **27**(7), 986–995 (2006). doi:10.1016/j.biomaterials.2005.07.038
8. Li, C.M., Buurma, N.J., Haq, I., Turner, C., Armes, S.P., Castelletto, V., Hamley, I.W., Lewis, A.L.: Synthesis and characterization of biocompatible, thermoresponsive ABC and ABA triblock copolymer gelators. Langmuir **21**(24), 11026–11033 (2005). doi:10.1021/la0515672

9. Li, C.M., Tang, Y.Q., Armes, S.P., Morris, C.J., Rose, S.F., Lloyd, A.W., Lewis, A.L.: Synthesis and characterization of biocompatible thermo-responsive gelators based on ABA triblock copolymers. Biomacromolecules **6**(2), 994–999 (2005). doi:10.1021/bm049331k
10. Lin, H.H., Cheng, Y.L.: In situ thermoreversible gelation of block and star copolymers of poly(ethylene glycol) and poly(N-isopropylacrylamide) of varying architectures. Macromolecules **34**(11), 3710–3715 (2001). doi:10.1021/ma001852m
11. Tang, T., Castelletto, V., Parras, P., Hamley, I.W., King, S.M., Roy, D., Perrier, S., Hoogenboom, R., Schubert, U.S.: Thermo-responsive poly(methyl methacrylate)-block-poly(N-isopropylacrylamide) block copolymers synthesized by RAFT polymerization: micellization and gelation. Macromol. Chem. Phys. **207**(19), 1718–1726 (2006). doi:10.1002/macp.200600309
12. Glatter, O., Scherf, G., Schillen, K., Brown, W.: Characterization of a poly(ethylene oxide) poly(propylene oxide) triblock copolymer (eo(27)-po39-eo(27)) in aqueous-solution. Macromolecules **27**(21), 6046–6054 (1994). doi:10.1021/ma00099a017
13. Jorgensen, E.B., Hvidt, S., Brown, W., Schillen, K.: Effects of salts on the micellization and gelation of a triblock copolymer studied by rheology and light scattering. Macromolecules **30**(8), 2355–2364 (1997). doi:10.1021/ma9616322
14. Mortensen, K., Brown, W.: Poly(ethylene oxide)-poly(propylene oxide)-poly(ethylene oxide) triblock copolymers in aqueous-solution - the influence of relative block size. Macromolecules **26**(16), 4128–4135 (1993). doi:10.1021/ma00068a010
15. Song, M.J., Lee, D.S., Ahn, J.H., Kim, D.J., Kim, S.C.: Dielectric behavior during sol-gel transition of PEO-PPO-PEO triblock copolymer aqueous solution. Polym. Bull. **43**(6), 497–504 (2000). doi:10.1007/s002890050007
16. Sosnik, A., Cohn, D.: Reverse thermo-responsive poly(ethylene oxide) and poly(propylene oxide) multiblock copolymers. Biomaterials **26**(4), 349–357 (2005). doi:10.1016/j.biomaterials.2004.02.041
17. Wanka, G., Hoffmann, H., Ulbricht, W.: The aggregation behavior of poly-(oxyethylene)-poly-(oxypropylene)-poly-(oxyethylene)-block-copolyme rs in aqueous-solution. Colloid Polym. Sci. **268**(2), 101–117 (1990). doi:10.1007/bf01513189
18. Bae, S.J., Suh, J.M., Sohn, Y.S., Bae, Y.H., Kim, S.W., Jeong, B.: Thermogelling poly(caprolactone-b-ethylene glycol-b-caprolactone) aqueous solutions. Macromolecules **38**(12), 5260–5265 (2005). doi:10.1021/ma050489m
19. Fujiwara, T., Mukose, T., Yamaoka, T., Yamane, H., Sakurai, S., Kimura, Y.: Novel thermo-responsive formation of a hydrogel by stereo-complexation between PLLA-PEG-PLLA and PDLA-PEG-PDLA block copolymers. Macromol. Biosci. **1**(5), 204–208 (2001). doi:10.1002/1616-5195(20010701)1:5<204:aid-mabi204>3.0.co;2-h
20. Jeong, B., Bae, Y.H., Lee, D.S., Kim, S.W.: Biodegradable block copolymers as injectable drug-delivery systems. Nature **388**(6645), 860–862 (1997)
21. Lee, J., Bae, Y.H., Sohn, Y.S., Jeong, B.: Thermogelling aqueous solutions of alternating multiblock copolymers of poly(L-lactic acid) and poly(ethylene glycol). Biomacromolecules **7**(6), 1729–1734 (2006). doi:10.1021/bm0600062
22. Li, F., Li, S.M., El Ghzaoui, A., Nouailhas, H., Zhuo, R.X.: Synthesis and gelation properties of PEG-PLA-PEG triblock copolymers obtained by coupling monohydroxylated PEG-PLA with adipoyl chloride. Langmuir **23**(5), 2778–2783 (2007). doi:10.1021/la0629025
23. Loh, X.J., Goh, S.H., Li, J.: New biodegradable thermogelling copolymers having very low gelation concentrations. Biomacromolecules **8**(2), 585–593 (2007). doi:10.1021/bm0607933
24. Jeong, B., Gutowska, A.: Lessons from nature: stimuli-responsive polymers and their biomedical applications. Trends Biotechnol. **20**(7), 305–311 (2002). doi:10.1016/s0167-7799(02)01962-5
25. Loh, X.J., Li, J.: Biodegradable thermosensitive copolymer hydrogels for drug delivery. Expert Opin. Ther. Pat. **17**(8), 965–977 (2007). doi:10.1517/13543776.17.8.965
26. Allcock, H.R.: Polyphosphazenes as New Biomedical and Bioactive Materials. In: Langer, R., Chasin, M. (eds.) Biodegradable Polymers as Drug Delivery System, pp. 163–193. Marcel Dekker, New York (1990)

27. Allcock, H.R.: Rational design and synthesis of polyphosphazenes for tissue engineering. In: Atala, A., Lanza, R. (eds.) Methods of Tissue Engineering, pp. 597–607. Academic Press, New York (2001)
28. Scopelianos, A.G.: Polyphosphazenes as new biomaterials. In: Shalaby, S. (ed.) Biomedical Polymers, pp. 153–171. Hanser Publishers, Munich and New York (1994)
29. Allcock, H.R., Kugel, R.L.: Synthesis of high polymeric alkoxy- and aryloxphosphonitriles. J. Am. Chem. Soc. **87**(18), 4216 (1965). doi:10.1021/ja01096a056
30. Allcock, H.R., Kugel, R.L.: Phosphonitrilic compounds. 7. High molecular weight poly(diaminophosphazenes). Inorg. Chem. **5**(10), 1716 (1966). doi:10.1021/ic50044a017
31. Allcock, H.R., Kugel, R.L., Valan, K.J.: Phosphonitrilic compounds.6. High molecular weight poly(alkoxy- and arylox-phosphazenes). Inorg. Chem. **5**(10), 1709 (1966). doi:10.1021/ic50044a016
32. Gettleman, L., Farris, C.L., Rawls, H.R., LeBouef, R.: Soft and firm fluoroalkoxyphosphazene rubber denture linear for a composite denture (1984)
33. Wade, C.W.R., Gourlay, S., Rice, R., Hegyeli, A., Singler, R., White, J.: Biocompatibility of Eight Poly(organophosphazenes). In: Carraher, C.E., Sheats, J.E., Pittman, C.U. (eds.) Organometallic Polymers, p. 298. Academic Press, New York (1978)
34. Welle, A., Grunze, M., Tur, D.: Plasma protein adsorption and platelet adhesion on poly bis(trifluoroethoxy)phosphazene and reference material surfaces. J. Colloid Interface Sci. **197**(2), 263–274 (1998). doi:10.1006/jcis.1997.5238
35. Bostman, O., Pihlajamaki, H.: Clinical biocompatibility of biodegradable orthopaedic implants for internal fixation: a review. Biomaterials **21**(24), 2615–2621 (2000). doi:10.1016/s0142-9612(00)00129-0
36. Allcock, H.R., Fuller, T.J., Mack, D.P., Matsumura, K., Smeltz, K.M.: Synthesis of poly [(amino acid alkyl ester)phosphazenes]. Macromolecules **10**(4), 824–830 (1977). doi:10.1021/ma60058a020
37. Allcock, H.R., Fuller, T.J., Matsumura, K.: Hydrolysis pathways for aminophosphazenes. Inorg. Chem. **21**(2), 515–521 (1982). doi:10.1021/ic00132a009
38. Allcock, H.R., Pucher, S.R., Scopelianos, A.G.: Poly (amino-acid-ester)phosphazenes—synthesis, crystallinity, and hydrolytic sensitivity in solution and the solid-state. Macromolecules **27**(5), 1071–1075 (1994). doi:10.1021/ma00083a001
39. Allcock, H.R., Pucher, S.R., Scopelianos, A.G.: Poly (amino acid ester)phosphazenes as substrates for the controlled-release of small molecules. Biomaterials **15**(8), 563–569 (1994). doi:10.1016/0142-9612(94)90205-4
40. Hindenlang, M.D., Soudakov, A.A., Imler, G.H., Laurencin, C.T., Nair, L.S., Allcock, H.R.: Iodine-containing radio-opaque polyphosphazenes. Polym. Chem. **1**(9), 1467–1474 (2010). doi:10.1039/c0py00126k
41. Deng, M., Nair, L.S., Nukavarapu, S.R., Jiang, T., Kanner, W.A., Li, X.D., Kumbar, S.G., Weikel, A.L., Krogman, N.R., Allcock, H.R., Laurencin, C.T.: Dipeptide-based polyphosphazene and polyester blends for bone tissue engineering. Biomaterials **31**(18), 4898–4908 (2010). doi:10.1016/j.biomaterials.2010.02.058
42. Deng, M., Kumbar, S.G., Nair, L.S., Weikel, A.L., Allcock, H.R., Laurencin, C.T.: Biomimetic structures: biological implications of dipeptide-substituted polyphosphazene-polyester blend nanofiber matrices for load-bearing bone regeneration. Adv. Funct. Mater. **21**(14), 2641–2651 (2011). doi:10.1002/adfm.201100275
43. Kim, J.I., Jun, Y.J., Seong, J.Y., Jun, M.J., Sohn, Y.S.: Synthesis and characterization of nanosized poly (organophosphazenes) with methoxy-poly(ethylene glycol) and dipeptide ethyl esters as side groups. Polymer **45**(21), 7083–7089 (2004). doi:10.1016/j.polymer.2004.08.031
44. Weikel, A.L., Krogman, N.R., Nguyen, N.Q., Nair, L.S., Laurencin, C.T., Allcock, H.R.: Polyphosphazenes that contain dipeptide side groups: synthesis, characterization, and sensitivity to hydrolysis. Macromolecules **42**(3), 636–639 (2009). doi:10.1021/ma802423c
45. Crommen, J.H.L., Schacht, E.H., Mense, E.H.G.: Biodegradable polymers.1. Synthesis of hydrolysis-sensitive poly (organo)phosphazenes. Biomaterials **13**(8), 511–520 (1992). doi:10.1016/0142-9612(92)90102-t

46. Crommen, J.H.L., Schacht, E.H., Mense, E.H.G.: Biodegradable polymers. 2. Degradation characteristics of hydrolysis-sensitive poly (organo)phosphazenes. Biomaterials **13**(9), 601–611 (1992). doi:10.1016/0142-9612(92)90028-m
47. Schacht, E., Vandorpe, J., Dejardin, S., Lemmouchi, Y., Seymour, L.: Biomedical applications of degradable polyphosphazenes. Biotechnol. Bioeng. **52**(1), 102–108 (1996). doi:10.1002/(sici)1097-0290(19961005)52:1<102:aid-bit10>3.0.co;2-q
48. Allcock, H.R., Scopelianos, A.G.: Synthesis of sugar-substituted cyclic and polymeric phosphazenes and their oxidation, reduction and acetylation reactions. Macromolecules **16**(5), 715–719 (1983). doi:10.1021/ma00239a001
49. Allcock, H.R., Singh, A., Ambrosio, A.M.A., Laredo, W.R.: Tyrosine-bearing polyphosphazenes. Biomacromolecules **4**(6), 1646–1653 (2003). doi:10.1021/bm030027i
50. Krogman, N.R., Hindenlang, M.D., Nair, L.S., Laurencin, C.T., Allcock, H.R.: Synthesis of purine- and pyrimidine-containing polyphosphazenes: physical properties and hydrolytic behavior. Macromolecules **41**(22), 8467–8472 (2008). doi:10.1021/ma8008417
51. Krogman, N.R., Weikel, A.L., Nguyen, N.Q., Nair, L.S., Laurencin, C.T., Allcock, H.R.: Synthesis and characterization of new biomedical polymers: serine- and threonine-containing polyphosphazenes and poly(L-lactic acid) grafted copolymers. Macromolecules **41**(21), 7824–7828 (2008). doi:10.1021/ma801961m
52. Morozowich, N.L., Weikel, A.L., Nichol, J.L., Chen, C., Nair, L.S., Laurencin, C.T., Allcock, H.R.: Polyphosphazenes containing vitamin substituents: synthesis, characterization, and hydrolytic sensitivity. Macromolecules **44**(6), 1355–1364 (2011). doi:10.1021/ma1027406
53. Weikel, A.L., Owens, S.G., Fushimi, T., Allcock, H.R.: Synthesis and characterization of methionine- and cysteine-substituted phosphazenes. Macromolecules **43**(12), 5205–5210 (2010). doi:10.1021/ma1007013
54. Weikel, A.L., Owens, S.G., Morozowich, N.L., Deng, M., Nair, L.S., Laurencin, C.T., Allcock, H.R.: Miscibility of choline-substituted polyphosphazenes with PLGA and osteoblast activity on resulting blends. Biomaterials **31**(33), 8507–8515 (2010). doi:10.1016/j.biomaterials.2010.07.094
55. Ahn, S., Ahn, S.W., Song, S.C.: Thermosensitive amphiphilic polyphosphazenes and their interaction with ionic surfactants. Colloids Surf. A **330**(2–3), 184–192 (2008). doi:10.1016/j.colsurfa.2008.07.059
56. Cho, Y.W., An, S.W., Song, S.C.: Effect of inorganic and organic salts on the thermogelling behavior of poly(organophosphazenes). Macromol. Chem. Phys. **207**(4), 412–418 (2006). doi:10.1002/macp.200500483
57. Kang, G.D., Heo, J.Y., Jung, S.B., Song, S.C.: Controlling the thermosensitive gelation properties of poly(organophosphazenes) by blending. Macromol. Rapid Commun. **26**(20), 1615–1618 (2005). doi:10.1002/marc.200500472
58. Lee, S.B., Song, S.C., Jin, J.I., Sohn, Y.S.: A new class of biodegradable thermosensitive polymers. 2. Hydrolytic properties and salt effect on the lower critical solution temperature of poly(organophosphazenes) with methoxypoly(ethylene glycol) and amino acid esters as side groups. Macromolecules **32**(23), 7820–7827 (1999). doi:10.1021/ma990645n
59. Lee, S.B., Song, S.C., Jin, J.I., Sohn, Y.S.: Thermosensitive cyclotriphosphazenes. J. Am. Chem. Soc. **122**(34), 8315–8316 (2000). doi:10.1021/ja001542j
60. Lee, B.H., Lee, Y.M., Sohn, Y.S., Song, S.C.: Thermosensitive and hydrolysis-sensitive poly(organophosphazenes). Polym. Int. **51**(7), 658–660 (2002). doi:10.1002/pi.1019
61. Lee, B.H., Lee, Y.M., Sohn, Y.S., Song, S.C.: A thermosensitive poly(organophosphazene) gel. Macromolecules **35**(10), 3876–3879 (2002). doi:10.1021/ma012093q
62. Song, S.C., Lee, S.B., Jin, J.I., Sohn, Y.S.: A new class of biodegradable thermosensitive polymers. I. Synthesis and characterization of poly(organophosphazenes) with methoxypoly(ethylene glycol) and amino acid esters as side groups. Macromolecules **32**(7), 2188–2193 (1999). doi:10.1021/ma981190p
63. Chun, C., Lee, S.M., Kim, C.W., Hong, K.Y., Kim, S.Y., Yang, H.K., Song, S.C.: Doxorubicin-polyphosphazene conjugate hydrogels for locally controlled delivery of cancer therapeutics. Biomaterials **30**(27), 4752–4762 (2009). doi:10.1016/j.biomaterials.2009.05.031

64. Chun, C., Lee, S.M., Kim, S.Y., Yang, H.K., Song, S.C.: Thermosensitive poly(organophosphazene)-paclitaxel conjugate gels for antitumor applications. Biomaterials **30**(12), 2349–2360 (2009). doi:10.1016/j.biomaterials.2008.12.083
65. Chun, C., Lim, H.J., Hong, K.Y., Park, K.H., Song, S.C.: The use of injectable, thermosensitive poly(organophosphazene)-RGD conjugates for the enhancement of mesenchymal stem cell osteogenic differentiation. Biomaterials **30**(31), 6295–6308 (2009). doi:10.1016/j.biomaterials.2009.08.011
66. Lee, S.M., Chun, C.J., Heo, J.Y., Song, S.C.: Injectable and Thermosensitive Poly(organophosphazene) Hydrogels for a 5-Fluorouracil Delivery. J. Appl. Polym. Sci. **113**(6), 3831–3839 (2009). doi:10.1002/app.30397
67. Park, M.R., Chun, C., Ahn, S.W., Ki, M.H., Cho, C.S., Song, S.C.: Cationic and thermosensitive protamine conjugated gels for enhancing sustained human growth hormone delivery. Biomaterials **31**(6), 1349–1359 (2010). doi:10.1016/j.biomaterials.2009.10.022
68. Lee, B.H., Song, S.C.: Synthesis and characterization of biodegradable thermosensitive poly(organophosphazene) gels. Macromolecules **37**(12), 4533–4537 (2004). doi:10.1021/ma0305838
69. Park, M.R., Chun, C.J., Ahn, S.W., Ki, M.H., Cho, C.S., Song, S.C.: Sustained delivery of human growth hormone using a polyelectrolyte complex-loaded thermosensitive polyphosphazene hydrogel. J. Controlled Release **147**(3), 359–367 (2010). doi:10.1016/j.jconrel.2010.07.126
70. Seong, J.Y., Jun, Y.J., Jeong, B., Sohn, Y.S.: New thermogelling poly (organophosphazenes) with methoxypoly(ethylene glycol) and oligopeptide as side groups. Polymer **46**(14), 5075–5081 (2005). doi:10.1016/j.polymer.2005.04.024
71. Ahn, S., Ahn, S.W., Song, S.C.: Polymer structure-dependent ion interaction studied by amphiphilic nonionic poly(organophosphazenes). J. Polym. Sci., Part B: Polym. Phys. **46**(19), 2022–2034 (2008). doi:10.1002/polb.21537
72. Jiang, H.L., Kim, Y.K., Lee, S.M., Park, M.R., Kim, E.M., Jin, Y.M., Arote, R., Jeong, H.J., Song, S.C., Cho, M.H., Cho, C.S.: Galactosylated chitosan-g-PEI/DNA complexes-loaded poly(organophosphazene) hydrogel as a hepatocyte targeting gene delivery system. Arch. Pharm. Res. **33**(4), 551–556 (2010). doi:10.1007/s12272-010-0409-9
73. Park, K.H., Song, S.C.: A thermo-sensitive poly(organophosphazene) hydrogel used as an extracellular matrix for artificial pancreas. J. Biomater. Sci. Polym. Ed. **16**(11), 1421–1431 (2005). doi:10.1163/156856205774472272
74. Park, M.R., Cho, C.S., Song, S.C.: In vitro and in vivo degradation behaviors of thermosensitive poly(organophosphazene) hydrogels. Polym. Degrad. Stab. **95**(6), 935–944 (2010). doi:10.1016/j.polymdegradstab.2010.03.024
75. Ahn, S., Ahn, S.W., Song, S.C.: Thermothickening modification of the poly(ethylene glycol) and amino acid ester grafted polyphosphazenes by monomethyl end-capped poly(ethylene glycol) addition. Colloids Surf. A **333**(1–3), 82–90 (2009). doi:10.1016/j.colsurfa.2008.09.045
76. Al-Abd, A.M., Hong, K.Y., Song, S.C., Kuh, H.J.: Pharmacokinetics of doxorubicin after intratumoral injection using a thermosensitive hydrogel in tumor-bearing mice. J. Controlled Release **142**(1), 101–107 (2010). doi:10.1016/j.jconrel.2009.10.003
77. Cho, J.K., Hong, K.Y., Park, J.W., Yang, H.K., Song, S.C.: Injectable delivery system of 2-methoxyestradiol for breast cancer therapy using biodegradable thermosensitive poly(organophosphazene) hydrogel. J. Drug Target. **19**(4), 270–280 (2011). doi:10.3109/1061186x.2010.499461
78. Cho, J.K., Park, J.W., Song, S.C.: Injectable and biodegradable poly(organophosphazene) gel containing silibinin: its physicochemical properties and anticancer activity. J. Pharm. Sci. **101**(7), 2382–2391 (2012). doi:10.1002/jps.23137
79. Il Kim, J., Kim, B., Chun, C., Lee, S.H., Song, S.C.: MRI-monitored long-term therapeutic hydrogel system for brain tumors without surgical resection. Biomaterials **33**(19), 4836–4842 (2012). doi:10.1016/j.biomaterials.2012.03.048

80. Kang, G.D., Cheon, S.H., Song, S.C.: Controlled release of doxorubicin from thermosensitive poly(organophosphazene) hydrogels. Int. J. Pharm. **319**(1–2), 29–36 (2006). doi:10.1016/j.ijpharm.2006.03.032
81. Kim, J.I., Chun, C., Kim, B., Hong, J.M., Cho, J.K., Lee, S.H., Song, S.C.: Thermosensitive/magnetic poly(organophosphazene) hydrogel as a long-term magnetic resonance contrast platform. Biomaterials **33**(1), 218–224 (2012). doi:10.1016/j.biomaterials.2011.09.033
82. Kim, J.I., Lee, B.S., Chun, C., Cho, J.K., Kim, S.Y., Song, S.C.: Long-term theranostic hydrogel system for solid tumors. Biomaterials **33**(7), 2251–2259 (2012). doi:10.1016/j.biomaterials.2011.11.083
83. Kim, J.H., Lee, J.H., Kim, K.S., Na, K., Song, S.C., Lee, J., Kuh, H.J.: Intratumoral delivery of paclitaxel using a thermosensitive hydrogel in human tumor xenografts. Arch. Pharm. Res. **36**(1), 94–101 (2013). doi:10.1007/s12272-013-0013-x
84. Kwak, M.K., Hur, K., Yu, J.E., Han, T.S., Yanagihara, K., Kim, W.H., Lee, S.M., Song, S.C., Yang, H.K.: Suppression of in vivo tumor growth by using a biodegradable thermosensitive hydrogel polymer containing chemotherapeutic agent. Invest. New Drugs **28**(3), 284–290 (2010). doi:10.1007/s10637-009-9253-5
85. Park, M.R., Seo, B.B., Song, S.C.: Dual ionic interaction system based on polyelectrolyte complex and ionic, injectable, and thermosensitive hydrogel for sustained release of human growth hormone. Biomaterials **34**(4), 1327–1336 (2013). doi:10.1016/j.biomaterials.2012.10.033
86. Seo, B.B., Park, M.R., Chun, C., Lee, J.Y., Song, S.C.: The biological efficiency and bioavailability of human growth hormone delivered using injectable, ionic, thermosensitive poly(organophosphazene)-polyethylenimine conjugate hydrogels. Biomaterials **32**(32), 8271–8280 (2011). doi:10.1016/j.biomaterials.2011.07.033
87. Yu, J., Lee, H.J., Hur, K., Kwak, M.K., Han, T.S., Kim, W.H., Song, S.C., Yanagihara, K., Yang, H.K.: The antitumor effect of a thermosensitive polymeric hydrogel containing paclitaxel in a peritoneal carcinomatosis model. Invest. New Drugs **30**(1), 1–7 (2012). doi:10.1007/s10637-010-9499-y
88. Ahn, S., Monge, E.C., Song, S.C.: Ion and pH effect on the lower critical solution temperature phase behavior in neutral and acidic poly(organophosphazene) counterparts. Langmuir **25**(4), 2407–2418 (2009). doi:10.1021/la802815u
89. Cho, J.K., Lee, S.M., Kim, C.W., Song, S.C.: Synthesis and characterization of biodegradable thermosensitive neutral and acidic poly(organophosphazene) gels bearing carboxylic acid group. J. Polym. Res. **18**(4), 701–713 (2011). doi:10.1007/s10965-010-9466-5
90. Lee, B.B., Song, S.C.: Synthesis and characterization of thermosensitive poly(organophosphazene) gels with an amino functional group. J. Appl. Polym. Sci. **120**(2), 998–1005 (2011). doi:10.1002/app.33181
91. Allcock, H.R.: Chemistry and applications of polyphosphazenes. Wiley, New York (2003)
92. Chen, C., Liu, X., Tian, Z.C., Allcock, H.R.: Trichloroethoxy-substituted polyphosphazenes: synthesis, characterization, and properties. Macromolecules **45**(22), 9085–9091 (2012). doi:10.1021/ma301822m
93. Liu, X., Breon, J.P., Chen, C., Allcock, H.R.: Substituent Exchange Reactions of Linear Oligomeric Aryloxyphosphazenes with Sodium 2,2,2-Trifluoroethoxide. Inorg. Chem. **51**(21), 11910–11916 (2012). doi:10.1021/ic301808v
94. Liu, X., Breon, J.P., Chen, C., Allcock, H.R.: Substituent exchange reactions with high polymeric organophosphazenes. Macromolecules **45**(22), 9100–9109 (2012). doi:10.1021/ma302087a
95. Liu, X., Tian, Z.C., Chen, C., Allcock, H.R.: Synthesis and Characterization of Brush-Shaped Hybrid Inorganic/Organic Polymers Based on Polyphosphazenes. Macromolecules **45**(3), 1417–1426 (2012). doi:10.1021/ma202587z
96. Tian, Z.C., Liu, X., Chen, C., Allcock, H.R.: Synthesis and micellar behavior of novel amphiphilic poly bis(trifluoroethoxy)phosphazene -co-poly (dimethylamino)ethyl methacrylate block copolymers. Macromolecules **45**(5), 2502–2508 (2012). doi:10.1021/ma300139z

97. Chen, C., Hess, A.R., Jones, A.R., Liu, X., Barber, G.D., Mallouk, T.E., Allcock, H.R.: Synthesis of new polyelectrolytes via backbone quaternization of poly(aryloxy- and alkoxyphosphazenes) and their small molecule counterparts. Macromolecules **45**(3), 1182–1189 (2012). doi:10.1021/ma202619j
98. Liu, X., Zhang, H., Tian, Z.C., Sen, A., Allcock, H.R.: Preparation of quaternized organic-inorganic hybrid brush polyphosphazene-co-poly 2-(dimethylamino)ethyl methacrylate electrospun fibers and their antibacterial properties. Polym. Chem. **3**(8), 2082–2091 (2012). doi:10.1039/c2py20170d
99. Allcock, H.R., Morozowich, N.L.: Bioerodible polyphosphazenes and their medical potential. Polymer Chemistry **3**(3), 578–590 (2012). doi:10.1039/c1py00468a
100. Rose, S.H.: Synthesis of phosphonitrilic fluoroelastomers. Journal of Polymer Science Part B-Polymer Letters **6**(12PB), 837 (1968). doi:10.1002/pol.1968.110061203
101. Tate, D.P.: Polyphosphazene elastomers. J. Polym. Sci., Part C: Polym. Symp. **48**, 33–45 (1974)
102. Liu, X., Tian, Z.C., Chen, C., Allcock, H.R.: UV-cleavable unimolecular micelles: synthesis and characterization toward photocontrolled drug release carriers. Polym. Chem. **4**(4), 1115–1125 (2013). doi:10.1039/c2py20825c
103. Cho, Y.W., Lee, J.R., Song, S.C.: Novel thermosensitive 5-fluorouracil-cyclotriphosphazene conjugates: synthesis, thermosensitivity, degradability, and in vitro antitumor activity. Bioconjug. Chem. **16**(6), 1529–1535 (2005). doi:10.1021/bc049697u
104. Cho, Y.W., Choi, M., Lee, K., Song, S.C.: Cyclotriphosphazene-Pt-DACH conjugates with dipeptide spacers for drug delivery systems. J. Bioact. Compatible Polym. **25**(3), 274–291 (2010). doi:10.1177/0883911509356377
105. Lee, S.B., Song, S.C., Jin, J.I., Sohn, Y.S.: Structural and thermosensitive properties of cyclotriphosphazenes with poly(ethylene glycol) and amino acid esters as side groups. Macromolecules **34**(21), 7565–7569 (2001). doi:10.1021/ma010648b
106. Song, S.C., Lee, S.B., Lee, B.H., Ha, H.W., Lee, K.T., Sohn, Y.S.: Synthesis and antitumor activity of novel thermosensitive platinum(II)-cyclotriphosphazene conjugates. J. Controlled Release **90**(3), 303–311 (2003). doi:10.1016/s0168-3659(03)00199-8
107. Allcock, H.R., Dudley, G.K.: Lower critical solubility temperature study of alkyl ether based polyphosphazenes. Macromolecules **29**(4), 1313–1319 (1996). doi:10.1021/ma951129+
108. Allcock, H.R., Pucher, S.R., Turner, M.L., Fitzpatrick, R.J.: Poly(organophosphazenes) with poly(alkyl ether) side groups—a study of their water solubility and the swelling characteristics of their hydrogels. Macromolecules **25**(21), 5573–5577 (1992). doi:10.1021/ma00047a002
109. Allcock, H.R., Pucher, S.R., Visscher, K.B.: Activity of urea amidohydrolase immobilized within poly di(methoxyethoxyethoxy)phosphazene hydrogels. Biomaterials **15**(7), 502–506 (1994). doi:10.1016/0142-9612(94)90015-9
110. Zhang, J.X., Qiu, L.Y., Zhu, K.J., Jin, Y.: Thermosensitive micelles self-assembled by novel N-isopropylacrylamide oligomer grafted polyphosphazene. Macromol. Rapid Commun. **25**(17), 1563–1567 (2004). doi:10.1002/marc.200400180
111. Zhang, J.X., Qiu, L.Y., Wu, X.L., Jin, Y., Zu, K.J.: Temperature-triggered nanosphere formation through self-assembly of amphiphilic polyphosphazene. Macromol. Chem. Phys. **207**(14), 1289–1296 (2006). doi:10.1002/macp.200600139
112. Zhang, R.X., Li, X.J., Qiu, L.Y., Li, X.H., Yan, M.Q., Jin, Y., Zhu, K.J.: Indomethacin-loaded polymeric nanocarriers based on amphiphilic polyphosphazenes with poly (N-isopropylacrylamide) and ethyl tryptophan as side groups: Preparation, in vitro and in vivo evaluation. J. Controlled Release **116**(3), 322–329 (2006). doi:10.1016/j.jconrel.2006.09.013
113. Lee, S.B., Song, S.C.: Hydrolysis-improved thermosensitive polyorganophosphazenes with alpha-amino-omega-methoxy-poly(ethylene glycol) and amino acid esters as side groups. Polym. Int. **54**(9), 1225–1232 (2005). doi:10.1002/pi.1702
114. Lee, S.B., Song, S.C., Jin, J.I., Sohn, Y.S.: Surfactant effect on the lower critical solution temperature of poly(organophosphazenes) with methoxy-poly(ethylene glycol) and amino acid esters as side groups. Colloid Polym. Sci. **278**(11), 1097–1102 (2000). doi:10.1007/s003960000368

115. Lee, S.B., Song, S.C., Jin, J.I., Sohn, Y.S.: Solvent effect on the lower critical solution temperature of biodegradable thermosensitive poly(organophosphazenes). Polym. Bull. **45**(4–5), 389–396 (2000). doi:10.1007/s002890070012
116. Allcock, H.R., Fuller, T.J.: Phosphazene high polymers with steroidal side groups. Macromolecules **13**(6), 1338–1345 (1980). doi:10.1021/ma60078a003
117. Allcock, H.R., Pucher, S.R.: Polyphosphazenes with glucosyl and methylamino, trifluoroethoxy, phenoxy, or (methoxyethoxy)ethoxy side groups. Macromolecules **24**(1), 23–34 (1991). doi:10.1021/ma00001a005
118. Andrianov, A.K., Marin, A.: Degradation of polyaminophosphazenes: effects of hydrolytic environment and polymer processing. Biomacromolecules **7**(5), 1581–1586 (2006). doi:10.1021/bm050959k
119. Andrianov, A.K., Marin, A., Peterson, P.: Water-soluble biodegradable polyphosphazenes containing N-ethylpyrrolidone groups. Macromolecules **38**(19), 7972–7976 (2005). doi:10.1021/ma0509309
120. Crommen, J., Vandorpe, J., Schacht, E.: Degradable polyphosphazenes for biomedical applications. J. Controlled Release **24**(1–3), 167–180 (1993). doi:10.1016/0168-3659(93)90176-6
121. Cui, Y.J., Zhao, M., Tang, X.Z., Luo, Y.P.: Novel micro-crosslinked poly(organophosphazenes) with improved mechanical properties and controllable degradation rate as potential biodegradable matrix. Biomaterials **25**(3), 451–457 (2004). doi:10.1016/s0142-9612(03)00532-5
122. Qiu, L.Y., Zhu, K.J.: Novel biodegradable polyphosphazenes containing glycine ethyl ester and benzyl ester of amino acethydroxamic acid as cosubstituents: Syntheses, characterization, and degradation properties. J. Appl. Polym. Sci. **77**(13), 2987–2995 (2000). doi:10.1002/1097-4628(20000923)77:13<2987:aid-app24>3.0.co;2-f
123. Singh, A., Krogman, N.R., Sethuraman, S., Nair, L.S., Sturgeon, J.L., Brown, P.W., Laurencin, C.T., Allcock, H.R.: Effect of side group chemistry on the properties of biodegradable L-alanine cosubstituted polyphosphazenes. Biomacromolecules **7**(3), 914–918 (2006). doi:10.1021/bm050752r
124. Tian, Z.C., Zhang, Y.F., Liu, X., Chen, C., Guiltinan, M.J., Allcock, H.R.: Biodegradable polyphosphazenes containing antibiotics: synthesis, characterization, and hydrolytic release behavior. Polymer Chemistry **4**(6), 1826–1835 (2013). doi:10.1039/c2py21064a
125. Yuan, W.Z., Song, Q., Zhu, L., Huang, X.B., Zheng, S.X., Tang, X.Z.: Asymmetric penta-armed poly(epsilon-caprolactone)s with short-chain phosphazene core: synthesis, characterization, and in vitro degradation. Polym. Int. **54**(9), 1262–1267 (2005). doi:10.1002/pi.1840
126. Singla, A.K., Garg, A., Aggarwal, D.: Paclitaxel and its formulations. Int. J. Pharm. **235**(1–2), 179–192 (2002). doi:10.1016/s0378-5173(01)00986-3
127. Maeda, H., Wu, J., Sawa, T., Matsumura, Y., Hori, K.: Tumor vascular permeability and the EPR effect in macromolecular therapeutics: a review. J. Controlled Release **65**(1–2), 271–284 (2000). doi:10.1016/s0168-3659(99)00248-5
128. Modok, S., Mellor, H.R., Callaghan, R.: Modulation of multidrug resistance efflux pump activity to overcome chemoresistance in cancer. Curr. Opin. Pharmacol. **6**(4), 350–354 (2006). doi:10.0116/j.coph.2006.01.009
129. Kwak, H.H., Shim, W.S., Choi, M.K., Son, M.K., Kim, Y.J., Yang, H.C., Kim, T.H., Lee, G.I., Kim, B.M., Kang, S.H., Shim, C.K.: Development of a sustained-release recombinant human growth hormone formulation. J. Controlled Release **137**(2), 160–165 (2009). doi:10.1016/j.jconrel.2009.03.014
130. Kim, H.K., Chung, H.J., Park, T.G.: Biodegradable polymeric microspheres with "open/closed" pores for sustained release of human growth hormone. J. Controlled Release **112**(2), 167–174 (2006). doi:10.1016/j.jconrel.2006.02.004
131. Kim, H.K., Park, T.G.: Microencapsulation of human growth hormone within biodegradable polyester microspheres: Protein aggregation stability and incomplete release mechanism. Biotechnol. Bioeng. **65**(6), 659–667 (1999). doi:10.1002/(sici)1097-0290(19991220)65:6<659:aid-bit6>3.0.co;2-9
132. Kim, Y.M., Park, M.R., Song, S.C.: Injectable polyplex hydrogel for localized and long-term delivery of siRNA. ACS Nano **6**(7), 5757–5766 (2012). doi:10.1021/nn300842a

133. Park, K.H., Song, S.C.: Morphology of spheroidal hepatocytes within injectable, biodegradable, and thermosensitive poly(organophosphazene) hydrogel as cell delivery vehicle. J. Biosci. Bioeng. **101**(3), 238–242 (2006). doi:10.1263/jbb.101.238
134. Potta, T., Chun, C., Song, S.C.: Chemically crosslinkable thermosensitive polyphosphazene gels as injectable materials for biomedical applications. Biomaterials **30**(31), 6178–6192 (2009). doi:10.1016/j.biomaterials.2009.08.015
135. Potta, T., Chun, C., Song, S.C.: Injectable, dual cross-linkable polyphosphazene blend hydrogels. Biomaterials **31**(32), 8107–8120 (2010). doi:10.1016/j.biomaterials.2010.07.029
136. Potta, T., Chun, C., Song, S.C.: Dual cross-linking systems of functionally photo-cross-linkable and thermoresponsive polyphosphazene hydrogels for biomedical applications. Biomacromolecules **11**(7), 1741–1753 (2010). doi:10.1021/bm100197y
137. Potta, T., Chun, C., Song, S.C.: Controlling the degradation rate of thermoresponsive photo-cross-linked poly(organophosphazene) hydrogels with compositions of depsipeptide and PEG chain lengths. Polym. Degrad. Stab. **96**(7), 1261–1270 (2011). doi:10.1016/j.polymdegradstab.2011.04.010
138. Potta, T., Chun, C., Song, S.C.: Rapid photocrosslinkable thermoresponsive injectable polyphosphazene hydrogels. Macromol. Rapid Commun. **31**(24), 2133–2139 (2010). doi:10.1002/marc.201000350
139. Potta, T., Chun, C., Song, S.C.: Design of polyphosphazene hydrogels with improved structural properties by use of star-shaped multithiol crosslinkers. Macromol. Biosci. **11**(5), 689–699 (2011). doi:10.1002/mabi.201000438

Designing Hydrogels by ATRP

Haifeng Gao, Nicky Chan, Jung Kwon Oh and Krzysztof Matyjaszewski

Abstract This review summarizes the recent progress on the synthesis and application of covalently crosslinked hydrogels prepared using atom transfer radical polymerization (ATRP) technique. ATRP has been employed as an effective means to synthesize well-controlled polymeric materials with narrow molecular weight distributions, compositions, chain-end functionalities, and macromolecular architectures. These ATRP-processed materials include not only linear polymer chains but also various branched architectures such as star, gradient, and graft copolymers with a very high grafting density. The techniques can be successfully used in water under homogeneous or heterogeneous conditions opening new avenues for the preparation of hydrogels and other networks, including functional materials, responsive, injectable and supersoft elastomers suitable for multiple bio-related applications.

Keywords ATRP · Hydrogel · Hydrophilic monomers · Gel points · Emulsion · Heterogeneous media

H. Gao (✉)
Department of Chemistry and Biochemistry, 365 Stepan Chemistry Hall, University of Notre Dame, Notre Dame, IN 46556, USA
e-mail: hgao@nd.edu

N. Chan · J.K. Oh (✉)
Department of Chemistry and Biochemistry and Center for Nanoscience Research, Concordia University, Montreal, QC H4B 1R6, Canada
e-mail: John.Oh@concordia.ca

K. Matyjaszewski (✉)
Department of Chemistry, Carnegie Mellon University, 4400 Fifth Avenue, Pittsburgh, PA 15213, USA
e-mail: km3b@andrew.cmu.edu

X.J. Loh (ed.), *In-Situ Gelling Polymers*, Series in BioEngineering,
DOI 10.1007/978-981-287-152-7_4

1 Introduction

Hydrogels are hydrophilic polymer networks that can be swollen in water. Special features of hydrogels include their three-dimensional (3D) physical structure, good mechanical property, high water content, tunable chemical composition and functionality. These advantages attract significant commercial attention to hydrogel materials for a broad number of applications including super-absorbents, polymer catalysts, tissue scaffolds, biomedical implants and biomedicines [1–4]. In addition, hydrogels can be easily hybridized with various inorganic materials, such as clays, silica, fullerenes, carbon nanotubes and graphenes, to achieve specific properties and functions.

The hydrogels are hydrophilic polymer network that can be crosslinked via either physical interactions or covalent bonds. Physically crosslinked hydrogels have been prepared based on various physical interactions, including hydrogen bonds, crystallization, hydrophobic interactions, stereo-complexation, sol-gel transition, host-guest interactions and aggregation. The physical hydrogels benefit from the ability to participate in reversible degradation into the corresponding precursors under appropriate conditions. Alternatively, polymer networks based on covalent chemical bonds are prepared by chemical crosslinking reactions [5–10]. The most common strategy among the various chemical crosslinking reactions employed to prepare covalently crosslinked hydrogels, is the use of radical copolymerization of hydrophilic monomers and crosslinkers in water or polar solvents. The polymerization of crosslinkers connects multiple linear primary chains into one branched molecule with high molecular weight. Gelation occurs when the system changes from a viscous liquid (sol) to an elastic gel.

Over the last two decades, the field of polymer chemistry has witnessed an explosive development of a number of procedures for conducting a controlled/"living" radical polymerization (CRP) [11, 12]. CRP allows for synthesis of various types of functional polymeric materials and provides the capability of designing polymers with controlled molecular weight and molecular weight distribution (MWD), in addition to controlled chemical composition, chain-sequence distribution, site-specific functionality and predeterminable topology [11, 13–16]. Various CRP techniques, including atom transfer radical polymerization (ATRP) [17–23], nitroxide mediated polymerization (NMP) [24–26] and reversible addition fragmentation chain transfer (RAFT) [27–30] polymerization, have been applied in the copolymerization of monomers and crosslinkers to synthesize either soluble branched polymers or insoluble polymer networks.

This review summarizes the recent progress on the synthesis and application of covalently crosslinked hydrogels prepared using ATRP techniques. Section 2 briefly covers the fundamentals of the ATRP mechanism with particular emphasis on the recent progress to understand the structure/reactivity relationship and the development of new ATRP conditions that decrease the amount Cu catalyst. In Sect. 3, theoretical gel points and experimental gel points based on vinyl conversions are described. Emphasis focuses on understanding of the gelation process in

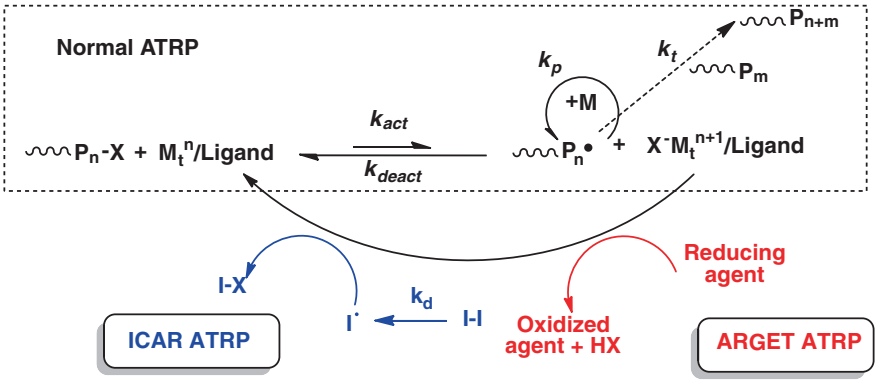

Scheme 1 General schemes for normal ATRP, ARGET and ICAR ATRP processes

ATRP and the influence of various experimental parameters on the experimental gel points. Section 4 discusses the development of aqueous ATRP in both homogenous and biphasic heterogeneous media. Sections 5–7 discuss the preparation of hydrogels and nanogels by ATRP and their applications, particularly as biomaterials. Section 8 summarizes the development of one-component supersoft gels using ATRP. Supersoft materials are as soft as hydrogels but contain no solvent and will never dry. It is followed by a brief section providing some conclusions.

2 ATRP Fundamentals

The rapid development of CRP techniques over the last two decades has resulted in the synthesis of various types of hydrophilic polymers with predeterminable molecular weights, distributed functionalities, and controlled architectures tailored for an expanding number of applications. All CRPs proceed through the same radical intermediates as conventional radical polymerization (RP) and therefore exhibit similar chemo-, regio- and stereo-selectivities [12]. However, in contrast to conventional RP, a fundamental feature of all CRPs is that the reactions are based on creation of a dynamic equilibrium between a low concentration of propagating radicals and a large amount of dormant reactivatable species. Specifically in ATRP, the dormant species, predominately in the form of alkyl halide initiators (R–X) and the corresponding macromolecular species (P–X) [31] periodically react with transition metal complexes in their lower oxidation state (activators) to intermittently form propagating radicals and deactivators in their higher oxidation states (Scheme 1). Thus, ATRP is a catalytic process and is kinetically controlled by the persistent radical effect (PRE) [32–34] in which every radical–radical termination leads to an irreversible accumulation of deactivator and shifts the equilibrium towards the dormant species consequently decreasing the probability

of termination reactions. ATRP is different from NMP, which is another PRE-regulated reaction that requires a stoichiometric amount of mediating agent (e.g., nitroxides) to cap all dormant chains. ATRP allows use of sub-stoichiometric amounts of metal catalysts because the catalytic process employs a halogen atom (or pseudo-halogen group) as the capping group [35–40].

2.1 Structure/Reactivity

Equilibrium constants in an ATRP depend on the reaction medium, the structure of the initiators, monomers and catalysts. Generally speaking, the ATRP equilibrium constants (K_{ATRP}) increase strongly with solvent polarity by better stabilization of the more polar Cu(II) species thereby decreasing the deactivation rate. The activation rate constants (k_{act}) are significantly affected by the structure of the N-containing ligands [41] and the alkyl halide initiators [42]. In contrast, the deactivation rate constants (k_{deact}) are usually very high and may approach diffusion control limits ($k_{deact} > 10^7\ M^{-1}\ s^{-1}$). They are less influenced by the structure of the involved reagents than the activation rate constants. Figures 1 and 2 show how k_{act} varies with the ligand structure and

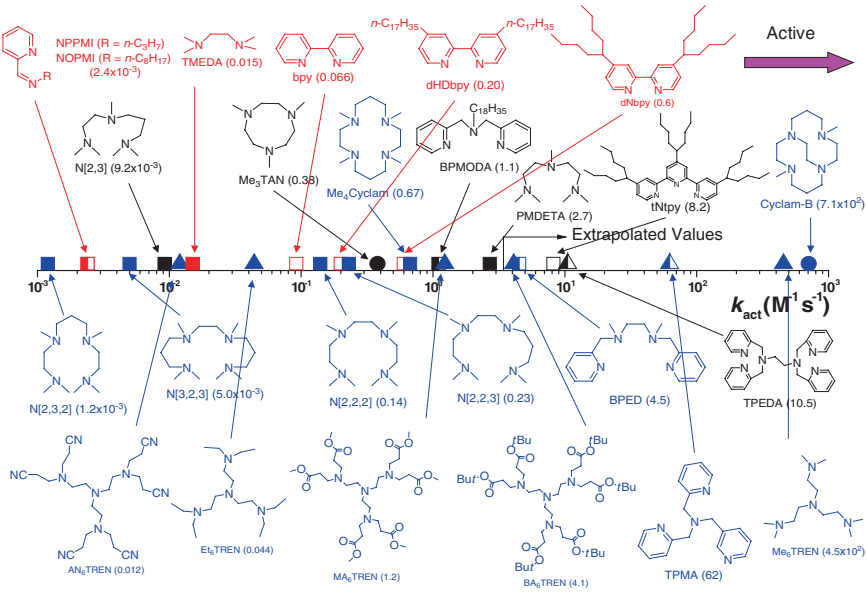

Fig. 1 Effect of ligand structures on ATRP activation rate constants (k_{act}) with ethyl 2-bromoisobutyrate (*EtBriB*) activated by Cu^IBr complexes in the presence of MeCN at 35 °C. N2: *red*; N3: *black*; N4: *blue*; amine/imine: *solid*; pyridine: *open*; mixed: *left-half solid*; linear: *open square*; branched: *filled triangle*; cyclic: *open circle*. Reprinted with permission from American Chemical Society [41]

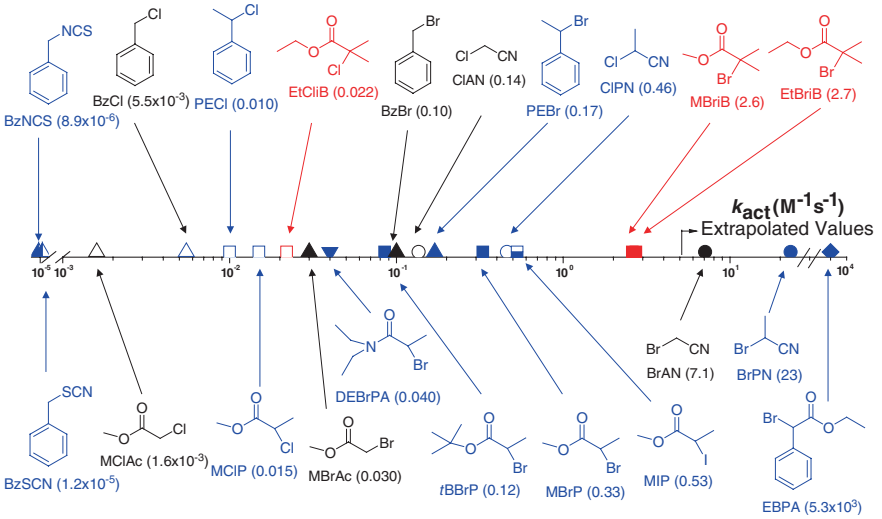

Fig. 2 Effect of initiator structures on ATRP activation rate constants (k_{act}) with $Cu^{I}X$/N,N,N′,N′,N″-pentamethyldiethylenetriamine (*PMDETA*) (X = Br or Cl) in MeCN at 35 °C. 3°: *red*; 2°: *blue*; 1°: *black*; isothiocyanate/thiocyanate: *left half-filled*; chloride: *open*; bromide: *filled*; iodide: *bottom half-filled*; amide: *inverted filled triangle*; benzyl: *filled triangle*; ester: *open square*; nitrile: *open circle*; phenyl ester: *open diamond*. Reprinted with permission from American Chemical Society [42]

selected alkyl (pseudo)halides. The range of k_{act} spans over six orders of magnitude and an examination of the structure of the ligands shows that the general order of Cu complex activity for ligands is: tetradentate (cyclic-bridged) > tetradentate (branched) > tetradentate (cyclic) > tridentate > bidentate ligands. Bridged cyclam (Cyclam–B), tris(2-dimethylaminoethyl)amine (Me_6TREN) and tris(2-pyridylmethyl)amine (TPMA) are among the most active while 2,2′-bipyridine (bpy) and pyridineimine are the least active. The nature of the nitrogen atoms in the ligands also plays a role in the activity of the Cu complexes and follows the order pyridine ≈ aliphatic amine > imine < aromatic amines. Generally, alkyl amines complex to Cu(II) more strongly than pyridines. A C2 bridge between N atoms generates complexes with higher activities than those with C3 or C4 bridges. Steric effects around the Cu center are very important, with a Me_6TREN catalyst complex being 10,000 times more active than the Et_6TREN complex [41]. Electronic effects are also very important and copper complexes formed with bpy containing two p-dimethylamino groups are 10^6 times more active than the unsubstituted ligand and a substituted TPMA, formed from three 3,5-dimethyl-4-methoxypuridine rings, is 10^3 times more reducing than TPMA [43, 44].

The reactivity of different alkyl halides in ATRP depends on the structure of the alkyl group and transferable (pseudo)halogen. It is important to select a sufficiently reactive species for an efficient ATRP initiation of the polymerization

of the selected monomer. Reactivity of alkyl halides follows the order of 3° > 2° > 1°, in agreement with the bond dissociation energy needed for homolytic bond cleavage. Also, radical stabilization is enhanced by the presence of a α-cyano group which is more activating than either a α-phenyl or ester group. Ethyl α-bromophenylacetate, which combines the activation effect of both benzyl and ester species, is the most active initiator and is >10,000 times more reactive than 1-phenylethyl bromide (PEBr) and >100,000 times more active than methyl 2-bromopropionate (MBrP). The reactivity of alkyl halides follow the order I > Br > Cl and is higher than that of alkyl pseudohalides [42].

In ATRP, the dynamics of the exchange reactions may be even more important than the overall values of the equilibrium constants. Radicals must be very quickly deactivated, and the value of k_{deact} should be as large as possible. This requires very rapid rearrangement of the catalyst complex from the L/Cu(II)–X to L/Cu(I) species, resulting from minimal reorganization of the complex, as accomplished with branched tetrapodal ligands. Figures 3a, b [31, 45] show the correlation of k_{act} and k_{deact} with K_{ATRP} for various $Cu^{I}Br$/ligand complexes with a standard alkyl halide, ethyl 2-bromoisobutyrate (EtBriB), and for various initiators in the presence of a Cu^{I}/TPMA at 22 °C in MeCN. The equilibrium constants increase as a consequence of a large increase in k_{act} accompanied by a small decrease in k_{deact}. The ideal catalyst for ATRP of less reactive monomers, or when used at lower concentrations, should have a large value for K_{ATRP} (i.e., larger k_{act}) but also preserve a very large value for k_{deact}. The values of equilibrium and rate constants in ATRP scale very well with the electrochemical activity of the complexes, as shown in Fig. 4 [31, 46]. A complex with a 300 mV more negative redox potential is ca. 100,000 times more reactive than the less reducing catalyst complex.

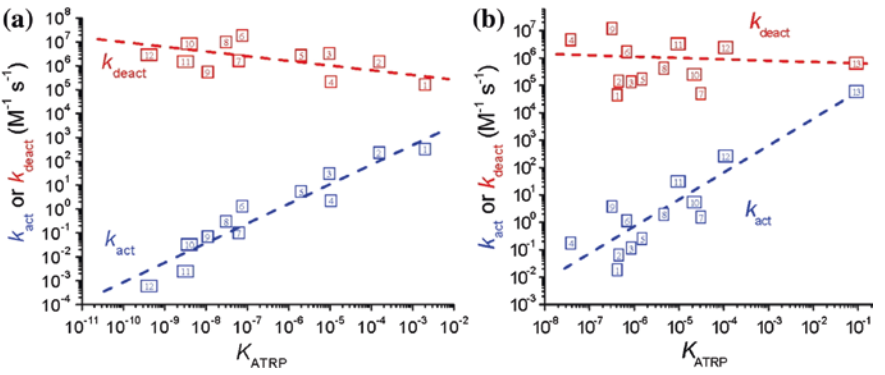

Fig. 3 **a** Ligands: *1* Cyclam-B, *2* Me6TREN, *3* TPMA, *4* BPED, *5* TPEDA, *6* PMDETA, *7* BPMPA, *8* dNbpy, *9* HMTETA, *10* bpy, *11* N4[3,2,3], *12* N4[2,3,2]. **b** Initiators: *1* MClAc, *2* BzCl, *3* PECl, *4* MClP, *5* EtCliB, *6* BzBr, *7* ClAN, *8* PEBr, *9* MBrP, *10* ClPN, *11* EtBriB, *12* BrPN, *13* EBPA. Reprinted with permission from American Chemical Society [45]

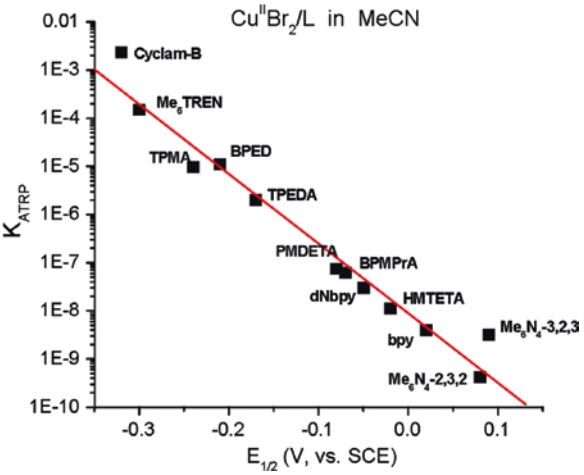

Fig. 4 Correlation between K_{ATRP} and redox potentials of different ATRP active $CuBr_2$/L complexes in MeCN at 25 °C. Reprinted with permission from American Chemical Society [46]

2.2 New Developments for ppm Cu

ATRP procedures have evolved significantly since the seminal report in 1995 [19] with continuous developments in normal ATRP and reverse ATRP [47, 48] resulting in simultaneous reverse and normal initiation (SR&NI) [35, 49] ATRP, activators generated by electron transfer (AGET) [36, 37] ATRP, activators regenerated by electron transfer (ARGET) [38–40] ATRP, initiators for continuous activator regeneration (ICAR) [40] ATRP, zero-valent metals as supplemental activators and reducing agents (SARA) ATRP [31, 50–54], photoATRP [55] and electrochemical ATRP (*e*ATRP) [56]. All these developments were supported by a constant motivation to ultimately develop ATRP into a powerful and robust technique applicable in different environments to a broad range of monomer species under facile polymerization conditions. Particularly, the recent progress on ARGET ATRP, ICAR ATRP, SARA ATRP and *e*ATRP allows for a significant decrease in the amount of copper catalyst in the reactions, down to ppm levels, without sacrificing control over the polymerization. The low amount of added Cu catalysts is continuously regenerated either by a reducing agent, e.g., in ARGET ATRP and SARA ATRP, or by radicals decomposed from conventional radical initiator in ICAR ATRP, or by electric potential in *e*ATRP to compensate for the unavoidable low fraction of radical termination reactions. The initial addition of excess amounts of reducing agents and radical initiators can even consume the inhibitors and limited amounts of air in the system before activating the Cu(II) species simplifying the steps of monomer purification and deoxygenation procedures.

Therefore, the steady progress in understanding ATRP procedures has allowed ATRP to become a robust controlled polymerization technique employed by numerous material scientists, and non-polymer specialists, to carry out their own polymerizations in a facile setup to produce the materials

of interest for their specific needs. Since its invention, ATRP has been broadly applied to the preparation of well-defined polymers with controlled chemical compositions, molecular weights and MWDs, chain sequence distributions, functionalities and topologies.

3 Networks and Crosslinking in ATRP

Radical polymerization of monovinyl monomers with divinyl crosslinkers has been broadly used for synthesis of various branched copolymers and gels. During the copolymerization, incorporation of a free crosslinker unit into the growing chain generates a pendant vinyl group which is consumed via its reaction with a propagating radical to produce a crosslinkage. The molecular weight and/or size of the branched polymers increase rapidly with the progress of intermolecular crosslinking reactions, and finally reach an "infinite" value with the formation of a polymeric network (gel). The transition from sol to gel is defined as the "gel point". It is evident that accurately predicting the gel point in a polymerization reaction is critical when the synthesis is targeting either a soluble branched polymer or an insoluble gel.

In the 1940's, Flory and Stockmayer developed a statistical mean-field theory (FS theory) for an ideal polymer network based on two assumptions: (1) equal reactivity of all vinyl species and (2) absence of intramolecular cyclization reactions. The FS theory pointed out that the theoretical gel point should occur when the weight-average number of crosslinking units per primary chain reached unity [57, 58] Eq. 1, derived from the FS theory, indicates that the theoretical gel point (p_c) based on the conversion of vinyl groups is determined by the concentration of primary chains $[PC]_t$ at time t, the initial concentration of divinyl crosslinker ($[X]_0$), and the polydispersity of primary chains (M_w/M_n) [59]

$$p_c = \sqrt{\frac{[PC]_t}{2[X]_0} \frac{1}{M_w/M_n}} \tag{1}$$

The theoretical gel point based on the FS theory provides important guidelines for experimental designs seeking to obtain branched polymers and gels, although the assumptions, particularly the "no intramolecular cyclization" assumption, are not completely valid during the experiments [8, 60–62]. When soluble branched polymers are targeted during the polymerization of monomer and crosslinker, the reaction should be stopped before the critical gel point (p_c) in order to exclusively obtain soluble sols. Based on Eq. 1, several strategies are applicable in order to delay gelation in a system and push gelation to higher conversion, including: (1) increasing the initial primary chain concentration [63–67] e.g., using more initiator or chain transfer agent; (2) using initiators with high initiation efficiency; [68] (3) using less crosslinker; and (4) stopping the reaction at lower monomer conversion. Furthermore,

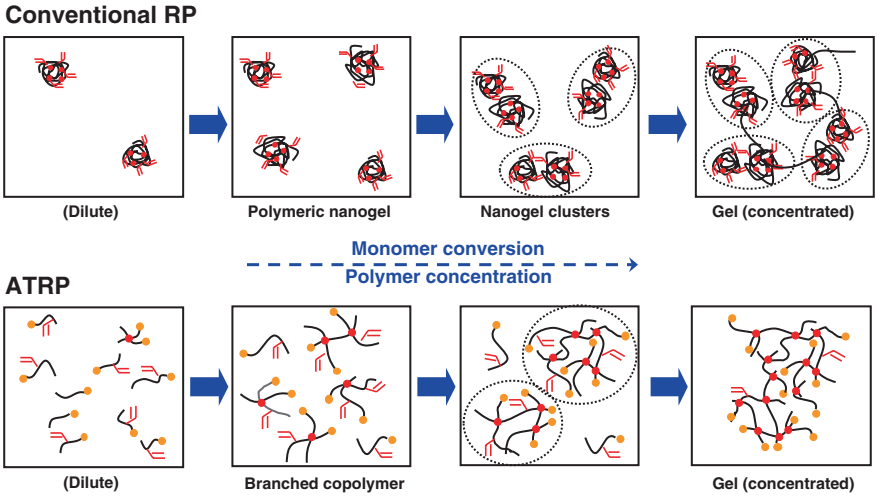

Scheme 2 Different gelation processes in conventional RP and ATRP. Reprinted with permission from Elsevier [59]

intramolecular cyclization reactions could be enhanced by performing the copolymerization under dilute conditions [69] in a selective solvent and/or in a confined space [70] e.g., emulsion, which usually delays and prevents macroscopic gelation and produces microgels.

Highly branched polymers and/or gels with inhomogeneous structures are formed during most conventional RP reactions due to the intrinsic limitations of the RP method, which include slow initiation, fast chain propagation, and exclusive radical termination reactions [5, 8, 71–73]. Due to the slow initiation, primary radicals are slowly but continuously generated in the system, resulting in formation of a very dilute polymer solution at the beginning ($[PC]_t \sim \mu M$). Thus, based on Eq. 1, a conventional RP reaction with bulk condition ($[M]_0 = 10$ M), 1 mol% of crosslinker ($[X]_0 = 0.1$ M) and $M_w/M_n = 2$ for the primary chains should gel at very low conversion, e.g., $p_c = 0.16$ %,. However, the experimental gel point based on monomer conversion in conventional RP is typically 1 or 2 orders of magnitude larger than the predicted value. This is mainly due to an excluded volume effect of polymer chains in dilute conditions and a significant contribution of intramolecular cyclization reactions (Scheme 2) [5, 8, 74]. At the beginning of the polymerization, the polymer chains formed in the reaction contain numerous pendent vinyl groups, but seldom overlap with each other because of the extremely low polymer concentration. Consequently, most of the pendent vinyl groups are consumed via intramolecular cyclization reactions, producing a less-swollen nanogel with highly crosslinked domains. As the reaction proceeds, the number of these nanogels increases and radicals generated later in the reaction connect these preformed overlapping nanogels into a macroscopic heterogeneous network [5, 8, 59].

In contrast to conventional RP, ATRP has several advantages that allow the preparation of more homogeneous polymer networks, due to the fast initiation and reversible deactivation reactions. Fast initiation reactions, relative to propagation reactions, result in a quick conversion of all initiators into primary chains and a nearly constant number of growing primary chains throughout the polymerization (Scheme 2). The dynamic equilibrium between a low concentration of growing radicals and a significantly higher fraction of dormant species ensures a slow but steady chain growth providing even incorporation of vinyl groups (from monomers, crosslinkers and pendent vinyl groups) into the polymer chains. Therefore, the branched sols and/or gels synthesized by an ATRP process have a more homogeneous structure than the polymers synthesized by a RP method at similar concentrations of monomers and crosslinkers [75]. In addition, the chain-end functionalities are preserved in the branched polymers and/or gels synthesized by ATRP, and can be further used for chain-end modification and chain extension reactions [76, 77].

Several research groups have exploited ATRP [78–82] as well as other CRP [75, 77, 83–87] of monomers and crosslinkers to study the gelation kinetics and synthesize soluble branched polymers. All these studies indicate a deviation of experimental gel points from the theoretical values, which is generally believed to be due to the unavoidable intramolecular cyclization reactions (both primary and secondary cyclizations) that consume pendant vinyl groups, but have no contribution to an increase in the molecular weight of the polymers. For instance, in an ATRP system with high initiation efficiency and good control over the dispersity of primary chains (low M_w/M_n), no gelation was observed when the initial molar ratio of crosslinker to initiator was less than 1, even under bulk conditions with complete conversion [80, 81, 88]. This result indicates that at least half of the vinyl groups in the crosslinker were consumed via intramolecular cyclizations.

The extent of cyclization reactions occurring during the copolymerization can be controlled by adjusting the initial concentration of reagents. For instance, during the ATRP of methyl acrylate (MA) and ethylene glycol diacrylate (EGDA) at fixed molar ratios of monomer, crosslinker and initiator, simply diluting the system, via addition of more solvent, dramatically postponed, or even prevented, the experimental gel point at higher monomer conversion, i.e., longer reaction time, than the value based on FS theory [89]. On the other hand, enhanced intramolecular cyclization can also be a practical method to produce soluble branched polymers when copolymerizing, or even homo-polymerizing, multivinyl crosslinkers. Since low-cost multivinyl crosslinkers are readily available, radical polymerization of crosslinkers represents a facile method to produce soluble (hyper)branched polymers. Common methods employed to avoid macroscopic gelation, include the use of (a) dilution, (b) high concentration of initiators, and (c) high concentration of transfer agents. Recently, a novel method named deactivation-enhanced ATRP was reported [90–92] that produced soluble cyclized polymers through homopolymerization of divinyl crosslinker by forming and keeping a high ratio of Cu(II) to Cu(I) in the reaction medium to

significantly decrease the kinetic chain length of a propagating radical during one activation/deactivation cycle.

Although intra-molecular cyclization has been well documented as the probable reason for delayed experimental gelation, it remains a challenge to quantify the degree of cyclization, primary due to the complicated structure of the branched polymers and the multiple pathways in the kinetics. However, very recently, two reports partially addressed this issue by designing a specific crosslinker [93] and/or polymerization system [94]. A disulfide-based divinyl crosslinker was used for RAFT copolymerization with methyl methacrylate (MMA). The interesting observation was that the disulfide crosslinker that participated in primary cyclization reactions showed different NMR shifts from the crosslinkers that reacted in inter-molecular reactions. The distinguished NMR shifts resolved in the spectrum was used to quantify the amount of primary intra-molecular reactions, although secondary cyclization are still elusive.

4 ATRP in Water and Formation of Water Soluble Polymers

Water is a safe, inexpensive and environmentally benign solvent that has been broadly used in industrial scale processes for conventional solution RP of hydrophilic monomers and for biphasic heterogeneous-mediated polymerizations of hydrophobic monomers (oil-in-water) and hydrophilic monomers (water-in-oil). Therefore it was highly desirable to develop conditions that allowed conducting ATRP in aqueous media [95–100].

4.1 Homogeneous Aqueous ATRP

Several groups have reported the ATRP of hydrophilic monomers (Scheme 3) in aqueous systems [24, 95, 97, 100–109]. However, in many cases, the level of control over the ATRP reactions was limited, leading to production of materials with broad MWD, significant tailing to low molecular weight, low initiation efficiency and loss of chain-end initiating groups [102, 103, 107]. There are several challenges associated with conducting an ATRP in water. First, the larger ATRP equilibrium constant in aqueous media generates a high concentration of radicals and consequently increases the rate of termination reactions. Second, the partial dissociation of halide ion from deactivator complex leads to loss of deactivator and inefficient deactivation of propagating radicals. Third, certain Cu(I)/L complexes disproportionate in water. Fourth, the potential hydrolysis of carbon-halogen bond diminishes chain–end functionality.

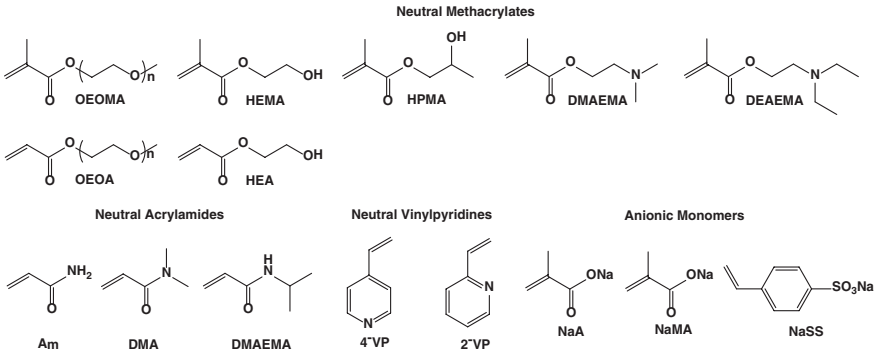

Scheme 3 Chemical structures of common hydrophilic monomers

To overcome these issues, conditions were intentionally developed that allowed ATRP in water to be performed: (a) creating a high ratio of Cu(II)/Cu(I), (b) using a high overall concentration of copper catalyst, (c) using excess of halide salts [95, 97, 110] (d) selecting a ligand, such as TPMA with significant Cu/TPMA stability in water [111] and (e) using chlorine as the chain end rather than bromine [42, 45] to reduce the concentration of radicals, and to minimize the loss of deactivator and polymer chain ends. Very recently, a few reports have demonstrated the preserved chain-end halide functionality for successful chain extension with another polymer block in a second batch reaction [97, 108].

The first well controlled ATRP of oligo(ethylene oxide) methacrylate (OEOMA) in water was reported in which excess amount of halide salts were intentionally added to suppress the dissociation of Cu(II) deactivators [11, 95]. In another report, a Cu(0) powder and large amount (10,000 ppm) of Cu(II) was generated by pre-disproportionation of CuBr/Me_6TREN in water before addition of monomer and initiator for the ATRP of *N*-isopropyl acrylamide (NIPAM), *N*,*N*-dimethyl acrylamide (DMA), oligo(ethylene oxide) acrylate (OEOA) and 2-hydroxyethyl acrylate (HEA) monomers [108]. The polymerization showed well controlled polymer chain structure with preserved bromine chain-end functionalities.

Alternatively, ATRP has been successfully conducted in organic solvents that dramatically decrease the K_{ATRP} equilibrium constants as compared to those in pure aqueous systems. The organic solvents suitable for the ATRP of hydrophilic monomers are largely determined by the solubility of the monomers and the produced polymers in the solvent. Several organic solvents, including dichlorobenzene [112], anisole [113], toluene [114], DMF, DMSO, alcohols [115–118] and their mixtures [119] have been successfully applied to the synthesis of neutral hydrophilic polymers of PHEMA, PDMAEMA and POEOMA (Scheme 3). When charged monomers are used in the ATRP for direct synthesis of charged polyelectrolytes, the choice of organic solvents becomes more limited and sometimes, water becomes an essential co-solvent, together with organic solvents including alcohol [120–122] DMF [123] DMSO and pyridine, to dissolve the polyelectrolytes and achieve a homogenous system.

4.2 ATRP in a Heterogeneous Oil–in–Water System

The interest in applying ATRP to aqueous dispersed media arose soon after the invention of ATRP. Initial attempts at conducting an ATRP in aqueous dispersed media, in particular, emulsion media were reported in early 1998 [124]. CuBr/bpy was used as catalyst and sodium dodecyl sulfate (SDS) was used as surfactant for ATRP of MMA at 60–80 °C. In spite of the relatively high polymer yield, the MWD was broad, indicating a poorly controlled polymerization. These initial failures were due to the problems associated with the partitioning and poisoning of the catalysts in the aqueous phase but stimulated extensive research on determining the feasibility and criteria required for a well-controlled ATRP in aqueous dispersed media [125–130]. In other words, the multiphase nature of aqueous dispersed media added new requirements to identify appropriate ligands, surfactants and even initiation methods to conduct a well-controlled ATRP. For instance, the chosen ligands should be highly hydrophobic since the Cu(II) species are usually more soluble and less stable than Cu(I) species in water. A hydrophobic ligand can complex with Cu(II) and minimize migration of deactivators into the aqueous phase, which was the main reason of the loss of control and excess termination in the initial experiments. A further consideration is that all the Cu/ligand complexes must be fully soluble in the monomer, unlike bulk or solution processes where heterogeneous catalysts are commonly used. The chemical structures of hydrophobic ligands reported to be successfully applied in ATRP in aqueous dispersed systems are shown in Scheme 4.

The choice of surfactants for ATRP in aqueous dispersed system is also critical. A good surfactant for a controlled ATRP in aqueous dispersed media should not only provide a stable dispersed system throughout the polymerization, but also have minimal interference in the equilibrium between the radicals and the dormant species. Therefore, anionic surfactants showed little success in ATRP since they interact with ATRP catalysts, especially the Cu(II) complexes. To date, non-ionic

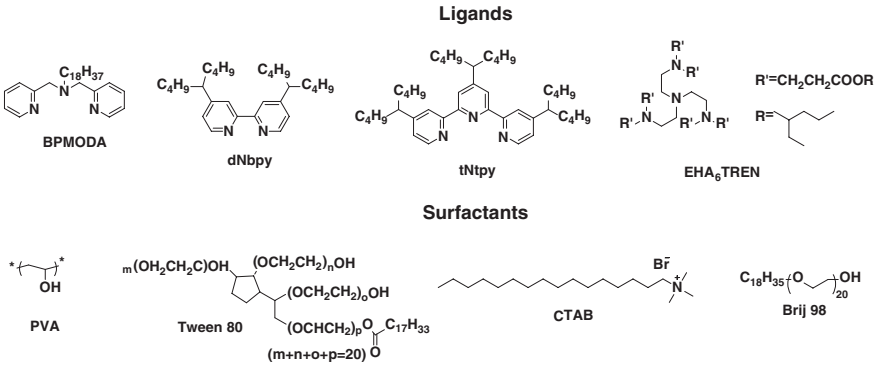

Scheme 4 Chemical structures of commonly used ligands and surfactants for ATRP in aqueous dispersed media

surfactants with hydrophilic lipophilic balance (HLB) values close to 14, such as commercially available polyoxyethylene(20) oleyl ether (Brij 98) were successfully applied to a controlled ATRP in aqueous dispersed media. Okubo et al. also reported the use of Tween 80 [131] and poly(vinyl alcohol) (PVA) [132] as nonionic surfactants for ATRP. Cationic surfactants, such as cetyltrimethylammonium bromide (CTAB), have also been used successfully for a controlled ATRP as well as preparation of stable latex particles [133]. The chemical structures of these surfactants are also illustrated in Scheme 4.

Another critical issue related to a controlled ATRP in aqueous dispersed media, in addition to the selection of proper ligands and surfactants, is the initiation technique. The biphasic nature of heterogeneous media precludes freeze-pump-thaw or vigorous N_2-bubbling to completely remove the oxygen from the reaction medium. As a result, any ATRP formulation with an initial addition of air-sensitive Cu(I) species could lose part of the Cu activator before initiating polymerization [134]. This issue is more pronounced in miniemulsion because it is very difficult to prevent oxygen diffusing into the samples during the ultrasonication procedure that is necessary for preparation of the submicron monomer droplets prior to polymerization [135]. Thus, ATRP techniques that start from air-stable Cu(II) species in the formula are desirable for conducting ATRP in aqueous dispersed systems. For instance, conducting a reverse ATRP of *n*-butyl methacrylate (*n*BMA) in an aqueous dispersed system using a water-soluble initiator (V-50), a nonionic surfactant (Brij 98), and a hydrophobic ligand (dNbpy) provided a controlled miniemulsion polymerization, as indicated by a linear increase of molecular weight with monomer conversion and a narrow MWD [134]. In another study, Simms and Cunningham reported a successful reverse ATRP of *n*BMA in miniemulsion using a cationic emulsifier, CTAB, at 90 °C with EHA_6TREN as ligand and VA-044 as thermal initiator [133]. A loading of CTAB as low as 1 wt%, relative to monomer, provided sufficient colloidal stability, i.e., a concentration considerably lower than that required when a nonionic surfactant, Brij 98, was used.

The successful development of SR&NI [49, 136, 137] ATRP, AGET [36, 138–143] ATRP and ARGET ATRP [144–146] significantly expanded the number of ATRP procedures that can be used in aqueous dispersed systems. The recent development of super-hydrophobic ligands with longer alkyl chains significantly decreased the partitioning of Cu(II) complexes in water and allowed the amount of catalyst to be as low as 50 ppm Cu while maintaining control in miniemulsion ATRP [145, 146]. In addition to the synthesis of linear and branched polymers, crosslinked latex particles containing degradable disulfide crosslinks were also prepared in miniemulsion by using SR&NI ATRP [147]. The efficient degradation of the latex particles into homopolymers, upon the addition of tri(*n*-butyl) phosphine reducing agent, was monitored by dynamic light scattering (DLS) measurements. When reactive surfactants with dual reactive sites were used, the polymerization provided direct methods to introduce surface and core functionalities into the nanoparticles for advanced applications [148, 149].

Most of the early reports of successful ATRP in aqueous dispersed media employed miniemulsion systems, since an ideal miniemulsion system has no mass transport

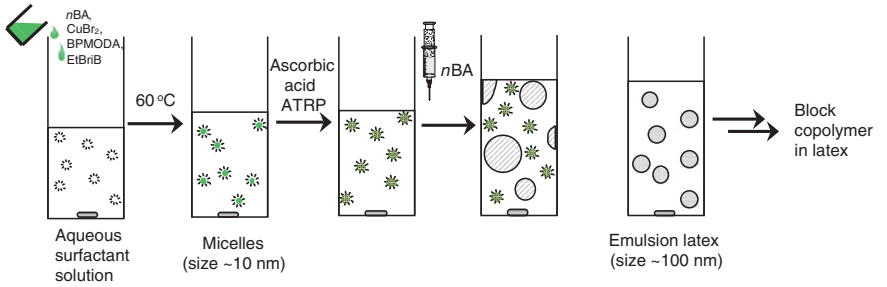

Scheme 5 Schematic illustration of a seeded emulsion ATRP using a continuous two-step procedure. Reprinted with permission from Springer [135]

between different droplets, indeed the miniemulsion system behaves as a mini-bulk system. In contrast, conducting a successful ATRP in a classic emulsion system is not straightforward because of the ineffective transport of hydrophobic catalysts from monomer droplets to polymerizing particles through aqueous phase. Instead, a two-step seeded emulsion polymerization was more practical than a classic emulsion polymerization since the catalysts can be confined to the seed particles [131]. In 2006, an effective two-step ab initio ATRP emulsion system was reported [138] in which an emulsion was formed by adding pure monomer to an ongoing microemulsion ATRP [141]. This ab initio emulsion method (Scheme 5) ensured that all ATRP initiators, catalysts and a small amount of monomer were encapsulated into microemulsion micelles in the absence of any high shear environment. After activating the catalyst and initiating the reaction, the rest of the pure monomer was fed to the polymerization system. During the polymerization, monomer diffused from monomer droplets to the polymerizing particles containing the catalyst, thereby mimicking a "normal" emulsion system. This procedure avoids the need to transport catalysts through the aqueous media during the polymerization and therefore facilitates a controlled ATRP in the active latex particles. The surfactant concentration was efficiently decreased to ~2 wt% (~10 wt% vs. monomer) by decreasing catalyst concentration and changing the ratio of the monomer added to the microemulsion stage and the monomer added afterwards to form the emulsion. A controlled emulsion ATRP was obtained, leading to the synthesis of polymers with narrow MWD ($M_w/M_n = 1.2–1.4$). In addition, copolymerization of monomers and divinyl crosslinkers in the microemulsion ATRP stage led to the direct synthesis of hairy nanoparticles in one-pot [139].

4.3 ATRP in an Inverse Water–in–Oil System

ATRP in inverse miniemulsion [150] and microemulsion [151] polymerizations has been applied to the production of water-soluble POEOMA homopolymer and copolymers. The first successful ATRP in inverse miniemulsion described the synthesis of stable nanoparticles of well-controlled water-soluble POEOMA

with $M_w/M_n < 1.3$ [150, 152]. When a hydrophilic divinyl crosslinker is used as comonomer, the prepared water-dispersible nanogels possess several useful features, including the preserved halide initiating groups for further chain extension and latex modification, relatively narrow MWD of the degraded product (linear primary chains), and more homogenous nanogel structure with better swelling properties and degradation behavior [153, 154]. These crosslinked nanogels prepared by ATRP in inverse heterogeneous systems have been applied to encapsulation and delivery of various hydrophobic drugs [153] carbohydrates [154] and siRNA molecules [155]. Detailed discussion of the nanogels prepared by ATRP in inverse miniemulsion will be presented in Sect. 6.

5 Hydrogels Prepared by ATRP

Hydrogels are three-dimensional crosslinked networks of hydrophilic polymers possessing unique properties such as tunable chemical and physical structure, good mechanical properties, high water content, and biocompatibility [1, 2]. These unique properties offer great potential for the use of hydrogels as the material of choice for various applications in the field of regenerative medicine, tissue engineering, drug delivery, and bio-nanotechnology [156]. Recently, several efforts have been made to develop advanced hydrogels as microfluidic biomaterials for tissue scaffolds [157] inverse opal for photonic crystals [158] and biosensors for sensing and detection applications [159]. Hydrogels are generally prepared from hydrophilic polymer matrices that are crosslinked through physical or chemical crosslinking [4, 160]. Physical crosslinking utilizes supramolecular association typically through hydrogen bonds, crystallized domains, ionic interactions, hydrophobic interactions, stereo-complexation, host-guest interactions, and temperature-induced sol-gel transitions. These physically crosslinked gels feature the absence of toxic crosslinkers and provide reversible degradation into the corresponding precursors upon application of external stimuli. In contrast, chemical crosslinking is a more versatile method that allows for the synthesis of a stable crosslinked gel network through the formation of new covalent bonds. Well-defined organic reactions such as click-type reactions as well as various polymerization methods such as free radical polymerization and step-growth polycondensation in the presence of various crosslinkers have been explored. Recently, ATRP has been utilized for the construction of well-defined crosslinked nanomaterials in the presence of crosslinkers. This section describes how ATRP, as a single polymerization method or in combination with other methods, has been utilized for the development of advanced hydrogels, including thermoresponsive hydrogels, nanostructured hybrid hydrogels, and degradable hydrogels.

Thermoresponsive hydrogels can swell or deswell in response to changes in temperature, thus undergoing a volume change at low critical solution temperature (LCST) in water. Above the LCST, the hydrogels are hydrophobic and expel water; below the LCST, they are hydrophilic and absorb water [161, 162]. Due

to concerns on potential cytotoxicity of poly(N-substituted acrylamide)s, polymethacrylates with pendant oligo(ethylene oxide) units, i.e. POEOMA, present a promising alternative for the preparation of thermoresponive materials [163]. POEOMA-based polymers exhibit tunable LCST between 20 and 90 °C simply by varying the composition of the POEOMA with different numbers of EO units in the side chains [164]. One desirable characteristic for the development of thermoresponsive hydrogels is the ability to rapidly respond to changes in temperature thereby providing fast deswelling or volume change.

One limiting factor for generation of rapid thermoresponsiveness is the formation of an impenetrable hydrophobic "skin layer" on the surface of the material; this skin layer delays the release of water from the core of the hydrogel, which contributes to a slow LCST transition from hydrophilicity to hydrophobicity of thermoresponsive polymers [165–169]. Rapid response is achieved by allowing fast water release from the gel matrix, and preventing formation of skin layers on the surface of hydrogels caused by LCST transition of the thermoresponsive polymers. The use of ATRP techniques for the preparation of hydrogels has resulted in the preparation of materials that demonstrated rapid deswelling kinetics with higher swelling ratio at a temperature above LCST of the hydrogels, compared to counterparts prepared by conventional RP [170]. The rapid thermoresponsiveness of ATRP gels is attributed to the formation of homogenous and uniform networks. In contrast, FRP leads to non-uniform crosslinking [171]. Taking advantage of this, several approaches utilizing ATRP have been explored to enhance the release rate of water from thermoresponsive hydrogels (Fig. 5). A grafting strategy, utilizing incorporation of dangling polymeric chains from the thermoresponsive network of crosslinked hydrogels, was reported. The resulting hydrogels exhibit thermoresponsive properties which can be customized by changing grafting density, grafting chain length, and chain composition [178].

Strategies utilizing disulfide-thiol degradation chemistry have also been explored. Star-shaped macromolecular pore precursors, with degradable disulfide crosslinked cores and hydrophilic poly(ethylene oxide) (PEO) arms, were incorporated into the gel network. The cleavage of disulfide linkages generated thermoresponsive porous hydrogels with efficient water-release channels, suppressing skin layer formation, thus facilitating the release of water molecules [178]. Evaluation of these hydrogels from a biomedical perspective takes advantage of the fact that the porous thermoresponsive hydrogels are non-cytotoxic and exhibit enhanced release of encapsulated model drugs, suggesting potential application as effective tissue scaffolds.

Two approaches utilizing polymerizable POEOMA-based nanogels as multifunctional crosslinkers have been reported for the development of nanostructured hybrid hydrogels. The polymerizable crosslinked nanogels were prepared by post-polymerization modification of carboxylic acid (COOH)-functionalized nanogels with methacrylate groups. The methacrylate-functionalized nanogels were used as multi-functional crosslinkers for a photo-induced FRP of dimethacrylates [173] or thiol-ene polyaddition with hyaluronic acids having pendant thiols [174] yielding hydrogels covalently embedded with nanogels domains.

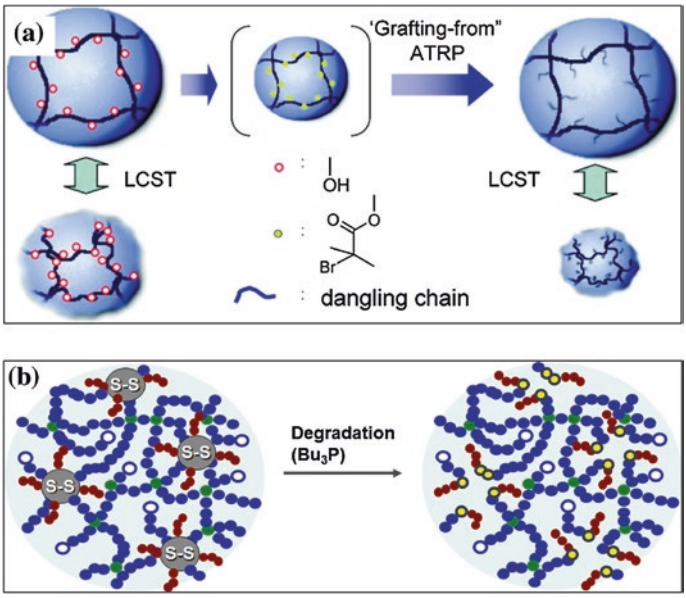

Fig. 5 Illustration of approaches utilizing ATRP to enhance the release rate of water from thermoresponsive hydrogels, including **a** grafting strategy [178] and **b** disulfide-thiol chemistry to generate nanopores [172]. Reprinted with permission from American Chemical Society

The development of several degradable hydrogels utilizing ATRP technique has also been reported; they include preparation of acidic pH-responsive hydrogels based on thermoresponsive poly(N-isopropylacrylamide-co-5,6-methylene-1,3-dioxepane) [175], redox-responsive hydrogels based on thiol/disulfide-functionalized star polymers [176, 179] and radical-responsive gels based on a dynamic covalent trithiocarbonate cross-linkers [177].

6 Nanogels by ATRP

Nanogels are a class of crosslinked hydrogels confined to nanometer-sized particles. In addition to displaying properties typical for hydrogels, nanogels have tunable size varying from submicron to tens of nanometers in diameter with large surface area, suitable for multivalent bioconjugation, and an interior network for incorporation of therapeutics. Because of these advantageous properties, they hold great promise as effective polymer-based drug delivery systems [180, 181]. Several methods have been proposed for the preparation of nanogels incorporating both chemical and physical crosslinkages. As described in a recent review, typical methods include photolithographic, micro-molding, and microfluidic methods, as well as aqueous homogeneous gelation and heterogeneous polymerization

methods [160]. Furthermore, ATRP techniques have been utilized to develop unique methodologies to synthesize and fabricate well-defined nanogels.

Nanogels can be prepared by inverse miniemulsion polymerization, an water–in–oil (W/O) process consisting of dispersions of aqueous droplets, including water-soluble monomers and difunctional crosslinkers, in organic media with the aid of oil-soluble surfactants. Polymerization occurs in the aqueous droplets upon addition of water-soluble initiators and yields colloidally-stable crosslinked hydrophilic nanogels [182]. Conducting an ATRP in inverse miniemulsion has been reported. This method enables the preparation of well-defined degradable nanogels crosslinked with disulfide linkages, which exhibit reduction-responsive degradation through disulfide-thiol exchange reactions. This methodology provides nanogels which possess a number of unique features specifically targeted toward drug delivery applications [183]. First, the incorporation of reduction-responsive degradability in the presence of cellular glutathione (GSH), a tripeptide containing cysteine with a pendent thiol group, facilitates biodegradation, enabling the enhanced release of encapsulated biomolecules including anticancer drugs, carbohydrate drugs, and protein drugs while ensuring the removal of the original device after the release of drugs in the body. Second, the retention of high chain–end functionalities enable further chain extension to form functional block copolymers, and facile bioconjugation with cell targeting agents such as peptides, proteins, and antibodies. Third, facile cellular internalization of the nanogels through clathrin-medicated endocytosis was confirmed through laser confocal fluorescent microscopy (LCFM) and flow cytometry experiments. Indeed, this methodology is so versatile that it has been utilized to synthesize other advanced functional nanomaterials; including thermoresponsive degradable magnetic microgels for hyperthermia applications [184] green florescent protein loaded nanogels for protein-polymer hybrids [106, 185] dual-responsive surfactants for functional nanocapsules [148] and OH-functionalized nanogels for nanostructured hybrid hydrogels [176]. Similarly, the ATRP technique has additionally been explored for inverse microemulsion [186] dispersion [187] and precipitation polymerizations [188].

Self-assembled micellar aggregates based on amphiphilic block copolymers (ABPs) resulted in formation of a broad range of materials that show promise as tumor-targeting nanocarriers [189, 190]. However, retaining colloidal stability of physically aggregated micelles upon dilution remains a challenge. Dilution, far below critical micellar concentration during circulation in the body, causes the micelles to destabilize or dissociate, which in turn leads to premature release of encapsulated drugs. Covalent crosslinking has been explored as a strategy to improve the in vivo stability of micelles by converting aggregates to crosslinked micelles or nanogels [191]. In this procedure, two reactive functional groups of ABPs and/or external crosslinkers react to form new covalent crosslinks in the shell or core of the micelles, endowing the micelles with enhanced colloidal stability. However, the use of permanent crosslinks hampers the controlled release of encapsulated drugs [192]. Recently, stimuli-responsive degradation has been explored as a smart response platform to synthesize degradable nanogels crosslinked with labile

crosslinks such as photo-cleavable coumarin dimers, acid-labile acetal, hydrazine, and imine linkages, and disulfides [193–195]. A general approach involves the use of multifunctional crosslinkers bearing cleavable linkages [196, 197]. In contrast, in situ formation of disulfide linkages as new cleavable crosslinks can be incorporated by using ABPs with pendant disulfide linkages [198]. In the presence of catalytic amounts of reducing agents, pendant disulfides on polymer chains undergo thiol-disulfide exchange reactions to generate crosslinked micelles with new labile disulfide crosslinks, affording enhanced colloidal stability [199]. This approach is advantageous in that the synthesis of triblock copolymers consisting of a middle block having pendant disulfide linkages allows for the development of disulfide degradable interlayer-crosslinked micelles with enhance colloidal stability as well as rapid drug release [200]. After injection, the newly-formed disulfide crosslinks are cleaved in the presence of excess thiols (preferably, glutathione in living cells), causing the crosslinked micelles to dissociate, and thus enhancing the release of encapsulated drugs in targeted cells.

7 In Situ Formed Hydrogels

In certain clinical settings where surgical implantation of a macroscopic hydrogel is an overly invasive procedure and may lead to undesired patient complications, the use of injectable or in situ formed physically crosslinked hydrogels provide a minimally invasive therapeutic technique [201–205]. Physically crosslinked hydrogels are more suitable for in situ gelation as chemical crosslinking may cause localized cytotoxicity and cell damage due to the use of reactive chemical compounds and residual organic molecules. Injectable hydrogels are also beneficial in that the precursor aqueous polymer solutions can be easily mixed with bioactive molecules such as drugs, proteins, genes, DNA, or cells prior to injection allowing for facile drug loading. Subsequent injection of the solution forms a macroscopic hydrogel in situ, which can act as a tissue scaffold or facilitate local delivery of active compounds.

The precise control over polymer microstructure afforded by ATRP has promoted its use to engineer block copolymers with stimuli-responsive hydrophilic blocks which respond to temperature and/or pH for formation of injectable hydrogels suitable for biomedical applications. Block copolymer based injectable hydrogels characteristically follow a micellar gelation mechanism. Linear stimuli-responsive amphiphilic block copolymers or doubly hydrophilic block copolymers can exist as micellar aggregates or free polymer chains in solution. Physical gelation is then triggered through a change in solubility of the initially dissolved polymer upon external stimuli such as an increase in temperature, which changes the solubility of one polymer block inducing the self-assembly of the polymer chins to form micellar structures. At sufficiently high polymer concentration, micellar coronas can overlap, thus inducing long range order in the polymer solution and physical gelation. This gelation mechanism is most common for linear AB type

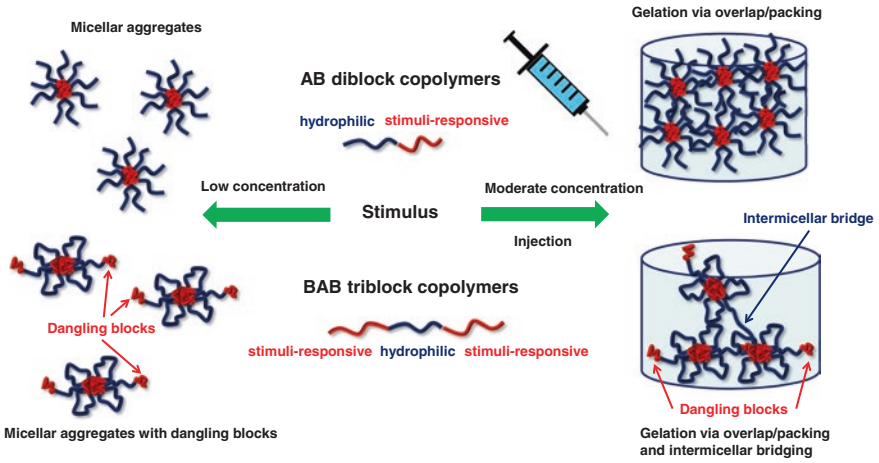

Fig. 6 Illustration of in situ gelation of well-defined thermoresponsive block copolymers

diblock copolymers, which have a critical gelation concentration of approximately 20 wt% in solution [206]. Alternatively, stimuli-responsive triblock copolymers such as ABA or BAB triblock copolymers, where the A block is hydrophilic and B block hydrophobic can be used to reduce the critical gelation concentration. Gelation of ABA triblock copolymers is also caused by an overlap of micellar coronas, although a lower polymer concentration may be used as the micellar aggregates formed are typically larger than those from AB diblock copolymers. BAB triblock copolymers however, can undergo gelation via an additional intermicelle bridging mechanism. Micellar aggregates formed from BAB triblocks require folding of two B hydrophobic blocks into one micelle core, which can be energetically unfavorable and, some B blocks can exist as dangling blocks in solution, which can form bridges when incorporated into other micelles (Fig. 6).

A series of BAB triblock copolymers, utilizing 2-methacryloyloxyethyl phosphorylcholine (MPC) as the central hydrophilic block, have been studied for production of in situ formed hydrogels [207–210]. MPC contains a phosphorylcholine functional group, which when incorporated into coatings makes the surface resistant to protein adsorption and cellular adhesion without negatively impacting cell viability [211–214]. The central MPC block was synthesized from a difunctional ATRP initiator, and then subsequently chain extended with pendant amine-containing methacylates, for example 2-(diethylamino)ethyl methacrylate (DEA) a class of pH and temperature responsive monomers. These MPC–containing triblock solutions with approximately 10 wt% polymer formed physical gels at body temperature and neutral pH. Release of encapsulated molecules could be enhanced at acidic pH's due to dissolution of the gel as the polymer becomes protonated [207, 208]. Alternatively, MPC was copolymerized with NIPAM, a well-known thermo-responsive monomer with a LCST transition ≈32 °C. The P(NIPAM-b-MPC-b-NIPAM) copolymers underwent gelation at a lower polymer content

(≈7 wt%) as PNIPAM undergoes a sharp thermo-response [210]. When a difunctional initiator containing a dynamic disulfide linkage was used, the synthesized P(NIPAM-b-MPC-ss-MPC-b-NIPAM) copolymers formed thiol and temperature responsive gels. Physical gelation was triggered by an increase in temperature, while the physically crosslinked gel could be permanently degraded/dissolved upon exposure to a reducing agent such as glutathione, making the thiol-responsive injectable hydrogel a suitable anticancer drug delivery depot [209]. In addition to incorporating thiol-responsive gel dissolution, injectable thermoresponsive hydrogels from BAB copolymers have been designed to incorporate light triggered [214] or enzyme catalyzed [215] gel-sol transitions to enhance delivery of encapsulated compounds. Recently, a phosphorylated BAB triblock copolymer was demonstrated to be an effective scaffold for bone tissue engineering. The copolymer was synthesized through consecutive ATRP of *tert*-butyl acrylate and NIPAM, followed by hydrolytic cleavage of the esters in the acrylate block to generate a central hydrophilic poly(acrylic acid) block. O-phosphoethanolamine was conjugated to the central A block to enhance mineralization and mimic naturally occurring hydroxyapatite in healthy bone structures [216]. Building on the concept of BAB triblocks, ABC triblock [217, 218] and CBABC pentablock copolymers [219–221] with various distributed chemical functionalities have also been synthesized and shown to form hydrogels in situ. The presence of a third monomer can introduce additional stimuli-responsive properties and alter the critical gelation concentration.

Multi-arm star ($n\mathrm{BA_n}$) block copolymers with central hydrophilic A blocks and stimuli-responsive B blocks possess lower critical gelation concentrations than linear analogues due to extra chain entanglement and inter-micelle bridging [222, 223]. Conveniently, one of the primary advantages of ATRP over competing CRP techniques is the ease with which multifunctional initiators can be prepared. A 3-arm star diblock copolymer with a MCP core and various AMA arms was found to form physically robust free standing gels at lower polymer concentrations than comparable BAB triblock copolymers [224]. Depending on the ratio and type of AMA monomer used, both thermoresponsive and pH responsive behavior was observed. In another study, AMA was used as the core forming segment in a 4-arm star copolymer, and gelation and gel dissolution was also found to be pH and temperature dependent [225].

Due to concerns over potential cytotoxicity of poly(N-substituted acrylamide) and poly(amino methacrylate), methacrylates with pendant ethylene oxide units (OEOMA) have been investigated as a class of promising alternative monomers to synthesize polymers with high biocompatibility and thermoresponsive behavior. A series of 4-arm star diblock copolymers containing OEOMA segments were synthesized from a PEO macroinitiator. By tuning the ratio of different OEOMA monomers, the LCST response of the arms occurred below body temperature, allowing for the formation of biocompatible free standing gels in various buffer solutions and cell culture media [226, 227].

Enhanced gel degradation can also be incorporated through the use of biodegradable polymers. A 4-arm diblock copolymer containing a biodegradable

hydrophobic poly(ε-caprolactone) (PCL) segment was synthesized by ring opening polymerization (ROP) followed by ATRP of hydrophilic OEOMA. The (PCL-b-POEOMA)$_4$ star block copolymers formed micelles at room temperature, and underwent a sol-gel transition below body temperature, demonstrating the ability to form an injectable hydrogel with a biodegradable core [228]. The rate of drug release can then be tuned through diffusion of active compounds through the gel as well as the degradation rate of the PCL chains. In addition to multi-arm star block copolymers, polymers with grafted stimuli-responsive chains can be used to form hydrogels with low critical gelation concentrations due to extra chain entanglement from dangling chains [229].

8 One-Component Supersoft Gels

Hydrogels in a swollen state are very soft materials with moduli in a range of 1 kPa. However, they become much harder after water evaporation. Thus, it would be very desirable to develop hydrogel-like single-component materials that would never dry. Such materials should act as supersoft elastomers.

Bulk polymers in a glassy state are hard materials with moduli in the range of 1 GPa. Above their glass transition temperature they soften and eventually flow. This depends on the molecular weight and nature of the polymers, i.e. entanglement MW. If the chains are slightly crosslinked they form rubbers or elastomers with typical moduli in the range of 100–1,000 kPa. Such crosslinked polymers can swell and, depending on degree of crosslinking, can reach softness typical for hydrogels. But after they dry, moduli return to the original values.

A new concept has been recently introduced to dilute a loose network of polymer chains not with a solvent (water) but with multiple short covalently attached unentangled side chains. In such a case, they could never evaporate and would provide a permanent non-leachable diluent that would reduce the moduli to a value of ca 1 kPa, forming a new class of stable supersoft elastomers [230, 231].

Scheme 6 illustrates two routes for the preparation of such supersoft elastomers. The left pathway relies on formation of bottlebrush macromolecules with

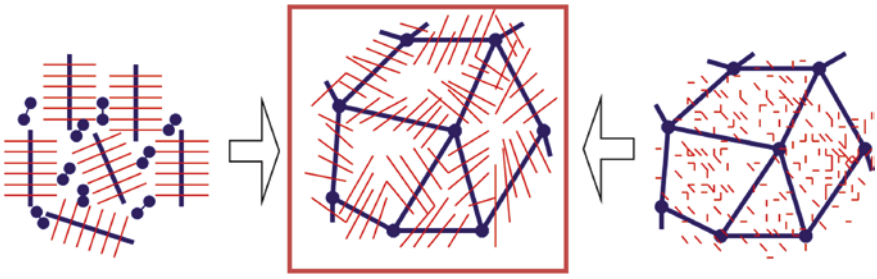

Scheme 6 Two pathways to supersoft elastomers

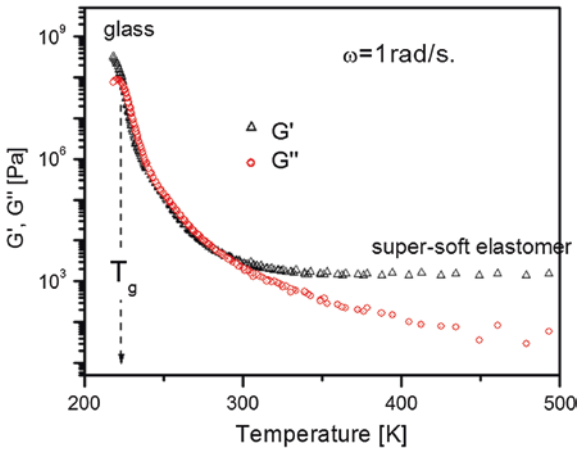

Fig. 7 Mechanical properties of supersoft elastomers with modules in the range of 1 kPa. The material obtained from loose crosslinking of bottlebrushes. Reprinted with permission from American Chemical Society [231]

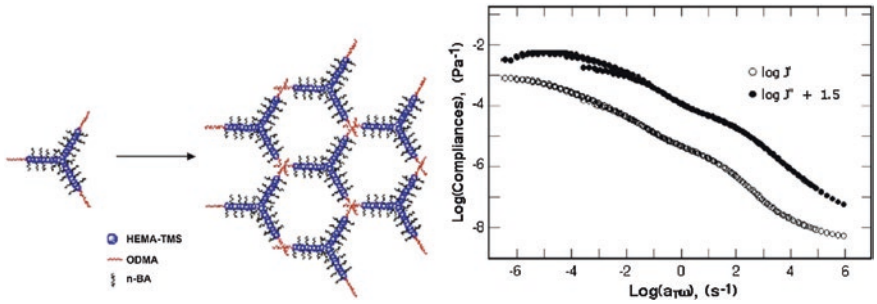

Fig. 8 Supersoft elastomer network formed via physical crosslinking and the resulting compliance data. Reprinted with permission from Elsevier [232]

very densely grafted side chains [15, 16]. Such molecular brushes typically have a backbone with DP_{bb} ca. 300–5,000 and correspondingly the same number of short side chains with DP_{sc} ca. 20–100. Brushes with the longest backbone may exhibit plateau in the range 1 kPa and after slight crosslinking form permanent supersoft elastomers that cannot flow (as shown in Fig. 7). The alternative pathway is grafting side chains from a loose network backbone, containing initiating sites.

As noted above supersoft elastomers can be prepared with permanent chemical crosslinkage but can also be formed by physical crosslinking, as in thermoplastic elastomers. Figure 8 presents a structure consisting of 3 arm stars bottlebrushes that can phase separate to form such a network and also the resulting mechanical properties of the thermoplastic network. Each arm of the star had a methacrylate backbone of $DP_{bb} = 300$ grafted with soft P*n*BA with $DP_{sc} = 35$. Each arm was

chain extended with poly(octadecyl methacrylate) with $DP_{ODMA} = 360$, leading to overall 8 wt% content of crystallizable outer segments. The resulting modulus of the physically crosslinked material was in the range of 1 kPa [232].

Similar materials were prepared by grafting from a loose network [233]. First, four-arm star-like polymers, poly(trimethylsilyloxyethyl acrylate), were synthesized and cross-linked to form a relatively uniform polymer gel network. Then, short P*n*BA side chains were grown from the initiating sites placed along the network backbone via atom transfer radical polymerization. These soft side chains act as low molecular weight diluent that swelled the cross-linked network forming supersoft materials with shear modulus less than 5 kPa, depending on the length and fraction of grafted side chain were formed. Such supersoft elastomers could be considered as materials appropriate for intraocular lenses, wound-healing or tissue engineering, and also ionic conductors [230].

9 Conclusions

ATRP and other CRP methods provide excellent tools for controlling polymer architecture. The procedures can not only provide linear chains but also branched architecture such as stars, graft copolymers with a very high grafting density, like bottlebrushes, and eventually well defined networks. These techniques can be successfully used in water under homogeneous or heterogeneous conditions opening new avenues for the preparation of designed hydrogels and other networks, including functional materials, responsive, injectable and also supersoft elastomers suitable for multiple bio-applications.

Acknowledgements H.G. thanks the University of Notre Dame and the Center for Sustainable Energy at Notre Dame (cSEND) for financial support. N.C. and J.K.O thank the financial support from Canada Research Chair Award and NSERC Canada. K.M. thanks the financial support from NSF (DMR 09-69301) and DoE (ER 45998).

References

1. Hoffman, A.S.: Applications of thermally reversible polymers and hydrogels in therapeutics and diagnostics. J. Control Release **6**, 297–305 (1987)
2. Langer, R., Vacanti, J.P.: Tissue engineering. Science **260**(5110), 920–926 (1993)
3. Langer, R.: Drug delivery: drugs on target. Science **293**(5527), 58–59 (2001)
4. Peppas, N.A., Hilt, J.Z., Khademhosseini, A., Langer, R.: Hydrogels in biology and medicine: from molecular principles to bionanotechnology. Adv. Mater. **18**(11), 1345–1360 (2006)
5. Matsumoto, A.: Free-radical crosslinking polymerization and copolymerization of multivinyl compounds. Adv. Polym. Sci. **123**, 41–80 (1995)
6. Erdodi, G., Janecska, A., Ivan, B.: Novel intelligent amphiphilic conetworks. In: The Wiley Polymer Networks Group Review, vol. 2, Synthetic versus Biological Networks, pp. 73–87 (1999)

7. Hild, G.: Model networks based on 'endlinking' processes: synthesis, structure and properties. Prog. Polym. Sci. **23**(6), 1019–1149 (1998)
8. Dusek, K., Duskova-Smrckova, M.: Network structure formation during crosslinking of organic coating systems. Prog. Polym. Sci. **25**(9), 1215–1260 (2000)
9. Patrickios, C.S., Georgiou, T.K.: Covalent amphiphilic polymer networks. Curr. Opin. Colloid Interface Sci. **8**(1), 76–85 (2003)
10. Kloxin, A.M., Kloxin, C.J., Bowman, C.N., Anseth, K.S.: Mechanical properties of cellularly responsive hydrogels and their experimental determination. Adv. Mater. **22**(31), 3484–3494 (2010)
11. Matyjaszewski, K., Davis, T.P. (eds.): Handbook of Radical Polymerization. Wiley, Hoboken (2002)
12. Braunecker, W.A., Matyjaszewski, K.: Controlled/living radical polymerization: features, developments, and perspectives. Prog. Polym. Sci. **32**(1), 93–146 (2007)
13. Patten, T.E., Xia, J.H., Abernathy, T., Matyjaszewski, K.: Polymers with very low polydispersities from atom transfer radical polymerization. Science **272**(5263), 866–868 (1996)
14. Coessens, V., Pintauer, T., Matyjaszewski, K.: Functional polymers by atom transfer radical polymerization. Prog. Polym. Sci. **26**(3), 337–377 (2001)
15. Lee, H-i, Pietrasik, J., Sheiko, S.S., Matyjaszewski, K.: Stimuli-responsive molecular brushes. Prog. Polym. Sci. **35**(1–2), 24–44 (2010)
16. Sheiko, S.S., Sumerlin, B.S., Matyjaszewski, K.: Cylindrical molecular brushes: synthesis, characterization, and properties. Prog. Polym. Sci. **33**(7), 759–785 (2008)
17. Tsarevsky, N.V., Matyjaszewski, K.: "Green" atom transfer radical polymerization: from process design to preparation of well-defined environmentally friendly polymeric materials. Chem. Rev. **107**(6), 2270–2299 (2007)
18. Kamigaito, M., Ando, T., Sawamoto, M.: Metal-catalyzed living radical polymerization. Chem. Rev. **101**(12), 3689–3745 (2001)
19. Wang, J.S., Matyjaszewski, K.: Controlled living radical polymerization—atom-transfer radical polymerization in the presence of transition-metal complexes. J. Am. Chem. Soc. **117**(20), 5614–5615 (1995)
20. Matyjaszewski, K., Xia, J.H.: Atom transfer radical polymerization. Chem. Rev. **101**(9), 2921–2990 (2001)
21. Kwak, Y., Matyjaszewski, K.: Effect of initiator and ligand structures on ATRP of styrene and methyl methacrylate initiated by alkyl dithiocarbamate. Macromolecules **41**(18), 6627–6635 (2008)
22. Matyjaszewski, K., Tsarevsky, N.V.: Nanostructured functional materials prepared by atom transfer radical polymerization. Nat. Chem. **1**(4), 276–288 (2009)
23. di Lena, F., Matyjaszewski, K.: Transition metal catalysts for controlled radical polymerization. Prog. Polym. Sci. **35**(8), 959–1021 (2010)
24. Georges, M.K., Veregin, R.P.N., Kazmaier, P.M., Hamer, G.K.: Narrow molecular weight resins by a free-radical polymerization process. Macromolecules **26**(11), 2987–2988 (1993)
25. Hawker, C.J., Bosman, A.W., Harth, E.: New polymer synthesis by nitroxide mediated living radical polymerizations. Chem. Rev. **101**, 3661–3688 (2001)
26. Nicolas, J., Guillaneuf, Y., Lefay, C., Bertin, D., Gigmes, D., Charleux, B.: Nitroxide-mediated polymerization. Prog. Polym. Sci. **38**(1):63–235 (2013)
27. Chiefari, J., Chong, Y.K., Ercole, F., Krstina, J., Jeffery, J., Le, T.P.T., Mayadunne, R.T.A., Meijs, G.F., Moad, C.L., Moad, G., Rizzardo, E., Thang, S.H.: Living free-radical polymerization by reversible addition–fragmentation chain transfer: the RAFT process. Macromolecules **31**(16), 5559–5562 (1998)
28. Moad, G., Rizzardo, E., Thang, S.H.: Living radical polymerization by the RAFT process. Aust. J. Chem. **58**(6), 379–410 (2005)
29. Moad, G., Rizzardo, E., Thang, S.H.: Toward living radical polymerization. Acc. Chem. Res. **41**(9), 1133–1142 (2008)

30. Gregory, A., Stenzel, M.H.: Complex polymer architectures via RAFT polymerization: from fundamental process to extending the scope using click chemistry and nature's building blocks. Prog. Polym. Sci. **37**(1), 38–105 (2012)
31. Matyjaszewski, K.: Atom transfer radical polymerization (ATRP): current status and future perspectives. Macromolecules **45**(10), 4015–4039 (2012)
32. Goto, A., Fukuda, T.: Kinetics of living radical polymerization. Prog. Polym. Sci. **29**(4), 329–385 (2004)
33. Tang, W., Tsarevsky, N.V., Matyjaszewski, K.: Determination of equilibrium constants for atom transfer radical polymerization. J. Am. Chem. Soc. **128**(5), 1598–1604 (2006)
34. Fischer, H.: The persistent radical effect: a principle for selective radical reactions and living radical polymerizations. Chem. Rev. **101**(12), 3581–3610 (2001)
35. Gromada, J., Matyjaszewski, K.: Simultaneous reverse and normal initiation in atom transfer radical polymerization. Macromolecules **34**(22), 7664–7671 (2001)
36. Min, K., Gao, H., Matyjaszewski, K.: Preparation of homopolymers and block copolymers in miniemulsion by ATRP using activators generated by electron transfer (AGET). J. Am. Chem. Soc. **127**(11), 3825–3830 (2005)
37. Jakubowski, W., Matyjaszewski, K.: Activator generated by electron transfer for atom transfer radical polymerization. Macromolecules **38**(10), 4139–4146 (2005)
38. Jakubowski, W., Min, K., Matyjaszewski, K.: Activators regenerated by electron transfer for atom transfer radical polymerization of styrene. Macromolecules **39**(1), 39–45 (2006)
39. Jakubowski, W., Matyjaszewski, K.: Activators regenerated by electron transfer for atom-transfer radical polymerization of (meth)acrylates and related block copolymers. Angew. Chem. Int. Ed. **45**(27), 4482–4486 (2006)
40. Matyjaszewski, K., Jakubowski, W., Min, K., Tang, W., Huang, J., Braunecker, W.A., Tsarevsky, N.V.: Diminishing catalyst concentration in atom transfer radical polymerization with reducing agents. Proc. Natl. Acad. Sci. U. S. A. **103**(42), 15309–15314 (2006)
41. Tang, W., Matyjaszewski, K.: Effect of ligand structure on activation rate constants in ATRP. Macromolecules **39**(15), 4953–4959 (2006)
42. Tang, W., Matyjaszewski, K.: Effects of initiator structure on activation rate constants in ATRP. Macromolecules **40**(6), 1858–1863 (2007)
43. Magenau, A.J.D., Kwak, Y., Schroder, K., Matyjaszewski, K.: Highly active bipyridine-based ligands for atom transfer radical polymerization. ACS Macro. Lett. **1**(4), 508–512 (2012)
44. Schröder, K., Mathers, R.T., Buback, J., Konkolewicz, D., Magenau, A.J.D., Matyjaszewski, K.: Substituted tris(2-pyridylmethyl)amine ligands for highly active ATRP catalysts. ACS Macro Lett. **1**, 1037–1040 (2012)
45. Tang, W., Kwak, Y., Braunecker, W., Tsarevsky, N.V., Coote, M.L., Matyjaszewski, K.: Understanding atom transfer radical polymerization: effect of ligand and initiator structures on the equilibrium constants. J. Am. Chem. Soc. **130**(32), 10702–10713 (2008)
46. Braunecker, W.A., Tsarevsky, N.V., Gennaro, A., Matyjaszewski, K.: Thermodynamic components of the atom transfer radical polymerization equilibrium: quantifying solvent effects. Macromolecules **42**(17), 6348–6360 (2009)
47. Wang, J.-S., Matyjaszewski, K.: "Living"/controlled radical polymerization. Transition-metal-catalyzed atom transfer radical polymerization in the presence of a conventional radical initiator. Macromolecules **28**(22), 7572–7573 (1995)
48. Xia, J.H., Matyjaszewski, K.: Controlled/"living" radical polymerization. Homogeneous reverse atom transfer radical polymerization using AIBN as the initiator. Macromolecules **30**(25), 7692–7696 (1997)
49. Li, M., Min, K., Matyjaszewski, K.: ATRP in waterborne miniemulsion via a simultaneous reverse and normal initiation process. Macromolecules **37**(6), 2106–2112 (2004)
50. Zhang, Y., Wang, Y., Matyjaszewski, K.: ATRP of methyl acrylate with metallic zinc, magnesium, and iron as reducing agents and supplemental activators. Macromolecules **44**(4), 683–685 (2011)

51. Zhong, M., Wang, Y., Krys, P., Konkolewicz, D., Matyjaszewski, K.: Reversible-deactivation radical polymerization in the presence of metallic copper. Kinetic Simulation. Macromolecules **46**(10), 3816–3827 (2013)
52. Peng, C.-H., Zhong, M., Wang, Y., Kwak, Y., Zhang, Y., Zhu, W., Tonge, M., Buback, J., Park, S., Krys, P., Konkolewicz, D., Gennaro, A., Matyjaszewski, K.: Reversible-deactivation radical polymerization in the presence of metallic copper. Activation of alkyl halides by CuO. Macromolecules **46**(10), 3803–3815 (2013)
53. Wang, Y., Zhong, M., Zhu, W., Peng, C.-H., Zhang, Y., Konkolewicz, D., Bortolamei, N., Isse, A.A., Gennaro, A., Matyjaszewski, K.: Reversible-deactivation radical polymerization in the presence of metallic copper. Comproportionation–disproportionation equilibria and kinetics. Macromolecules **46**(10), 3793–3802 (2013)
54. Konkolewicz, D., Wang, Y., Zhong, M., Krys, P., Isse, A.A., Gennaro, A., Matyjaszewski, K.: Reversible-deactivation radical polymerization in the presence of metallic copper. A critical assessment of the SARA ATRP and SET-LRP mechanisms. Macromolecules (2013)
55. Konkolewicz, D., Schroder, K., Buback, J., Bernhard, S., Matyjaszewski, K.: Visible light and sunlight photoinduced ATRP with ppm of Cu catalyst. ACS Macro. Lett. **1**(10), 1219–1223 (2012)
56. Magenau Andrew, J.D., Strandwitz Nicholas, C., Gennaro, A., Matyjaszewski, K.: Electrochemically mediated atom transfer radical polymerization. Science **332**(6025), 81–84 (2011)
57. Stockmayer, W.H.: Theory of molecular size distribution and gel formation in branched polymers. II. General cross linking. J. Chem. Phys. **12**, 125–131 (1944)
58. Flory, P.J.: Principles of polymer chemistry. Cornell University Press, Ithaca (1953)
59. Gao, H., Matyjaszewski, K.: Synthesis of functional polymers with controlled architecture by CRP of monomers in the presence of cross-linkers: from stars to gels. Prog. Polym. Sci. **34**(4), 317–350 (2009)
60. Walling, C.J.: Gel formation in addition polymerization. J. Am. Chem. Soc. **67**(3), 441–447 (1945)
61. Gordon, M.: Network theory of the gel point and the "incestuous" polymerization of diallyl phthalate. J. Chem. Phys. **22**, 610–613 (1954)
62. Matsumoto, A.: Polymerization of multiallyl monomers. Prog. Polym. Sci. **26**(2), 189–257 (2001)
63. O'Brien, N., McKee, A., Sherrington, D.C., Slark, A.T., Titterton, A.: Facile, versatile and cost effective route to branched vinyl polymers. Polymer **41**(15), 6027–6031 (2000)
64. Isaure, F., Cormack, P.A.G., Sherrington, D.C.: Facile synthesis of branched poly(methyl methacrylate)s. J. Mater. Chem. **13**(11), 2701–2710 (2003)
65. Sato, T., Ihara, H., Hirano, T., Seno, M.: Formation of soluble hyperbranched polymer through the initiator-fragment incorporation radical copolymerization of ethylene glycol dimethacrylate with N-methylmethacrylamide. Polymer **45**(22), 7491–7498 (2004)
66. Sato, T., Arima, Y., Seno, M., Hirano, T.: Initiator-fragment incorporation radical polymerization of divinyl adipate with dimethyl 2,2′-azobis(isobutyrate): kinetics and formation of soluble hyperbranched polymer. Macromolecules **38**(5), 1627–1632 (2005)
67. Weaver, J.V.M., Williams, R.T., Royles, B.J.L., Findlay, P.H., Cooper, A.I., Rannard, S.P.: PH-responsive branched polymer nanoparticles. Soft Matter **4**(5), 985–992 (2008)
68. Li, W., Gao, H., Matyjaszewski, K.: Influence of initiation efficiency and polydispersity of primary chains on gelation during atom transfer radical copolymerization of monomer and cross-linker. Macromolecules **42**(4), 927–932 (2009)
69. Li, W., Yoon, J.A., Zhong, M., Matyjaszewski, K.: Atom transfer radical copolymerization of monomer and cross-linker under highly dilute conditions. Macromolecules **44**(9), 3270–3275 (2011)
70. Li, W., Matyjaszewski, K.: Star polymers via cross-linking amphiphilic macroinitiators by AGET ATRP in aqueous media. J. Am. Chem. Soc. **131**(30), 10378–10379 (2009)

71. Bastide, J., Leibler, L.: Large-scale heterogeneities in randomly cross-linked networks. Macromolecules **21**(8), 2647–2649 (1988)
72. Kannurpatti, A.R., Anseth, J.W., Bowman, C.N.: A study of the evolution of mechanical properties and structural heterogeneity of polymer networks formed by photopolymerizations of multifunctional (meth)acrylates. Polymer **39**(12), 2507–2513 (1998)
73. Funke, W., Okay, O., Joos-Muller, B.: Microgels-intramolecularly crosslinked macromolecules with a globular structure. Advances in Polymer Science (Microencapsulation, Microgels, Iniferters), vol. 136, pp. 138–234 (1998)
74. Gordon, M., Roe, R.-J.: Diffusion and gelation in polyadditions. IV. Statistical theory of ring formation and the absolute gel point. J. Polym. Sci. **21**, 75–90 (1956)
75. Ide, N., Fukuda, T.: Nitroxide-controlled free-radical copolymerization of vinyl and divinyl monomers. 2. Gelation. Macromolecules **32**(1), 95–99 (1999)
76. Tsarevsky, N.V., Matyjaszewski, K.: Combining atom transfer radical polymerization and disulfide/thiol redox chemistry: a route to well-defined (bio)degradable polymeric materials. Macromolecules **38**(8), 3087–3092 (2005)
77. Taton, D., Baussard, J.-F., Dupayage, L., Poly, J., Gnanou, Y., Ponsinet, V., Destarac, M., Mignaud, C., Pitois, C.: Water soluble polymeric nanogels by xanthate-mediated radical crosslinking copolymerization. Chem. Commun. **18**, 1953–1955 (2006)
78. Isaure, F., Cormack, P.A.G., Graham, S., Sherrington, D.C., Armes, S.P., Buetuen, V.: Synthesis of branched poly(methyl methacrylate)s via controlled/living polymerisations exploiting ethylene glycol dimethacrylate as branching agent. Chem. Commun. (9), 1138–1139 (2004)
79. Yu, Q., Zeng, F., Zhu, S.: Atom transfer radical polymerization of poly(ethylene glycol) dimethacrylate. Macromolecules **34**(6), 1612–1618 (2001)
80. Bannister, I., Billingham, N.C., Armes, S.P., Rannard, S.P., Findlay, P.: Development of branching in living radical copolymerization of vinyl and divinyl monomers. Macromolecules **39**(22), 7483–7492 (2006)
81. Gao, H., Min, K., Matyjaszewski, K.: Determination of gel point during atom transfer radical copolymerization with cross-linker. Macromolecules **40**(22), 7763–7770 (2007)
82. Yu, Q., Zhang, J., Cheng, M., Zhu, S.: Kinetic behavior of atom transfer radical polymerization of dimethacrylates. Macromol. Chem. Phys. **207**(3), 287–294 (2006)
83. Ide, N., Fukuda, T.: Nitroxide-controlled free-radical copolymerization of vinyl and divinyl monomers. Evaluation of Pendant-Vinyl Reactivity. Macromolecules **30**(15), 4268–4271 (1997)
84. Liu, B., Kazlauciunas, A., Guthrie, J.T., Perrier, S.: One-pot hyperbranched polymer synthesis mediated by reversible addition fragmentation chain transfer (RAFT) polymerization. Macromolecules **38**(6), 2131–2136 (2005)
85. Liu, B., Kazlauciunas, A., Guthrie, J.T., Perrier, S.: Influence of reaction parameters on the synthesis of hyperbranched polymers via reversible addition fragmentation chain transfer (RAFT) polymerization. Polymer **46**(17), 6293–6299 (2005)
86. Saka, Y., Zetterlund, P.B., Okubo, M.: Gel formation and primary chain lengths in nitroxide-mediated radical copolymerization of styrene and divinylbenzene in miniemulsion. Polymer **48**(5), 1229–1236 (2007)
87. Vo, C.-D., Rosselgong, J., Armes, S.P., Billingham, N.C.: RAFT synthesis of branched acrylic copolymers. Macromolecules **40**(20), 7119–7125 (2007)
88. Bouhier, M.-H., Cormack, P., Graham, S., Sherrington, D.C.: Synthesis of densely branched poly(methyl methacrylate)s via ATR copolymerization of methyl methacrylate and ethylene glycol dimethacrylate. J. Polym. Sci. Part A Polym. Chem. **45**(12), 2375–2386 (2007)
89. Gao, H., Li, W., Matyjaszewski, K.: Synthesis of polyacrylate networks by ATRP: parameters influencing experimental gel points. Macromolecules **41**(7), 2335–2340 (2008)
90. Zhao, T., Zheng, Y., Poly, J., Wang, W.: Controlled multi-vinyl monomer homopolymerization through vinyl oligomer combination as a universal approach to hyperbranched architectures. Nat. Commun. **4**, Article number: 1873 (2013)

91. Zheng, Y., Cao, H., Newland, B., Dong, Y., Pandit, A., Wang, W.: 3D single cyclized polymer chain structure from controlled polymerization of multi-vinyl monomers: beyond flory-stockmayer theory. J. Am. Chem. Soc. **133**(33), 13130–13137 (2011)
92. Wang, W., Zheng, Y., Roberts, E., Duxbury, C.J., Ding, L., Irvine, D.J., Howdle, S.M.: Controlling chain growth: a new strategy to hyperbranched materials. Macromolecules **40**(20), 7184–7194 (2007)
93. Rosselgong, J., Armes, S.P.: Quantification of intramolecular cyclization in branched copolymers by 1H NMR spectroscopy. Macromolecules **45**(6), 2731–2737 (2012)
94. Zhou, H., Woo, J., Cok, A.M., Wang, M., Olsen, B.D., Johnson, J.A.: Counting primary loops in polymer gels. Proc. Natl. Acad. Sci. U. S. A. **109**, 19119–19124 (2012)
95. Bortolamei, N., Isse, A.A., Magenau, A.J.D., Gennaro, A., Matyjaszewski, K.: Controlled aqueous atom transfer radical polymerization with electrochemical generation of the active catalyst. Angew. Chem. Int. Ed. **50**(48), 11391–11394 (2011)
96. Oh, J.K., Min, K., Matyjaszewski, K.: Preparation of poly(oligo(ethylene glycol) monomethyl ether methacrylate) by homogeneous aqueous AGET ATRP. Macromolecules **39**(9), 3161–3167 (2006)
97. Simakova, A., Averick, S.E., Konkolewicz, D., Matyjaszewski, K.: Aqueous ARGET ATRP. Macromolecules **45**(16), 6371–6379 (2012)
98. Wang, X.S., Armes, S.P.: Facile atom transfer radical polymerization of methoxy-capped oligo(ethylene glycol) methacrylate in aqueous media at ambient temperature. Macromolecules **33**(18), 6640–6647 (2000)
99. He, W., Jiang, H., Zhang, L., Cheng, Z., Zhu, X.: Atom transfer radical polymerization of hydrophilic monomers and its applications. Polym. Chem. **4**(10), 2919–2938 (2013)
100. Chung, I.-D., Britt, P., Xie, D., Harth, E., Mays, J.: Synthesis of amino acid-based polymers via atom transfer radical polymerization in aqueous media at ambient temperature. Chem. Commun. **8**, 1046–1048 (2005)
101. Coca, S., Jasieczek, C.B., Beers, K.L., Matyjaszewski, K. Polymerization of acrylates by atom transfer radical polymerization. Homopolymerization of 2-hydroxyethyl acrylate. J. Polym. Sci. Part A Polym. Chem. **36** (9), 1417–1424 (1998)
102. Wang, X.S., Lascelles, S.F., Jackson, R.A., Armes, S.P.: Facile synthesis of well-defined water-soluble polymers via atom transfer radical polymerization (ATRP) in aqueous media at ambient temperature. Chem. Commun. **18**, 1817–1818 (1999)
103. Wang, X.S., Jackson, R.A., Armes, S.P.: Facile synthesis of acidic copolymers via atom transfer radical polymerization in aqueous media at ambient temperature. Macromolecules **33**(2), 255–257 (2000)
104. Heredia, K.L., Bontempo, D., Ly, T., Byers, J.T., Halstenberg, S., Maynard, H.D.: In situ preparation of protein–"smart" polymer conjugates with retention of bioactivity. J. Am. Chem. Soc. **127**(48), 16955–16960 (2005)
105. Lele, B.S., Murata, H., Matyjaszewski, K., Russell, A.J.: Synthesis of uniform protein–polymer conjugates. Biomacromolecules **6**(6), 3380–3387 (2005)
106. Peeler, J.C., Woodman, B.F., Averick, S., Miyake-Stoner, S.J., Stokes, A.L., Hess, K.R., Matyjaszewski, K., Mehl, R.A.: Genetically encoded initiator for polymer growth from proteins. J. Am. Chem. Soc. **132**(39), 13575–13577 (2010)
107. Wever, D.A.Z., Raffa, P., Picchioni, F., Broekhuis, A.A.: Acrylamide homopolymers and acrylamide–n-isopropylacrylamide block copolymers by atomic transfer radical polymerization in water. Macromolecules **45**(10), 4040–4045 (2012)
108. Zhang, Q., Wilson, P., Li, Z., McHale, R., Godfrey, J., Anastasaki, A., Waldron, C., Haddleton, D.M.: Aqueous copper-mediated living polymerization: exploiting rapid disproportionation of CuBr with Me6TREN. J. Am. Chem. Soc. **135**(19), 7355–7363 (2013)
109. Nguyen, N.H., Rodriguez-Emmenegger, C., Brynda, E., Sedlakova, Z., Percec, V.: SET-LRP of N-(2-hydroxypropyl)methacrylamide in H_2O. Polym. Chem. **4**(8), 2424–2427 (2013)

110. Konkolewicz, D., Magenau, A.J.D., Averick, S.E., Simakova, A., He, H., Matyjaszewski, K.: ICAR ATRP with ppm Cu Catalyst in Water. Macromolecules **45**(11), 4461–4468 (2012)
111. Tsarevsky, N.V., Braunecker, W.A., Matyjaszewski, K.: Electron transfer reactions relevant to atom transfer radical polymerization. J. Organomet. Chem. **692**(15), 3212–3222 (2007)
112. Zhang, X., Xia, J.H., Matyjaszewski, K.: Controlled/"living" radical polymerization of 2-(dimethylamino)ethyl methacrylate. Macromolecules **31**(15), 5167–5169 (1998)
113. Dong, H., Matyjaszewski, K.: ARGET ATRP of 2-(dimethylamino)ethyl methacrylate as an intrinsic reducing agent. Macromolecules **41**(19), 6868–6870 (2008)
114. Even, M., Haddleton, D.M., Kukulj, D.: Synthesis and characterization of amphiphilic triblock polymers by copper mediated living radical polymerization. Eur. Polym. J. **39**(4), 633–639 (2003)
115. Li, Y., Armes, S.P., Jin, X., Zhu, S.: Direct synthesis of well-defined quaternized homopolymers and diblock copolymers via ATRP in protic media. Macromolecules **36**(22), 8268–8275 (2003)
116. Xia, Y., Yin, X., Burke, N.A.D., Stöver, H.D.H.: Thermal response of narrow-disperse poly(N-isopropylacrylamide) prepared by atom transfer radical polymerization. Macromolecules **38**(14), 5937–5943 (2005)
117. Weaver, J.V.M., Bannister, I., Robinson, K.L., Bories-Azeau, X., Armes, S.P., Smallridge, M., McKenna, P.: Stimulus-responsive water-soluble polymers based on 2-hydroxyethyl methacrylate. Macromolecules **37**(7), 2395–2403 (2004)
118. Jin, X., Shen, Y., Zhu, S.: Atom transfer radical block copolymerization of 2-(N,N-dimethylamino)ethyl methacrylate and 2-hydroxyethyl methacrylate. Macromol. Mater. Eng. **288**(12), 925–935 (2003)
119. Oh, J.K., Matyjaszewski, K.: Synthesis of poly(2-hydroxyethyl methacrylate) in protic media through atom transfer radical polymerization using activators generated by electron transfer. J. Polym. Sci. Part A Polym. Chem. **44**(12), 3787–3796 (2006)
120. Lee, S.B., Russell, A.J., Matyjaszewski, K.: ATRP synthesis of amphiphilic random, gradient, and block copolymers of 2-(dimethylamino)ethyl methacrylate and n-butyl methacrylate in aqueous media. Biomacromolecules **4**(5), 1386–1393 (2003)
121. Iddon, P.D., Robinson, K.L., Armes, S.P.: Polymerization of sodium 4-styrenesulfonate via atom transfer radical polymerization in protic media. Polymer **45**(3), 759–768 (2004)
122. Ma, I.Y., Lobb, E.J., Billingham, N.C., Armes, S.P., Lewis, A.L., Lloyd, A.W., Salvage, J.: Synthesis of biocompatible polymers. 1. Homopolymerization of 2-methacryloyloxyethyl phosphorylcholine via ATRP in protic solvents: an optimization study. Macromolecules **35**(25), 9306–9314 (2002)
123. Tang, X., Liang, X., Gao, L., Fan, X., Zhou, Q.: Water-soluble triply-responsive homopolymers of N,N-dimethylaminoethyl methacrylate with a terminal azobenzene moiety. J. Polym. Sci. Part A Polym. Chem. **48**(12), 2564–2570 (2010)
124. Gaynor, S.G., Qiu, J., Matyjaszewski, K.: Controlled/"living" radical polymerization applied to water-borne systems. Macromolecules **31**(17), 5951–5954 (1998)
125. Qiu, J., Charleux, B., Matyjaszewski, K.: Controlled/living radical polymerization in aqueous media: homogeneous and heterogeneous systems. Prog. Polym. Sci. **26**(10), 2083–2134 (2001)
126. Cunningham, M.F.: Living/controlled radical polymerizations in dispersed phase systems. Prog. Polym. Sci. **27**(6), 1039–1067 (2002)
127. Save, M., Guillaneuf, Y., Gilbert, R.G.: Controlled radical polymerization in aqueous dispersed media. Aust. J. Chem. **59**(10), 693–711 (2006)
128. McLeary, J.B., Klumperman, B.: RAFT mediated polymerisation in heterogeneous media. Soft Matter **2**(1), 45–53 (2006)
129. Cunningham, M.F.: Controlled/living radical polymerization in aqueous dispersed systems. Prog. Polym. Sci. **33**(4), 365–398 (2008)
130. Zetterlund, P.B., Kagawa, Y., Okubo, M.: Controlled/living radical polymerization in dispersed systems. Chem. Rev. **108**(9), 3747–3794 (2008)

131. Okubo, M., Minami, H., Zhou, J.: Preparation of block copolymer by atom transfer radical seeded emulsion polymerization. Colloid Polym. Sci. **282**(7), 747–752 (2004)
132. Kagawa, Y., Zetterlund, P.B., Minami, H., Okubo, M.: Atom transfer radical polymerization in miniemulsion: partitioning effects of copper(I) and copper(II) on polymerization rate, livingness, and molecular weight distribution. Macromolecules **40**(9), 3062–3069 (2007)
133. Simms, R.W., Cunningham, M.F.: Reverse atom transfer radical polymerization of butyl methacrylate in a miniemulsion stabilized with a cationic surfactant. J. Polym. Sci. Part A Polym. Chem. **44**(5), 1628–1634 (2006)
134. Qiu, J., Pintauer, T., Gaynor, S.G., Matyjaszewski, K., Charleux, B., Vairon, J.P.: Mechanistic aspect of reverse atom transfer radical polymerization of n-butyl methacrylate in aqueous dispersed system. Macromolecules **33**(20), 7310–7320 (2000)
135. Min, K., Matyjaszewski, K.: Atom transfer radical polymerization in aqueous dispersed media. Cent. Eur. J. Chem. **7**(4), 657–674 (2009)
136. Li, M., Jahed, N.M., Min, K., Matyjaszewski, K.: Preparation of linear and star-shaped block copolymers by ATRP using simultaneous reverse and normal initiation process in bulk and miniemulsion. Macromolecules **37**(7), 2434–2441 (2004)
137. Min, K.E., Li, M., Matyjaszewski, K.: Preparation of gradient copolymers via ATRP using a simultaneous reverse and normal initiation process. I. spontaneous gradient. J. Polym. Sci. Part A Polym. Chem. **43**(16), 3616–3622 (2005)
138. Min, K., Gao, H., Matyjaszewski, K.: Development of an ab initio emulsion atom transfer radical polymerization: from microemulsion to emulsion. J. Am. Chem. Soc. **128**(32), 10521–10526 (2006)
139. Min, K., Gao, H., Yoon, J.A., Wu, W., Kowalewski, T., Matyjaszewski, K.: One-pot synthesis of hairy nanoparticles by emulsion ATRP. Macromolecules **42**(5), 1597–1603 (2009)
140. Min, K., Jakubowski, W., Matyjaszewski, K.: AGET ATRP in the presence of air in miniemulsion and in bulk. Macromol. Rapid Commun. **27**(8), 594–598 (2006)
141. Min, K., Matyjaszewski, K.: Atom transfer radical polymerization in microemulsion. Macromolecules **38**(20), 8131–8134 (2005)
142. Dong, H., Matyjaszewski, K.: Thermally responsive P(M(EO)2MA-co-OEOMA) copolymers via AGET ATRP in miniemulsion. Macromolecules **43**(10), 4623–4628 (2010)
143. Min, K., Gao, H.: New method to access hyperbranched polymers with uniform structure via one-pot polymerization of inimer in microemulsion. J. Am. Chem. Soc. **134**(38), 15680–15683 (2012)
144. Stoffelbach, F., Griffete, N., Bui, C., Charleux, B.: Use of a simple surface-active initiator in controlled/living free-radical miniemulsion polymerization under AGET and ARGET ATRP conditions. Chem. Commun. **39**, 4807–4809 (2008)
145. Elsen, A.M., Burdynska, J., Park, S., Matyjaszewski, K.: Activators regenerated by electron transfer atom transfer radical polymerization in miniemulsion with 50 ppm of copper catalyst. ACS Macro. Lett. **2**(9), 822–825 (2013)
146. Elsen, A.M., Burdynska, J., Park, S., Matyjaszewski, K.: Active ligand for low PPM miniemulsion atom transfer radical polymerization. Macromolecules **45**(18), 7356–7363 (2012)
147. Tsarevsky, N.V., Min, K., Jahed, N.M., Gao, H., Matyjaszewski, K.: Functional degradable polymeric materials prepared by atom transfer radical polymerization. In: ACS Symposium Series, vol. 939. Degradable Polymers and Materials, pp. 184–200 (2006)
148. Li, W., Yoon Jeong, A., Matyjaszewski, K.: Dual-reactive surfactant used for synthesis of functional nanocapsules in miniemulsion. J. Am. Chem. Soc. **132**(23), 7823–7825 (2010)
149. Li, W., Matyjaszewski, K., Albrecht, K., Moller, M.: Reactive surfactants for polymeric nanocapsules via interfacially confined miniemulsion ATRP. Macromolecules **42**(21), 8228–8233 (2009)
150. Oh, J.K., Tang, C., Gao, H., Tsarevsky, N.V., Matyjaszewski, K.: Inverse miniemulsion ATRP: a new method for synthesis and functionalization of well-defined water-soluble/cross-linked polymeric particles. J. Am. Chem. Soc. **128**(16), 5578–5584 (2006)
151. Li, W., Matyjaszewski, K.: AGET ATRP of oligo(ethylene glycol) monomethyl ether methacrylate in inverse microemulsion. Polym. Chem. **3**, 1813–1819 (2012)

152. Oh, J.K., Perineau, F., Matyjaszewski, K.: Preparation of nanoparticles of well-controlled water-soluble homopolymers and block copolymers using an inverse miniemulsion ATRP. Macromolecules **39**(23), 8003–8010 (2006)
153. Oh, J.K., Siegwart, D.J., Lee, H-i, Sherwood, G., Peteanu, L., Hollinger, J.O., Kataoka, K., Matyjaszewski, K.: Biodegradable nanogels prepared by atom transfer radical polymerization as potential drug delivery carriers: synthesis, biodegradation, in vitro release, and bioconjugation. J. Am. Chem. Soc. **129**(18), 5939–5945 (2007)
154. Oh, J.K., Siegwart, D.J., Matyjaszewski, K.: Synthesis and biodegradation of nanogels as delivery carriers for carbohydrate drugs. Biomacromolecules **8**(11), 3326–3331 (2007)
155. Averick, S.E., Paredes, E., Irastorza, A., Shrivats, A.R., Srinivasan, A., Siegwart, D.J., Magenau, A.J., Cho, H.Y., Hsu, E., Averick, A.A., Kim, J., Liu, S., Hollinger, J.O., Das, S.R., Matyjaszewski, K.: Preparation of cationic nanogels for nucleic acid delivery. Biomacromolecules **13**(11), 3445–3449 (2012)
156. Slaughter, B.V., Khurshid, S.S., Fisher, O.Z., Khademhosseini, A., Peppas, N.A.: Hydrogels in regenerative medicine. Adv. Mater. **21**(32–33), 3307–3329 (2009)
157. Cabodi, M., Choi, N.W., Gleghorn, J.P., Lee, C.S.D., Bonassar, L.J., Stroock, A.D.: A microfluidic biomaterial. J. Am. Chem. Soc. **127**(40), 13788–13789 (2005)
158. Choi, S.-W., Xie, J., Xia, Y.: Chitosan-based inverse opals: three-dimensional scaffolds with uniform pore structures for cell culture. Adv. Mater. **21**(29), 2997–3001 (2009)
159. Tanaka, H., Isojima, T., Hanasaki, M., Ifuku, Y., Takeuchi, H., Kawaguchi, H., Shiroya, T.: Porous protein-based nanoparticle hydrogel for protein chips with improved sensitivity. Macromol. Rapid Commun. **29**(15), 1287–1292 (2008)
160. Oh, J.K., Drumright, R., Siegwart, D.J., Matyjaszewski, K.: The development of microgels/nanogels for drug delivery applications. Prog. Polym. Sci. **33**(4), 448–477 (2008)
161. Aoshima, S., Kanaoka, S.: Synthesis of stimuli-responsive polymers by living polymerization: poly(N-isopropylacrylamide) and poly(vinyl ether)s. Adv. Polym. Sci. **210**, 169–208 (2008)
162. Rapoport, N.: Physical stimuli-responsive polymeric micelles for anti-cancer drug delivery. Prog. Polym. Sci. **32**(8–9), 962–990 (2007)
163. Lutz, J.F., Akdemir, O., Hoth, A.: Point by point comparison of two thermosensitive polymers exhibiting a similar LCST: is the age of poly(NIPAM) over? J. Am. Chem. Soc. **128**, 13046–13047 (2006)
164. Lutz, J.-F.: Polymerization of oligo(ethylene glycol) (meth)acrylates: toward new generations of smart biocompatible materials. J. Polym. Sci. Part A Polym. Chem. **46**(11), 3459–3470 (2008)
165. Morimoto, N., Ohki, T., Kurita, K., Akiyoshi, K.: Thermo-responsive hydrogels with nanodomains: rapid shrinking of a nanogel-crosslinking hydrogel of poly(N-isopropyl acrylamide). Macromol. Rapid Commun. **29**(8), 672–676 (2008)
166. Cho, E.C., Kim, J.W., Fernandez-Nieves, A., Weitz, D.A.: Highly responsive hydrogel scaffolds formed by three-dimensional organization of microgel nanoparticles. Nano Lett. **8**(1), 168–172 (2008)
167. Tan, Y., Xu, K., Wang, P., Li, W., Sun, S., Dong, L.: High mechanical strength and rapid response rate of poly(N-isopropyl acrylamide) hydrogel crosslinked by starch-based nanospheres. Soft Matter **6**, 1467–1471 (2010)
168. Liu, R., Saunders, J.M., Freemont, T.J., Saunders, B.R.: Doubly crosslinked microgel-polyelectrolyte complexes: three simple methods to tune and improve gel mechanical properties. Soft Matter **8**(42), 10932–10940 (2012)
169. Serizawa, T., Wakita, K., Kaneko, T., Akashi, M.: Thermoresponsive properties of porous poly(N-isopropylacrylamide) hydrogels prepared in the presence of nanosized silica particles and subsequent acid treatment. J. Polym. Sci. Part A Polym. Chem. **40**(23), 4228–4235 (2002)
170. Yoon, J.A., Gayathri, C., Gil, R.R., Kowalewski, T., Matyjaszewski, K.: Comparison of the thermoresponsive deswelling kinetics of poly(2-(2-methoxyethoxy)ethyl methacrylate) hydrogels prepared by ATRP and FRP. Macromolecules **43**(10), 4791–4797 (2010)

171. Kanamori, K., Hasegawa, J., Nakanishi, K., Hanada, T.: Facile synthesis of macroporous cross-linked methacrylate gels by atom transfer radical polymerization. Macromolecules **41**(19), 7186–7193 (2008)
172. Yoon, J.A., Bencherif, S.A., Aksak, B., Kim, E.K., Kowalewski, T., Oh, J.K., Matyjaszewski, K. Thermoresponsive hydrogel scaffolds with tailored hydrophilic pores. Chem. Asian J. **6**(1), 128–136 (2011)
173. Bencherif, S.A., Siegwart, D.J., Srinivasan, A., Horkay, F., Hollinger, J.O., Washburn, N.R., Matyjaszewski, K.: Nanostructured hybrid hydrogels prepared by a combination of atom transfer radical polymerization and free radical polymerization. Biomaterials **30**, 5270–5278 (2009)
174. Bencherif, S.A., Washburn, N.R., Matyjaszewski, K.: Synthesis by AGET ATRP of degradable nanogel precursors for in situ formation of nanostructured hyaluronic acid hydrogel. Biomacromolecules **10**, 2499–2507 (2009)
175. Siegwart, D.J., Bencherif, S.A., Srinivasan, A., Hollinger, J.O., Matyjaszewski, K.: Synthesis, characterization, and in vitro cell culture viability of degradable poly(N-isopropylacrylamide-co-5,6-benzo-2-methylene-1,3-dioxepane)-based polymers and crosslinked gels. J. Biomed. Mater. Res. Part A **87A**(2), 345–358 (2008)
176. Kamada, J., Koynov, K., Corten, C., Juhari, A., Yoon, J.A., Urban, M.W., Balazs, A.C., Matyjaszewski, K.: Redox responsive behavior of thiol/disulfide-functionalized star polymers synthesized via atom transfer radical polymerization. Macromolecules **43**(9), 4133–4139 (2010)
177. Nicolay, R., Kamada, J., Van Wassen, A., Matyjaszewski, K.: Responsive gels based on a dynamic covalent trithiocarbonate cross-linker. Macromolecules **43**(9), 4355–4361 (2010)
178. Yoon, J.A., Kowalewski, T., Matyjaszewski, K.: Comparison of thermoresponsive deswelling kinetics of poly(oligo(ethylene oxide) methacrylate)-based thermoresponsive hydrogels prepared by "Graft-from" ATRP. Macromolecules **44**(7), 2261–2268 (2011)
179. Aleksanian, S., Chan, N., Wen, Y., Oh J.K.: Thial–responsive hydrogel scaffolds for rapid change in thermoresponsiveness. RSC Adv. **4**, 3713–3721 (2014)
180. Hamidi, M., Azadi, A., Rafiei, P.: Hydrogel nanoparticles in drug delivery. Adv. Drug Delivery Rev. **60**(15), 1638–1649 (2008)
181. Kabanov, A.V., Vinogradov, S.V.: Nanogels as pharmaceutical carriers: finite networks of infinite capabilities. Angew. Chem. Int. Ed. **48**(30), 5418–5429 (2009)
182. Antonietti, M., Landfester, K.: Polyreactions in miniemulsions. Prog. Polym. Sci. **27**(4), 689–757 (2002)
183. Oh, J.K., Bencherif, S.A., Matyjaszewski, K.: Atom transfer radical polymerization in inverse miniemulsion: a versatile route toward preparation and functionalization of microgels/nanogels for targeted drug delivery applications. Polymer **50**(19), 4407–4423 (2009)
184. Dong, H., Mantha, V., Matyjaszewski, K.: Thermally responsive PM(EO)2MA magnetic microgels via activators generated by electron transfer atom transfer radical polymerization in miniemulsion. Chem. Mater. **21**(17), 3965–3972 (2009)
185. Averick, S.E., Magenau, A.J.D., Simakova, A., Woodman, B.F., Seong, A., Mehl, R.A., Matyjaszewski, K.: Covalently incorporated protein-nanogels using AGET ATRP in an inverse miniemulsion. Polym. Chem. **2**(7), 1476–1478 (2011)
186. Li, W., Matyjaszewski, K.: AGET ATRP in an inverse microemulsion. PMSE Prepr. **106**, 142–144 (2012)
187. Sugihara, S., Sugihara, K., Armes, S.P., Ahmad, H., Lewis, A.L.: Synthesis of biomimetic Poly(2-(methacryloyloxy)ethyl phosphorylcholine) nanolatexes via atom transfer radical dispersion polymerization in alcohol/water mixtures. Macromolecules **43**(15), 6321–6329 (2010)
188. Kim, K.H., Kim, J., Jo, W.H.: Preparation of hydrogel nanoparticles by atom transfer radical polymerization of N-isopropylacrylamide in aqueous media using PEG macro-initiator. Polymer **46**(9), 2836–2840 (2005)
189. Mikhail, A.S., Allen, C.: Block copolymer micelles for delivery of cancer therapy: transport at the whole body, tissue and cellular levels. J. Controlled Release **138**(3), 214–223 (2009)

190. Xiong, X.-B., Falamarzian, A., Garg, S.M., Lavasanifar, A.: Engineering of amphiphilic block copolymers for polymeric micellar drug and gene delivery. J. Controlled Release **155**(2), 248–261 (2011)
191. O'Reilly, R.K., Joralemon, M.J., Hawker, C.J., Wooley, K.L.: Preparation of orthogonally-functionalized core click cross-linked nanoparticles. New J. Chem. **31**(5), 718–724 (2007)
192. Huang, H., Remsen, E.E., Kowalewski, T., Wooley, K.L.: Nanocages derived from shell cross-linked micelle templates. J. Am. Chem. Soc. **121**(15), 3805–3806 (1999)
193. Zhang, Q., Ko, N.R., Oh, J.K.: Recent advances in stimuli-responsive degradable block copolymer micelles: synthesis and controlled drug delivery applications. Chem. Commun. **48**(61), 7542–7552 (2012)
194. Binauld, S., Stenzel, M.H.: Acid-degradable polymers for drug delivery: a decade of innovation. Chem. Commun. **49**(21), 2082–2102 (2013)
195. Zhao, Y.: Light-responsive block copolymer micelles. Macromolecules **45**(9), 3647–3657 (2012)
196. Duong, H.T.T., Marquis, C.P., Whittaker, M., Davis, T.P., Boyer, C.: Acid degradable and biocompatible polymeric nanoparticles for the potential codelivery of therapeutic agents. Macromolecules **44**(20), 8008–8019 (2011)
197. Zhang, Z., Yin, L., Tu, C., Song, Z., Zhang, Y., Xu, Y., Tong, R., Zhou, Q., Ren, J., Cheng, J.: Redox-responsive, core cross-linked polyester micelles. ACS Macro. Lett. **2**(1), 40–44 (2013)
198. Ryu, J.-H., Chacko, R.T., Jiwpanich, S., Bickerton, S., Babu, R.P., Thayumanavan, S.: Self-cross-linked polymer nanogels: a versatile nanoscopic drug delivery platform. J. Am. Chem. Soc. **132**(48), 17227–17235 (2010)
199. Zhang, Q., Aleksanian, S., Noh, S.M., Oh, J.K.: Thiol-responsive block copolymer nanocarriers exhibiting tunable release with morphology changes. Polym. Chem. **4**(2), 351–359 (2012)
200. Chan, N., An, S.Y., Oh, J.K.: Dual location disulfide degradable interlayer-crosslinked micelles with extended sheddable coronas exhibiting enhanced colloidal stability and rapid release Polym. Chem. **5**, 1637–1649 (2014)
201. Kretlow, J.D., Klouda, L., Mikos, A.G.: Injectable matrices and scaffolds for drug delivery in tissue engineering. Adv. Drug Deliv. Rev. **59**(4–5), 263–273 (2007)
202. He, C., Kim, S.W., Lee, D.S.: In situ gelling stimuli-sensitive block copolymer hydrogels for drug delivery. J. Controlled Release **127**(3), 189–207 (2008)
203. Yu, L., Ding, J.: Injectable hydrogels as unique biomedical materials. Chem. Soc. Rev. **37**(8), 1473–1481 (2008)
204. Park, M., Joo, M., Choi, B., Jeong, B.: Biodegradable thermogels. Acc. Chem. Res. **45**(3), 424–433 (2012)
205. Moon, H., Ko, Y., Park, M., Joo, M., Jeong, B.: Temperature-responsive compounds as in situ gelling biomedical materials. Chem. Soc. Rev. **41**(14), 4860 (2012)
206. Hamley, I.W.: The physics of block copolymers, vol. 19 (Oxford University Press, New York, 1998)
207. Ma, Y., Tang, Y., Billingham, N., Armes, S., Lewis, A.: Synthesis of biocompatible, stimuli-responsive, physical gels based on ABA triblock copolymers. Biomacromolecules **4**(4), 864–868 (2003)
208. Castelletto, V., Hamley, I., Ma, Y., Bories-Azeau, X., Armes, S., Lewis, A.: Microstructure and physical properties of a pH-responsive gel based on a novel biocompatible ABA-type triblock copolymer. Langmuir **20**(10), 4306–4309 (2004)
209. Li, C., Madsen, J., Armes, S., Lewis, A.: A new class of biochemically degradable, stimulus-responsive triblock copolymer gelators. Angew. Chem. Int. Ed. **45**(21), 3510–3513 (2006)
210. Li, C., Tang, Y., Armes, S., Morris, C., Rose, S., Lloyd, A., Lewis, A.: Synthesis and characterization of biocompatible thermo-responsive gelators based on ABA triblock copolymers. Biomacromolecules **6**(2), 994–999 (2005)
211. Hayward, J., Chapman, D.: Biomembrane surfaces as models for polymer design: the potential for haemocompatibility. Biomaterials **5**(3), 135–142 (1984)

212. Lewis, A., Cumming, Z., Goreish, H., Kirkwood, L., Tolhurst, L., Stratford, P.: Crosslinkable coatings from phosphorylcholine-based polymers. Biomaterials **22**(2), 99–111 (2001)
213. Lewis, A., Hughes, P., Kirkwood, L., Leppard, S., Redman, R., Tolhurst, L., Stratford, P.: Synthesis and characterisation of phosphorylcholine-based polymers useful for coating blood filtration devices. Biomaterials **21**(18), 1847–1859 (2000)
214. Woodcock, J., Wright, R., Jiang, X., O'Lenick, T., Zhao, B.: Dually responsive aqueous gels from thermo- and light-sensitive hydrophilic ABA triblock copolymers. Soft Matter **6**(14), 3325 (2010)
215. Gao, W., Durham, D., Xu, D., Lim, D., Gyeonggi-do, O., Craig, S., Chilkoti, A.: In situ growth of a thermoresponsive polymer from a genetically engineered elastin-like polypeptide. Polym. Chem. **2**(7):1561 (2011)
216. Lin, Z., Cao, S., Chen, X., Wu, W., Li, J.: Thermoresponsive hydrogels from phosphorylated ABA triblock copolymers: a potential scaffold for bone tissue engineering. Biomacromolecules **14**(7), 2206–2214 (2013)
217. Reinicke, S., Schmalz, H.: Combination of living anionic polymerization and ATRP via "click" chemistry as a versatile route to multiple responsive triblock terpolymers and corresponding hydrogels. Colloid Polym. Sci. **289**(5–6), 497–512 (2011)
218. Shunmugam, R., Massachusetts, U., Smith, C., Tew, G.: Atrp synthesis of abc lipophilic–hydrophilic–fluorophilic triblock copolymers. J. Polym. Sci. Part A Polym. Chem. **45**(13), 2601–2608 (2007)
219. Dayananda, K., Pi, B., Kim, B., Park, T., Lee, D.: Synthesis and characterization of pH/temperature-sensitive block copolymers via atom transfer radical polymerization. Polymer **48**(3), 758–762 (2007)
220. Beheshti, N., Oslo, U., Zhu, K., Kjøniksen, A.-L., Pharmacy, S., Knudsen, K., Box, K., Nyström, B.: Characterization of temperature-induced association in aqueous solutions of charged ABCBA-type pentablock tercopolymers. Soft Matter **7**(3), 1168 (2011)
221. Abandansari, H., Aghaghafari, E., Nabid, M., Niknejad, H.: Preparation of injectable and thermoresponsive hydrogel based on penta-block copolymer with improved sol stability and mechanical properties. Polymer **54**(4), 1329–1340 (2013)
222. Lin, H.-H., Cheng, Y.-L.: In situ thermoreversible gelation of block and star copolymers of poly(ethylene glycol) and poly(-isopropylacrylamide) of varying architectures. Macromolecules **34**(11), 3710–3715 (2001)
223. Hietala, S., Mononen, P., Strandman, S., Järvi, P., Torkkeli, M., Jankova, K., Hvilsted, S., Tenhu, H.: Synthesis and rheological properties of an associative star polymer in aqueous solutions. Polymer **48**(14), 4087–4096 (2007)
224. Li, Y., Tang, Y., Narain, R., Lewis, A., Armes, S.: Biomimetic stimulus-responsive star diblock gelators. Langmuir **21**(22), 9946–9954 (2005)
225. Schmalz, A., Schmalz, H., Müller, A.: Smart hydrogels based on responsive star-block copolymers. Soft Matter **8**(36), 9436 (2012)
226. Fechler, N., Badi, N., Schade, K., Pfeifer, S., Lutz, J.-F.: Thermogelation of PEG-based macromolecules of controlled architecture. Macromolecules **42**(1), 33–36 (2009)
227. Badi, N., Lutz, J.-F.: PEG-based thermogels: applicability in physiological media. J. Controlled Release **140**(3), 224–229 (2009)
228. Zhu, W., Nese, A., Matyjaszewski, K.: Thermoresponsive star triblock copolymers by combination of ROP and ATRP: from micelles to hydrogels. J. Polym. Sci. Part A Polym. Chem. **49**(9), 1942–1952 (2011)
229. Jin, S., Liu, M., Chen, S., Gao, C.: Synthesis, characterization and the rapid response property of the temperature responsive PVP-g-PNIPAM hydrogel. Eur. Polym. J. **44**(7), 2162–2170 (2008)
230. Zhang, Y., Costantini, N., Mierzwa, M., Pakula, T., Neugebauer, D., Matyjaszewski, K.: Super soft elastomers as ionic conductors. Polymer **45**(18), 6333–6339 (2004)
231. Neugebauer, D., Zhang, Y., Pakula, T., Sheiko, S.S., Matyjaszewski, K.: Densely-grafted and double-grafted PEO brushes via ATRP. A route to soft elastomers. Macromolecules **36**(18), 6746–6755 (2003)

232. Pakula, T., Zhang, Y., Matyjaszewski, K., Lee, H-i, Boerner, H., Qin, S., Berry, G.C.: Molecular brushes as super-soft elastomers. Polymer **47**(20), 7198–7206 (2006)
233. Mpoukouvalas, A., Li, W., Graf, R., Koynov, K., Matyjaszewski, K.: Soft elastomers via introduction of poly(butyl acrylate) "diluent" to poly(hydroxyethyl acrylate)-based gel networks. ACS Macro Lett **2**(1), 23–26 (2013)

Supramolecular Soft Biomaterials for Biomedical Applications

Enyi Ye, Pei Lin Chee, Ankshita Prasad, Xiaotian Fang, Cally Owh, Valerie Jing Jing Yeo and Xian Jun Loh

Abstract Rapidly aging societies, demands for improved organ functions and repair of damaged tissues has led to the use of synthetic materials in different parts of our body. Traditional covalent chemistry has served us well in terms of the design of materials. The future of soft biomaterials demands the ease of synthesis, multi-functionality and efficacy. Supramolecular hydrogels are the next-generation materials to enter the biomedical arena. These materials are three-dimensional entities built from crosslinking agents which bond non-covalently (via hydrogen bonds, π-π stacking and van der Waals interactions) to produce fibers and crosslinking among fibers. The properties of these materials are vastly different from their covalent counterparts and the exciting developments are summarized in this review.

Keywords Supramolecular · Dynamic systems · Host-guest · Biomaterials · Hierarchical self-assembly

1 Introduction

According to the classical explanation of the Nobel Laureate Jean-Marie Lehn, supramolecular chemistry is the chemistry of molecular assemblies (supramolecular system with specific structure and functionality) formed through the intermolecular interactions among two or more chemical species [1, 2]. Polymeric hydrogels

E. Ye · P.L. Chee · A. Prasad · X. Fang · C. Owh · V.J.J. Yeo · X.J. Loh (✉)
Institute of Materials Research and Engineering (IMRE), A*STAR, 3 Research Link, Singapore 117602, Singapore
e-mail: lohxj@imre.a-star.edu.sg; XianJun_Loh@scholars.a-star.edu.sg

X.J. Loh
Department of Materials Science and Engineering, National University of Singapore, 9 Engineering Drive 1, Singapore 117576, Singapore

X.J. Loh
Singapore Eye Research Institute, 11 Third Hospital Avenue, Singapore 168751, Singapore

X.J. Loh (ed.), *In-Situ Gelling Polymers*, Series in BioEngineering,
DOI 10.1007/978-981-287-152-7_5

can be categorized in numerous ways depending on the type of polymer and their structural characteristics. Chemically crosslinked hydrogels are formed by polymer chains linked permanently by non-reversible covalent bonds. This causes the hydrogels to be brittle, at times opaque and not having the self-healing property when the network is disrupted. These covalent bonds can be made using various reactions such as Michael type addition, Schiff base formation, thiol-ene photopolymerizations, free radical photopolymerisation, enzyme-triggered reactions and "click" reactions. Chemical crosslinking can be modulated in order to sufficiently modify the mechanical properties of hydrogels and it has been frequently used when tough and stable hydrogels are desired. Unlike traditional chemistry which relies on covalent interactions, supramolecular chemistry focuses on weaker and reversible non-covalent interactions between molecules. A supramolecular polymer can be defined as an ordered array of repeating units of monomeric building blocks formed by reversible and directional non-covalent interactions [3, 4]. Supramolecular polymers can form through various intermolecular interactions such as hydrogen bonding, metal-ligand complexation, hydrophobic forces, van der Waals forces, π-π interactions and electrostatic effects, together with their synergetic interactions. Important concepts that have been demonstrated by supramolecular chemistry include molecular self-assembly, folding, molecular recognition, host-guest chemistry, mechanically-interlocked molecular architectures, and dynamic covalent chemistry. Highly complex functional materials can be built from seemingly simple modular blocks. Supramolecular chemistry offers possibilities whereby modular structures self-assemble into intricate structures. The extension of these systems beyond the level of the individual molecule relies on several key non-covalent interactions leading to a directed self-assembly step. Here, we can observe the development of structures from the primary molecular level to the secondary polymeric level and further to the tertiary networked structure. This network structure is the classical example of a hydrogel structure [5–7]. While offering the dynamic modulation of the intrinsic properties of the materials, these materials can also be assembled into novel supramolecular structures such as hydrogels, micelles and vesicles [8]. In this review, we will highlight several examples of how the supramolecular hydrogels are prepared through hydrogen bonding, ionic and associative interactions, host-guest complexation and metal-ligand complexation. These interactions have extremely high biomedical relevance as will be explained in the review. The literature reviewed here is not meant to be exhaustive but rather meant to be a primer of this research area.

2 Preparation of Supramolecular Hydrogels

2.1 Hydrogen Bonding

Hydrogen bonding is one of the main driving forces that direct the self-assembly of molecules, and it plays important roles in numerous biomedical applications. In particular, hydrogen bonding serves as the basis for the formation of a large

class of supramolecular hydrogels which have desirable properties such as sensitivity to the environment, facile formation processes and an almost universal mode of attachment. Here, we will discuss the role of hydrogen bonding on the different peptides and polymers that can form supramolecular hydrogels. It is well known that peptides can self-assemble through hydrogen bonding [9, 10]. With self-assembly, the molecules will either co-assemble in a random manner or self-sort to form an aggregated structure. With growing applications in drug delivery and tissue engineering areas, there exists a need to control the manner in which the molecules self-assemble. The use of peptides as hydrogelators in the formation of the hydrogel can potentially improve the biocompatibility of the hydrogel as peptides occur naturally in the human body, making it more suitable for any biomedical application than any other synthetic materials. Morris et al. has developed a pH-based system that is able to control the self-sorting of naphthalene-functionalized dipeptide hydrogelators to form self-assembled networks in water [11]. By hydrolysing glucono-δ-lactone (GdL) to gluconic acid, they were able to gradually modify the pH level in the system, leading to the formation of the hydrogels. The pH triggered methodology introduced in this paper utilizes kinetic self-sorting, which ensures that a self-sorted local energetic minimum is reached due to its fast formation. The advantage of this technique is that it enables the preparation of complex structures that would otherwise be difficult to achieve by conventional chemical reactions. Responsive photo-luminescent dipeptide gels were reported by Bardelang and colleagues [12]. Quantum dots (QD) have been extensively explored for bioimaging applications [13, 14]. The incorporation of QDs into hydrogels has previously been used for the development of materials for sensing and drug delivery applications [15]. Here, QDs were incorporated into soft supramolecular materials, and with the use of ultrasound, QD-gel nanocomposites were prepared. In a typical experiment, the mixture of dipeptide with hexane suspensions of CdSe/ZnS QDs covered with trioctylphosphine oxide (TOPO) as surface ligands forms gels in minutes with the use of ultrasound (Fig. 1a–c). The gels are luminescent under UV light and can revert into the sol state by the application of heat. The ability of these small peptides to generate supramolecular hydrogels demonstrates great promise for biological applications for which QDs have also shown a great potential such as biochemical sensing. In another report, Yang et al. reported the use of enzymes as a tool to regulate both the formation and the dissociation of self-assembled nanostructures and its subsequent transition into a supramolecular hydrogel [16]. This work utilised a kinase/phosphatase switch to regulate the pentapeptidic hydrogelator, Nap-FFGEY by controlling its phosphorylation and dephosphorylation. When the kinase is added to Nap-FFGEY, the self-assembling property of the hydrogel is disrupted. But with addition of a phosphatase, the self-assembling property of the hydrogel is restored (Fig. 2). The in vivo study done showed that with the subcutaneous injection of the phosphate in the mice, a supramolecular hydrogel is able to form. Given its biocompatibility, this suggests the possibility of using minimally invasive methods to introduce the hydrogel into the body as well as a better and more precise way to control the hydrogel. Other self-assembled peptide hydrogels have been investigated for

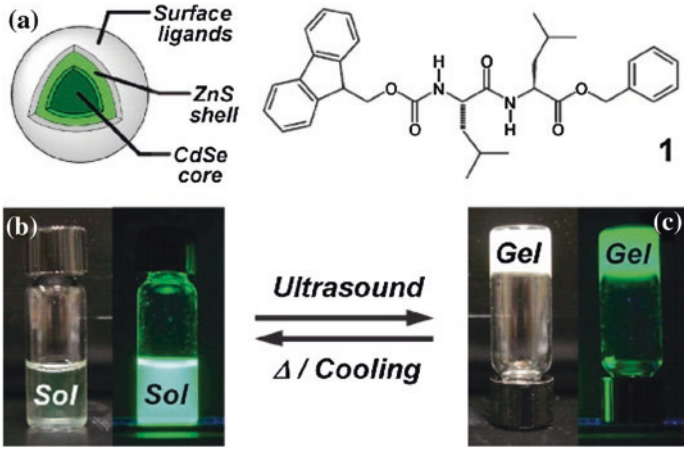

Fig. 1 **a** Structure of dipeptide 1 and hexane solution of green-light emitting CdSe/ZnS QDs with TOPO as surface ligands before (**b**) and after (**c**) application of ultrasound. **a–c** Reproduced with permission from Ref. [12]

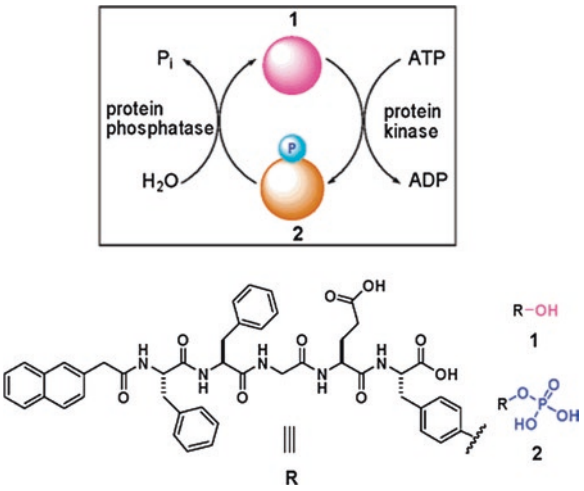

Fig. 2 Scheme of enzyme-switch-regulated supramolecular hydrogel reproduced with permission from Ref. [16]

the attenuation of hematoma and the possibility of providing a therapeutic effect in a spinal cord injury model [17]. Peptide hydrogels have also been used for the encapsulation of neural cells for up to 5 months, showing good viability [18].

In a similar way, some polymers can form a supramolecular hydrogel through H-bonding. Light as a gelation trigger is favoured due to the ease of control and convenience of usage. Peng and colleagues created a hydrogel by mixing dextran functionalized with acrylate-modified o-nitrobenzyl moieties (Dex-AN) and dithiolated poly(ethylene glycol) (DSPEG) via a Michael addition between the acrylate

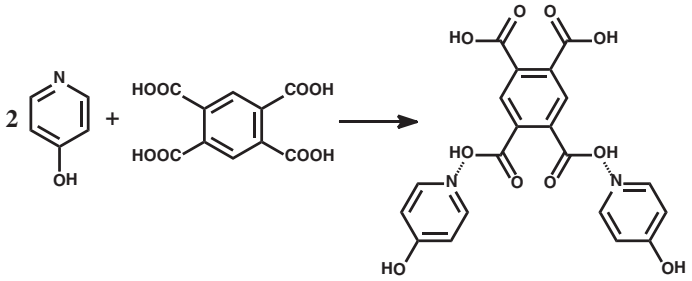

Fig. 3 Molecular structure of hydrogelator used for microfabrication of supramolecular hydrogel microspheres

and thiol groups [19]. The hydrogel that was formed from the components is light sensitive and decomposes upon irradiation as a result of the photo-labile moiety being cleaved. In this experiment, a green fluorescent protein (GFP) was used as a model protein and hence it can be seen that the GFP was released from hydrogel and migrated into the solution. The use of such hydrogels could be extended for the delivery of bioactive molecules due to its unique properties. In order to fabricate hydrogel with greater sensitivity, Chen and coworkers developed a novel strategy to fabricate supramolecular hydrogel microspheres with diameters of 15 to 105 μm using a microfluidic device from the hydrogelator shown in Fig. 3 [20]. The hydrogelator as shown in the figure is synthesized using 1,2,4,5-benzene tetracarboxylic acid and 4-hydroxy pyridine. High temperatures are used to form the droplets and allowed to cool to promote the self-assembly of the hydrogelator. The encapsulation ability of the hydrogel microspheres allows unstable or toxic biomolecules to be transported safely. With each microsphere fabricated uniformly, there exists the possibility to improve drug-loading and release kinetics.

2.2 Ionic and Associative Interactions

The formation of hydrogels through ionic interactions is possible when ionic liquids are in the presence of gelators. The presence of polymer chains with positive and negative charges at the end results in the attraction of opposite charges, thus leading to the gelation of the ionic liquids to form ionic-liquid supramolecular gels. These gels have attractive properties that include high mechanical strength and stimuli-responsive capabilities. With these enhanced properties, hydrogels formed through electrostatic interactions have found roles in applications in various areas such as microfluidics, drug delivery and artificial organ fabrication [21–23]. Interesting work done on such hydrogels include the development of fluoride-responsive fluorescent hydrogel which was embedded with CdTe quantum dots (QDs) by Zhou and coworkers [24]. The hydrogel, namely DC5700-QDs, was prepared by electrostatic

interactions of ammonium cations and carboxylate anions. Upon treating DC5700-QDs with fluoride, a highly fluorescent hydrogel formation was observed. For comparison, other anions solutions such as carbonate, sulphate, chloride and bromide was also added to DC5700-QDs, but no hydrogel was formed, confirming the unique gelation effect of the fluoride anion. DC5700-QDs with fluoride added was characterized by FT-IR and steady-state fluorescence emission. This material exists as a gel when it is below 68 °C, while above this temperature, it exists in sol state. This work is particularly useful due to the large number of applications of fluoride, especially in the biomedical and dental field [25, 26]. Besides studying the applications of ionic supramolecular hydrogels, much has been dedicated to the investigation of the synthesis and characterization of novel ionic supramolecular hydrogels. One major area of the structures that has been of great interest is the rod-coil block copolymer assembly, which has unique assembly characteristics. Due to these characteristics, the copolymers enable the organization of functional materials, such as π-conjugate polymers, into supramolecular assemblies. Huo and coworkers describe in their paper the synthesis process, as well as the characterization results of a coil-rod-coil triblock copolymer [27]. This polymer, which showed unique aggregation behaviour in a solution, was designed from oligo(p-phenylene ethynylene) (OPE) and polystyrene (PS), polystyrene–oligo(p-phenyleneethynylene)–polystyrene (PS–OPE–PS) through a novel approach that omitted the α-position substitutes into OPE blocks during the linking of the units. This method has many advantages as compared to more conventional methods, for example circumventing the solubility problems of the OPE blocks, allowing for the generation of longer OPEs, as well as increasing the tendency of parallel aligned OPE assembly formation. The strong π-π stacking interactions of rigid aromatic segments results in the distinctive gelation capability of the gel.

2.3 Host-Guest Complexation

A host-guest complex is an interesting structure where the ‘host’ is a molecular structure that resembles the shape of a ring, with the central cavity playing an essential role of hosting other “threads” of polymer. The “thread” polymer, which is often referred to as the ‘guest’, resides in the cavity in the host as a result of the host-guest interaction. For the formation of supramolecular hydrogels, cyclodextrins (CD) and cucurbit[n]urils (CB) are commonly used as the host molecule [5, 28–33]. Lin and coworkers used the reaction between cucurbit[8]uril (Q[8]) and a chitosan derivative, N-(4-diethylaminobenzyl)chitosan (EBCS) to form a supramolecular hydrogel [34]. Characteristics of the Q[8]/EBCS gel were noted, such as the thermosensitivity of the gel, as proven by repeated sol-gel transitions. Upon heating to 50 °C, a clear gel-to-sol transition was observed, indicating weak non-covalent host-guest interactions. With regards to pH, when the gel has higher pH value, supramolecular assembling was hindered due to the increase in electrostatic repulsion. On an interesting note, gelation does not occur

between Q[8] and chitosan due to the absence of diethylamino group. The gel also showed cross-linked network structure with many cavities, shown by images obtained using scanning electron microscopy. The drug release property of the hydrogel across different pH was also studied. Results showed that drug release is significantly slower in gels with a lower pH, compared to those at a higher pH. This implies that the rate of release of selected protein can be varied based on different pH media. Possible explanations for the slower release include the higher concentration of ammonium cations, which boosts the electrostatic interactions and enhances the structure. Hence this demonstrates that the Q[8]/EBCS gel is a possible pH-sensitive drug carrier. In another work, Appel and coworkers used cucurbit[8]uril (CB[8]) as host molecules to form reversible cross-links of multivalent copolymers with high binding constants leading to formation of a supramolecular hydrogel [35]. Two types of polymers involved were viologen (MV) and 2-naphthoxy (Np) derivatives. The supramolecular hydrogels were then prepared, by first adding equal amounts of the two polymers, after which CB[8] was added. An interesting point to note is that the colourless clear solution turns bright red upon the addition of CB[8], with simultaneous formation of hydrogel observed. The high association of functional polymer was due to the presence of CB[8], that holds onto the two polymers in its cavity, thus forming a network in the gel. The work then moved on to characterise the gel that was formed in terms of its rheological properties. The hydrogel pore size was controlled by the amount of CB[8] that was added into the solution. As more CB[8] was added, the gel was observed to have smaller pores in scanning electron microscopy images. Higher concentrations of CB[8] in gels appear to form a hydrogel that is a darker shade of red. This unique gel thus could have industrial applications that need such controlled viscosity or smart hydrogels. Using the same concept, self-assembled hydrogels with extremely high water content and tunable mechanical properties were prepared from cellulose derivatives [36]. These hydrogels are easily processed and the simplicity of their preparation, their availability from inexpensive renewable resources, and the tunability of their mechanical properties are distinguishing for important biomedical applications. The protein release characteristics were investigated to determine the effect of both the protein molecular weight and polymer loadings of the hydrogels on the protein release rate. Extremely sustained release of bovine serum albumin is observed over the course of 160 days from supramolecular hydrogels containing only 1.5 wt% polymeric constituents. CD is used as another popular host molecule. In a recent report, Hou and coworkers copolymerised modified gelatin with PLA-PEG-PLA under UV light illumination, which was later added to α-CDs in order to obtain a new biodegradable gel (Fig. 4) [37]. The gel was observed to have good elasticity and appears opaque in water, in contrast to being transparent in DMSO. This new hydrogel was then characterised using techniques like thermal gravimetry analysis in order determine interactions between the host and guest molecules. It was found that the gel has a two-step thermal degradation process, the first being the decomposition of α-CDs, and the second step being the decomposition of the guest polymer. The increased decomposition temperature suggests that the structure of the hydrogel is stabilized by the

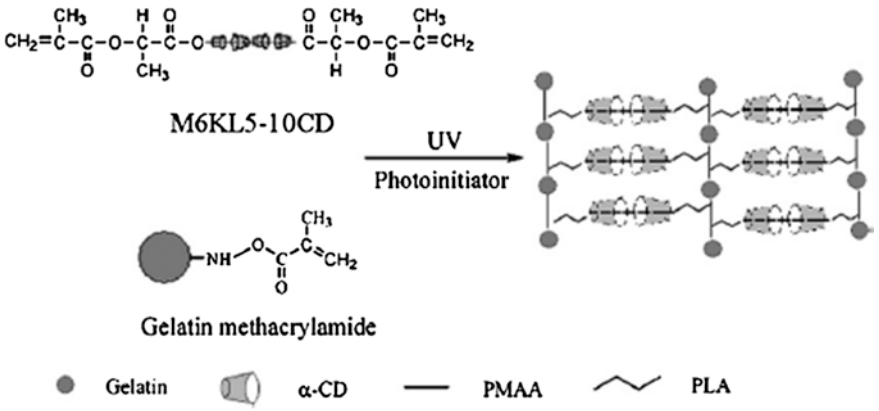

Fig. 4 Preparation route of biodegradable CD-based supramolecular hydrogels. Reproduced from Ref. [37]

interaction of these host-guest molecules. The swelling ratio of the gel was then investigated and it was shown that the swelling ratios of hydrogels increases with the increasing content of modified gelatin, due to the hydrophilic nature of gelatin. Connected pores were observed in the hydrogel, which could be used for cell adhesion and growth which are important in tissue engineering.

2.4 Metal-Ligand Complexation

The incorporation of metal ions within supramolecular gels can enhance the properties of the polymeric hydrogels and increase their utility. Metal complexes can be used as organogelators to develop hydro- and/or organogels by virtue of their rich optical, electronic, redox, or magnetic properties which increases the stability of metal complexes in common organic solvents, and also imparts new physical and chemical properties to the resulted supramolecular gels. Metal ligand ions incorporated in polymeric hydrogels can lead to the formation of ordered 2D and 3D structures with increased complexity and functions, which can serve many functions such as the separation of heavy metal ions or creating new nanostructures. Another added advantage of this approach is that they provide self-assembled superstructures with specific physiochemical properties of metal ions. In recent work, Zhang et al. incorporated a ruthenium-(II)tris(bipyridine), which is a metal complex in a hydrogelator [38]. The hydrogelator demonstrates self-assembly in water and is able to form nanofibers at low concentrations hydrogels over a range of pH. The optical images together with the emission spectrum of the hydrogel in water at pH 7 show the fluorescent ability of the hydrogel upon excitation (Fig. 5). It was discovered that lower pH values decrease the solubility of the complex and hence favours formation of the hydrogel. The hydrogel turns

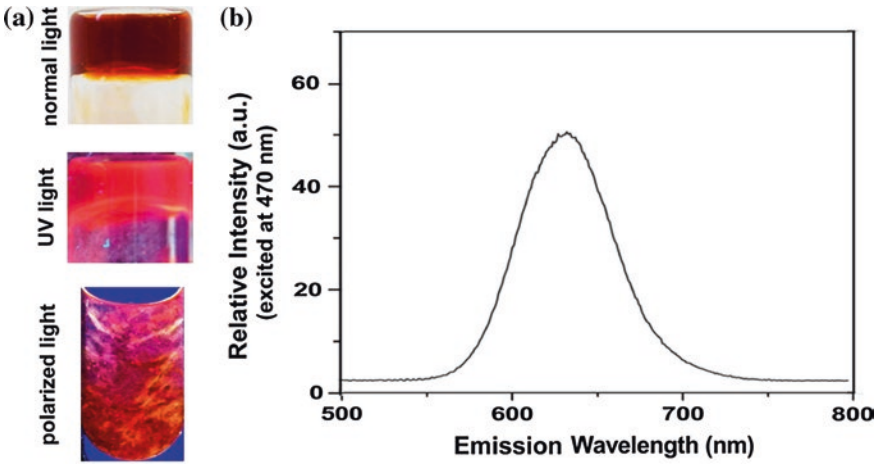

Fig. 5 **a** Optical images of hydrogel formed by 3 (0.8 % w/v) in water at pH = 7 under normal light, UV (long wavelength) light, and polarized light. **b** Emission (excited at 470 nm) spectrum of the hydrogel in (**a**). Reproduced from Ref. [38]

into a solution with oxidation, suggesting that a redox change of the ruthenium(II) tris(bipyridine) center of the complex induces a transition of the self-assembly of the complex in water. The incorporation of a metal complex with a hydrogelator helps to explore the possibility of prearranging the self-assembly motif prior to self-assembling. This work demonstrates the use of this material as a multipurpose hydrogelator and could potentially find application in live-cell imaging. In another work, Peng et al. reports a reversible gel-sol/sol-gel transition in poly-(acrylic acid) (PAA) aqueous solutions triggered by the redox state of ferric ions conjugated with photo-reduction and oxidation (Fig. 6) [39]. When Fe(III) ions in the PAA hydrogel containing citric acid are reduced to Fe(II) by light irradiation, the PAA hydrogel dissolves into a soluble state. The PAA solution can be recovered to the homogeneous hydrogel again by oxidating Fe(II) to Fe(III). This reversible transition can be observed visually and can be repeated, provided there is enough citric acid. The photochemical or electrochemical control to this transition will be a convenient method. With irradiation by stimulated sunlight, homogeneous hydrogel of PAA + Fe(III) was dissolved into solution. This process is reversible with exposure to oxygen in dark for 5 days. The redox-responsive hydrogel is also promising as a unique material that can encapsulate and localize bioactive molecules and cells within the gel matrix.

In a study by Shen et al., a series of experiments were conducted on structurally similar bile acid derivatives (BAs) to test the effects of concentration and molar ratio of BAs to M^{n+} on the gelation properties. It was reported that metal ions like Ca^{2+}, Au^{3+}, $Mg^{2+}$and Ag^{+} could trigger the self-assembly of most BAs. It was also observed that irradiation of light facilitates the formation of Au NPs in Ba-Au^{3+}. Ba-Ag^{+} hydrogel systems were found to have a temperature sensitive

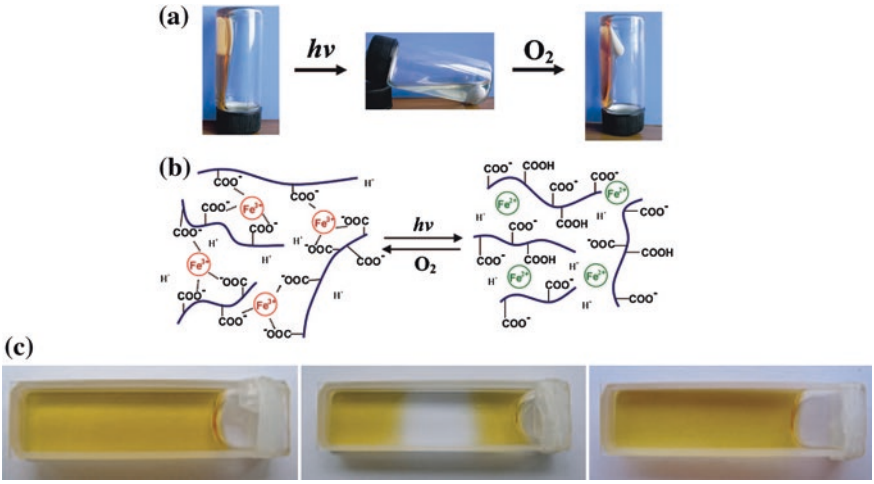

Fig. 6 **a** Switching gel-sol-gel transition in PAA (20 wt%) + Fe(III) (0.02 mol/L)- citrate (0.04 mol/L) aqueous system at pH 4.0 and room temperature. **b** Schematic illustration of the gel-sol transition in the PAA + Fe(III)-citrate aqueous system switched by photoreduction and oxidation. **c** *Left*: PAA + Fe(III) gel 3 days after preparation. *Center*: the gel irradiated for 12 min at the center part. *Right*: the same gel after exposure to oxygen for 5 days. Reproduced from Ref. [39]

reversible gel-sol state transition, with pH showing considerable effect on both BA-Ag^{+} and Ba-Au^{3+} systems. The rheological behavior indicated that irradiation helps to increase the strength of the gels. Moreover, photo-reduction was found to be a more simple and environment friendly method in comparison with using a reducing agent such as $NaBH_4$. The systems studied here provide a general strategy for incorporating AuNP or AgNPs, thereby opening up the possibility of creating effective chemo-sensing platforms, catalytic and anti-bacterial functional materials by exploiting the interesting properties of metal NPs and hydrogels.

2.5 Low Molecular Weight Hydrogels

Given the constraints of covalent bonds found in traditional polymer gels, low molecular weight hydrogels are increasingly sought as alternative replacements. These gels are made of small constituent molecules that self-assemble in water to form nanofibers that have the ability to entrap water and subsequently form a 3D network. Low molecular weight hydrogels have been attractive materials due to their biocompatibility and responsiveness to external stimuli such as temperature, pH, and mechanical force, as well as the simplicity of the gel preparation. In addition, these gels serve as biomaterials for biomedical applications as they undergo gel-sol phase transitions, which allow for the release of

the encapsulated drug. Thus, some areas of applications that have been explored include bioactive substance delivery and the regulation of enzymatic activity. In particular, low molecular weight hydrogels have been widely employed in various applications [40]. Cell targeting by the drugs is desirable as it serves to further enhance the effectiveness of drug delivery systems. With this, Ikeda et al. have demonstrated the possibility of incorporating cell sensing and targeting property into supramolecular hydrogel capsules (SH-capsule) [41]. By assembling the PSA-cleavable additive with the hydrogen capsule, responsiveness of SH-capsule to the prostate-specific antigen (PSA) was achieved. This allowed the SH-capsule to detect the prostate cancer cells through the PSA released from them, which diffused into the developed capsule to cause cleavage of the additive. Consequently, the hydrophilic fragment that was released from the capsule could target the prostate cancer cell via a plasma membrane-associated glycoprotein targeting ligand known as DUPA (2-[3-(1,3-dicarboxypropyl) ureido]pentanedioic acid), which was previously attached to the fragment. This success in sensing and targeting the prostate cancer cells can provide valuable knowledge on the applications of supramolecular hydrogels in regulating the release of bioactive substances and in tissue engineering. Apart from functioning as effective drug delivery systems, the numerous properties of the low molecular weight hydrogels also means that biomaterial can be tailor-made for different applications. This was done by Qiu and co-workers, where photo-sensitive spiropyran, D-Ala-D-Ala (a dipeptide residue which is responsive to the antibiotic vancomycin) with D-alanine and 1,3,3-trimethyl-2-methyleneindoline were assembled [42]. They found that the hydrogel formed disassembled within 5 min upon exposure to high-pressure mercury lamp of 500 W with cut-off wavelength below 400 nm. Addition of vancomycin hydrochloride on the gel surface also successfully induced the gradual transition from the gel to solution phase. The lack of the response of hydrogel incorporated with L-Ala–L-Ala to vancomycin hydrochloride illustrated that the hydrogel has assimilated the specific ligand-receptor interaction property. Thus, a hydrogel with dual response has been created which can provide insight to further development of such hydrogels tailored to different applications. Low molecular weight hydrogels can also be used as barriers to control the release of bioactive substances. This was illustrated in the study done by Komatsu and his co-workers, where they demonstrated that the phosphate-type hydrogelator formed from HO-$(CH_2)_8$-Fum-Glu-(O-cyclohexyl)$_2$ responded to four stimuli: temperature, pH, Ca^{2+} and light (Fig. 7) [43]. This meant that any of the four stimuli was able to cause a gel-sol phase transition that could control the release of the bioactive substances. This work was also further extended to the development of four fundamental logic gates (AND, OR, NAND and NOR) which were intended for regulating the release of these bioactive substances. For instance, the OR logic gate could take inputs from UV light and heat, and hence the presence of either one would be able to induce the gel-sol phase transition. Such an invention of intelligent supramolecular soft materials will be very useful in the applications of environment-sensitive actuators, tissue engineering and controlled-release systems.

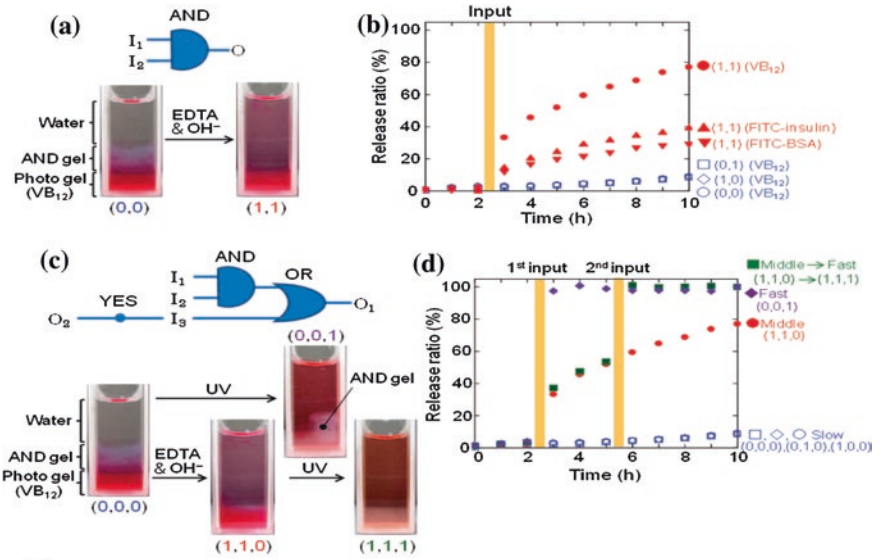

(e)

Input (I_1, I_2, I_3)			Output / 0 = Gel, 1 = Sol		
I_1 (EDTA)	I_2 (OH^-)	I_3 (UV)	O_1 (AND gel)	O_2 (Photo gel)	Release speed
0	0	0	0	0	Slow
0	1	0	0	0	Slow
1	0	0	0	0	Slow
1	1	0	1	0	Middle
0	0	1	1	1	Fast
0	1	1	1	1	Fast
1	0	1	1	1	Fast
1	1	1	1	1	Fast

Fig. 7 Controlled release of bioactive substances by supramolecular hydrogel **1** (as a logic-gate barrier) and photogel **2** (as a holding matrix) and fine-tuning of the release function through a combination of AND logic gate operation and UV light stimulation. **a** Photographs displaying a supramolecular hydrogel gate composed of AND logic gate gel **1** and photogel **2** containing vitamin B12 in a 1 cm cell before and after the AND input; the logic scheme is also shown. **b** Corresponding time courses for the release of the bioactive substances (vitamin B12, FITC-insulin, and FITC-BSA). **c** Photographs showing the supramolecular hydrogel gate holding vitamin B12 before and after application of UV light and the AND input and then after application of UV light subsequently; the combinatorial logic scheme is also shown. **d** Corresponding time courses of the vitamin B12 release. **e** Truth table for the combinational logic circuit. (**a**–**e**) are reproduced with permission from Ref. [43]

Anions which are bonded on the supramolecular hydrogel surface can also act as the growth center for biomineralization. Low molecular weight hydrogels have also found applicability in aiding bone repair, a burgeoning area of medical science given significant increases in average lifespan. The significance of bone repair has encouraged Shi et al. to study the technique of promoting growth of biominerals, which can be used as artificial bone material [44]. In the study,

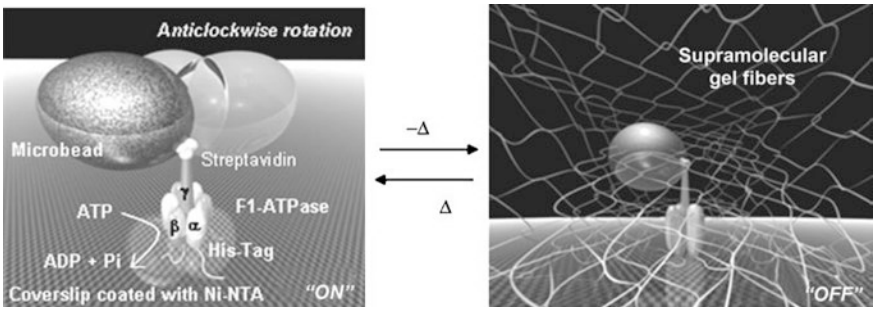

Fig. 8 Schematic illustrations of the on/off switching of F1-ATPase rotation by entanglement of the stimuli responsive supramolecular hydrogel fibers (nanomeshes). To clearly show the component of rotary motor, F1-ATPase is represented enlarged. The figure is reproduced with permission from Ref. [45]

a supramolecular hydrogel that consisted of *N*,*N*′,*N*′-tris(3-pyridyl)-trimesic amide was formed. The nitrogen heterocyclic ring and amide groups presented in the gel were chosen to function as the biomineralization active sites where the growth of the biominerals could begin. The role that the supramolecular hydrogel played was evident in their tests, as they proved that the immersion of the hydrogel into the aqueous Na_2CO_3 solution followed by $CaCl_2$ solution led to the formation of $CaCO_3$ while only layered structured calcite $CaCO_3$ was observed in the absence of the hydrogel-Na_2CO_3 composite matrix. A similar trend was also observed for the calcium phosphate-hydrogel composite, where nanoplate-like calcium phosphate was found to have enclosed the hydrogel scaffold surface. With the results from their study, Shi et al. have successfully demonstrated that, while the conventional sites are carboxylate groups binding Ca^{2+}, amide and pyridyl groups binding PO_4^{3-} can also be used as biomineralization active sites. Furthermore, the biodegradability of the hydrogel developed in this study suggests that it can be useful for the advancement of organic matrices which display high affinity for mineral ions and allow for clearance from the body. Studies have also been conducted in the area of thermally responsive supramolecular hydrogels, where the changes in temperature can elicit a phase-change response in the gels, allowing them to serve various purposes. For example, Yamaguchi and his co-workers have constructed supramolecular nanomeshes from glycolipids and adapted them to regulate the rotary motion of F1-ATPase [45]. In the experiment, a microbead unit was attached to the F1-ATPase and also embedded in the sol/gel (Fig. 8). Being thermally responsive, nanomeshes were formed at low temperature which trapped the microbead that serves as a physical hindrance to the rotary motion and switch off the ATPase motion. Conversely, a high temperature can destroy the nanomeshes and switch on the ATPase motion. The advantage of such regulating system would be beneficial in the future investigation on the use of matrices to control the microbiomachines that are powered by biological motors.

2.6 Other Methods

Apart from their various conventional formations, supramolecular hydrogels have also found use as novel hybrid materials. With the incorporation of other substances, the hybrid materials formed possess significantly enhanced inherent characteristics that could potentially aid in serving their purposes. To name a few, supramolecular hydrogels have been successfully hybridized with enzymes, silica particles, and even metal ions to create functional materials that work as drug release substances, fluorescent probes and more. One of the significant finds with regards to hybrid hydrogels resulted in the creation of a novel cancer diagnosis system. Compared to conventional methods, which require expensive equipment and long procedures, the spermine and spermidine hybrid hydrogel detection system developed by Ikeda et al. is desirable due to its simple and quick process [46]. The hydrogel therein was formed through the encapsulation of a cationic fluorescent dye, which served as a probe, in an inorganic anionic layered host, montmorillonite. This host was then embedded in a supramolecular hydrogel matrix, which served to intensify the fluorescence emitted by the probe upon the detection of spermine. This resulted in a change in the intensity of the fluorescence, which, along with the shift in the emission peak, allowed for the direct detection of the substances with only the naked eye. With this, rapid and relatively uncomplicated detections can be achieved with the sensitivities at levels almost within the range required for clinical usage. In addition to their potential uses in cancer diagnosis, hybrid supramolecular hydrogels have also been discovered to be effective in functioning as photo-responsive materials that serve many purposes in localizing bioactive molecules and more. By incorporating a stimulus-responsive molecule into a small molecule that serves as a constituent of the final hybrid hydrogel, supramolecular hydrogels that respond to stimuli can be achieved. In particular, photo-responsiveness is an attractive quality in the gels due to its ability to exert spatially and temporally controlled remote input to achieve the desired effects. Matsumoto et al. created a hybrid supramolecular hydrogel by making use of a photo-switching module, which replaced the gelator's spacer units to effectively cause the central hydrogel-network to assemble and/or diassemble through the photo-isomerization of the module [47]. This resulted in pseudo-reversible gel-sol and sol-gel transitions that could be achieved through light stimuli. Such a property allowed for the exertion of photo-control over the release of substrates, where sustained release of longer than 10 h could be accelerated to rapid releases of approximately 10 min through gel-sol transitions induced by the presence of UV light. Through the same transitions, photo-controlled starting and stopping of bacteria and enzymatic motion could also be achieved, the latter through tethering to nanobeads. Thus, this hydrogel is a novel method to control or localize bioactive molecules through light stimuli, and could hence serve as a unique biomaterial. Besides studying various potential uses of the supramolecular hydrogels, research has also been devoted to developing novel approaches that seek to improve current fabrication procedures. For example, Wang et al. reported a new method to

create polyoxometalate-based (POM-based) supramolecular hydrogels that could potentially play important roles in optics, medicine, catalysis, as well as magnetism [48]. They made use of the dispersion of POM-based building blocks in certain solvents to create the even hybrid gels. To achieve this, POMs were modified through the exchange of their counter ions with cationic surfactants, resulting in the formation of surfactant-encapsulated (SEP) POM complexes. This allowed for hybrid self-assemblings as the surface properties of the inorganic clusters were largely improved. With these properties, grafting into both organic and inorganic matrices was also made possible, and the SEPs could also be used to fabricate organogels. Thus, through appropriate selections of particular solvents and SEPs, POM-based hybrid supramolecular hydrogels could be fabricated. In addition, the relationships between the properties of the gelators and the alkyl chain density, alkyl chain length SEP, as well as the shape of the POM were investigated, and the authors have concluded that the formation of the hybrid gels was due to the effect of the electrostatic interaction and solvents. This research could hence serve as basis for the development of organic-inorganic hybrid gels through complexes with similar structures to SEPs in hydrophobic environments.

Schubert et al. reported the synthesis of poly(methyl methacrylate) based copolymers with different amounts of terpyridine units in the side chain [49]. The addition of transition metal ions, Fe (II) or Zn (II), was used to trigger supramolecular crosslinking in diluted solutions. It was found that the stability of the metal-terpyridine complexes affects the physical properties of the gel concentrations. The dissolution of the gel could be accomplished by the addition of a strong competing ligand to obtain the soluble phase. Another report focuses on poly(vinyl chloride) crosslinking in organic solvent using a variety of transition metal ions, leading to an increase in the polymer molecular weight [50]. In another report, the gelation of the amphiphilic quaternary ammonium oligoether-based ionic liquid with water is presented [51]. The thermoreversible ionogels have high ionic conductivity (up to 60 mS cm^{-1}), and storage moduli above 10^5 Pa. Upon heating, these gels melt with melting points ranging from 20 to 53 °C. These properties can be easily tuned in a broad range by varying the aqueous (and/or inorganic salts) concentration in the ionogels. The observed gelation phenomenon is purported to occur via the formation of a hydrogen bonded network between water and the ionic liquid.

Weck et al. reported the preparation of complementary hydrogen bonded cross-linked polymer networks based on two distinct hydrogen bonding recognition motifs [52]. The hydrogen bonding recognition units were based on either three-point cyanuric acid-2,4-diaminotriazine or six-point cyanuric acid-Hamilton wedge interactions. The polymer scaffold, which was functionalized with cyanuric acid functional groups, was cross-linked in 1-chloronaphthalene through complementary interchain hydrogen bonding interactions. These gels are thermally reversible and possess tunable mechanical properties that are controlled by the molecular structure of the cross-linking agent. In related work by the same group, side-chain-functionalized polymers containing hydrogen bonding and metal coordination sites were synthesized [53]. The crosslinking of these polymers can be

achieved through hydrogen bonding or metal coordination or simultaneously using both interactions through the addition of small molecule cross-linking agents. The hydrogen bonding motifs utilized for reversible cross-linking are similarly based on cyanuric acid residues hydrogen bonded to 2,4-diaminotriazine-based crosslinking agents. The metal coordination motifs are based on palladated SCS pincer complexes coordinated to bispyridine cross-linking agents. The rheology of the polymer networks from a free-flowing liquid to a highly elastic gel can be controlled and the mechanical properties of the gel can be tuned by varying the temperature and ligand displacement agents.

3 Conclusion

This review provides a snapshot of the different types of supramolecular hydrogels and their associated potential biomedical applications. The different types of interactions that drive the formation of these hydrogels have their own advantages in relation to their application as biomaterials. Hydrogen bonds are important to the body. For example, the double helix structure of DNA is held by hydrogen bonds. The folding of proteins, which is necessary for proper protein function, is also governed by hydrogen bonds. The similarities of the peptide hydrogel systems with the naturally occurring systems make them highly attractive for bioapplications. Host-guest complexations for the formation of hydrogels are attractive due to their ability to be "unlocked" by chemical triggers. This has multiple advantages. On the one hand, such a material can be expected to have multi-stimuli, on the other hand, these systems offer ease of assembly due to the high binding constants of such systems. On another aspect, with such numerous useful properties, low molecular weight hydrogels are likely to be widely used in various biomedical applications. For instance, they can be used to target specific cells and deliver drugs concurrently. They can also provide a platform to promote the growth of bone mineral. The ease of mixing low molecular weight components for the formation of a hydrogel could be a clinically attractive option. Recent developments on hybrid materials have uncovered numerous applications that hybrid hydrogels can serve. Through acting as a complement to the embedded substances by enhancing their natural properties, such hybrid supramolecular hydrogels could possibly be highly applicable in raising the effectiveness of the current substances used. The progress of supramolecular soft biomaterials has vast potential in the landscape of medical care. This area of research is one to watch for the future.

References

1. Lehn, J.M.: Supramolecular chemistry—scope and perspectives molecules, supermolecules, and molecular devices. Angew. Chem. Int. Ed. Engl. **27**(1), 89–112 (1988). doi:10.1002/anie.198800891

2. Lehn, J.M.: Perspectives in supramolecular chemistry—from molecular recognition towards molecular information-processing and self-organization. Angew. Chem. Int. Ed. Engl. **29**(11), 1304–1319 (1990). doi:10.1002/anie.199013041
3. Folmer, B.J.B., Sijbesma, R.P., Versteegen, R.M., van der Rijt, J.A.J., Meijer, E.W.: Supramolecular polymer materials: Chain extension of telechelic polymers using a reactive hydrogen-bonding synthon. Adv. Mater. **12**(12), 874–878 (2000). doi:10.1002/1521-4095(200006)12:12<874:AID-ADMA874>3.0.CO;2-C
4. Lehn, J.M.: Supramolecular polymer chemistry—scope and perspectives. Polym. Int. **51**(10), 825–839 (2002). doi:10.1002/pi.852
5. Appel, E.A., del Barrio, J., Loh, X.J., Scherman, O.A.: Supramolecular polymeric hydrogels. Chem. Soc. Rev. **41**(18), 6195–6214 (2012). doi:10.1039/c2cs35264h
6. Loh, X.J., Vu, P.N.N., Kuo, N.Y., Li, J.: Encapsulation of basic fibroblast growth factor in thermogelling copolymers preserves its bioactivity. J. Mater. Chem. **21**(7), 2246–2254 (2011). doi:10.1039/c0jm03051a
7. Nguyen, V.P.N., Kuo, N.Y., Loh, X.J.: New biocompatible thermogelling copolymers containing ethylene-butylene segments exhibiting very low gelation concentrations. Soft Matter **7**(5), 2150–2159 (2011). doi:10.1039/c0sm00764a
8. Loh, X.J.: Supramolecular host-guest polymeric materials for biomedical applications. Mater. Horiz. **2014**(1), 185–195 (2013). doi:10.1039/C3MH00057E
9. Lutolf, M.P., Hubbell, J.A.: Synthetic biomaterials as instructive extracellular microenvironments for morphogenesis in tissue engineering. Nat. Biotechnol. **23**(1), 47–55 (2005). doi:10.1038/nbt1055
10. Zhang, S.G.: Fabrication of novel biomaterials through molecular self-assembly. Nat. Biotechnol. **21**(10), 1171–1178 (2003). doi:10.1038/nbt874
11. Morris, K.L., Chen, L., Raeburn, J., Sellick, O.R., Cotanda, P., Paul, A., Griffiths, P.C., King, S.M., O'Reilly, R.K., Serpell, L.C.: Chemically programmed self-sorting of gelator networks. Nature Commun. **4**, 1480 (2013)
12. Bardelang, D., Zaman, M., Moudrakovski, I.L., Pawsey, S., Margeson, J.C., Wang, D., Wu, X., Ripmeester, J.A., Ratcliffe, C.I., Yu, K.: Interfacing supramolecular gels and quantum dots with ultrasound: smart photoluminescent dipeptide gels. Adv. Mater. **20**(23), 4517–4520 (2008)
13. Cao, L., Wang, X., Meziani, M.J., Lu, F.S., Wang, H.F., Luo, P.J.G., Lin, Y., Harruff, B.A., Veca, L.M., Murray, D., Xie, S.Y., Sun, Y.P.: Carbon dots for multiphoton bioimaging. J. Am. Chem. Soc. **129**(37), 11318 (2007). doi:10.1021/ja073527l
14. Kim, J., Piao, Y., Hyeon, T.: Multifunctional nanostructured materials for multimodal imaging, and simultaneous imaging and therapy. Chem. Soc. Rev. **38**(2), 372–390 (2009). doi:10.1039/b709883a
15. Ye, E., Loh, X.J.: Polymeric hydrogels and nanoparticles: a merging and emerging field. Aust. J. Chem. **66**(9):997–1007 (2013). http://dx.doi.org/10.1071/CH13168
16. Yang, Z., Liang, G., Wang, L., Xu, B.: Using a kinase/phosphatase switch to regulate a supramolecular hydrogel and forming the supramolecular hydrogel in vivo. J. Am. Chem. Soc. **128**(9), 3038–3043 (2006)
17. Cigognini, D., Silva, D., Paloppi, S., Gelain, F.: Evaluation of mechanical properties and therapeutic effect of injectable self-assembling hydrogels for spinal cord injury. J. Biomed. Nanotechnol. **10**(2), 309–323 (2014). doi:10.1166/jbn.2014.1759
18. Koutsopoulos, S., Zhang, S.: Long-term three-dimensional neural tissue cultures in functionalized self-assembling peptide hydrogels, matrigel and collagen I. Acta Biomater. **9**(2), 5162–5169 (2013). doi:10.1016/j.actbio.2012.09.010
19. Peng, K., Tomatsu, I., van den Broek, B., Cui, C., Korobko, A.V., van Noort, J., Meijer, A.H., Spaink, H.P., Kros, A.: Dextran based photodegradable hydrogels formed via a Michael addition. Soft Matter. **7**(10), 4881–4887 (2011)
20. Chen, W., Yang, Y., Rinadi, C., Zhou, D., Shen, A.Q.: Formation of supramolecular hydrogel microspheres via microfluidics. Lab Chip **9**(20), 2947–2951 (2009)

21. Calvert, P.: Hydrogels for Soft Machines. Adv. Mater. **21**(7), 743–756 (2009). doi:10.1002/adma.200800534
22. Murdan, S.: Electro-responsive drug delivery from hydrogels. J. Controlled Release **92**(1–2), 1–17 (2003). doi:10.1016/s0168-3659(03)00303-1
23. Ziaie, B., Baldi, A., Lei, M., Gu, Y.D., Siegel, R.A.: Hard and soft micromachining for BioMEMS: review of techniques and examples of applications in microfluidics and drug delivery. Adv. Drug Deliv. Rev. **56**(2), 145–172 (2004). doi:10.1016/j.addr.2003.09.001
24. Zhou, J., Li, H.: Highly Fluorescent Fluoride-Responsive Hydrogels Embedded with CdTe Quantum Dots. ACS Appl. Mater. Interfaces **4**(2), 721–724 (2012)
25. Jha, L.J., Best, S.M., Knowles, J.C., Rehman, I., Santos, J.D., Bonfield, W.: Preparation and characterization of fluoride-substituted apatites. J. Mater. Sci. Mater. Med. **8**(4), 185–191 (1997). doi:10.1023/a:1018531505484
26. Moszner, N., Salz, U.: New developments of polymeric dental composites. Prog. Polym. Sci. **26**(4), 535–576 (2001). doi:10.1016/s0079-6700(01)00005-3
27. Huo, H., Li, K., Wang, Q., Wu, C.: Self-assembly and optical property of triblock copolymers made of polystyrene and oligo(p-phenyleneethynylene) in different mixtures of toluene and hexane. Macromolecules **40**(18), 6692–6698 (2007). doi:10.1021/ma071247k
28. Appel, E.A., Rowland, M.J., Loh, X.J., Heywood, R.M., Watts, C., Scherman, O.A.: Enhanced stability and activity of temozolomide in primary glioblastoma multiforme cells with cucurbit[n]uril. Chem. Commun. **48**(79), 9843–9845 (2012). doi:10.1039/c2cc35131e
29. Jiao, D.Z., Geng, J., Loh, X.J., Das, D., Lee, T.C., Scherman, O.A.: Supramolecular peptide amphiphile vesicles through host-guest complexation. Angew. Chem. Int. Ed. **51**(38), 9633–9637 (2012). doi:10.1002/anie.201202947
30. Lan, Y., Loh, X.J., Geng, J., Walsh, Z., Scherman, O.A.: A supramolecular route towards core-shell polymeric microspheres in water via cucurbit[8]uril complexation. Chem. Commun. **48**(70), 8757–8759 (2012). doi:10.1039/c2cc34016j
31. Loh, X.J., del Barrio, J., Toh, P.P.C., Lee, T.C., Jiao, D.Z., Rauwald, U., Appel, E.A., Scherman, O.A.: Triply triggered doxorubicin release from supramolecular nanocontainers. Biomacromolecules **13**(1), 84–91 (2012). doi:10.1021/bm201588m
32. Loh, X.J., Tsai, M.H., del Barrio, J., Appel, E.A., Lee, T.C., Scherman, O.A.: Triggered insulin release studies of triply responsive supramolecular micelles. Polym. Chem. **3**(11), 3180–3188 (2012). doi:10.1039/c2py20380d
33. Rauwald, U., del Barrio, J., Loh, X.J., Scherman, O.A.: "On-demand'' control of thermoresponsive properties of poly(N-isopropylacrylamide) with cucurbit[8]uril host-guest complexes. Chem. Commun. **47**(21), 6000–6002 (2011). doi:10.1039/c1cc11214g
34. Lin, Y., Li, L., Li, G.: A new supramolecular gel via host-guest complexation with cucurbit [8] uril and N-(4-diethylaminobenzyl) chitosan. Carbohydr Polym. **92**(1), 429–434 (2012)
35. Appel, E.A., Biedermann, F., Rauwald, U., Jones, S.T., Zayed, J.M., Scherman, O.A.: Supramolecular cross-linked networks via host—guest complexation with cucurbit[8]uril. J. Am. Chem. Soc. **132**(40), 14251–14260 (2010)
36. Appel, E.A., Loh, X.J., Jones, S.T., Dreiss, C.A., Scherman, O.A.: Sustained release of proteins from high water content supramolecular polymer hydrogels. Biomaterials **33**(18), 4646–4652 (2012). doi:10.1016/j.biomaterials.2012.02.030
37. Hou, D., Tong, X., Yu, H., A-y, Zhang, Z-g, Feng: A kind of novel biodegradable hydrogel made from copolymerization of gelatin with polypseudorotaxanes based on α-CDs. Biomed. Mater. **2**(3), S147 (2007)
38. Zhang, Y., Zhang, B., Kuang, Y., Gao, Y., Shi, J., Zhang, X.X., Xu, B.: A Redox Responsive, Fluorescent Supramolecular Metallohydrogel Consists of Nanofibers with Single-Molecule Width. J. Am. Chem. Soc. **135**(13), 5008–5011 (2013)
39. Peng, F., Li, G., Liu, X., Wu, S., Tong, Z.: Redox-responsive gel–sol/sol−gel transition in poly (acrylic acid) aqueous solution containing Fe (III) ions switched by light. J. Am. Chem. Soc. **130**(48), 16166–16167 (2008)
40. Ikeda, M., Ochi, R., Hamachi, I.: Supramolecular hydrogel-based protein and chemosensor array. Lab Chip **10**(24), 3325–3334 (2010)

41. Ikeda, M., Ochi, R., Wada, A., Hamachi, I.: Supramolecular hydrogel capsule showing prostate specific antigen-responsive function for sensing and targeting prostate cancer cells. Chem. Sci. **1**(4), 491–498 (2010)
42. Qiu, Z., Yu, H., Li, J., Wang, Y., Zhang, Y.: Spiropyran-linked dipeptide forms supramolecular hydrogel with dual responses to light and to ligand–receptor interaction. Chem. Commun. **23**, 3342–3344 (2009)
43. Komatsu, H., Matsumoto, S., S-i, Tamaru, Kaneko, K., Ikeda, M., Hamachi, I.: Supramolecular hydrogel exhibiting four basic logic gate functions to fine-tune substance release. J. Am. Chem. Soc. **131**(15), 5580–5585 (2009)
44. Shi, N., Yin, G., Han, M., Xu, Z.: Anions bonded on the supramolecular hydrogel surface as the growth center of biominerals. Colloids Surf. B **66**(1), 84–89 (2008)
45. Yamaguchi, S., Matsumoto, S., Ishizuka, K., Iko, Y., Tabata, K.V., Arata, H.F., Fujita, H., Noji, H., Hamachi, I.: Thermally responsive supramolecular nanomeshes for on/off switching of the rotary motion of F1-ATPase at the single-molecule level. Chemistry **14**(6), 1891–1896 (2008)
46. Ikeda, M., Yoshii, T., Matsui, T., Tanida, T., Komatsu, H., Hamachi, I.: Montmorillonite—supramolecular hydrogel hybrid for fluorocolorimetric sensing of polyamines. J. Am. Chem. Soc. **133**(6), 1670–1673 (2011)
47. Matsumoto, S., Yamaguchi, S., Ueno, S., Komatsu, H., Ikeda, M., Ishizuka, K., Iko, Y., Tabata, K.V., Aoki, H., Ito, S.: Photo Gel–Sol/Sol–Gel Transition and Its Patterning of a Supramolecular Hydrogel as Stimuli-Responsive Biomaterials. Chemistry **14**(13), 3977–3986 (2008)
48. He, P., Xu, B., Liu, H., He, S., Saleem, F., Wang, X.: Polyoxometalate-based supramolecular gel. Scientific reports 3 (2013)
49. Hofmeier, H., Schubert, U.S.: Supramolecular branching and crosslinking of terpyridine-modified copolymers: complexation and decomplexation studies in diluted solution. Macromol. Chem. Phys. **204**(11), 1391–1397 (2003). doi:10.1002/macp.200350003
50. Meier, M.A.R., Schubert, U.S.: Terpyridine-modified poly(vinyl chloride): Possibilities for supramolecular grafting and crosslinking. Journal of Polymer Science Part a-Polymer Chemistry **41**(19), 2964–2973 (2003). doi:10.1002/pola.10881
51. Ribot, J.C., Guerrero-Sanchez, C., Hoogenboom, R., Schubert, U.S.: Thermoreversible ionogels with tunable properties via aqueous gelation of an amphiphilic quaternary ammonium oligoether-based ionic liquid. J. Mater. Chem. **20**(38), 8279–8284 (2010). doi:10.1039/c0jm02061c
52. Nair, K.P., Breedveld, V., Weck, M.: Complementary hydrogen-bonded thermoreversible polymer networks with tunable properties. Macromolecules **41**(10), 3429–3438 (2008). doi:10.1021/ma800279w
53. Nair, K.P., Breedveld, V., Weck, M.: Multiresponsive Reversible Polymer Networks Based on Hydrogen Bonding and Metal Coordination. Macromolecules **44**(9), 3346–3357 (2011). doi:10.1021/ma102462y

Peptidic Hydrogels

Jessie E.P. Sun and Darrin Pochan

Abstract This chapter looks into the hierarchical structures of peptide sequences and hydrogels constructed with physical solution assembly in an attempt to discuss the fundamental properties of peptide hydrogels and the molecular foundations. Peptide hydrogels are great candidates in the ever-growing field of biological and medical applications due to their ease of synthesis and customizable molecular and material features. The natural cytocompatibility and degradability of peptides make peptide hydrogels great candidates for cell encapsulation and drug delivery. There is immense potential in using new peptide molecules to make new hydrogel materials with both designed properties as well as unanticipated, excellent properties.

Keywords Peptides · Injectable · Drug delivery · Cell encapsulation · Tissue engineering

Within the increasingly expansive field of polymer hydrogels is the subset of peptide hydrogels. Peptides in nature and biology are critical for structure and function and involved in every bodily process from cell reproduction and tissue generation to simple enzymatic reactions. In the design of synthetic peptides, the scientist and engineer has twenty one natural amino acids in addition to a large and growing number of man-made amino acids to choose from for molecule formation. This amino acid toolbox provides for an almost limitless array of characteristics and function in new molecules and hydrogel materials. Amino acid attributes can include more traditional characteristics, such as hydrophobicity, polarity, or charge, or more exotic functionality such as the ability to crosslink with specificity in a "click" ligation reaction [1–9]. Therefore, these inherent

J.E.P. Sun · D. Pochan (✉)
Materials Science and Engineering, University of Delaware, Newark, DE, USA
e-mail: pochan@udel.edu

X.J. Loh (ed.), *In-Situ Gelling Polymers*, Series in BioEngineering,
DOI 10.1007/978-981-287-152-7_6

amino acid characteristics are taken full advantage of in creating a rich library of peptide hydrogel sequences with drastically varied chemistries.

The piece-by-piece amino acid chemical connection during peptide synthesis, combined with the range of amino acid properties, gives peptide hydrogels tunable characteristics and capabilities for a multitude of chemical, material or biological uses. After molecular peptide synthesis, many peptide hydrogels are constructed with solution assembly mechanisms and can be made in situ with the introduction of the proper trigger, or change in environment, such as changes in temperature, pH, or ionic concentration. [1, 2, 6, 10–18]. While the starting peptide sequences are straightforward to synthesize, the resulting structures after triggered molecular assembly can take on secondary, tertiary or quaternary structures like peptides and proteins in nature.

There are many different types of peptide hydrogels presently being researched, from those created from short peptide sequences that exist as conjugates with other synthetic polymer constructs [11, 14, 15, 19–27] to hydrogels made from high molecular weight, protein-like molecules [17, 28–35]. The focus in this chapter will be mainly on shorter peptide sequences that can be triggered in situ to form higher order structure and, consequently, form supramolecular, physical hydrogels [10, 13, 36–38]. These sequences are shorter than typical proteins, and their solution self-assembling capabilities to form higher order, intra- and intermolecular structures can result in a variety of hydrogels with beneficial and interesting material properties such as shear-thinning capabilities for injectable solid behavior for therapy delivery [1, 13, 20, 36, 39–45].

Peptide hydrogel structural hierarchy sets them apart from synthetic polymer hydrogels. Peptides, and their resultant shapes after folding and intermolecular assembly, are categorized by four different levels of structure: primary, secondary, tertiary, and quaternary. With adaptable and precise synthesis methods, peptide structures have the ability to achieve naturally-inspired structures such as those observed in known protein crystal structures as well as completely new, de novo designed structures by proper design of a peptide sequence. Starting with a designed sequence, peptides can be constructed faithfully into a final, desired structure and function. Additional functional groups or amino acids can be added, exchanged, or removed from a known natural or designed sequence to change the final material structure, the kinetics of intermolecular assembly, the material properties or other behaviors (e.g. biological properties) of the resultant peptide hydrogel. The molecular assembly processes designed into peptide hydrogels readily can be made to be efficient, fast, and easily modified based on the desired hydrogel performance environment. From synthesis to assembly, a considerable amount of organization of intermolecular and intramolecular interactions is needed. Each structure and its final properties as a hydrogel is defined and affected by these interactions.

Regardless of final hydrogel structure, the driving forces of peptide assembly into hierarchical structures and materials are physical, non-covalent interactions such as hydrogen bonding and π-stacking, hydrophobic and van der Waals

interactions, as well as electrostatic interactions. In aqueous solutions, all of the above interactions have been used, primarily in concert, in bringing peptides together and to hold the assembled structure together after assembly and gelation [11, 14, 15, 22, 25–27, 33, 34, 46–48]. Change of the pH, ionic concentration, or temperature of a solution can be used to trigger the solution assembly of the peptide sequences. These changes force single molecules to intramolecularly fold into desired secondary structures, such as β-sheets or α-helices, and/or collections of molecules that begin intermolecularly assembling to form local nanostructure such as nanofibrils or nanotubes. The entire process results in a hydrogel with quaternary structure (i.e. hydrogel network structure) organization [1, 2, 6, 10–18, 26, 28, 29, 31, 34–36, 48–50]. This chapter explores the formation of primary and secondary structures with small peptides as well as resultant, physical hydrogels and underlying peptide tertiary and quaternary (i.e. hydrogel network) structure.

1 Primary Structures

Primary structure is first order peptide structure—the amino acid linear sequence. The diversity in the natural amino acids as well as numerous synthetic, non-natural amino acids allows for a great and constantly growing number of possibilities of primary sequences. Linked together with amide bonds between the carboxylic acid and amine ends of neighboring amino acids, peptides are predominantly linear in architecture although chemistry can be designed to make branched peptides, particularly when peptides are combined as a hybrid with other organic molecules. For example, peptide primary structure can also be seen in hybrid polymer-peptide or aliphatic hydrocarbon conjugates that can introduce new architecture and other characteristics (e.g. peptide amphiphiles that exhibit branches or helical behavior [11, 14–16, 19–27, 33, 51–55]; or polymer-peptide conjugates that have star or branched architecture [17, 18, 28–35, 56–62]). However, the focus here will be on linear peptide architecture.

Previously, the synthesis of peptidic materials was seen as a cumbersome and expensive method that lacked the precision of other polymeric synthesis methods [3, 10, 13, 16, 18, 33, 36–38, 63]. Synthesis of peptides has quickly advanced with cheaper methods, larger yield quantities, greater precision, and more adaptive equipment and methodology. There are two main pathways of creating a large number of customized peptide sequences, (a) engineered/recombinant DNA synthesis or (b) synthetic solid phase peptide synthesis (SPPS) [1, 13, 18, 20, 33, 36, 39–45, 64, 65]. These methods are preferred to traditional methods because of the yield, automation, and time saved when compared to manual organic synthesis.

Recombinant DNA peptide synthesis refers to the use of introducing modified DNA to a host, typically *E. coli*, to subsequently produce the designed peptide

sequence [11, 14–18, 22, 25–27, 33–37, 46–48, 56, 60, 66]. Recombinant synthesis is advantageous when one desires to synthesize a longer sequence. Typically, using SPPS to produce sequences with greater than 40 amino acid residues is difficult and requires synthesis by parts where the separate molecule parts are synthesized separately with additional reactions [3, 19–21, 23, 24, 26, 37, 42, 61, 67, 68]. Additionally, one can synthesize large amounts of peptide easily with recombinant methods, a main advantage with recombinant DNA for peptide production over solid phase peptide synthesis. The DNA sequences required to prescribe specific amino acids in a peptide chain are known and established for the natural amino acids and are constantly being discovered and engineered for non-natural amino acids. To begin making a peptide sequence, the desired DNA sequence is constructed with primers, reproduced to create thousands of copies, and introduced to plasmid DNA, which transfers the designed DNA sequence to *E. coli* colonies. The colonies take up the plasmid DNA and begin producing the desired peptide sequences. Numerous research groups using recombinant DNA peptide synthesis have investigated the many possible different molecular products that produce hydrogel materials after assembly [32, 45, 48, 68, 69].

The other method of peptide synthesis is commonly known as solid phase peptide synthesis (SPPS). This method is synthetic and allows for more straightforward incorporation of noncanonical amino acids than with recombinant DNA [20, 23, 26, 29, 37, 43, 70–73]. Additionally, the synthesis process can be done by automation through machine or by hand. The convenience of using a machine is the automated process of many repeat steps for longer peptide sequences. The ease of use allows for a greater number of novel peptide sequences to be created. Synthesis begins with a resin support made of small, porous polymer beads that are functionalized so that the amino acid attaches with an amide bond. The functionalization of the bead depends on the protection group used for the attaching amino acids and cleavage conditions [74]. Amino acids are added sequentially onto the solid phase-supported growing sequence, c-terminus to n-terminus. To ensure only one coupling reaction per amino acid, the n-terminus of each amino acid added to the reaction vessel has one of two possible protection groups, fluorenylmethyloxycarbonyl chloride (Fmoc) or tert-butyloxycarbonyl (Boc). Traditionally, Boc was the protection group, but the need for hydrogen fluoride (HF) in the final cleavage step brought about the Fmoc group for protection [74, 75]. The system is washed after each coupling step to get rid of unattached amino acids, and then the n-terminus of the growing peptide chain is deprotected for the next amino acid. After the desired sequence is created, the resin and attached amino acids go through filtration to get rid of unwanted amino acids with the peptide sequence ultimately cleaved from the resin. As mentioned before, HF, an acid, is needed in the cleavage step for Boc protected synthesis, while a base such as piperidine is needed for Fmoc protected synthesis. Because of the sequential definition of amino acids by either synthesis method, peptide hydrogels can be readily designed with different characteristics by specifically altering the primary sequence. This primary structure design can affect directly the solution conditions in which the peptides intermolecularly assemble, the nanostructure formed by the

peptides after assembly, as well as hydrogel properties such as the solution conditions desired for encapsulated payload release.

There are also hybrid molecules produced through traditional organic or polymer chemistry methods with desired peptide primary sequences attached to polymers, hydrocarbon chains, or even other peptide chains as conjugates. One of the most common sequences used as a conjugate is the three amino acid sequence of RGD (arginine, glycine, aspartic acid), used because of its ability to trigger cell adhesion, a desired feature for cell-hydrogel constructs [2, 4, 6, 8, 10, 36–38]. Because RGD works as an integrin-binding site, there are many variations of this three amino acid sequence, as well as other integrin-recognized amino acid sequences, that can be synthesized [1, 2, 6, 36, 41, 43–45]. RGD does not create hydrogels itself; rather, RGD is incorporated into other polymer sequences that go on to create hydrogels through physical assembly or chemical reactions. While RGD is used biologically to imitate RGD found naturally, there are peptide sequences that are used for non-natural, non-hydrogel purposes. Taking advantage of the structure, solution conditions, and availability of peptides, many groups are using peptide sequences and resultant higher order structure to direct the synthesis, growth and organization of non-peptide, disparate materials, such as graphene, metallic nanoparticles, or silica dioxide [76–78].

With the ease of synthesis, there are a vast number of the possible combinations and permutations of natural and non-natural amino acids with varying sequence lengths. The length of a peptide sequence affects many of the characteristics of the hydrogel created. Shorter peptide sequences will generally assemble faster intermolecularly with less defective assembly than longer sequences that can coil and entangle during assembly. Mono- [20], di- [79, 80], and tri-peptide [17, 26, 36, 40] sequences that are created as supramolecular gelators tend to be made of amino acids with naturally hydrophobic or polar but uncharged functional groups [11, 34–37, 40]. Some mono-, di- and tri-peptide sequences retain the Fmoc protection group at the end of the n-terminus, which is observed to be an integral part in hydrogel formation with π-stacking from the aromatic rings. A change in pH [20, 40, 42, 57, 59, 61] to force hydrophobic collapse or the addition of enzymes [3, 16, 26, 33, 47, 63] can be used to induce hydrogelation. Figure 1 shows two di-peptides used in combination to create three different hydrogels and the TEM images of the fibrils formed [80].

When triggered, short amino acid sequences form long fibril networks of peptides to form hydrogels. The peptides generally start as primary structures soluble in solution, but then self assemble intermolecularly into higher order structures and hydrogels [1, 29, 31, 33–35, 48, 50, 64, 65, 81, 82]. In order for longer sequences to self-assemble, longer peptide sequences generally have both hydrophobic, uncharged amino acids, while also including hydrophilic and polar groups to help drive secondary bonding as well as hydrophobic collapse of sequences. The trigger for longer sequences to intermolecularly assemble into higher order structures will usually be a change in pH, temperature or ion concentration although many other stimuli have been designed and will be discussed later in the chapter. The properties and applications of these higher order structures will

be discussed in greater detail further on with quaternary structures. Figure 2 is an example from the Hartgerink group, showing fibril formation and hydrogel formation [50]. First, the primary order peptide structures assembled into fibrous quaternary structures. Gelation is triggered with the introduction of multivalent ions, inducing interfibrillar assembly. The barely entangled or branched fibril structures between the short sequence peptide hydrogels of Fig. 1 is visibly different from the longer sequence fibrils after gelation in Fig. 2.

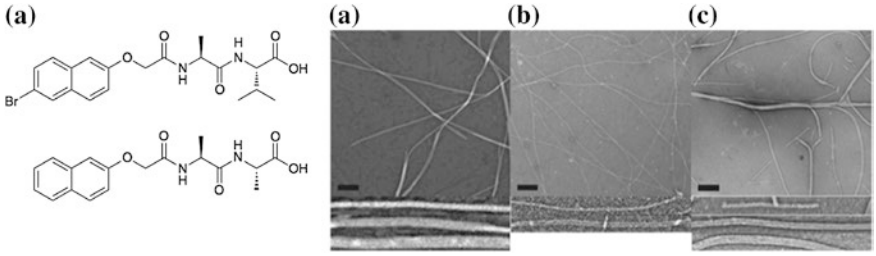

Fig. 1 Top dipeptide structure (I) and bottom peptide structure (II) and a combination of the two shown with TEM and with *inset* to better show local fibril structure. The *scale bar* is 200 nm. **a** I alone, **b** II alone, **c** combination of I and II [80]

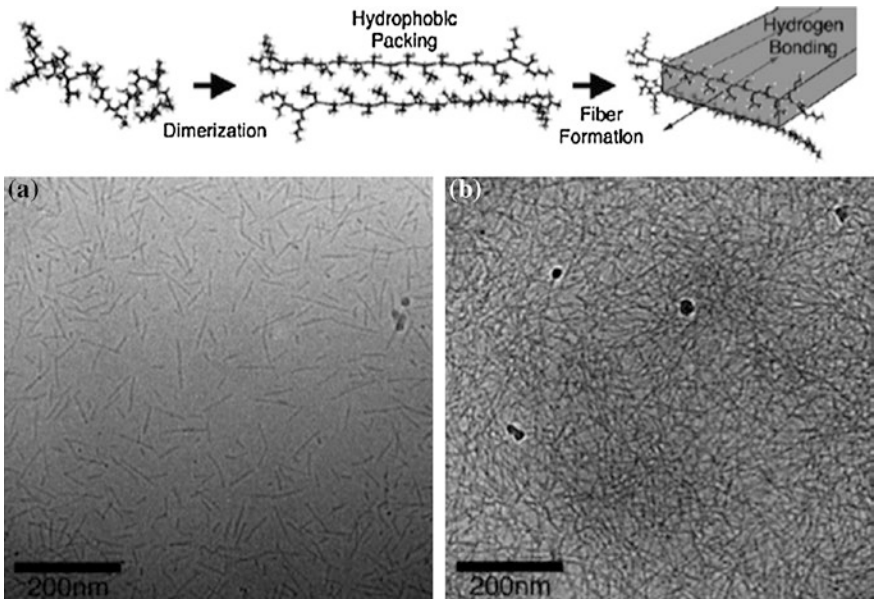

Fig. 2 Dimers and folding mechanism of primary peptide sequences. TEM images show $E(QL)_6E$ from the Hartgerink group **a** before gelation and **b** after gelation with Mg^{2+} [50]

2 Secondary Structures

Secondary structures in peptides display a specific conformation of the peptide chain. The two main secondary structures are the α-helix and the β-sheet. For both structures, there has been extensive research to define, dictate, and predict structural and folding behaviors of primary sequences of peptides [36]. Before a triggering event for secondary structure formation (i.e. intramolecular folding), the unfolded peptide sequence may be a random coil, lacking specific three-dimensional structure. Figure 3 shows the secondary order structures discussed in this chapter and their potential quaternary order structures [36].

As indicated by the name, α-helices form a unimolecular helix when triggered to fold. Figure 3b shows an external model of an α-helix and Fig. 4 shows a top

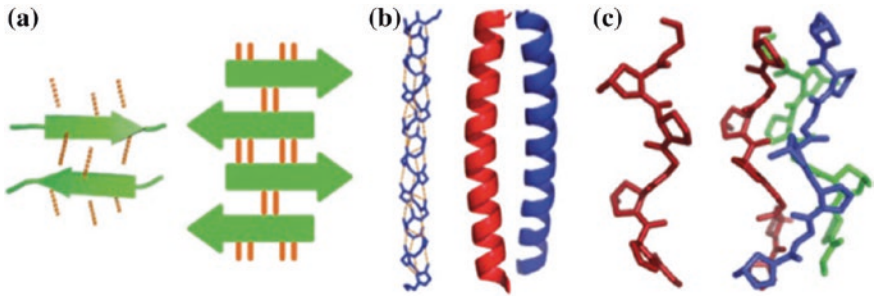

Fig. 3 Basic secondary structures **a** beta strands; extended peptide chains held together by hydrogen bonds shown in *orange* between CO and NH groups in the peptide backbones, and resultant beta-sheets formed by several or more beta strands (actually an example of quaternary structure). **b** An α-helix with *orange* hydrogen bonds along the length of the helix and a coiled coil quaternary structure made of two alpha-helices. **c** A proline helix that goes on to form a collagen helix with other proline helices [36]

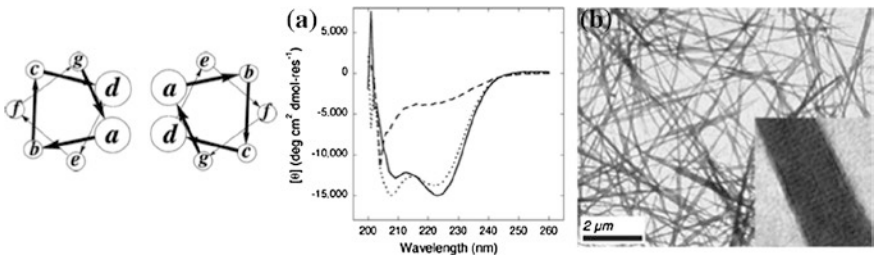

Fig. 4 Diagram of typical alpha helical heptad organization for coiled-coil formation and the protection of hydrophobic residues at **a** and **d** for two coiled-coils. **a** CD data proving alpha helix confirmation (two minima at 208 and 222 nm) for the peptide at 37 °C (*solid line*) when cooled to 37 °C from 85 °C (*dotted line*); 85 °C (*broken line*) shows typical random coil behavior. **b** Shows TEM of the resultant larger fibril organization with higher magnification to show striations [13]

down view of the helix. Each turn of an α-helix is 3.6 amino acid residues. The α-helical structure is held together by hydrogen bonds between backbone CO and NH functionalities along the helix, holding the helix together tightly, and creating a fairly rigid secondary structure [13, 36]. A common helix design for gelation involves helices that are composed of amino acid heptads labeled ***abcdefg***, where the first and fourth amino acids are typically hydrophobic while the remaining amino acids are polar [10, 13, 34]. This design places the hydrophobic residues alternatingly 3 or 4 residues apart along the chain, giving the helix a hydrophobic face that winds around the surface of the helix. The exposed hydrophobic face after helix formation is one of the driving forces for higher order structure formation and gelation. This driving force is discussed further in the quaternary structure section, as helices collapse into what are called coiled-coils and, ultimately, into fibrils and hydrogels (cf. Figs. 3b and 4) [13, 34]. Certain amino acids are more likely to be found in α-helices such as lysine, glutamine, glutamic acid, or alanine [1, 44]. α-Helices can be left or right-handed [36] and can be modified with additional functional groups [1]. For example, the Woolfson group uses peptide customization to functionalize α-helices with "sticky ends" designed to link helices together to propagate longer fibrils upon self-assembly [1, 10, 12, 13].

The other dominant secondary structure is the β-strand that can further hydrogen bond together to form β-sheets. Strictly speaking, the strand is the intramolecular secondary structure while interstrand sheet formation is a quaternary structure. β-Sheets have a distance of 4.7 angstroms between each neighboring strand, since hydrogen bonds form laterally between the CO and NH functionalities of opposite β-strand backbones, as shown schematically in Fig. 3a. Just as there are certain amino acids primarily associated with α-helices, hydrophobic and aromatic amino acids such as phenylalanine, valine, and isoleucine are associated with the formation of β-sheets [13, 36, 44, 83]. The presence of hydrophobic residues in a β-sheet can create hydrophobic faces that build up as β-sheet formation occurs, causing the β-sheet fibrils to collapse forming hierarchical fibrillar and fiber nanostructures, further examined later in quaternary structures [28].

Another variation of the β-sheet is the β-hairpin formed by two β-strands held together by short amino acid sequence known as a β-turn. The Schneider and Pochan groups created the family of MAX β-hairpin structures that intramolecularly fold and intermolecularly assemble into nanofibrils with a hydrophobic core. Figure 5 shows an example of the β-hairpin structure from the group's flagship MAX1 peptide sequence that collapses to protect hydrophobic valines when triggered [28, 49]. The hairpin collapse throughout the solution creates a bilayer fibril, where hydrogen bonds between carboxyl and amine groups of opposing amino acid backbones stabilize the parallel structures (dotted lines in the Fig. 5 [28, 49]).

Figure 6 shows AFM images of two very similar primary sequences that appear similar after quaternary structure formation and gelation, but one forms α-helices while the other forms β-sheets [44]. Beyond the most common α-helices and β-sheets, there are other secondary structures that are less observed in peptide hydrogels [19, 34, 36]. One example is the polyproline helix seen in Fig. 3c, a common secondary structure observed in collagen materials and hydrogels [84].

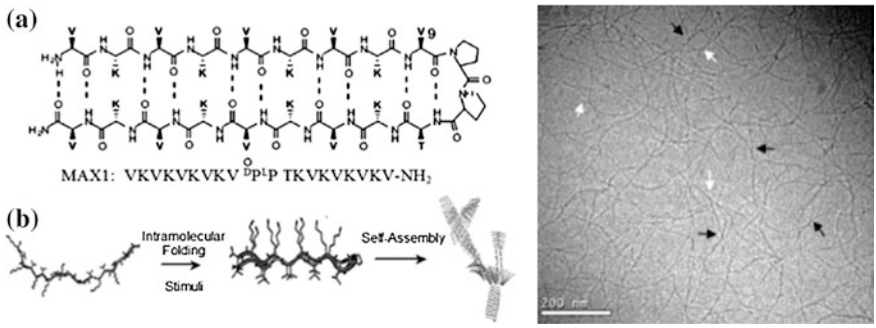

Fig. 5 A diagram of a beta-hairpin molecule, showing the hydrogen bonds (*dotted lines*) that stabilize the folded conformation between carboxyl and amide groups [28]. On folding, the hydrophobic, valine side chain-rich face collapses together with a neighbor to form a bilayered fibril cross-section. The hairpins also hydrogen bond with neighbors to form fibrils that branch and entangle with physical crosslinks as indicated by the *arrows* in the Cryo-TEM image [49]

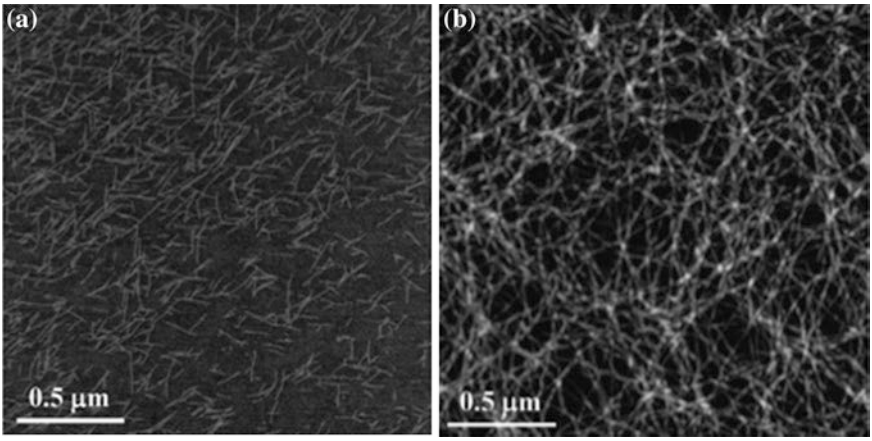

Fig. 6 AFM micrographs on negatively charged mica of freshly prepared **a** α-helix forming AEAKAEAK solution and **b** β-sheet forming FEFEFKFK. Alanine based peptide sequence to phenylalanine changes folding properties. Both form secondary structures that go on to create fibrils into a higher order structures [44]

A benefit of peptide synthesis is that one can easily fine tune amino acid content (i.e. primary structure) of peptides to customize final molecular conformations, gelation times, or other molecular interactions. This allows the creation of an array of peptides with minute differences in sequences but vast differences in final properties. Characterization is important to understanding the secondary structures formed by individual peptides and, consequently, the higher order structures that are formed during gelation. To confirm and characterize second order structure, two spectroscopic methods, circular dichroism spectroscopy (CD) and Fourier-transform infrared spectroscopy (FTIR) are frequently used. Both methods examine light absorption

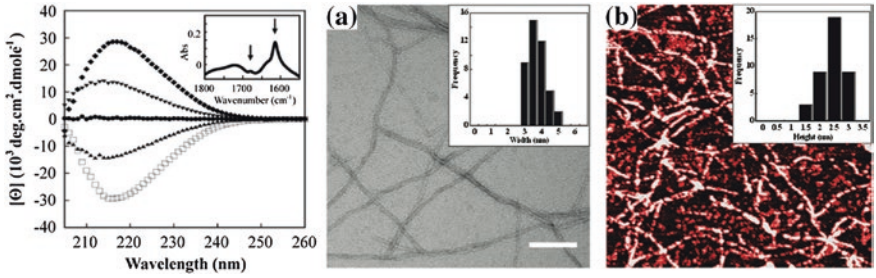

Fig. 7 *Left* CD spectra of 1 wt% hydrogels containing (from *top* to *bottom*) pure DMAX1, 3:1DMAX1:MAX1, 1:1DMAX1:MAX1, 1:3DMAX1:MAX1, and pure MAX1. The *inset* shows the IR spectra of 1:1DMAX1:MAX to prove beta-strand behavior. *Right* 1 wt% 1:1DMAX1:MAX1gel as **a** TEM and **b** AFM images, with insets of average fibrillar widths. *Scale bar* is 100 nm [85]

by molecular bonds to identify the presence of random coils, α-helices, or β-sheets. Figure 4 shows CD measurements with typical α-helical characteristics (two minima at 208 and 222 nm) when the peptide is at 37 °C (solid line) or when cooled to 37 °C from 85 °C (dotted line). The broken line demonstrates the sequence exhibiting random coil behavior at 85 °C [13, 39]. Figure 7 shows CD data with an FTIR inset of the Schneider and Pochan groups' MAX1 along with varying ratios of its stereoisomer DMAX1 [85]. The FTIR inset confirms β-sheet structure that was not clear in the CD due to a racemic mixture of both D and L peptide stereoisomers, which eliminates clear CD signal. The inset shows clear absorption at 1,615 and 1,680 cm^{-1} indicative of β-strand behavior. These spectroscopy methods are used for confirming and analyzing secondary structures, but as the peptide sequences go on to form desired intermolecular structures, microscopy and rheology techniques are required. These techniques for examining quaternary structures are discussed later in the chapter.

Most of the peptide hydrogels that currently exist exhibit a specific secondary structure before and during gelation. While there are many secondary structures available, only those that are able to induce intermolecular assembly into quaternary structure formation are important to the formation of peptide hydrogels. In current peptide hydrogels, the secondary structure utilized most frequently in peptide hydrogel design is the β-sheet due to its propensity to form fibrillar intermolecular nanostructure and, thus, entangled and branched fibrillar networks for hydrogel formation. The examples presented herein contain hydrogels of both major secondary structures but focus mostly on β-sheet constructions.

3 Tertiary Structures

Tertiary structures, like primary and secondary structures, are observed within single peptide chains. Unlike primary or secondary structures, tertiary structures can exhibit primary and/or secondary structures all within the same molecule. Tertiary

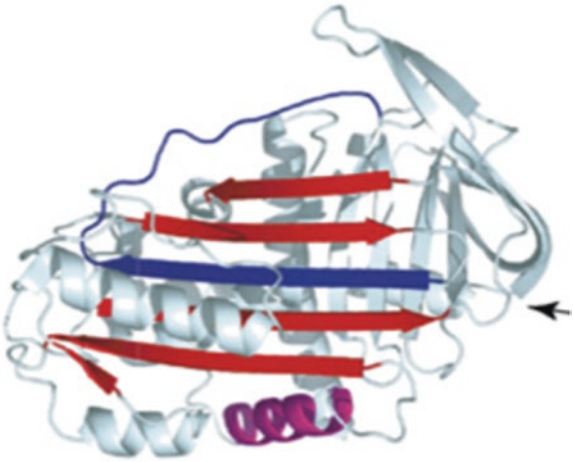

Fig. 8 Serpin molecule with tertiary order. β-strands are represented by *arrows* with visible α-helices throughout the entire protein as well as disordered, random coils and turns that connect the areas of more regular secondary structure [86]

structures are stabilized by a wide variety of intramolecular interactions in addition to hydrogen bonding and hydrophobic interactions. These bonds, including salt-bridges or disulfide cysteine bonds, can also be covalent bonds unlike primary or secondary structures [16, 33, 51]. Figure 8 shows a protein example of tertiary structure from the serpin family of proteins naturally found in the body [86]. In the diagram there are visible α-helices, one of which is highlighted in purple, and there are β-strands highlighted in red and blue all within the same molecule.

While there are many proteins that exhibit tertiary order in their globular, functional form, in peptide hydrogels currently there are very few tertiary order structures. Inspirations for some synthetic globular proteins come from naturally occurring tertiary structures such as bovine serum albumin, β-lactoglobulin, or ovalalbumin [18, 56, 58, 60, 62]. Assembling globular proteins into quaternary structures for hydrogels are examined later in the chapter. As the field of peptide hydrogels grows and more complex sequences are created, there may be more tertiary order structures for peptide hydrogels on the horizon [87].

4 Quaternary Structures

While previous sections described molecular structures peptide sequences can adopt before interacting with other sequences, the actual peptide hydrogel network itself has an intermolecular quaternary structure. When exposed to the proper triggers in solution, the previously mentioned primary, secondary, and tertiary structures create quaternary structures. The solution triggers include, but are not limited to, changes in pH [19, 37, 42, 61, 67, 68] or ionic concentration [45, 48, 68]. The desired hydrogel characteristics and properties dictate the solution and triggering conditions sought for gel formation as peptide sequences fold and assemble into

the network quaternary structure. The dominant peptide hydrogel network quaternary structure is the peptide nanofibril.

Fibrils and fibrillar structure are critical for peptide hydrogel formation; the entanglement and branching of fibrils define the quaternary structures of most peptide hydrogel networks. The fibrils formed during gelation can be well-defined nanofibrils alone that entangle or branch. Nanofibrils can also hierarchically assemble into larger fibrils or fibers to form a network. Non-covalent crosslinking is a critical attribute of physical peptide hydrogels. As the fibrils develop, natural entanglement of the fibrils with themselves as well as physical crosslinking of hydrogen bonds along the backbones of the fibrils and hydrophobic interactions between fibrils, form networks of the peptide hydrogel. The kinetics of the hydrogel formation can affect fibril widths and branching as well as ultimate hydrogel properties.

The kinetics of β-sheet fibril formation and growth can be strongly affected by the hydrophobic interactions of the constituent amino acids. [17, 37, 41, 42, 48]. The hydrogen bonding and hydrophobic collapse during β-sheet formation and gelation can form homogeneous fibrillar nanostructures with a hydrophobic core [28, 50, 72] or can lead to hierarchical assembly of nanofibrils into fibers of a wide variety of length scales [65, 88, 89]. For peptide sequences that assume other secondary structure before fibrillar growth, such as α-helices, hydrophobic collapse can also cause a rather specific intermolecular interaction to form supramolecular structure. For α-helices, two or more helices can collapse together to form what are known as coiled-coils [90–93]. Figure 4 demonstrates how two α-helices would interact to form a coiled-coil by burying their hydrophobic faces [19, 37, 41, 72]. The number of helices that come together in fibril formation to form the coiled-coil dictates the width of assembled fibrils. As mentioned previously, the α-helices can be functionalized with sticky ends, altering the mechanical strengths of the overall hydrogel [1, 10, 12, 13].

There are fewer tertiary structures that go on to form peptide hydrogels. One group of molecules that form tertiary structures is synthetic globular proteins. While forming hydrogels, some globular proteins will aggregate to create a particulate gel whereas others form fibrils, usually rich in β-sheet, that entangle into a hydrogel network [18]. As with the folding characteristics of secondary structure, the gelation of proteins can be triggered by temperature, ionic concentration, or pH [18, 56, 60, 66]. While there may be less of a definite hydrophobic surface to facilitate peptide collapse for fibril formation, hydrophobicity is still the main driving source for aggregation and gelation after a trigger event as seen in Fig. 9 [18].

Changing the peptide primary structure itself can alter the kinetics and structure of fibril formation. With gelation/peptide folding and assembly dependent on the peptide charge and hydrophobicity, faster gelation kinetics can be realized by reducing the overall charge of the peptide sequence. For example, the Schneider and Pochan groups substitute a single glutamic acid for a lysine forming a slightly less charged MAX8 hydrogel, rather than the MAX1 hydrogel shown in Fig. 10 [73]. This change greatly increases the speed of hydrogel formation as compared to MAX1 in identical solution conditions. An increase in the rate of intramolecular folding leads to a faster intermolecular assembly with more branched fibrils and

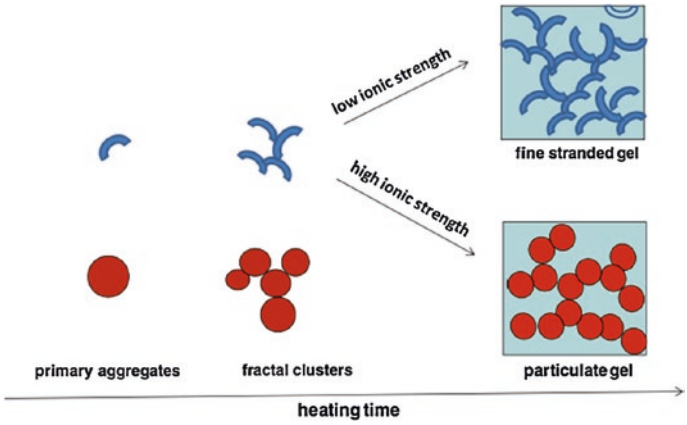

Fig. 9 Different pathways to form a globular protein hydrogel; a tertiary structure as it gels into a hydrogel with quaternary structure [18]

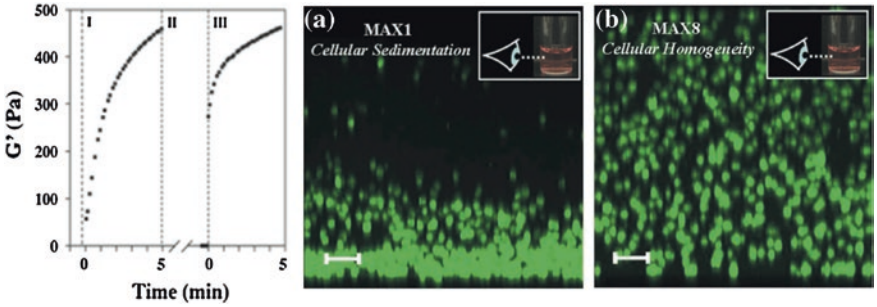

Fig. 10 *Left* Rheology data showing the storage modulus of 0.5 wt% MAX8 (*I*) during initial gelation, (*II*) as MAX8 undergoes steady-state shear, it becomes liquid like, (*III*) when shear ceases, the gel immediately displays solid like behavior with $G' > 250$ Pa and quickly recovers original storage modulus. *Right* **a** MAX1 after a single substitution difference for reduced overall charge is known as **b** MAX8. The reduced charge leads to faster kinetics and gelation time for MAX8, as evidenced by the effects of gravity on encapsulated MSCs [73]

more fibrillar entanglements overall in the quaternary structure. The consequently stiffer hydrogels formed more quickly than more highly charged MAX1 networks show affects on the distribution of encapsulated payloads. The faster gelation prevents heavier items, such as cells, from sinking due to gravity before the fibrillar network finishes gelation, as seen in Fig. 10 [73]. The fibrillar network and resultant molecular diffusion properties within the gel do not change significantly between peptide gels because the method of fibrillar growth does not change [51]. One can also change the solution peptide folding and assembly triggering conditions in order to change the amount of branching of the gel, which changes the

number of physical crosslinks of the gel, ultimately affecting the stiffness of the MAX hydrogel created [73, 94, 95]. The Schneider group has also looked at substituting all L-amino (left handed) acids for D-amino acids (right handed), thereby reversing the natural chirality of MAX1 [85]. The assembly kinetics and mechanical stiffness of the hydrogel were found to depend on the chirality of the peptide. Combining equal amounts of MAX1 and its stereoisomer resulted in a racemic hydrogel that was an order of magnitude stiffer than the individual stereoisomer gels. Clearly, there is ample opportunity to alter quaternary structure in peptide hydrogels through new primary structure design in peptide molecules.

Methods that help to visualize the hydrogel intermolecular quaternary structure include microscopies such as transmission electron microscopy (TEM), cryo-TEM, scanning electron microscopy (SEM), and atomic force microscopy (AFM). TEM, SEM, and cryo-TEM can image at higher resolutions than light microscopes and routinely image nanostructure of hydrogel networks. TEM and SEM use dried samples while cryo-TEM uses vitrified samples at cryogenic temperatures to preserve a sample in a hydrated state. TEM images of fibrillar nanostructure can be seen in Figs. 1, 2, 4, and 5 [13, 50, 80, 85]. Hydrogel fibrils taken with cryo-TEM can be seen in Fig. 5 [49]. AFM uses a mechanical nanoprobe to scan along the surface of a sample, obtaining information with regards to the surface topography and nanostructure. Figure 7 shows a nanostructure comparison of the same sample obtained with both TEM and AFM image [85].

Rheology is an important technique to identify if a hydrogel network is present and to measure properties such as mechanical rigidity and timing of gelation. Unlike the other characterization techniques, which examine the static structure of the hydrogel, rheology subjects the hydrogel to shear forces in order to better understand bulk gel mechanical properties and structure such as gel stiffness, flow properties, assembly time and overall network structure. For the same peptide sequences, the solution conditions and peptide concentration can cause drastic differences in gelation time and ultimate gel properties. A simple example of the utility of rheology is shown in Fig. 8 [86]. MAX1 peptide is assembled with the same peptide concentration but different salt concentration in Fig. 11a showing clear differences in gel stiffness as indicated by different storage moduli, G′, when hydrogelation occurs with a higher salt concentration in solution. The higher the salt concentration, the faster the intramolecular folding and secondary structure formation and the faster the intermolecular quaternary structure hydrogel network formation. Consequently, the faster the assembly, the more crosslinks in the gel and the stiffer the final network. This observation is only possible with rheology during and after the gelation process. In Fig. 11b, the stiffness (G′) and viscous properties (G″ or loss modulus) are measured for a MAX1 gel versus frequency in order to gain insight into the material properties relative to time scale of shear applied to the gel [28]. Rheology is a critical tool to defining quaternary structures and ultimately peptide hydrogel properties. Yan et al. have defined and examined the importance and uses for rheology to better understand peptide hydrogels as the field expands [38].

An exciting property of some physical peptide hydrogels due to the entangled and branched nanostructure is the ability of the solid gel to flow like a liquid when

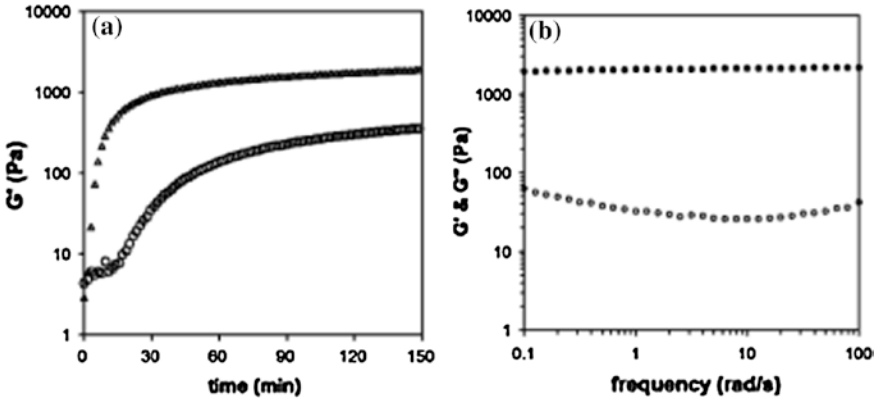

Fig. 11 Showing a difference in rheology data in for 2 wt% MAX1 in a **a** dynamic time sweep at 20 °C (*circles*) and at 37 °C (*triangles*), and **b** a frequency sweep at 37 °C showing G′ (*filled*) and G″ (*empty*) [28]

under stress, otherwise known as shear-thinning. The property allows a gel network quaternary structure to be set and then subsequently processed (i.e. injected from a syringe) to a secondary site. Rheology is an important tool in understanding and confirming shear-thinning behavior. Many of these materials after the cessation of shear are able to fully recover into solid hydrogel materials similar to the preshear state [37, 43, 72, 73]. The Pochan group studied at length the causes for shear-thinning behavior in β-hairpin peptide hydrogels and how the hydrogel is able to recover into a solid. The shear-thinning capability comes from the physical crosslinking, primarily the fibril branching present in the quaternary order. When the gel experiences shear forces, the fibril network can fracture, breaking the gel into domains that are able to move past each other. When shear forces cease, the gel domains come into contact with each other and immediately percolate to reform a gel network [72]. Figure 10 shows an example of rheology data for MAX8 where it first gels, then shear-thins under steady-state shear, exhibits solid properties directly after shear has ceased and ultimately recovers to preshear stiffness after a short amount of time. This property is critical in defining the properties of hydrogel-encapsulated payload constructs where one would like to know the exact properties of the construct, e.g. drug delivery profile [96] or encapsulated cell state, after in vivo injection [73, 97].

5 Hydrogel Properties

Peptide hydrogels have many properties that allow for a wide range of possible applications from drug delivery to tissue scaffolding. In addition, the customizable synthesis of peptide sequences for use as hydrogels allows for the tailoring of

hydrogel properties. Some of these supramolecular hydrogel properties, like cytocompatibility or customizable gelation conditions, are properties seen regularly in peptide hydrogels and are necessary for biomedical peptide hydrogel applications.

Like many other nature-inspired materials, peptides and proteins are often cytocompatible. This makes peptide hydrogels excellent candidates in providing growth conditions that mimic the natural, in vivo environment of cells. Cytocompatibility is a broad, general term that describes whether or not a cell is able to survive near, in, with, or on a peptide hydrogel. Many peptide hydrogels, regardless of structure and composition, have shown good cytocompatibility with many different cell lines such as mesenchymal stem cells (MSCs) [73, 97, 98], embryonic stem cells (ESCs) [84, 99], rat adrenal pheochromocytoma cells [100], or macrophages [101]. Many of these cell types have not only stayed alive while encapsulated, but also continued to grow and proliferate, indicating a high degree of cytocompatibility in the peptide hydrogels.

Self-assembly methods and the solid structure of hydrogels, combined with biological compatibility, leads to many biomedical applications specific to drug, cell, or molecule delivery. In addition, these materials are excellent candidates as scaffolding for tissue regeneration or for 3D cell growth environments. Drug, protein, and molecule delivery systems include targeted treatment for eradication of cancers [6, 55, 96], diabetes [43], and other illnesses [37, 38, 102, 103]. As the following examples will discuss, successfully encapsulated drugs and molecules are varied in size, hydrophobicity, charge, origin, and pH.

The Zhang group encapsulated biologically native proteins of varying charge and hydrophobicity to better understand diffusion kinetics through the Ac-$(RADA)_4$-$CONH_2$ peptide hydrogels in vitro [103]. Using a single molecule approach, the kinetics showed potential for sustained release of proteins, where diffusion of the protein was dependent on size and not charge. The Schneider group also encapsulated proteins of varying charge and hydrophobicity in MAX8 hydrogels, but instead examined bulk release after syringe delivery [104]. Unlike the Zhang group, the charge of the protein greatly affected the release and diffusion profile, suggesting the importance of the native hydrogel environment for molecule encapsulation. Instead of looking at proteins, the Pochan group examined drug molecule release through encapsulation of hydrophobic curcumin, a derivative of the naturally occurring Indian spice turmeric [96]. In this study, the hydrophobic curcumin was encapsulated and protected from quick degradation in a mostly aqueous situation in the MAX8 peptide hydrogel. The encapsulated curcumin remained active after release well beyond its chemical stability half-life of 8 h. In addition, the compound continued very low, sustained concentrations of release over 2 weeks, enough for cancer cell eradication in vitro. Since many chemotherapeutics can be equally detrimental to healthy cells, this ability to release chemotherapeutic compounds locally and at low but effective concentrations is advantageous for minimizing side effects while maintaining meaningful treatments.

Peptide hydrogels can be delivered into the body through several different methods, depending on the gel assembly mechanism and desired application of the

hydrogel. Peptide hydrogels can be introduced by injection [27, 33, 34, 45, 48, 68, 72] or surgical placement [26, 29, 37]. While injection is a common delivery tactic, most polymer material hydrogels being injected are liquids that are designed to be crosslinked covalently in vivo [45, 68]. This requires additional external stimuli to trigger gelation after injection. For example, a gel pre-cursor is injected, and gelation is then triggered using UV [105, 106], a crosslinking chemical, or infrared light [107]. Not only does external stimuli increase the possibility of contamination or side effects, these delayed crosslinking steps do not guarantee uniformity in gel structures or payload distribution. In the cases when peptides are injected as a liquid, usually a biological stimulus in vivo is used to cause desired secondary and quaternary structure formation i.e. gelation. These gelation stimuli include using body temperature [108], cell environments [15, 55], or native enzymes [109].

An alternative to liquid injection that is made possible by some physical peptide hydrogels is the idea of an injectable solid. The Pochan and Schneider groups are able to take advantage of the structural organization of MAX gels to inject solids that have already assembled because the hydrogels have shear-thinning behavior and reheal at the cessation of shear forces. This advantage is the result of the physical crosslinking of the hydrogel nanostructures, causing the hydrogel to break up into smaller domains of intact gel when undergoing shear. Because the system is not chemically cross-linked, when shear forces cease, the nanofibrils remake physical crosslink contacts and do not need the introduction of another trigger to reform a hydrogel network. As a shear-thinning and rehealing hydrogel is injected through a syringe, only the hydrogel at the edges, along the surface of the syringe, experiences shear, leaving the rest of the hydrogel intact. This creates a plug flow of hydrogel [37, 41]. The resultant plug flow allows the hydrogel to protect payloads from shear and maintain the distribution and viability of cells, drugs, or proteins encapsulated within [29, 37, 41, 72].

Besides drugs and large molecules, peptide hydrogels are also used in the delivery of cells [41, 43, 45, 73, 96–99]. MSCs are encapsulated for injection in hopes of influencing or better understanding stem cell differentiation, with the goal of depositing the cells in a specific-cell type deficient area [73, 97, 98]. Instead of encapsulating cells for cell growth, the Hartgerink group cultures ESCs and their $E_2(SL)_6E_2$GRGDS hydrogel separated by a permeable membrane [43]. The separated peptide hydrogels act as sponges, harnessing secreted growth factors and secretomes from ESCs. Then, the protein-infused peptide hydrogels are injected in vivo or used for tissue culture at a later time with concurrent release of or metabolism of the infused ESC proteins.

In addition to delivery, peptide hydrogels are ideal for tissue scaffolding and 3D cell growth environments. 3D environments can be used to provide a working model of systems within the body that may be hard to observe and difficult to mimic in vitro. Some of these systems include the culture of endothelial stem cells [31], blood vessel formation [63], chondrocyte development [11], and stem cells of many types [73, 98]. 3D environments also provide a more natural environment than 2D cell culturing methods with ability to control material details in 3D such as morphology and matrix stiffnesses [1, 61, 110–113]. Extracellular matrix (ECM)

mimetic 3D structures are also highly desirable to better understand the intricate physical networks that cells need for growth and replication. The inherent fibrillar network of the gels provides a similar ECM-like structure on which cells may anchor, as well as a hydrogel porous enough for growth factors and important biochemical signals to diffuse through [11, 34, 35, 37, 114–117]. Some of the many encapsulated cell lines include MSCs [73, 98], endothelial cells [31], chondrocytes [118], or fibroblasts [99]. The Schneider and Pochan groups have successfully encapsulated MSCs in a 3D environment as seen in Fig. 10, showing homogenous distribution of cells with desired cell density and spacing—a feature unavailable in 2D growth environments [73, 97]. Additionally, the 3D environment also provides the starting structure for the cells to deposit ECM [73, 97] with the opportunity to observe in vivo-like behavior recreated in the 3D peptide hydrogel construct.

Because of the nature-inspired origins of peptide hydrogels, the natural degradation of peptide hydrogels is also an important property. This is a feature that is inherent in peptide hydrogels that is less characteristic in polymeric hydrogels. Because of the amino acid origins of peptide hydrogels, there is natural degradation [19, 98, 115] that occurs from enzymes secreted by the body in vivo, without major immune reactions [19, 37, 43, 61, 67, 68]. Macrophages and neutrophils are cells typically associated with an immune response in the body that are observed to have little or no reaction when cultured with hydrogels [70, 84, 101] or in vivo [84]. The interaction of enzyme with peptides to affect hydrogel properties is not surprising, since one of the possible triggers for self-assembly is the introduction of enzymes to linear peptides as seen by the Xu and Ulijn groups [26, 47]. In degradation, however, instead of assembling short peptides into fibrils and hydrogels, the hydrogels are being broken down into smaller pieces through enzymolysis [115, 119, 120]. When designing the peptide sequences, specific segments that act as reaction substrates for enzymes such as MMP13 [119] or MMP2 [120] can be incorporated into the initial peptide synthesis.

The bulk of this chapter explained the hierarchical structures of peptide sequences and hydrogels constructed with physical solution assembly in an attempt to discuss the fundamental properties of peptide hydrogels and the molecular foundations thereof. Peptide sequences can be categorized with primary, secondary, tertiary, and/or quaternary structures, spanning the molecular level through the hydrogel network. Peptide hydrogels are great candidates in the ever-growing field of biological and medical applications. Not only are peptide sequences easy to synthesize, the synthesis process allows for customizable molecular and material features such as peptide length, amino acid substitution, gelation time, mechanical properties (e.g. stiffness), or functionalities for cell targeting or encapsulations. The natural cytocompatibility and degradability of peptides make peptide hydrogels great candidates for cell encapsulation, 3D growth environments, tissue scaffolding, and injectable payload delivery. Peptide hydrogels are not only able to successfully encapsulate cells, but also able to encapsulate proteins and drugs of varying charge, size, or hydrophobicity. Unlike traditional liquid-based delivery systems that rely on gelation after injection while simultaneously

delivering encapsulated payloads, some peptide hydrogels can be injected as solids without need of external stimuli or interactions to reform into a solid similar to the preinjected material. It is clear that the future is bright for the discovery of new peptide molecules to make new hydrogel materials with both designed properties as well as unanticipated, excellent properties.

References

1. Bromley, E.H.C., Channon, K.J., King, P.J.S., et al.: Assembly pathway of a designed alpha-helical protein fiber. Biophys. J. **98**, 1668–1676 (2010). doi:10.1016/j.bpj.2009.12.4309
2. Ruoslahti, E.: RGD and other recognition sequences for integrins. Annu. Rev. Cell Dev. Biol. **12**, 697–715 (1996). doi:10.1146/annurev.cellbio.12.1.697
3. Nilsson, B.L., Soellner, M.B., Raines, R.T.: Chemical synthesis of proteins. Annu. Rev. Biophys. Biomol. Struct. **34**, 91 (2005)
4. Hersel, U., Dahmen, C., Kessler, H.: RGD modified polymers: biomaterials for stimulated cell adhesion and beyond. Biomaterials **24**, 4385–4415 (2003)
5. Iha, R.K., Wooley, K.L., Nyström, A.M., et al.: Applications of orthogonal "click" chemistries in the synthesis of functional soft materials. Chem. Rev. **109**, 5620–5686 (2009)
6. Collier, J.H., Segura, T.: Evolving the use of peptides as components of biomaterials. Biomaterials **32**, 4198–4204 (2011). doi:10.1016/j.biomaterials.2011.02.030
7. DeForest, C.A., Sims, E.A., Anseth, K.S.: Peptide-functionalized click hydrogels with independently tunable mechanics and chemical functionality for 3D cell culture. Chem. Mater. **22**, 4783–4790 (2010). doi:10.1021/cm101391y
8. Ruoslahti, E.: Integrins. J. Clin. Invest. **87**, 1–5 (1991). doi:10.1172/JCI114957
9. DeForest, C.A., Polizzotti, B.D., Anseth, K.S.: Sequential click reactions for synthesizing and patterning three-dimensional cell microenvironments. Nat. Mater. **8**, 659–664 (2009). doi:10.1038/nmat2473
10. Ulijn, R.V., Smith, A.M.: Designing peptide based nanomaterials. Chem. Soc. Rev. **37**, 664–675 (2008)
11. Kyle, S., Aggeli, A., Ingham, E., McPherson, M.J.: Production of self-assembling biomaterials for tissue engineering. Trends Biotechnol. **27**, 423–433 (2009). doi:10.1016/j.tibtech.2009.04.002
12. Woolfson, D.N., Mahmoud, Z.N.: More than just bare scaffolds: towards multi-component and decorated fibrous biomaterials. Chem. Soc. Rev. **39**, 3464–3479 (2010). doi:10.1039/c0cs00032a
13. Smith, A.M., Banwell, E.F., Edwards, W.R., et al.: Engineering increased stability into self-assembled protein fibers. Adv. Funct. Mater. **16**, 1022–1030 (2006). doi:10.1002/adfm.200500568
14. Schneider, J., Pochan, D., Ozbas, B., et al.: Responsive hydrogels from the intramolecular folding and self-assembly of a designed peptide. J. Am. Chem. Soc. **124**, 15030–15037 (2002). doi:10.1021/ja027993g
15. Bowerman, C.J., Nilsson, B.L.: A reductive trigger for peptide self-assembly and hydrogelation. J. Am. Chem. Soc. **132**, 9526–9527 (2010). doi:10.1021/ja1025535
16. Kopecek, J., Yang, J.: Smart self-assembled hybrid hydrogel biomaterials. Angew. Chem. Int. Ed. **51**, 7396–7417 (2012). doi:10.1002/anie.201201040
17. Ryan, D.M., Nilsson, B.L.: Self-assembled amino acids and dipeptides as noncovalent hydrogels for tissue engineering. Polym. Chem. **3**, 18–33 (2011). doi:10.1039/c1py00335f
18. Nicolai, T., Durand, D.: Controlled food protein aggregation for new functionality. Curr. Opin. Colloid Interface Sci. **18**, 249–256 (2013). doi:10.1016/j.cocis.2013.03.001

19. Kopecek, J., Yang, J.: Peptide-directed self-assembly of hydrogels. Acta Biomater. **5**, 805–816 (2009). doi:10.1016/j.actbio.2008.10.001
20. Zhang, Y., Gu, H., Yang, Z., Xu, B.: Supramolecular hydrogels respond to ligand–receptor interaction. J. Am. Chem. Soc. **125**, 13680–13681 (2003). doi:10.1021/ja036817k
21. Shu, J.Y., Panganiban, B., Xu, T.: Peptide–polymer conjugates: from fundamental science to application. Annu. Rev. Phys. Chem. **64**, 631–657 (2013)
22. Bowerman, C.J., Liyanage, W., Federation, A.J., Nilsson, B.L.: Tuning beta-sheet peptide self-assembly and hydrogelation behavior by modification of sequence hydrophobicity and aromaticity. Biomacromolecules **12**, 2735–2745 (2011). doi:10.1021/bm200510k
23. Li, J., Gao, Y., Kuang, Y., et al.: Dephosphorylation of d-peptide derivatives to form biofunctional, supramolecular nanofibers/hydrogels and their potential applications for intracellular imaging and intratumoral chemotherapy. J. Am. Chem. Soc. **135**, 9907–9914 (2013). doi:10.1021/ja404215g
24. Kim, M., Tang, S., Olsen, B.D.: Physics of engineered protein hydrogels. J. Polym. Sci. B Polym. Phys. **51**, 587–601 (2013). doi:10.1002/polb.23270
25. Khakshoor, O., Nowick, J.S.: Artificial beta-sheets: chemical models of beta-sheets. Curr. Opin. Chem. Biol. **12**, 722–729 (2008). doi:10.1016/j.cbpa.2008.08.009
26. Das, A.K., Collins, R., Ulijn, R.V.: Exploiting enzymatic (reversed) hydrolysis in directed self-assembly of peptide nanostructures. Small **4**, 279–287 (2008)
27. Ozbas, B., Rajagopal, K., Schneider, J., Pochan, D.: Semiflexible chain networks formed via self-assembly of β-hairpin molecules. Phys. Rev. Lett. **93**, 268106 (2004). doi:10.1103/PhysRevLett.93.268106
28. Ozbas, B., Kretsinger, J., Rajagopal, K., et al.: Salt-triggered peptide folding and consequent self-assembly into hydrogels with tunable modulus. Macromolecules **37**, 7331–7337 (2004)
29. Bakota, E.L., Aulisa, L., Galler, K.M., Hartgerink, J.D.: Enzymatic cross-linking of a nanofibrous peptide hydrogel. Biomacromolecules **12**, 82–87 (2011). doi:10.1021/bm1010195
30. Olsen, B.D.: Engineering materials from proteins. AIChE J. **59**, 3558–3568 (2013). doi:10.1002/aic.14223
31. Jung, J.P., Nagaraj, A.K., Fox, E.K., et al.: Co-assembling peptides as defined matrices for endothelial cells. Biomaterials **30**, 2400–2410 (2009)
32. DiMarco, R.L., Heilshorn, S.C.: Multifunctional materials through modular protein engineering. Adv. Mater. **24**, 3923–3940 (2012). doi:10.1002/adma.201200051
33. Estroff, L.A., Hamilton, A.D.: Water gelation by small organic molecules. Chem. Rev. **104**, 1201–1218 (2004)
34. Bromley, E.H.C., Channon, K., Moutevelis, E., Woolfson, D.N.: Peptide and protein building blocks for synthetic biology: from programming biomolecules to self-organized biomolecular systems. ACS Chem. Biol. **3**, 38–50 (2008). doi:10.1021/cb700249v
35. Kyle, S., Aggeli, A., Ingham, E., McPherson, M.J.: Recombinant self-assembling peptides as biomaterials for tissue engineering. Biomaterials **31**, 9395–9405 (2010). doi:10.1016/j.biomaterials.2010.08.051
36. Woolfson, D.N.: Building fibrous biomaterials from alpha-helical and collagen-like coiled-coil peptides. Pept. Sci. **94**, 118–127 (2010). doi:10.1002/bip.21345
37. Guvendiren, M., Lu, H.D., Burdick, J.A.: Shear-thinning hydrogels for biomedical applications. Soft Matter **8**, 260–272 (2011). doi:10.1039/c1sm06513k
38. Yan, C., Pochan, D.J.: Rheological properties of peptide-based hydrogels for biomedical and other applications. Chem. Soc. Rev. **39**, 3528–3540 (2010)
39. Smith, T.J., Khatcheressian, J., Lyman, G.H., et al.: 2006 update of recommendations for the use of white blood cell growth factors: an evidence-based clinical practice guideline. J. Clin. Oncol. **24**, 3187–3205 (2006)
40. Jayawarna, V., Richardson, S.M., Hirst, A.R., et al.: Introducing chemical functionality in Fmoc-peptide gels for cell culture. Acta Biomater. **5**, 934–943 (2009). doi:10.1016/j.actbio.2009.01.006
41. Olsen, B.D., Kornfield, J.A., Tirrell, D.A.: Yielding behavior in injectable hydrogels from telechelic proteins. Macromolecules **43**, 9094–9099 (2010). doi:10.1021/ma101434a

42. Adams, D.J., Butler, M.F., Frith, W.J., et al.: A new method for maintaining homogeneity during liquid–hydrogel transitions using low molecular weight hydrogelators. Soft Matter **5**, 1856 (2009). doi:10.1039/b901556f
43. Bakota, E.L., Wang, Y., Danesh, F.R., Hartgerink, J.D.: Injectable multidomain peptide nanofiber hydrogel as a delivery agent for stem cell secretome. Biomacromolecules **12**, 1651–1657 (2011)
44. Saiani, A., Mohammed, A., Frielinghaus, H., et al.: Self-assembly and gelation properties of alpha-helix versus beta-sheet forming peptides. Soft Matter **5**, 193–202 (2009). doi:10.1039/b811288f
45. Macaya, D., Spector, M.: Injectable hydrogel materials for spinal cord regeneration: a review. Biomed. Mater. **7**, 012001 (2012). doi:10.1088/1748-6041/7/1/012001
46. Doose, S., Neuweiler, H., Barsch, H., Sauer, M.: Probing polyproline structure and dynamics by photoinduced electron transfer provides evidence for deviations from a regular polyproline type II helix. Proc. Natl. Acad. Sci. **104**, 17400–17405 (2007). doi:10.1073/pnas.0705605104
47. Yang, Z., Gu, H., Fu, D., et al.: Enzymatic formation of supramolecular hydrogels. Adv. Mater. **16**, 1440–1444 (2004). doi:10.1002/adma.200400340
48. Raeburn, J., Zamith Cardoso, A., Adams, D.J.: The importance of the self-assembly process to control mechanical properties of low molecular weight hydrogels. Chem. Soc. Rev. **42**, 5143–5156 (2013). doi:10.1039/c3cs60030k
49. Yucel, T., Micklitsch, C.M., Schneider, J.P., Pochan, D.J.: Direct observation of early-time hydrogelation in beta-hairpin peptide self-assembly. Macromolecules **41**, 5763–5772 (2008). doi:10.1021/ma702840q
50. Aulisa, L., Dong, H., Hartgerink, J.D.: Self-assembly of multidomain peptides: sequence variation allows control over cross-linking and viscoelasticity. Biomacromolecules **10**, 2694–2698 (2009). doi:10.1021/bm900634x
51. Branco, M.C., Pochan, D.J., Wagner, N.J., Schneider, J.P.: Macromolecular diffusion and release from self-assembled beta-hairpin peptide hydrogels. Biomaterials **30**, 1339–1347 (2009). doi:10.1016/j.biomaterials.2008.11.019
52. Lin, B.F., Megley, K.A., Viswanathan, N., et al.: pH-responsive branched peptide amphiphile hydrogel designed for applications in regenerative medicine with potential as injectable tissue scaffolds. J. Mater. Chem. **22**, 19447 (2012). doi:10.1039/c2jm31745a
53. Tagalakis, A.D., Saraiva, L., McCarthy, D., et al.: Comparison of nanocomplexes with branched and linear peptides for SiRNA delivery. Biomacromolecules **14**, 761–770 (2013)
54. Dong, H., Dube, N., Shu, J.Y., et al.: Long-circulating 15 nm micelles based on amphiphilic 3-helix peptide–PEG conjugates. ACS Nano **6**, 5320–5329 (2012). doi:10.1021/nn301142r
55. Cui, H., Webber, M.J., Stupp, S.I.: Self-assembly of peptide amphiphiles: from molecules to nanostructures to biomaterials. Biopolymers **94**, 1–18 (2010). doi:10.1002/bip.21328
56. Gosal, W.S., Clark, A.H., Ross-Murphy, S.B.: Fibrillar β-lactoglobulin gels: part 1. Fibril formation and structure. Biomacromolecules **5**, 2408–2419 (2004). doi:10.1021/bm049659d
57. Liu, T.-Y., Hussein, W.M., Jia, Z., et al.: Self-adjuvanting polymer–peptide conjugates as therapeutic vaccine candidates against cervical cancer. Biomacromolecules **14**, 2798–2806 (2013). doi:10.1021/bm400626w
58. Gosal, W.S., Clark, A.H., Pudney, P.D., Ross-Murphy, S.B.: Novel amyloid fibrillar networks derived from a globular protein: β-lactoglobulin. Langmuir **18**, 7174–7181 (2002)
59. Lin, Y.-A., Ou, Y.-C., Cheetham, A.G., Cui, H.: Supramolecular polymers formed by ABC miktoarm star peptides. ACS Macro Lett **2**, 1088–1094 (2013). doi:10.1021/mz400535g
60. Kavanagh, G.M., Clark, A.H., Ross-Murphy, S.B.: Heat-induced gelation of globular proteins. Part 5. Creep behaviour of β-lactoglobulin gels. Rheol. Acta **41**, 276–284 (2002). doi:10.1007/s00397-001-0220-0
61. Hamley, I.W.: Self-assembly of amphiphilic peptides. Soft Matter **7**, 4122–4138 (2011). doi:10.1039/c0sm01218a

62. Kroes-Nijboer, A., Venema, P., Linden, E.V.D.: Fibrillar structures in food. Food Funct. **3**, 221–227 (2012). doi:10.1039/c1fo10163c
63. Lee, K., Mooney, D.: Hydrogels for tissue engineering. Chem. Rev. **101**, 1869–1879 (2001). doi:10.1021/cr000108x
64. Bowerman, C.J., Nilsson, B.L.: Review self-assembly of amphipathic β-sheet peptides: Insights and applications. Pept. Sci. **98**, 169–184 (2012). doi:10.1002/bip.22058
65. Cheng, R.P., Gellman, S.H., DeGrado, W.F.: β-Peptides: from structure to function. Chem. Rev. **101**, 3219–3232 (2001)
66. Totosaus, A., Montejano, J.G., Salazar, J.A., Guerrero, I.: A review of physical and chemical protein-gel induction. Int. J. Food Sci. Technol. **37**, 589–601 (2002). doi:10.1046/j.1365-2621.2002.00623.x
67. Hauser, C.A., Zhang, S.: Designer self-assembling peptide nanofiber biological materials. Chem. Soc. Rev. **39**, 2780–2790 (2010). doi:10.1039/b921448h
68. Li, Y., Rodrigues, J., Tomás, H.: Injectable and biodegradable hydrogels: gelation, biodegradation and biomedical applications. Chem. Soc. Rev. **41**, 2193–2221 (2012). doi:10.1039/c1cs15203c
69. Heilshorn, S.C., Liu, J.C., Tirrell, D.A.: Cell-binding domain context affects cell behavior on engineered proteins. Biomacromolecules **6**, 318–323 (2005). doi:10.1021/bm049627q
70. Ngo, J.T., Tirrell, D.A.: Noncanonical amino acids in the interrogation of cellular protein synthesis. Acc. Chem. Res. **44**, 677–685 (2011). doi:10.1021/ar200144y
71. Gauthier, M.A., Klok, H.-A.: Peptide/protein–polymer conjugates: synthetic strategies and design concepts. Chem. Commun. 2591–2611 (2008). doi:10.1039/b719689j
72. Yan, C., Altunbas, A., Yucel, T., et al.: Injectable solid hydrogel: mechanism of shear-thinning and immediate recovery of injectable β-hairpin peptide hydrogels. Soft Matter **6**, 5143–5156 (2010). doi:10.1039/c0sm00642d
73. Haines-Butterick, L., Rajagopal, K., Branco, M., et al.: Controlling hydrogelation kinetics by peptide design for three-dimensional encapsulation and injectable delivery of cells. Proc. Natl. Acad. Sci. U.S.A. **104**, 7791–7796 (2007). doi:10.1073/pnas.0701980104
74. Moss, J.A.: Unit 18.7: Guide for resin and linker selection in solid-phase peptide synthesis. Curr. Protoc. Prot. Sci. 1–19 (2005)
75. Barany, G., Albericio, F.: Three-dimensional orthogonal protection scheme for solid-phase peptide synthesis under mild conditions. J. Am. Chem. Soc. **107**, 4936–4942 (1985)
76. Naik, R.R., Stringer, S.J., Agarwal, G., et al.: Biomimetic synthesis and patterning of silver nanoparticles. Nat. Mater. **1**, 169–172 (2002). doi:10.1038/nmat758
77. Akdim, B., Pachter, R., Kim, S.S., et al.: Electronic properties of a graphene device with peptide adsorption: insight from simulation. ACS Appl. Mater. Interfaces **5**, 7470–7477 (2013). doi:10.1021/am401731c
78. Dickerson, M.B., Sandhage, K.H., Naik, R.R.: Protein- and peptide-directed syntheses of inorganic materials. Chem. Rev. **108**, 4935–4978 (2008)
79. Helen, W., de Leonardis, P., Ulijn, R.V., et al.: Mechanosensitive peptide gelation: mode of agitation controls mechanical properties and nano-scale morphology. Soft Matter **7**, 1732 (2011). doi:10.1039/c0sm00649a
80. Morris, K.L., Chen, L., Raeburn, J., et al.: Chemically programmed self-sorting of gelator networks. Nat. Commun. **4**, 1480 (2013)
81. Ramachandran, S., Taraban, M.B., Trewhella, J., et al.: Effect of temperature during assembly on the structure and mechanical properties of peptide-based materials. Biomacromolecules **11**, 1502–1506 (2010). doi:10.1021/bm100138m
82. Feng, Y., Taraban, M., Yu, Y.B.: The effect of ionic strength on the mechanical, structural and transport properties of peptide hydrogels. Soft Matter **8**, 11723–11731 (2012). doi:10.1039/c2sm26572a
83. Kim, C.A., Berg, J.M.: Thermodynamic β-sheet propensities measured using a zinc-finger host peptide. Nature **362**, 267–270 (1993). doi:10.1038/362267a0
84. Jung, J.P., Gasiorowski, J.Z., Collier, J.H.: Fibrillar peptide gels in biotechnology and biomedicine. Biopolymers **94**, 49–59 (2010). doi:10.1002/bip.21326

85. Nagy, K.J., Giano, M.C., Jin, A., et al.: Enhanced mechanical rigidity of hydrogels formed from enantiomeric peptide assemblies. J. Am. Chem. Soc. **133**, 14975–14977 (2011). doi:10.1021/ja206742m
86. Whisstock, J.C., Bottomley, S.P.: Molecular gymnastics: serpin structure, folding and misfolding. Curr. Opin. Struct. Biol. **16**, 761–768 (2006). doi:10.1016/j.sbi.2006.10.005
87. Nagarkar, R.P., Hule, R.A., Pochan, D.J., Schneider, J.P.: Domain swapping in materials design. Biopolymers **94**, 141–155 (2010). doi:10.1002/bip.21332
88. Rajagopal, K., Lamm, M.S., Haines-Butterick, L.A., et al.: Tuning the pH responsiveness of beta-hairpin peptide folding, self-assembly, and hydrogel material formation. Biomacromolecules **10**, 2619–2625 (2009). doi:10.1021/bm900544e
89. Freire, F., Almeida, A.M., Fisk, J.D., et al.: Impact of strand length on the stability of parallel-beta-sheet secondary structure. Angew. Chem. Int. Ed. **50**, 8735–8738 (2011). doi:10.1002/anie.201102986
90. Apostolovic, B., Danial, M., Klok, H.-A.: Coiled coils: attractive protein folding motifs for the fabrication of self-assembled, responsive and bioactive materials. Chem. Soc. Rev. **39**, 3541–3575 (2010). doi:10.1039/b914339b
91. Moutevelis, E., Woolfson, D.N.: A periodic table of coiled-coil protein structures. J. Mol. Biol. **385**, 726–732 (2009). doi:10.1016/j.jmb.2008.11.028
92. Marsden, H.R., Kros, A.: Self-assembly of coiled coils in synthetic biology: inspiration and progress. Angew. Chem. Int. Ed. **49**, 2988–3005 (2010). doi:10.1002/anie.200904943
93. Jing, P., Rudra, J.S., Herr, A.B., Collier, J.H.: Self-assembling peptide–polymer hydrogels designed from the coiled coil region of fibrin. Biomacromolecules **9**, 2438–2446 (2008)
94. Hule, R.A., Nagarkar, R.P., Altunbas, A., et al.: Correlations between structure, material properties and bioproperties in self-assembled β-hairpin peptide hydrogels. Faraday Discuss. **139**, 251–264 (2008)
95. Branco, M.C., Nettesheim, F., Pochan, D.J., et al.: Fast dynamics of semiflexible chain networks of self-assembled peptides. Biomacromolecules **10**, 1374–1380 (2009)
96. Altunbas, A., Lee, S.J., Rajasekaran, S.A., et al.: Encapsulation of curcumin in self-assembling peptide hydrogels as injectable drug delivery vehicles. Biomaterials **32**, 5906–5914 (2011). doi:10.1016/j.biomaterials.2011.04.069
97. Yan, C., Mackay, M.E., Czymmek, K., et al.: Injectable solid peptide hydrogel as a cell carrier: effects of shear flow on hydrogels and cell payload. Langmuir **28**, 6076–6087 (2012). doi:10.1021/la2041746
98. Anderson, S.B., Lin, C.-C., Kuntzler, D.V., Anseth, K.S.: The performance of human mesenchymal stem cells encapsulated in cell-degradable polymer–peptide hydrogels. Biomaterials **32**, 3564–3574 (2011)
99. Tian, Y.F., Devgun, J.M., Collier, J.H.: Fibrillized peptide microgels for cell encapsulation and 3D cell culture. Soft Matter **7**, 6005–6011 (2011)
100. Jabbari, E.: Bioconjugation of hydrogels for tissue engineering. Curr. Opin. Biotechnol. **22**, 655–660 (2011)
101. Haines-Butterick, L.A., Salick, D.A., Pochan, D.J., Schneider, J.P.: In vitro assessment of the pro-inflammatory potential of β-hairpin peptide hydrogels. Biomaterials **29**, 4164–4169 (2008). doi:10.1016/j.biomaterials.2008.07.009
102. Rudra, J.S., Mishra, S., Chong, A.S., et al.: Self-assembled peptide nanofibers raising durable antibody responses against a malaria epitope. Biomaterials **33**, 6476–6484 (2012)
103. Koutsopoulos, S., Unsworth, L.D., Nagai, Y., Zhang, S.: Controlled release of functional proteins through designer self-assembling peptide nanofiber hydrogel scaffold. Proc. Natl. Acad. Sci. **106**, 4623–4628 (2009). doi:10.1073/pnas.0807506106
104. Branco, M.C., Pochan, D.J., Wagner, N.J., Schneider, J.P.: The effect of protein structure on their controlled release from an injectable peptide hydrogel. Biomaterials **31**, 9527–9534 (2010)
105. Weber, L.M., Lopez, C.G., Anseth, K.S.: Effects of PEG hydrogel crosslinking density on protein diffusion and encapsulated islet survival and function. J. Biomed. Mater. Res. **90A**, 720–729 (2009). doi:10.1002/jbm.a.32134

106. Burdick, J.A., Anseth, K.S.: Photoencapsulation of osteoblasts in injectable RGD-modified PEG hydrogels for bone tissue engineering. Biomaterials **23**, 4315–4323 (2002)
107. Van Tomme, S.R., Storm, G., Hennink, W.E.: In situ gelling hydrogels for pharmaceutical and biomedical applications. Int. J. Pharm. **355**, 1–18 (2008)
108. Collier, J.H., Hu, B.H., Ruberti, J.W., et al.: Thermally and photochemically triggered self-assembly of peptide hydrogels. J. Am. Chem. Soc. **123**, 9463–9464 (2001). doi:10.1021/ja011535a
109. Collier, J.H., Messersmith, P.B.: Enzymatic modification of self-assembled peptide structures with tissue transglutaminase. Bioconjug. Chem. **14**, 748–755 (2003). doi:10.1021/bc034017t
110. Engler, A.J., Sen, S., Sweeney, H.L., Discher, D.E.: Matrix elasticity directs stem cell lineage specification. Cell **126**, 677–689 (2006). doi:10.1016/j.cell.2006.06.044
111. Kim, I.L., Mauck, R.L., Burdick, J.A.: Hydrogel design for cartilage tissue engineering: a case study with hyaluronic acid. Biomaterials **32**, 8771–8782 (2011)
112. Silva, D., Natalello, A., Sanii, B., et al.: Synthesis and characterization of designed BMHP1-derived self-assembling peptides for tissue engineering applications. Nanoscale **5**, 704–718 (2013)
113. Webber, M.J., Tongers, J., Renault, M.-A., et al.: Development of bioactive peptide amphiphiles for therapeutic cell delivery. Acta Biomater. **6**, 3–11 (2010). doi:10.1016/j.actbio.2009.07.031
114. Collier, J.H., Rudra, J.S., Gasiorowski, J.Z., Jung, J.P.: Multi-component extracellular matrices based on peptide self-assembly. Chem. Soc. Rev. **39**, 3413–3424 (2010). doi:10.1039/b914337h
115. Eliyahu-Gross, S., Bitton, R.: Environmentally responsive hydrogels with dynamically tunable properties as extracellular matrix mimetic. Rev. Chem. Eng. **29**, 159–168 (2013)
116. Romano, N.H., Sengupta, D., Chung, C., Heilshorn, S.C.: Protein-engineered biomaterials: nanoscale mimics of the extracellular matrix. Biochim. Biophys. Acta **1810**, 339–349 (2011). doi:10.1016/j.bbagen.2010.07.005
117. Matson, J.B., Stupp, S.I.: Self-assembling peptide scaffolds for regenerative medicine. Chem. Commun. **48**, 26 (2011). doi:10.1039/c1cc15551b
118. Jayawarna, V., Smith, A., Gough, J.E., Ulijn, R.V.: Three-dimensional cell culture of chondrocytes on modified di-phenylalanine scaffolds. Biochem. Soc. Trans. **35**, 535–537 (2007)
119. Giano, M.C., Pochan, D.J., Schneider, J.P.: Controlled biodegradation of self-assembling β-hairpin peptide hydrogels by proteolysis with matrix metalloproteinase-13. Biomaterials **32**, 6471–6477 (2011). doi:10.1016/j.biomaterials.2011.05.052
120. Galler, K.M., Hartgerink, J.D., Cavender, A.C., et al.: A customized self-assembling peptide hydrogel for dental pulp tissue engineering. Tissue Eng. Part A **18**, 176–184 (2012). doi:10.1089/ten.tea.2011.0222

Polymeric Supramolecular Hydrogels as Materials for Medicine

Sebastian Hackelbusch and Sebastian Seiffert

Abstract This chapter describes some recent research in the field of supramolecular polymeric hydrogels. Eight examples are discussed that represent a small view of the plethora of these advanced functional materials. The examples described herein exhibit tunable physicochemical properties that allow for adjustment towards targeted applications in the biomedical field, including protein immobilization, tissue engineering, drug delivery, and dermocosmetics. The highly adaptive supramolecular polymeric hydrogels are likely to have a bright future as materials for medicine.

Keywords Supramolecular · Hydrogen bonding · Ionic bonding · Metal complexation · Adaptive materials

1 Introduction

Polymeric hydrogels consist of three-dimensional networks of crosslinked macromolecules that entrap large amounts of water. A common scheme of classification distinguishes physical and chemical hydrogels, depending on the thermodynamic and kinetic strength of chain crosslinking [1]. Chemical chain connection can be considered irreversible on experimental timescales; it is either achieved by covalent bond formation between functionalized precursor polymer chains, including Schiff-base formation [2–4], Michael-type addition [3, 5], and

S. Hackelbusch · S. Seiffert
Institute of Chemistry and Biochemistry, FU Berlin, Takustr. 3, 14195 Berlin, Germany

S. Seiffert (✉)
F-ISFM Soft Matter and Functional Materials,
Helmholtz-Zentrum Berlin, Hahn-Meitner-Platz 1, 14109 Berlin, Germany
e-mail: sebastian.seiffert@helmholtz-berlin.de

X.J. Loh (ed.), *In-Situ Gelling Polymers*, Series in BioEngineering,
DOI 10.1007/978-981-287-152-7_7

'click' chemistry [6], or by radical crosslinking copolymerization of suitable monomers and crosslinkers [2, 7, 8], both resulting in permanent polymer networks, as illustrated in Fig. 1a. Due to the irreversibility of chain connection, the mechanical properties of chemical gels are determined by their crosslinking density and chain flexibility [9]. Many materials, such as polymeric adhesives [10], artificial lenses [11, 12], and cements [13], require gels to be stable and tough; this is achieved by dense crosslinking. However, dense crosslinking also entails gel brittleness [14] and turbidity [15]. A decisive downside of covalent hydrogels is that extensive mechanical stress can cause irreversible bond breakage in chemical gels, impairing their utility.

The drawbacks of chemical gels are overcome by physical gels. In these materials, chain crosslinking occurs by transient and reversible supramolecular association, as illustrated in Fig. 1b. As a result, the interchain junctions continuously break and rearrange on experimental timescales; this causes the transient bonds to be susceptible to shear, decreasing the stability of the hydrogels [16]. This dynamic characteristic leads to two unique abilities of gels: shear-thinning [16] and self-healing [17, 18]. At shear-thinning, physical hydrogels display decrease of their viscosity upon application of stress. This effect makes them suitable for implantation via syringe, whereafter they can regain their original properties; it also allows them to be processed to obtain desired shapes in materials engineering. In self-healing, disrupted supramolecular bonds exhibit a tendency to reassociate upon contact. This effect allows the hydrogel to restore its original mechanical strength after damage; it also allows fusion of two independent gel fragments to a new composite [19]. As a complement to self-healing, another feature of supramolecular hydrogels is that they can be disintegrated by external stimulation, including change of pH [20, 21], temperature [22, 23], or solvent composition [24], thereby degrading them to their precursor polymers or building blocks. Because of

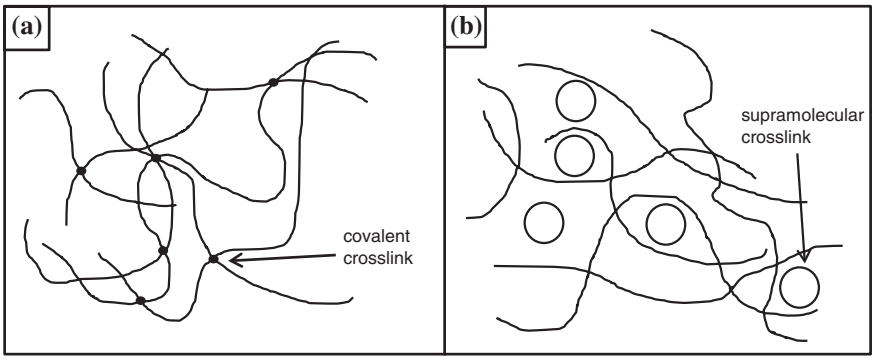

Fig. 1 Schematic structures of **a** permanent, chemically crosslinked and **b** transient, physically crosslinked polymer networks

these characteristics, physical hydrogels are suited for a plethora of applications as functional smart materials [25–29].

Physical chain crosslinking can be achieved by two different approaches. In one approach, junctions are formed directly between precursor polymer chains by mutual reversible association of suitable moieties on the polymer backbone [30, 31]. In another approach, supramolecular junctions are formed by chain association mediated by an additional linker [32, 33]. To realize these different strategies, different crosslinker motifs have been reported, including those based on hydrogen bonding [34, 35], metal complexation [36, 37], or ionic interaction [38, 39]. These different motifs have specific pros and cons, depending on the desired application of the hydrogel. For example, applications in the medicinal sector, such as tissue engineering [40, 41] or drug delivery [42, 43], are impaired by chain crosslinking through metal complexation, because many metal ions are toxic [44, 45]. Instead hydrogels used for these purposes are better crosslinked by hydrogen bonding or ionic interactions. However, hydrogels crosslinked by metal complexation find various use in other areas, including application as superabsorbers [46], optical devices [47, 48], soft semiconductors [49, 50], or fuel cells [51, 52].

Several starting materials can be used to prepare supramolecular polymeric hydrogels, including biopolymers, synthetic polymers, or hybrids of both. Many biomolecules, such as alginate [53–55], gelatin [56–58], or chitosan [59–61] can form hydrogels even without chemical modification of the polymer. In addition, these materials are biocompatible, bioavailable, biodegradable, and cheap. This makes them ideal candidates for applications in the medicinal sector. However, a downside of biopolymers is their batch-to-batch variation [62–64], entailing variation of the physical properties of gels that are formed from them. To avoid this problem, synthetic polymers like polyethylene glycol [65–67], polyhydroxyethylmethacrylate [68–70], and polyglycerol [71–73] can be used to substitute biopolymers. In their native form, these polymers are incapable of forming hydrogels. Thus, suitable chemical modification must be applied to use them for this purpose. This approach often entails increased costs and a high workload to prepare the hydrogels, but it introduces the advantage that chemical modification can be applied in a custom and versatile principle, thereby tailoring the precursor polymers in rational materials design. In another approach, hybrid gels that consist of biopolymers *and* synthetic polymers combine the utility of both [74–76].

The topic of supramolecular polymeric hydrogels is a wide field. In this chapter, we summarize some recent work on the formation, characterization, and application of hydrogels crosslinked by hydrogen bonding, metal complexation, or electrostatic interaction. The selected examples represent a cross-section of the recent research and development on physical polymeric hydrogels for biomedical applications. We emphasize on different approaches using biopolymers, synthetic polymers, or hybrids of both. A special focus is on the physical–chemical features and the resulting macroscopic properties of these functional materials in biotechnological applications.

2 Hydrogels Crosslinked by Hydrogen Bonding

The most important supramolecular interaction in Nature is hydrogen bonding. In biomolecules like dsRNA and DNA, two single strands are assembled by complementary base pairing, thymine–adenine, guanine–cytosine, and uracil–adenine, to form helixes. Even though a single hydrogen bond is rather weak, with binding energies of 10–65 kJ mol^{-1} [77], multiplicity of this interaction along with π–π stacking makes DNA double helixes stable against disintegration in water. The stability of DNA helixes is also increased by the ability of nucleobases to form secondary hydrogen bonds to one another [16, 34].

A typical form of hydrogen-bonded hydrogels found in Nature is those based on polysaccharides like cellulose [78–80], starch [26, 81], and agarose [82, 60]. In contrast to DNA, where hydrogen bonds link purine and pyrimidine bases, the bonds in polysaccharide-based physical networks connect hydroxy groups of the sugar units. In the case of cellulose, these interactions are so strong that without any prior modification, cellulose is not water soluble at room temperature. Thus, cellulose has been partly alkylated by etherification of the hydroxy groups to increase its solubility in water [83, 79]. The most abundant alkylated cellulose derivatives are methyl, ethyl, hydroxyethyl, and hydroxypropylmethyl cellulose. When solutions of these polymers are heated above certain temperatures, depending on the level of cellulose alkylation, hydrogels are obtained. The gelation mechanism involves hydrophobic interaction between the alkylated hydroxy groups: at low temperature, cellulose chains are hydrated, whereas at high temperature, water is repelled from the chains, and the alkylated hydroxy groups interact with one another to form a hydrogel. This sol–gel transition can also be achieved by addition of salts: the solvation of a salt is a competing reaction to polymer–water hydrogen bonding, thereby removing water from the hydrated polymer chains and entailing physical polymer crosslinking and hydrogel formation.

Alkylated derivatives of cellulose have applications throughout our daily lives, such as those as thickening agents in food industry, emulsion stabilizers in shampoos, and humectants in pharmacy [78, 3]. Inspired by these widespread applications, cellulose derivatives have also been tested for biomedical applications, but hydrogels based solely on hydrogen bonding turned out to degrade too fast for these areas of use. Therefore, blends of modified cellulose and polymers like synthetic polyvinyl alcohol [84, 85] or natural hyaluronic acid [86, 87] have been investigated.

Shoichet and coworkers used a blend of methylcellulose (MC) and hyaluronic acid (HA) to form hydrogels [87]. The aim of this effort was to design a hydrogel that can be injected into the spinal cord. To achieve this goal, five criteria must be met. First, the material has to gel suitably fast to prevent spreading of the hydrogel outside the target area. Second, injection of the hydrogel has to be minimally invasively. Third, the material should not be cell adhesive, thereby preventing formation of scar tissue due to decreased migration of fibroblasts into the gel [88]. Fourth, the hydrogel should be degradable to make further surgical interventions obsolete. Fifth, the material has to be biocompatible to avoid immune reactions.

To comply with these requirements, the authors prepared different blends and investigated them in vitro with a view to their gelation mechanisms, degradation profiles, and cell adhesion characteristics. In addition to these in vitro studies, the authors also investigated the injectability, biocompatibility, and therapeutic efficacy of these gels in vivo. The blends used were composed of 2 % hyaluronan and 7 % methylcellulose, whereby one of these polymers was modified with acetic hydrazide to investigate the effect of free carboxyl groups in the formation of the HAMC hydrogel. This composition of HAMC was found to gel rapidly and was therefore used for all further experiments. The two blends were compared to hydrogels composed of 7 and 9 % MC only.

The first experiments comprised gelation studies and characterization of the hydrogels by rheology. As a simple test, inverted-tube experiments were used to determine the gelation time. HAMC took 2 min to gel in this assessment, whereas the 9 % MC hydrogel took 10 min. The modified HAMC needed 20 min for gelation, such as the hydrogel with 7 % MC. As this type of gelation is affected by temperature, solutions of MC, HAMC, and modified HAMC were also investigated by rheology with a constant frequency at increasing temperature, showing that HAMC does gel at 18 °C, whereas the other samples gel between 27 and 32 °C, as shown in Fig. 2a. In addition to these gelation studies, the authors probed the resulting hydrogels in view of their thioxotropic response. This was done because the HAMC hydrogel should later be applied to the host via syringe; thus, the viscosity was measured as a function of increasing and decreasing shear stress, producing a thioxotropic loop of the materials. Whereas the viscosities of the MC hydrogels

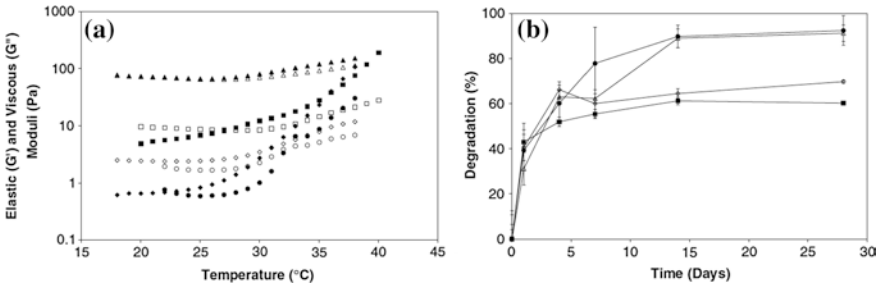

Fig. 2 Mechanical characterization of hydrogels based on hyaluonic acid and methyl cellulose. To investigate the mechanical characteristics of these hydrogels as a function of increasing temperature from room temperature to body temperature (37 °C), Shoichet and coworkers probed the gels using a rheometer with a cone-plate geometry at 1 Hz. The degradation of the gels was investigated in artificial cerebral spine fluid (*aCSF*) medium at 37 °C by the weight loss. **a** Temperature-dependence of the elastic (G') and the viscous (G'') part of the complex shear modulus of 7 % MC (*circles*), 9 % MC (*squares*), HAMC (*triangles*), and acet-HAMC (*diamonds*) (*filled symbols* represent G', *open symbols* represent G''). **b** In vitro degradation of 7 % MC (*filled circles*), 9 % MC (*filled squares*), HAMC (*open triangles*), and acet-HAMC (*open diamonds*) in aSCF medium determined by dry mass over time. Reprinted from Shoichet et al. [87]. Copyright 2006 Elsevier

Table 1 Quantative histological data of artificial cerebral spine fluid (aCSF) and hydrogels based on hyaluronic acid and methyl cellulose (HAMC) injected into rats

	aCSF	HAMC
Cavity volume (mm^3)	52.1 ± 20.1	36.6 ± 6.0
Lesion area at epicenter (%)	75.4 ± 8.6	71.5 ± 8.7
Number of aptotic cells	38.8 ± 10.56	38.9 ± 7.99
Inflammatory cells (μm^2)	$(3.79 \pm 1.39) \times 10^5$	$(2.42 \pm 0.35) \times 10^5$

Adopted from Shoichet et al. [87]. Copyright 2006 Elsevier

ranged over seven decades, the viscosities of the HAMC hydrogels spanned over four decades only, representing faster recovery from the applied stress.

In addition to mechanical studies, in vitro tests were conducted on the same samples to observe cell adhesion and degradation of the material. To qualitatively assess cell adhesion on HAMC, fibroplasts were cultured on macrogel specimen. Shoichet and coworkers observed formation of cell clusters with little spread on the surface of the gel; this finding indicates that the cells prefer to adhere to themselves rather than to the material. To conclude the in vitro experiments, the degradation was investigated in artificial cerebral spine fluid (aCSF) at 37 °C, showing that after 14 days of incubation, HAMC and 7 % MC were almost completely degraded (~90 %), whereas acet-HAMC and 9 % MC were eroded to ~65 %, as illustrated in Fig. 2b. These observations suggest that the hydrophobic interactions of the acetyl groups of the modified HAMC and the methyl groups of MC delay the erosion of the hydrogels.

The biocompatibility of the HAMC hydrogel was investigated by injection in both injured and uninjured rats. As a control experiment, Shoichet and coworkers also injected aCSF. 28 days later, these experiments revealed that the HAMC-treated rats showed no signs of scar formation, arachnoiditis, or syringomelia. Also, no cord compression or increased severity of the injury was observed. The injection site at the dura was sealed better and thicker than that in the control group with no accumulation of HAMC residue. Furthermore, Shoichet and colleagues investigated rats towards immune reactions that could have been caused by the hydrogels; HAMC-treated rats showed significantly fewer inflammatory cells than the control group, as compiled in Table 1.

In conclusion, Shoichet and coworkers designed a fast-gelling hydrogel that can be applied via syringe in a minimally invasive fashion. The hydrogel is biocompatible, not cell adhesive, and has the ability to support healing after lesion of the dura. In more recent publications, Shoichet and collaborators investigated this hydrogel as a scaffold for cell transplantation [89] and drug delivery [90], thereby pushing the applicability of this system towards use in treatment of injuries in the spinal cord.

Despite their numerous advantages, the mechanical strength of HAMC hydrogels is too low for applications like tissue engineering. To overcome this shortcoming, Zhang and coworkers prepared tough physical hydrogels based on a

blend of poly(vinyl alcohol) (PVA) with cellulose and compared them to chemically crosslinked gels of the same composition [91]. The physical gels were prepared by repeat freeze–thaw cycles, whereas the chemical gels were prepared by addition of epichlorohydrin to crosslink their hydroxy groups. The hydrogels were characterized with a view to their morphology, structure, and properties. With the help of differential scanning calorimetry (DSC), Zhang and colleagues could show that the melting point and the heat of melting of the physical gels both increase with their PVA content, as shown in Fig. 3a; this result indicates enhancement of the thermal stability of the gels. The covalent hydrogels exhibit an amorphous character, which is attributable to breakdown of the crystalline structure of PVA due to chemical crosslinking; this can also be seen by the degree of crystallinity in these gels, which is 10 % lower than in the physical hydrogels. To get more insight into the structure of these hydrogels, wide angle X-ray diffraction was measured. These experiments reveal that the physical hydrogels partly crystallize in the crystal plane of cellulose II, whereas the chemical hydrogels do not exhibit any diffraction pattern, as shown in Fig. 3b. These two results suggest that the structure of the physical hydrogels exhibits a dense packing with crystalline domains of cellulose, whereas the chemical gels exhibit an amorphous structure with no residual structural characteristics of the precursor polymers.

Scanning electron micrographs show regular pore structures in the physical hydrogels. The pore size and density can be tuned by the number of freeze–thaw

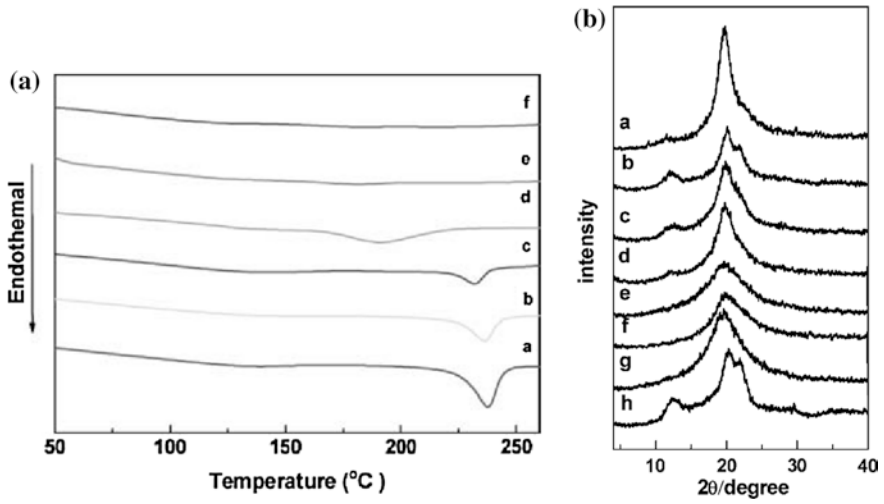

Fig. 3 Investigation of the melting and structure of gels based on PVA and cellulose by **a** differential scanning calorimetry (*DSC*) and **b** wide angle X-ray scattering (*WAXD*). **a** DSC thermograms of physical (*a–c*) and chemical (*d–f*) hydrogels. The PVA content decreases from *a* to *c* and from *d* to *f*, respectively. **b** WAXD patterns of cellulose–PVA hydrogels: (*a*) PVA; (*b–d*) physical hydrogels; (*e–g*) chemical hydrogels; (*h*) cellulose. The PVA content increases from *b* to *d* and from *e* to *g*, respectively. Reprinted from Zhang et al. [91]. Copyright 2008 Wiley VCH

cycles during the gel preparation, leading to smaller and denser pores at higher numbers of cycles. By contrast, the chemical hydrogels are less regularly structured, leading to a more porous structure; the average pore size is proportional to the PVA content of the gels. Zhang and coworkers argue that the PVA content controls the amount of water absorbed by the hydrogel and therefore expands the pores.

To investigate the mechanical properties of the hydrogels, they were probed by frequency sweeps in shear rheology. The physically crosslinked gels exhibit plateau moduli of 2–3 kPa, as shown in Fig. 4a, indicating that the polymer chains develop strong intra- and intermolecular hydrogen bonds if they are subjected to repeat freeze–thaw cycles; this also indicates reduction of the free volume between the chains, resulting in denser hydrogels. The chemical hydrogels exhibit elastic plateau moduli that are a decade less than that of the physical crosslinked gels, indicating high amounts of water within the chemical gels. This hypothesis is supported by swelling experiments: the porous structure of the chemical gels allows for maximum degrees of mass-swelling in the range from 3,000 to 7,000 %, depending on the content of PVA incorporated, as illustrated in Fig. 4b. By contrast, the physically crosslinked hydrogels exhibit maximum mass-swelling degrees of only 1,000 %, independent of their composition, as also illustrated in Fig. 4b; this finding can be explained by the dense structure of these gels that impairs penetration of water.

In conclusion, Zhang and coworkers demonstrated the preparation of hydrogels with strong interactions between cellulose and PVA chains, resulting in high storage moduli and strength. These materials show interesting properties to be used

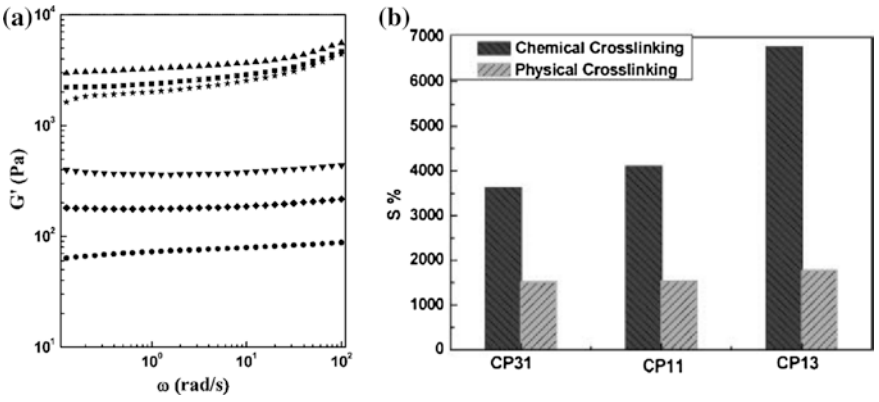

Fig. 4 Characterization of physical and chemical hydrogels based on PVA and cellulose by **a** shear rheology and **b** their maximum swelling degrees. **a** Frequency dependence of the storage modulus, $G'(\omega)$, of chemically (*circles*, *diamonds*, *nabla*) and physically (*square*, *triangle*, *star*) crosslinked hydrogels. **b** Comparison of the equilibrium swelling degrees, S %, of the same physical and chemical hydrogels. The swelling percentage of CP31 (ratio of cellulose to PVA of 3:1), CP11 (ratio of cellulose to PVA of 1:1), and CP13 (ratio of cellulose to PVA of 1:3) were determined by weighting the swollen gel and comparison to the dried gel. Reprinted from Zhang et al. [91]. Copyright 2008 Wiley VCH

in material sciences, since the swelling degree is too low for application in the medicinal sector.

The examples from the groups of Shoichet [87] and Zhang [91] are based on the use of biopolymer blends. Whereas natural hydrogels based on biopolymers that are crosslinked by hydrogen bonding are well known, successful *synthetic* approaches to prepare such hydrogels are rare. To overcome this limitation, Meijer and coworkers reported about tunable hydrogels based on poly(ethylene glycol) (PEG) chains that are end-group functionalized with ureidopyrimidinone (UPy) [92]. UPy is a self-complementary AADD–DDAA quadruple hydrogen-bonding motif (A = hydrogen-bond acceptor, D = hydrogen-bond donor). Meijer and coworkers were able to form hydrogels from these materials by dissolving dried polymers in an isotonic water solution at 70 °C and cooling it down to room temperature. In dilute solution, the polymers aggregate to form isolated nanofibers, as shown in Fig. 5a. With increasing concentration, these nanofibers form a transient network, as also shown in Fig. 5a. This process is tunable by the length of alkyl spacers between the UPy motif and the PEG chain. When the chain length of PEG is increased and the overall number of

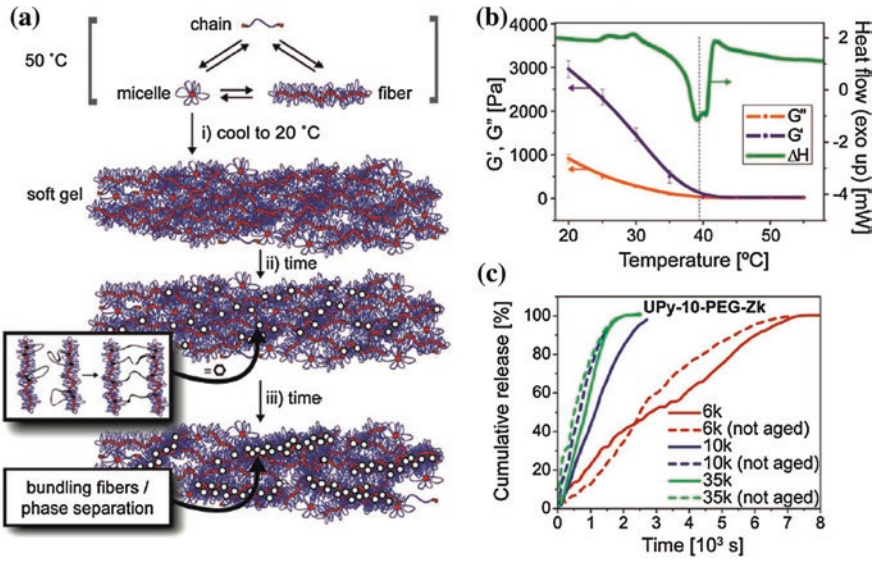

Fig. 5 Formation and characterization of hydrogels based on poly(ethylene glycol) (*PEG*) chains that are end-group functionalized with ureidopyrimidinone (*UPy*). **a** The process of hydrogel formation of Upy-modified PEG by hierarchical assembly of different structural units at 50 °C, comprising single chains, micelles, and fibers. (*i*) Upon cooling or increase of concentration, a soft hydrogel forms. (*ii*) Formation of supramolecular crosslinks after 16–24 h. (*iii*) Bundling of fibers, leading to phase-separating domains. **b** Rheological measurement (*left axis*) and DSC (*right axis*) showing the thermal collapse of a UPy-$PEG_{10\text{-}kDa}$ hydrogel (G': storage modulus, G'': loss modulus, ΔH: enthalpy). **c** Rhodamine B release from fresh and aged hydrogels depending on the chain length of the polymer used to form the hydrogels (*red* PEG 6 kDa, *blue* PEG 10 kDa, *green* PEG 35 kDa). Reproduced from Meijer et al. [92]. Copyright 2012 Wiley VCH

functional groups is decreased, the system shows an intriguing property: in rheology, these systems display a sol–gel transition at 40 °C, which can also be observed by micro-DSC, as compiled in Fig. 5b. When cooling the solution back to room temperature, the reformed hydrogel exhibits weaker mechanical strength than before heating, or the system does no longer form a hydrogel at all. After 24 h of relaxation, however, the original properties are restored. Meijer and colleagues argue that this property is similar to self-healing based on the reorganization of hydrogen bonds, but it takes the system long times to regain its initial mechanical properties. In addition to rheology, the authors investigated solutions of these polymers by static and dynamic light scattering at 20 °C to measure diffusion coefficients. Three different coefficients were observed, indicating three different structures present in the hydrogels: micelles, fibers, and single chains, which are resolved only when the samples are heated to 50 °C.

To investigate the erosion of the hydrogels, macrogel samples containing rhodamine B were probed in a flow chamber under a confocal microscope. This experiment shows that hydrogels formed from short PEG chains (6 kDa) release rhodamine B six times slower than hydrogels formed from long chains (35 kDa), as illustrated in Fig. 5c. When using 24-h aged hydrogels, the release is also

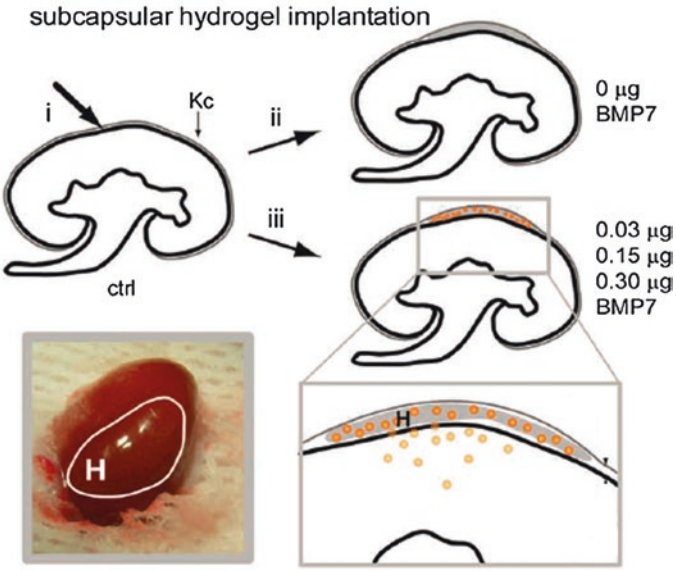

Fig. 6 Schematic of the implantation of a PEG–UPy hydrogel into kidneys of rats and localization of the gel in the kidney capsule with subsequent release of anti-fibrotic growth factor protein BMP7. (*i*) Introduction of a small pocket after loosening of the kidney capsule (*Kc*). (*ii*) Implantation of a hydrogel without any biorelevant additives in the Kc. (*iii*) Implantation of a bioactive hydrogel. The schematic representation illustrates the release of BMP7 (*orange dots*) in the kidney. The *left* picture shows an actual kidney indicating where the hydrogel (*H*) is located. Modified from Meijer et al. [92]. Copyright 2012 Wiley VCH

slower compared to a freshly prepared hydrogel, as also shown in Fig. 5c. To conclude these in vitro experiments, cyano-fluorescent proteins were encapsulated in the same hydrogels. The release of these proteins shows that hydrogels based on long PEG chains (20 kDa) have a slower release than gels based on short chains (10 kDa). The variation of the alkyl-spacer length also influences the release of the proteins; the longer the spacer, the slower the delivery. With these results in hand, Meijer and coworkers conducted in vivo studies on rats. These studies were performed with a gel loaded with a bone morphogenetic protein (BMP7) that was injected underneath the kidney capsule of rats, as shown in Fig. 6. Seven days after implantation, the hydrogels were completely eroded and the kidneys were examined by histology. The amount of myofibroplasts was estimated, showing no signs of any immune reaction towards the hydrogel.

With this latter work, Meijer and coworkers introduced the first synthetic polymeric hydrogel based on supramolecular crosslinking of UPy-modified PEG. These materials are biodegradable, non-immunogenic, and tunable. In a follow-up publication, Meijer and coworkers investigated the rheological properties in greater detail and exploited this system further, primarily in view of application for protein delivery into kidneys [93].

3 Hydrogels Crosslinked by Metal Complexation

A hydrogel based on metal-complexation crosslinking is formed when ion complexes interconnect polymer chains that are functionalized with suitable ligand-moieties. Depending on the metals and ligands used, the resulting coordinative bonds can exhibit binding energies of up to 400 kJ mol^{-1} [77]; as a result, this interaction allows for the design of hydrogels that exhibit stabilities ranging from very labile to covalent-like [33]. Hydrogels formed by metal–ligand complexation most commonly base on ions such as Mn, Fe, Co, Ni, Cu, Zn, Ru, Ag, Cd, Os, Ir, and Pt in their low oxidation states (+2 or +3). In a seminal series of work, Schubert and co-workers investigated the characteristics of different metal ions using terpyridine-modified polymers as the ligands, showing that Fe-crosslinked gels are thermally less stable than Ru-crosslinked gels [94]. In addition to terpyridine, other ligands such as benzimidazolpyridines [95, 96], bipyridines [97, 98], or catechols [99, 100], have been applied to prepare gels. The use of toxic transition metal ions like Ag, Cu, or Cd limits the use of these gels to applications in materials science. For more demanding biomedical applications, biologically inert metal ions or ions that are already present in the human body, including Mg, Ca, Fe, Zn, Pt, and Au, must be used [45, 101].

The most prominent example of a biopolymer hydrogel based on crosslinking by metal complexation is alginate. It is a polysaccharide composed of mannuronic and guluronic acid in three different fashions: blocks of guluronic acid, blocks of mannuronic acid, and alternating blocks of both. A hydrogel is formed when multivalent ions are added to a solution of algic acid in water, interacting with its

carboxy groups. The stiffness and degradability of the resulting hydrogel depends on the ratio of guluronic to mannuronic acid and on the amount of metal ions used [102]. Materials based on alginate are employed for diverse applications such as emulsifiers and gelling agents in food industry [103, 104], shear-thinning agents in the textile and paper industries [105], and in pharmaceutical industry for wound treatment [106] and dental impression [107]. Recent research has focused on the ability of alginate hydrogels to accelerate regeneration of mineralized tissues [108], in addition to recent applications as vessels for drug delivery [109] and as extracellular matrixes [110].

For the preparation of alginate-based hydrogels, calcium ions find predominant use as the crosslinking agent, whereas the preceding homologue, magnesium, is considered to be a non-gelling ion for alginate [111]. Groll and coworkers investigated the possibility to form alginate hydrogels with magnesium ions, supplementing a new alginate-based biomaterial [112]. For this purpose, different types of alginate were used, differing in the ratio of guluronic and mannuronic acid, in their respective block lengths, and in the composition of the blocks (plain guluronic, plain mannuronic, or alternating); the magnesium concentration was also varied, leading to a toolbox ranging from 0.5 to 8 wt% alginate concentration and ion concentrations of 10–400 mmol L^{-1}. Investigation of alginate solutions that are supplemented with magnesium ions in shear rheology for 24 h at a constant frequency of 1 Hz showed that hydrogels form on timescales longer than 10 min when an alginate batch that has an even distribution of mannuronic and guluronic acid is used. The next step was to investigate the impact of different ion concentrations at a constant alginate concentration of 5 wt%. At ion concentrations below 50 mmol L^{-1}, no gels form, whereas at concentrations above 50 mmol L^{-1}, hydrogel formation occurs on timescales from 800 min at 50 mmol L^{-1} down to only 2 min at 400 mmol L^{-1}, as shown in Fig. 7. A simplistic expectation is that the elastic moduli of the hydrogels increase with increasing concentration of magnesium ions, but this is not observed: at magnesium ion concentrations above 100 mmol L^{-1}, the elastic moduli of the gels slightly decrease and reach a maximum between 1,300 and 1,800 Pa, as also illustrated in Fig. 7. Groll and coworkers argue that at this threshold, a maximum concentration is reached. In this state, the helical structure of the polymer chains is disturbed, favoring formation of larger aggregates, which causes inhomogenous network formation; this effect has also been observed before in other metal-complexing systems [113, 114].

In addition to the concentrations of alginate and ions, temperature plays a crucial role for the formation of alginate-based hydrogels. To investigate this effect, the gelation was monitored at 15, 25, and 40 °C, showing that hydrogels prepared at lower temperatures have higher elastic moduli than hydrogels prepared at higher temperatures. Groll and colleagues argue that the formation of gels commences slowly at low temperature due to hindered diffusion of metal ions into the hydrogel, which leads to a more ordered microstructure with a higher degree of elastically effective crosslinks.

To conduct the preceding investigations, Groll and coworkers purchased three different types of alginates. The experiments were carried out with an alginate

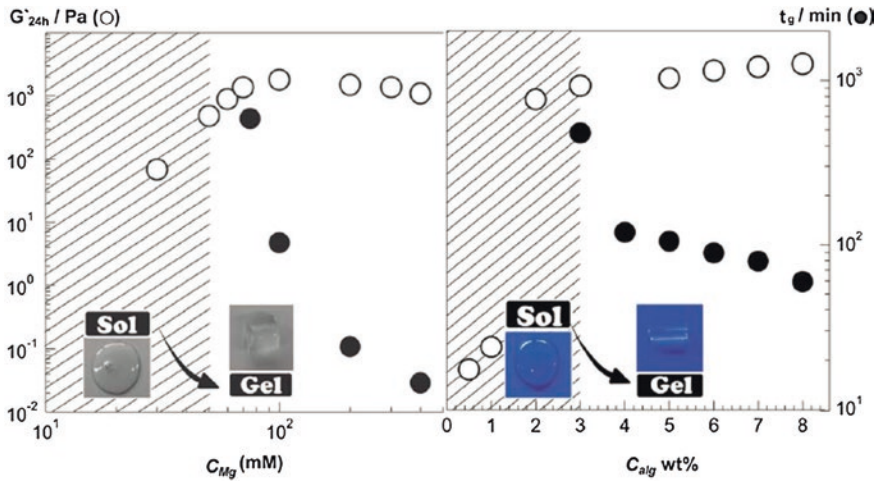

Fig. 7 Investigation of the elastic shear modulus, G', during formation of alginate–magnesium hydrogels along with the gelation time, t_g, depending on the concentration of precursor solutions of alginate, c_{alg}, and crosslinking magnesium ions, c_{Mg}. *Open circles* represent the elastic shear modulus after 24 h, whereas filled circles represent the gelation time as a function of the amount of Mg^{2+} added to 5 wt% alginate (*left*) and the amount of alginate supplemented by 100 mmol L^{-1} of Mg^{2+} (*right*). The *marked areas* show concentrations where no gel formation is observed. Reprinted from Groll et al. [112]. Copyright 2012 RSC Publishing Group

batch that had a close-to equal ratio of guluronic to mannuronic acid. To investigate the impact of the different acids, the experiments were repeated using alginate batches composed of either more guluronic or more mannuronic acid. This assessment shows that gluronic acid has a higher affinity towards magnesium ions than mannuronic acid, because hydrogels could be formed at lower concentrations of ions and alginate than with batches of alginate containing higher contents of mannuronic acid, which did not form gels at all.

For biomedical applications, hydrogels should be biodegradable. Therefore, hydrogels of the latter kind were stored within water, and the time of hydrogel erosion was measured. In these tests, hydrogels crosslinked by magnesium ions display full dissolution on a timescale of 2.5–5 h, depending on the concentration of alginate. Increasing the concentration of magnesium ions does not increase the stability of the hydrogels towards dissolution in water, but it increases their short-term elastic modulus. Groll and coworkers argue that the weak interaction of magnesium ions with the alginate chains and the slow exchange of these ions lead to an increased osmotic pressure; this causes gel swelling and finally rupture of the hydrogel. To overcome the fast degradation of the gel, hydrogels were treated with a calcium-ion solution, leading to additional crosslinking on the surface of the hydrogel; after 24 h in aqueous medium, the hydrogels treated with calcium did not dissolve. SEM micrographs of a magnesium-crosslinked hydrogel show a

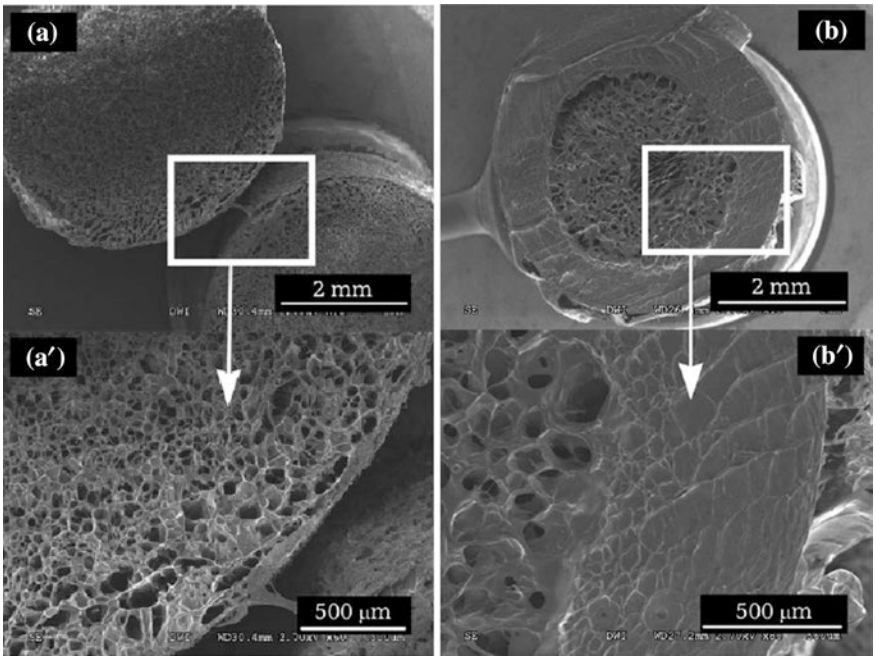

Fig. 8 Investigation of the structure of Mg–alginate hydrogels by Cryo SEM. The micrographs display Mg–alginate gels without (**a**, **a′**) and with (**b**, **b′**) Ca–alginate outer layer. Reprinted from Groll et al. [112]. Copyright 2012 RSC Publishing Group

porous structure, whereas the calcium-treated hydrogels have a porous structure in the core only, along with a much smoother surface, as shown in Fig. 8. This is because the calcium ions induce collapse of the pores at the surface of the hydrogel, resulting in a denser structure that prevents diffusive escape of the crosslinking ions from the core of the gel.

In conclusion, Groll and colleagues showed that alginate hydrogels can be formed by complexation with magnesium ions. Tuning the composition of the hydrogels changes their elastic modulus and stability towards dissolution in water, making this material a promising candidate for applications in the biomedical sector.

A common method in the design of synthetic hydrogels is to mimick Nature. There are many approaches to follow this idea, such as mimicking favorable properties like bone structure for lightweight but stable materials or utilization of unfavored effects like the adherence of mussels on almost any surface. This adherence has been widely investigated and it has been shown that mussels possess byssal threads that allow them to physically attach to surfaces [115–118]. The surfaces of these threads carry catechol units that can complex to Fe^{3+} ions. The strength of this complexation depends on the surrounding pH. Whereas pH values ≤ 5 entail formation of weak monocatechol complexes, pH $\geq$ 8 promotes formation of bis- and tris-complexes with a much higher equilibrium constant [119], as shown in

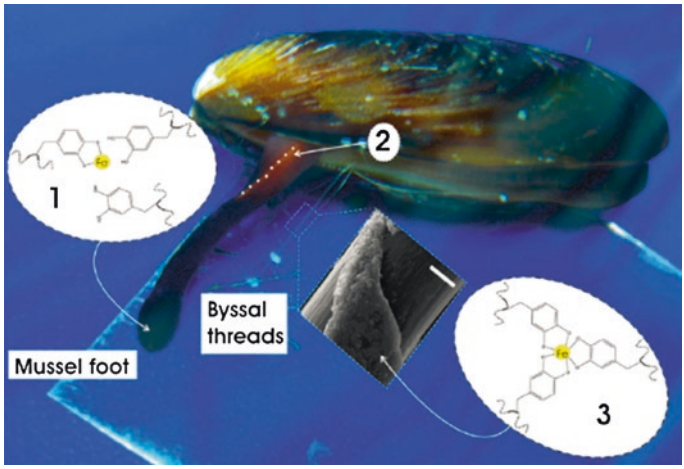

Fig. 9 Schematic of the adherence of mussels on surfaces by formation of catchol complexes. (*1*) Production and storage of byssal thread cells at pH 5 through monocatechol complexes. (*2*) Release of the threads from the ventral grove (indicated by the *white dashed line*). (*3*) Formation of bis- and triscatechol complexes in the byssal threads after exposure to seawater (pH 8). Reprinted from Waite et al. [121]. Copyright 2011 National Academy of Sciences of the United States

Fig. 9. Upon adherence to a surface, mussels excrete preassembled thread cells at a pH of 5–6; upon contact with seawater (pH $\approx$ 8), the stability constant of the complexes increases from the mono to the bis- and tris-complex. As a result, hydrogels interconnected by these tris-complexes exhibit high extensibilities, hardness, and most importantly self-healing [120].

Based on this model, Waite and coworkers reported a hydrogel complexed by dihydroxy-phenyalanin (dopa) modified PEG and Fe^{3+} ions [121]. Dopa is a metal-complexing ligand, exhibiting a modestly lower force needed to rupture the metal-dopa bond than a covalent bond, but it possesses the ability of self-healing [117]. This feature renders this motif attractive for use in supramolecular hydrogels. To pursue this goal, Waite and coworkers modified 4-arm PEG with four dopa functionalities. Upon mixing with iron ions (dopa:Fe = 3:1) at pH = 5, a green-blue fluid evolved that formed a sticky purple gel after increase of the pH to 8. At pH = 12, a red elastomeric gel was formed. UV–vis absorbance and Raman spectroscopies could show that upon increase of pH, higher-ordered complexes are formed. When comparing spectra taken of the native mussel cuticle to that of the triscatechol complex, both complexes show the same bands with almost same intensities. Probing the systems by dynamic oscillatory shear rheology showed that the elasticity of the systems decreases with increasing pH; the elastic modulus ranged from 30 Pa at pH 5 to 1,000 Pa at pH 12, as compiled in Fig. 10a. For comparison, a covalently crosslinked hydrogel was prepared by addition of sodium periodate to the modified 4-arm PEG, forming a covalent C–C bond between two catechol moieties. Probing the physical and the chemical hydrogels by shear rheology shows almost the same

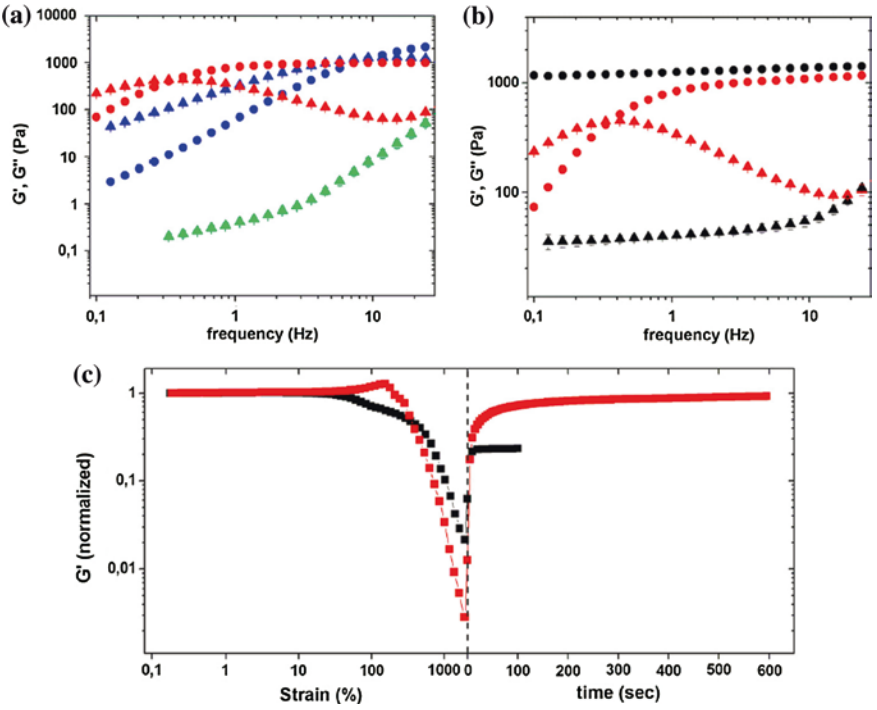

Fig. 10 Mechanical properties of polymeric hydrogels based on catechol-functiomalized PEG at different pH and comparison of a chemical and a physical hydrogel, assessed by their elastic (G') and viscous (G'') shear moduli. **a** Frequency-dependent loss (G'') and storage (G') moduli of gels at pH 5 (*green*), pH 8 (*blue*), and pH 12 (*red*) (G': *circles*; G'': *triangles*). **b** Comparison of physically (*red*) and chemically (*black*) crosslinked hydrogels. **c** Recovery of stiffness and cohesiveness after tearing by shear stress (same *color* code as in **b**). Modified from Waite et al. [121]. Copyright 2011 National Academy of Sciences of the United States

elastic modulus at high frequencies, as shown in Fig. 10b. After applying high strain to the gels, the physical hydrogel regained its elastic modulus within minutes, whereas the chemical hydrogel was damaged irreversibly, as illustrated in Fig. 10c; this observation indicates the ability of the catechol-based hydrogels to self-heal.

To investigate the degradability of the hydrogel, an EDTA solution (pH 4.7) was added, fully dissolving the gel after 1 h of exposure. Apart from the degradability of the hydrogel, it could be shown that Fe^{3+} ions do not oxidize the catechol functionalities, which would lead to covalent crosslinking.

With this work, Waite and coworkers were able to form a hydrogel mimicking the effect that byssal threads of mussels use to adhere on surfaces. The system is based on modified PEG, allowing possible applications in the fields of engineering and biomedicine.

4 Hydrogels Crosslinked by Ionic Interactions

Ionic interactions between polymer chains provide an alternative to covalent crosslinking due to their high binding constants and the unique swelling properties of the resulting hydrogels [122, 38]. Gels can be obtained through these interactions by combining cationic and anionic polymers, with the ability to be fully degraded by change of pH [123, 124] or salt concentration in the medium [125]. A well-investigated example is chitosan, a polycationic copolymer composed of 2-acetamido-2-deoxy-D-glucopyranose and 2-amino-2-deoxy-D-glucopyranose. It can be obtained by alkaline deacetylation of chitin, one of the most abundant biopolymers and main component of the exoskeleton of crustaceans and insects. Chitosan arose interest due to its biocompatability, biodegradability, and high natural abundance in form of chitin [126, 61]. Hydrogels based on chitosan have been investigated for topical ocular applications [127], wound healing [128], implantation [129], and injection [130].

An example of an anionic polyelectrolyte is xanthan. It is composed of a cellulose backbone that has a negatively charged trisaccharide side chain on every other glucose unit; this side chain is composed of α-mannose, α-glucoronic acid, and β-mannose with a pyruvic acid diketal moiety located on the terminus of the side chain [131]. Expressed by *Xanthomonas campestris*, a bacterium found on cabbage plants, xanthan is the first biopolymer produced on an industrial scale, serving for applications as food additive [132], in oil recovery [133], and in cosmetics [134].

In the mid 1990s, Dumitriu and coworkers reported a polyionic hydrogel based on chitosan and xanthan [135]. Since then, numerous publications and patents were released, pushing the applicability of this system from immobilization of enzymes to dermocosmetics [136–140]. However, little was known about how the composition of the precursor polymers influences the properties of these hydrogels. To close this gap, Dumitriu and coworkers investigated the swelling properties, microstructure, and mechanical traits of chitosan–xanthan hydrogels [141]. Mixing aqueous solutions of anionic xanthan and cationic chitosan forms hydrogels in a multistep process: after mixing, a common solution-pH value is established, causing structural changes of the polymer chains. The next step is formation of ionic interactions of the ammonium moities of chitosan with the carboxylate functions of xanthan. These two steps lead to phase separation, often referred to as coacervation [142]. In one phase, often called the coacervate phase, the polymers are concentrated, whereas the other phase is a dilute phase. In the coacervate phase, water molecules orient towards the polymer chains, leading to formation of hydrogen bonds. In the dilute phase, water molecules are not orientated. A hydrogel is formed when all water molecules have formed hydrogen bonds between the polymer chains, provided that the polymer chains are distributed properly, as compiled in Fig. 11. Dumitriu and coworkers investigated the effect of coacervation on the properties of these hydrogels by quantification of their viscolelastic properties and swelling degrees.

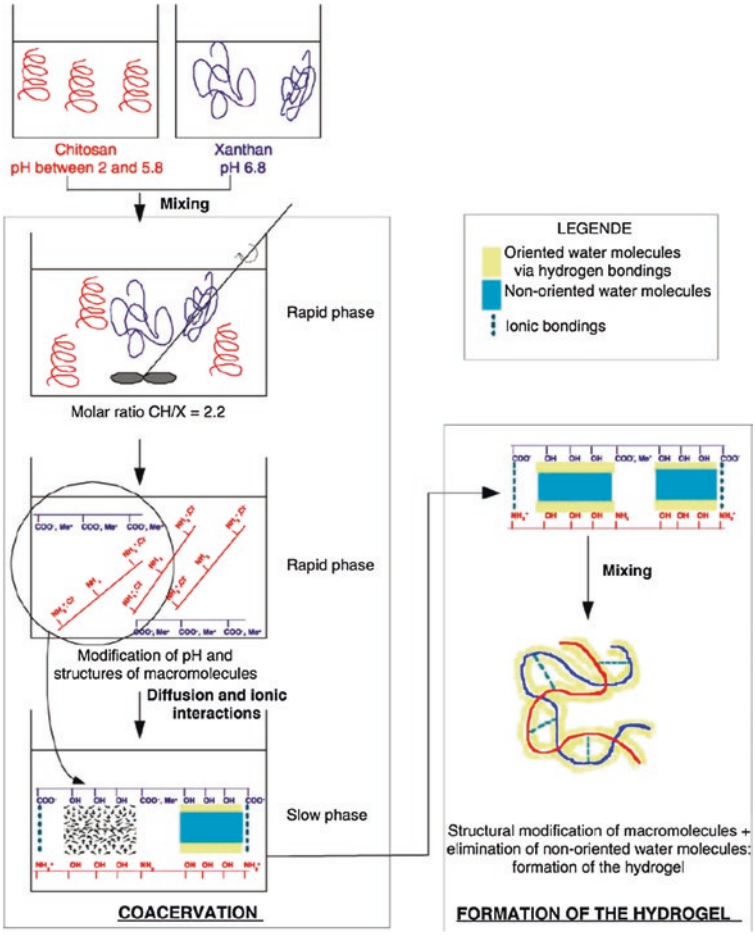

Fig. 11 Schematic representation of the formation of xanthan and chitosan polyelectrolyte hydrogels through mutual ionic interaction. When chitosan and xanthan are mixed, a common pH is established, and the polymer chains associate to each other. These first two steps are rapid processes, followed by slow phase separation that is referred to as coacervation. In the coacervation step, water molecules orient in between the polymer chains and form hydrogen bonds. When all surrounding water molecules are oriented in this fashion, a polyelectrolyte hydrogel is obtained. Reprinted from Dumitriu et al. [141]. Copyright 2004 Elsevier

At first, Dumitriu and collaborators investigated the swelling of hydrogels composed of a high and a low molecular-weight chitosan with different coacervation times before the preparation of the gels, spanning from no time of coacervation over 4–24 h. The lower molecular-weight sample with no coacervation time showed a high mass-swelling degree of 4,000 %, indicating weak association between the polymer chains. After 4 h of coacervation, the mass-swelling degree was smaller, 1,250 %, whereas the mass-swelling degree of the sample with high

molecular-weight chitosan decreased from 3,000 to 2,500 %; this trend progressed with the gels prepared after 24 h of coacervation time, with mass-swelling degrees of 250 % in case of the low molecular-weight chitosan and 1,000 % in case of the high molecular-weight chitosan, as compiled in Fig. 12a. Dumitriu and coworkers explained this observation by assuming slower diffusion of the longer polymer chains, resulting in a less ordered hydrogel compared to the material composed of shorter polymer chains. As a consequence, water molecules can penetrate the less ordered network easier, causing these gels to exhibit higher swelling degrees.

In addition to the internal structure of the gels, the swelling degree of ionic hydrogels depends on the pH of the swelling medium. To investigate this interplay, Dumtriu and collaborators probed a gel composed of high molecular-weight chitosan in view of its swelling characteristics as a function of pH. The swelling degree increases as a function of the pH from 3.5 to 5.8, explainable by gradual deprotonation of the ammonium moieties in the chitosan polymer, thereby screening the ionic interactions between xanthan and chitosan. Similarly, at pH $\leq$ 2, the degree of swelling is higher due to protonation of the carboxy moieties in the xanthan polymer, which also attenuates ionic interactions between xanthan and chitosan, as shown in Fig. 12b.

With the help of shear rheology, Dumitriu and coworkers investigated the formation of coacervates of a low and a high molecular-weight chitosan and xanthan. In the beginning, both systems showed a steep slope of the storage modulus as a function of time, indicating progressive formation of ionic interactions between the polymer chains that can still diffuse easily in the solution. This is followed by percolation to a gel state as a consequence of orientation of water molecules toward the polymer chains, resulting in a rigid network structure that entails hindered diffusion of the polymer chains; in this period, the slope of G' as a function of time decreases, but even after 24 h, the elastic part of the shear modulus, G', does not

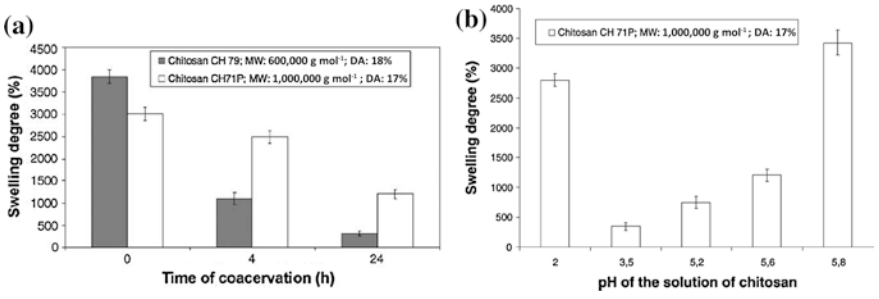

Fig. 12 Investigation of the swelling degree of polyelectrolyte hydrogels based on chitosan and xanthan depending on the composition, coacervation time, and pH. **a** Effect of the molecular weight and coacervation time of chitosan on the swelling charateristics of the resulting polyelectrolyte hydrogels. **b** Influence of pH on the swelling of the gel. Swelling degrees were determined by comparison of the mass of dried hydrogels with the mass of the swollen gels. DA represents the degree of acetylation of chitosan in mol%. CH79 (79 %) and CH71P (71 %) represent the degree of deacetylation of chitosan in mol%. Modified from Dumitriu et al. [141].

reach a plateau. This effect has been reported before for physical hydrogels based on biopolymers [143, 144]. The G' values of the high molecular-weight chitosan are lower during the whole experiment, with a final value of 950 Pa, compared to the low molecular-weight chitosan with a final value of 1,550 Pa, as shown in Fig. 13. Dumitriu and colleagues interpreted this observation by less efficient formation of elastically effective crosslinks in hydrogels prepared from high molecular-weight precursors than in hydrogels prepared from low molecular-weight precursors, without further explanation as to why this is.

To check for history-dependence of the gel mechanical properties, Dumitriu and coworkers compared rheology experiments on freshly prepared hydrogels (no coacervation time) to experiments on hydrogels prepared after 24 h of aging of the coacervates. Whereas the swelling degree of these hydrogels decreases during the aging process, the storage modulus increases; this observation can be explained by assuming formation of more homogenous networks during the ageing period, which increases the number of elastically effective crosslinks in the constituent polymer networks. This observation agrees with a postulate of Meijer and coworkers, who hypothesized that supramolecular polymer networks show self-repairing of network defects and thus evolve into more homogenous and mechanically stronger networks with time [145, 146].

To conclude the rheological probing of the coacervates and the hydrogels, Dumitriu and coworkers demonstrated their linear viscoelastic response to increasing strain. For this purpose, both freshly prepared and aged hydrogel samples, all based on low molecular-weight chitosan, were probed, and the data were fitted to a first-order approximation of the Kronig–Kramers equation as modified by Tschoegl [147]. Dumitriu and colleagues could show that the viscoelastic modulus increases with the time of preparation of the hydrogels, which is again addressable to formation of a denser network. The coacervate exhibits a viscoelastic modulus of 2 kPa, whereas the freshly prepared hydrogel displays a modulus of 9 kPa. The hydrogel prepared after 24 h of coacervation has a modulus of 12 kPa, as shown in Fig. 14. The values of G'' calculated with the Kronig–Kramers equation comply to the recorded G'', showing that the mechanical spectra lay in the linear viscoelastic domain.

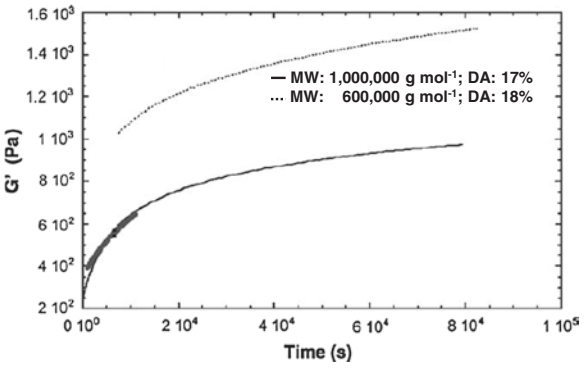

Fig. 13 Time-dependent evolution of the storage modulus of polyelectrolyte hydrogels formed from different molecular-weight chitosan precursors during coacervation. DA represents the degree of acetylation of chitosan in mol%. Modified from Dumitriu et al. [141]. Copyright 2004 Elsevier

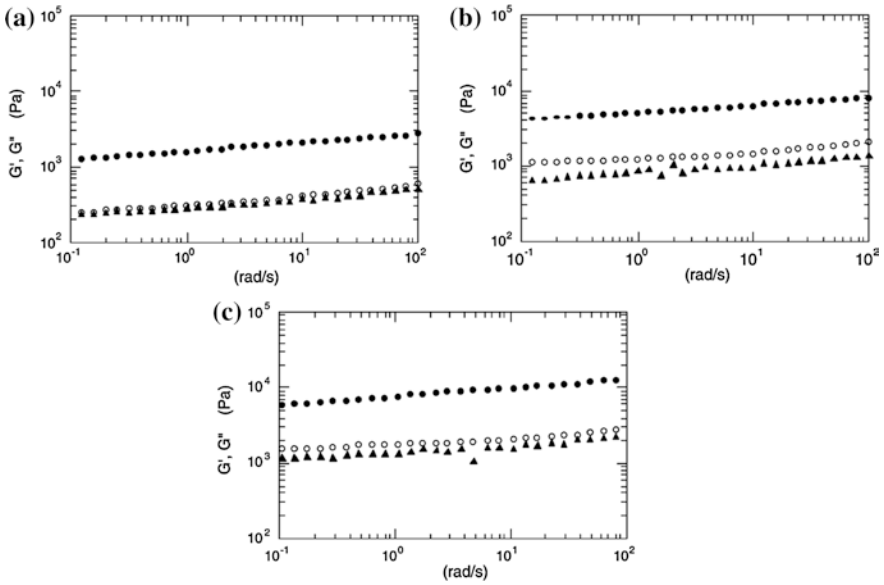

Fig. 14 Linear dependence of the storage (G') and loss (G'') shear moduli of low molecular-weight chitosan hydrogels as a function of strain (*filled circles G′*, *empty circles G′″*; *triangles* data calculated by the Kronig–Kramers equation). **a** Coacervate; **b** hydrogel prepared without coacervation; **c** hydrogel after 24 h of coacervation. Reprinted from Dumitriu et al. [141]. Copyright 2004 Elsevier

Dumitriu and coworkers finished their study with a structural analysis of the hydrogels by preparing hydrogel beads that were investigated by SEM. The beads exhibit fibrillar porous structures with pore sizes of 100–250 nm and fiber diameters of 1–10 μm. In previous publications, Dumitriu and Chornet observed the diffusion of immobilized enzymes out of similar chitosan–xanthan hydrogel beads [138]. This observation can be explained by the porous external and internal structure of the beads, as illustrated in Fig. 15a, b.

With this latter work, Dumitriu and coworkers investigated the formation, the physical–chemical properties, and the structural characteristics of chitosan–xanthan based polyelectrolyte hydrogels. They could show the dependence of the mechanical and swelling characteristics of the gels on to the length of the precursor polymer chains and the pH value during gel probing. Microstructural investigation of gel beads revealed a porous fibrillar structure, which makes this system interesting for biomedical applications such as those in drug delivery.

Implants based on hydrogels might someday replace the need for invasive surgery. A delicate example of invasive surgery is the epineural suture of nerves after traumatic lesions. The outcome of these surgeries are disillusioning: often, little or no functional recovery of the nerves can be obtained. In the worst case, transplanted nerve tissue that is needed to close gaps between the nerve stumps is rejected by the body and forms neuroma at the donor site [148]. To solve this

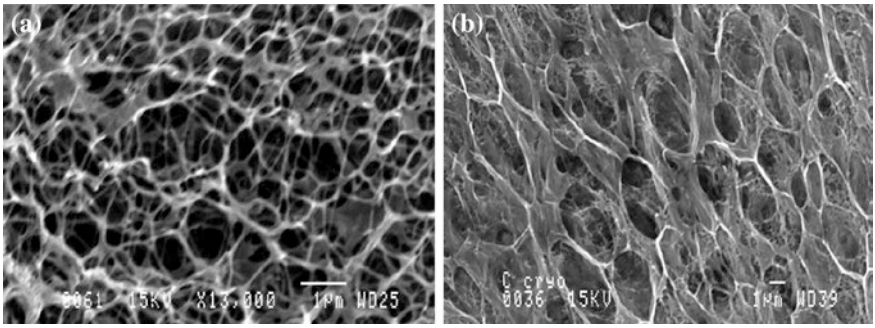

Fig. 15 Microstructures of hydrogels based on chitosan and xanthan. SEM micrographs of the porous inner (**a**) and outer (**b**) structure of hydrogel beads. Reprinted from Dumitriu et al. [141]. Copyright 2004 Elsevier

problem, tubular hydrogels can be envisioned to serve as nerve conduits, making future surgeries obsolete [149, 150]. To realize this concept, several criteria have to be met: the material has to be biocompatible and biodegradable after the regeneration is complete, its mechanical stability has to be constant during the entire regeneration process, it has to be flexible with a Young's modulus similar to that of the nerve tissue to avoid compression of the nerve, and the material has to be porous to allow for diffusive penetration of nutrients.

To pursue this goal, Gander and coworkers reported a hydrogel based on alginate and chitosan that possesses the required characteristics to act as a nerve conduit [151]. Tubular hydrogels were prepared using a spinning mandrel and investigated in view of their physical–chemical characteristics as well as their porosity, probed by diffusive penetration of dextran as a model substance for biologically relevant nutrients and growth factors. At first, the hydrogels were investigated with respect to their swelling in PBS buffer at pH 7.4; for this purpose, freeze-dried tubular gels were cut into 6-mm pieces that were immersed in the medium. After 20 min, the maximum swelling degree was reached: the outer diameter was swollen from 1.7 to 2.7 mm, whereas the inner diameter was still 1.3 mm, as shown in Fig. 16b. The water content of the tubes was determined gravimetrically to be 83 wt%. This high water content indicates a porous microstructure. SEM micrographs could confirm this indication in the dried state of the hydrogel, as illustrated in Fig. 16a. In addition to these experiments, the diffusivity of nutrients through the hydrogels was investigated with three differently sized fluorescein-labeled dextrans (4, 10, 20 kDa); for this purpose, the swollen tubes were filled with 5 g L^{-1} dextran solution, and the ends of the tubes were sealed. The amount of dextran that diffuses out of the conduit was determined fluorometrically, showing a dependence on the length of the dextran chains. The lowest molecular-weight dextran (4 kDa) showed the fastest diffusivity through the conduit wall: 35 % in 7 h. At higher size of the dextran probe, the diffusivity was slower: in case of 20-kDa dextran, only 2 % of the solution permeated out

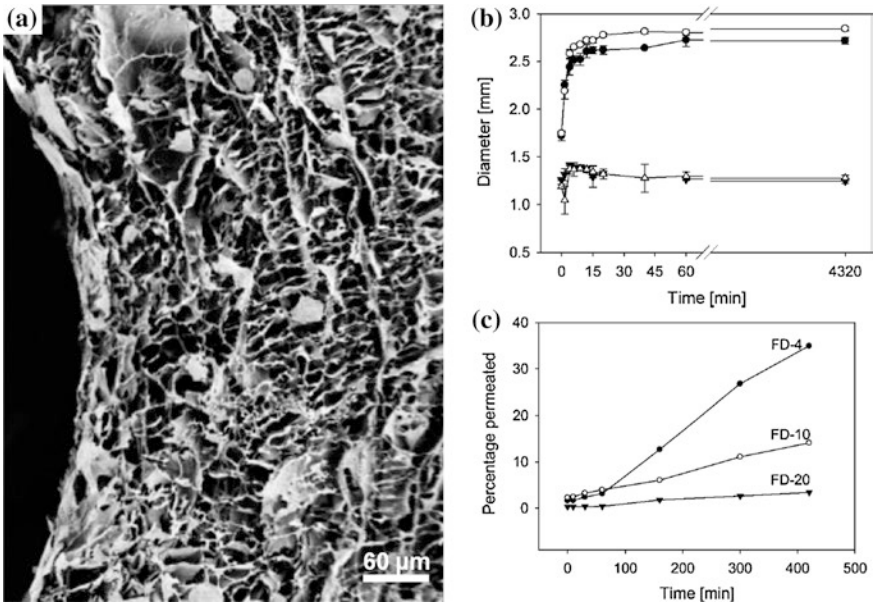

Fig. 16 Structural characteristics, swelling degrees, and diffusive permeability of nerve conduits composed of alginate and chitosan. **a** SEM micrograph of the porous structure of a freeze-dried nerve conduit. **b** Diameter of the nerve conduit of two different batches of hydrogel of the same composition (*circles* outer diameter; *triangles* inner diameter). **c** Permeation of fluorescein-labeled dextrans through the wall of a swollen alginate–chitosan hydrogel nerve conduit, as investigated by Gander and colleagues (*FD-4* 4.4-kDa dextran; *FD-10* 10-kDa dextran; *FD-20* 20-kDa dextran). Reprinted from Gander et al. [151]. Copyright 2006 Wiley VCH

of the conduit within 7 h, as shown in Fig. 16c. These experiments can serve as a model for the permeation of nutrients or growth factors through the conduit, which is dependent on their hydrodynamic radius. 20-kDa dextran exhibits a hydrodynamic radius of 3.3 nm [152], which is similar to the radius of proteins. This similarity indicates that the permeation of high molecular-weight proteins, cells, and immunoglobulins through the conduit wall is likely to be hindered, which could decrease the triggering of immune reactions during the regeneration. Growth factors and nutrients have a lower hydrodynamic radius and can permeate the wall of the nerve conduits easier, increasing the chance of regeneration of the tissue.

To supplement these assessments of diffusive permeability, rheological measurements were performed on hydrogel films under a normal force of 3, 10, and 30 N as a function of oscillatory shear strain. By inducing 3 and 10 N, no structural changes of the hydrogels could be observed. At 30 N, a high initial storage modulus was detected, which relaxed throughout the measurement, as shown in Fig. 17. The measurements were repeated on the same gel, showing that the initial storage modulus was lower than in the previous measurement. This observation indicates structural changes induced by the normal force. After relaxation times of

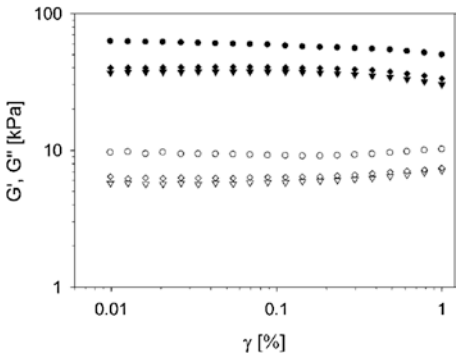

Fig. 17 Mechanical properties of alginate and chitosan hydrogel nerve conduits, assessed by the shear-strain dependencies of the storage (*G′ filled symbols*) and the loss moduli (*G″ open symbols*) as a function of the normal force during the measurement (*inverted filled triangle* 3N, *filled diamond* 10N, *filled circle* 30N). Reprinted from Gander et al. [151]. Copyright 2006 Wiley VCH

>7 h in buffer, the increased stiffness was reversed, showing the transient nature of the hydrogel. The Young's modulus of the hydrogels is 110 kPa, which is considerably lower than the modulus of whole nerves (500–70,000 kPa) [153, 154]. This should preclude possible mechanical irritation after implantation of the nerve conduits in the surrounding tissue as well as on the nerve.

In conclusion, Gander and coworkers showed the preparation and physicochemical characteristics of tubular hydrogels based on chitosan and alginate for applications as neural conduits. This system shows mechanical characteristics that are suitable for implantation without irritation of the nerve and the surrounding tissue. Furthermore, the walls of the conduit can most likely be penetrated by growth factors and nutrients, but they exclude cells, proteins, and immunoglubolins, which can trigger immune reactions that hinder regeneration of the neural tissue.

Another widely used biopolymer is starch, a polysaccharide composed of α-D-glucose units. Plants produce starch for energy storage; it is therefore one of the most abundant biopolymers on Earth. Starch arose interest in the biomedical sector due to its biocompatibility, degradability, and availability [155, 156]. However, unmodified starch is easily metabolized into saccharides under biological conditions, making chemical modifications necessary. A common way to functionalize starch is to chemically crosslink it with epichlorohydrin, along with further modification of the matrix by introduction of desired functionalities [157, 158]. To avoid toxic crosslinking conditions, physical hydrogels based on starch have been investigated.

Cukierman and coworkers presented a matrix for drug delivery based on polycationic starch (MS) and κ-carageenan (KC), an anionic polysaccharide based on sulfated α-D-galactopyranose units [159]. Investigation of the binding of the polymer chains of a granular mixture of freeze-dried KC and MS and a hydrogel prepared by solutions of both by FT-IR showed slight shifts of the C–N and of the sulfate bands, indicating formation of polyelectrolyte complexes in the hydrogel.

Turbidity measurements of solutions of MS and KC exhibit a maximum at a composition of 1:1, suggesting that at this point equivalent quantities of both polymers interacted with each other. The measurement could also prove that the formation of the hydrogel is not dependent on the order of mixing. To conclude this investigation, the elemental compositions of the hydrogels were studied, showing an equivalent amount of nitrogen and sulphur.

For further analysis, hydrogels were prepared, freeze-dried, and ground to $\leq$ 100-μm particles. SEM micrographs in Fig. 18 show the irregular structure of a dried hydrogel particle. The Brunauer–Emmet–Teller (BET) area could be determined to be 0.58 $m^2\ g^{-1}$, which agrees with the mean surface diameter of 91 μm observed by optical spectroscopy.

For oral drug release, tablets have to be prepared. To determine if the powder is suitable for this application, Cukierman and coworkers generated a compactability profile of tablets prepared by different pressures, showing that adequate values of hardness could be observed even at low compression of the powder. Tablets prepared from the granular mixture of freeze-dried KC and MS and the dried hydrogel, referred to as interpolyelectrolyte complex (IPEC), were used to investigate the swelling behavior. The swelling test was composed of two steps: in the first step, the tablets were immersed in 0.1 mol L^{-1} HCl for 2 h. In the second step, the medium was changed to phosphate buffer with pH 6.8 for additional 22 h. The swelling degree was calculated by weighting the sample in swollen and dry states. The granular mixture of KC and MS reached its maximum mass-swelling degree of 317 % after 30 min, and after 2 h the tablet was completely disintegrated. In the beginning of the swelling experiment, the turbidity of the tablet increased, indicating the onset of erosion of the tablet. This observation has been reported before on unmodified starch as well as on carageenan [160, 161]. The tablet made of the ground hydrogel exhibited a mass-swelling degree of 380 % after the first part of the experiment, with a rapid increase of swelling during the first hour. After change of the medium, the swelling degree slowly increases, reaching an equilibrium mass-swelling degree of 742 % after

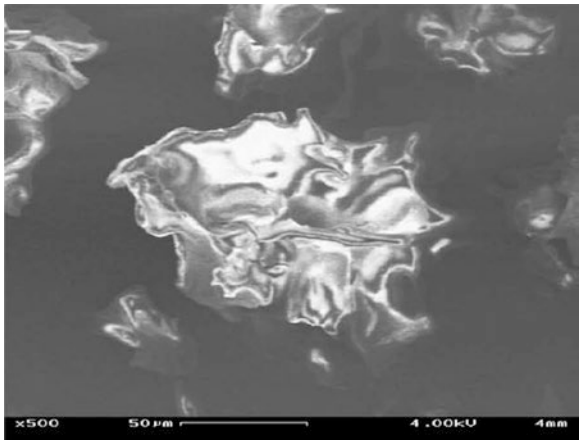

Fig. 18 Structure of hydrogel particles based on starch and carageenan as determined by SEM. For this purpose, hydrogels were freeze-dried and ground to sub-millimeter sized particles. Reprinted from Cukierman et al. [159]. Copyright 2009 Elsevier

24 h, as shown in Fig. 19. Cukierman and collaborators explained the high swelling degree with the composition of the hydrogel: MS has a degree of functionalization with ammonium moieties of 4 %, whereas KC has a degree of functionalization with sulfate moieties of 50 %. The hydrogels were prepared using equimolar amounts of functional groups, entailing a higher content of MS in the hydrogels than KC; this leads to formation of crosslinked domains that do not disentangle. The steady increase during the first hour of the experiment indicates that the polyionic complex is not influenced by the surrounding acidic medium.

To determine the applicability for oral drug delivery, the tablets were loaded with ibuprofen, a nonsteroidal anti-inflammatory drug, and investigated in regard of their drug release. The conditions were similar to the swelling experiments: during the first 2 h, the tablets were immersed within strongly acidic medium at pH 1, followed by 6 h of storage at pH 6.8 phosphate buffered medium. The granular mixture showed the same characteristics as in the swelling studies, releasing the drug completely within 2 h. Samples prepared of the dried hydrogel of 50 or 100 mg, each loaded with 50 mg of ibuprofen, showed slow release in the acidic stage that accelerated after change of the medium. After 6 h, the tablet composed of 50 mg hydrogel released all its drug content, whereas the tablet with 100 mg hydrogel needed 8 h for complete drug release, as illustrated in Fig. 20. The slow release in the acidic phase can be explained by the poor solubility of ibuprofen in acidic media. Fitting the data of these release experiments to model predictions could show that the hydrogels release the drug with zero-order kinetics.

In conclusion, Cukierman and coworkers presented a polyelectrolyte hydrogel system for drug delivery. The hydrogels can be formulated as tablets that can be loaded with drugs. The swelling degree and the release of ibuprofen with zero-order kinetics could be shown.

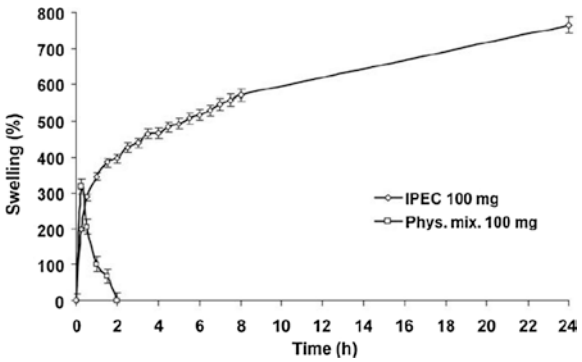

Fig. 19 Comparison of the swelling degree of hydrogels based on starch and carageenan. Tablets were composed of either a freeze-dried polyionic complex (IPEC; *diamonds*) or a granular mixture of dried polymers (phys. mix.; *squares*). The swelling degree was determined by comparison of the mass of swollen gel to dry gel. Reprinted from Cukierman et al. [159]. Copyright 2009 Elsevier

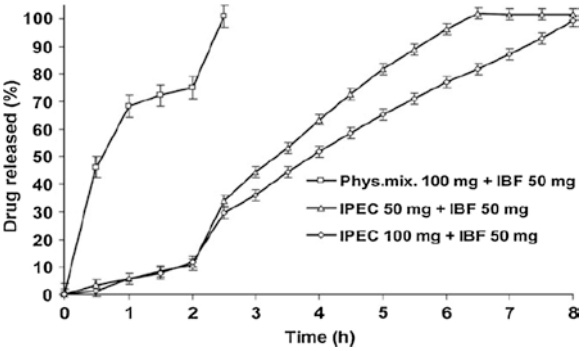

Fig. 20 Comparison of the release of ibuprofen (*IBF*) from tablets composed of a granular mixture of freeze-dried polymers (phys. mix.; *squares*) or freeze-dried polyionic complex (IPEC; *triangles and diamonds*). Reprinted from Cukierman et al. [159]. Copyright 2009 Elsevier

5 Conclusion and Outlook

The recent research in the field of supramolecular polymeric hydrogels is diverse; thus, the eight examples discussed in this chapter represent only a small view on the plethora of these advanced functional materials. All of the selected examples exhibit tunable physicochemical properties that allow for adjustment towards targeted applications in the biomedical field. This tunability permits the gels to have more than just one application in this area. For example, the chitosan and xanthan based hydrogels introduced and investigated by Dumitriu and coworkers have found several possible applications over the past years, including protein immobilization, tissue engineering, drug delivery, and dermocosmetics, and three related patents were claimed [139, 140, 162]. Because of this adaptability towards target applications, supramolecular polymeric hydrogels will most likely have a bright future as materials for medicine.

References

1. Peppas, N.A., Bures, P., Leobandung, W., Ichikawa, H.: Hydrogels in pharmaceutical formulations. Eur. J. Pharm. Biopharm. **50**(1), 27–46 (2000). doi:10.1016/S0939-6411(00)00090-4
2. Hennink, W., Van Nostrum, C.: Novel crosslinking methods to design hydrogels. Adv. Drug Deliv. Rev. **64**(3), 223–236 (2012)
3. Hoare, T.R., Kohane, D.S.: Hydrogels in drug delivery: progress and challenges. Polymer **49**(8), 1993–2007 (2008)
4. Tabata, Y., Ikada, Y.: Synthesis of gelatin microspheres containing interferon. Pharm. Res. **6**(5), 422–427 (1989)
5. Mather, B.D., Viswanathan, K., Miller, K.M., Long, T.E.: Michael addition reactions in macromolecular design for emerging technologies. Prog. Polym. Sci. **31**(5), 487–531 (2006). doi:10.1016/j.progpolymsci.2006.03.001
6. Nandivada, H., Jiang, X., Lahann, J.: Click chemistry: versatility and control in the hands of materials scientists. Adv. Mater. **19**(17), 2197–2208 (2007). doi:10.1002/adma.200602739
7. Langer, R., Peppas, N.: Present and future applications of biomaterials in controlled drug delivery systems. Biomaterials **2**(4), 201–214 (1981)
8. Wichterle, O., Lim, D.: Hydrophilic gels for biological use. Nature **185**(4706), 117–118 (1960)

9. Oelker, A.M., Morey, S.M., Griffith, L.G., Hammond, P.T.: Helix versus coil polypeptide macromers: gel networks with decoupled stiffness and permeability. Soft Matter **8**(42), 10887–10895 (2012). doi:10.1039/C2SM26487K
10. White, S.R., Sottos, N.R., Geubelle, P.H., Moore, J.S., Kessler, M.R., Sriram, S.R., Brown, E.N., Viswanathan, S.: Autonomic healing of polymer composites. Nature **409**(6822), 794–797 (2001)
11. Maldonado-Codina, C., Efron, N.: Impact of manufacturing technology and material composition on the mechanical properties of hydrogel contact lenses. Ophthalmic Physiol. Opt. **24**(6), 551–561 (2004). doi:10.1111/j.1475-1313.2004.00236.x
12. Sun, J.-Y., Zhao, X., Illeperuma, W.R.K., Chaudhuri, O., Oh, K.H., Mooney, D.J., Vlassak, J.J., Suo, Z.: Highly stretchable and tough hydrogels. Nature **489**(7414), 133–136 (2012). http://www.nature.com/nature/journal/v489/n7414/abs/nature11409.html#supplementary-information
13. Yiu, C., Tay, F., King, N., Pashley, D., Sidhu, S., Neo, J., Toledano, M., Wong, S.: Interaction of glass-ionomer cements with moist dentin. J. Dent. Res. **83**(4), 283–289 (2004)
14. Haraguchi, K., Takehisa, T., Fan, S.: Effects of clay content on the properties of nanocomposite hydrogels composed of poly(N-isopropylacrylamide) and clay. Macromolecules **35**(27), 10162–10171 (2002). doi:10.1021/ma021301r
15. Goycoolea, F.M., Heras, A., Aranaz, I., Galed, G., Fernández-Valle, M.E., Argüelles-Monal, W.: Effect of chemical crosslinking on the swelling and shrinking properties of thermal and pH-responsive chitosan hydrogels. Macromol. Biosci. **3**(10), 612–619 (2003). doi:10.1002/mabi.200300011
16. Appel, E.A., del Barrio, J., Loh, X.J., Scherman, O.A.: Supramolecular polymeric hydrogels. Chem. Soc. Rev. **41**(18), 6195–6214 (2012). doi:10.1039/C2CS35264H
17. Brochu, A.B.W., Craig, S.L., Reichert, W.M.: Self-healing biomaterials. J. Biomed. Mater. Res., Part A **96A**(2), 492–506 (2011). doi:10.1002/jbm.a.32987
18. van Gemert, G.M.L., Peeters, J.W., Söntjens, S.H.M., Janssen, H.M., Bosman, A.W.: Self-healing supramolecular polymers in action. Macromol. Chem. Phys. **213**(2), 234–242 (2012). doi:10.1002/macp.201100559
19. Phadke, A., Zhang, C., Arman, B., Hsu, C.-C., Mashelkar, R.A., Lele, A.K., Tauber, M.J., Arya, G., Varghese, S.: Rapid self-healing hydrogels. PNAS **109**(12), 4383–4388 (2012)
20. Lemmers, M., Sprakel, J., Voets, I.K., van der Gucht, J., Cohen Stuart MA, : Multiresponsive reversible gels based on charge-driven assembly. Angew. Chem. Int. Ed. **49**(4), 708–711 (2010). doi:10.1002/anie.200905515
21. Tokarev, I., Minko, S.: Stimuli-responsive hydrogel thin films. Soft Matter **5**(3), 511–524 (2009)
22. Grassi, G., Farra, R., Caliceti, P., Guarnieri, G., Salmaso, S., Carenza, M., Grassi, M.: Temperature-sensitive hydrogels. Am. J. Drug Deliv. **3**(4), 239–251 (2005)
23. Miyata, T., Asami, N., Uragami, T.: A reversibly antigen-responsive hydrogel. Nature **399**(6738), 766–769 (1999). http://www.nature.com/nature/journal/v399/n6738/suppinfo/399766a0_S1.html
24. Kuckling, D.: Responsive hydrogel layers—from synthesis to applications. Colloid Polym. Sci. **287**(8), 881–891 (2009). doi:10.1007/s00396-009-2060-x
25. Alves, M.H., Jensen, B.E., Smith, A.A., Zelikin, A.N.: Poly (vinyl alcohol) physical hydrogels: new vista on a long serving biomaterial. Macromol. Biosci. **11**(10), 1293–1313 (2011)
26. Farris, S., Schaich, K.M., Liu, L., Piergiovanni, L., Yam, K.L.: Development of polyion-complex hydrogels as an alternative approach for the production of bio-based polymers for food packaging applications: a review. Trends Food Sci. Technol. **20**(8), 316–332 (2009)
27. Geckil, H., Xu, F., Zhang, X., Moon, S., Demirci, U.: Engineering hydrogels as extracellular matrix mimics. Nanomedicine **5**(3), 469–484 (2010)
28. Hoffman, A.S.: Hydrogels for biomedical applications. Adv. Drug. Deliv. Rev. (2012)
29. Kaneko, T., Yamaoka, K., Osada, Y., Gong, J.P.: Thermoresponsive shrinkage triggered by mesophase transition in liquid crystalline physical hydrogels. Macromolecules **37**(14), 5385–5388 (2004)

30. Hoffman, A.S.: Hydrogels for biomedical applications. Adv. Drug Deliv. Rev. **64**(Supplement), 18–23 (2012). doi:10.1016/j.addr.2012.09.010
31. Talei Franzesi, G., Ni, B., Ling, Y., Khademhosseini, A.: A controlled-release strategy for the generation of cross-linked hydrogel microstructures. J. Am. Chem. Soc. **128**(47), 15064–15065 (2006). doi:10.1021/ja065867x
32. Kroll, E., Winnik, F.M., Ziolo, R.F.: In situ preparation of nanocrystalline γ-Fe_2O_3 in iron (II) cross-linked alginate gels. Chem. Mater. **8**(8), 1594–1596 (1996)
33. Rossow, T., Hackelbusch, S., Van Assenbergh, P., Seiffert, S.: A modular construction kit for supramolecular polymer gels. Polym. Chem. **4**(8), 2515–2527 (2013)
34. Krische, M., Lehn, J.-M.: The Utilization of Persistent H-Bonding Motifs in the Self-Assembly of Supramolecular Architectures. In: Fuiita, M. (ed.) Molecular Self-Assembly Organic Versus Inorganic Approaches. Structure and Bonding, vol. 96, pp. 3–29. Springer, Berlin Heidelberg (2000). doi:10.1007/3-540-46591-X_1
35. Steed, J.W., Atwood, J.L. The supramolecular chemistry of life. In: Supramolecular chemistry, pp. 49–104. Wiley (2009). doi:10.1002/9780470740880.ch2
36. Piepenbrock, M.-O.M., Lloyd, G.O., Clarke, N., Steed, J.W.: Metal- and anion-binding supramolecular gels. Chem. Rev. **110**(4), 1960–2004 (2009)
37. Schubert, U.S., Eschbaumer, C.: Macromolecules containing bipyridine and terpyridine metal complexes: towards metallosupramolecular polymers. Angew. Chem. Int. Ed. **41**(16), 2892–2926 (2002). doi:10.1002/1521-3773(20020816)41:16<2892:AID-ANIE2892>3.0.CO;2-6
38. Berger, J., Reist, M., Mayer, J., Felt, O., Peppas, N., Gurny, R.: Structure and interactions in covalently and ionically crosslinked chitosan hydrogels for biomedical applications. Eur. J. Pharm. Biopharm. **57**(1), 19–34 (2004)
39. Rastello De Boisseson, M., Leonard, M., Hubert, P., Marchal, P., Stequert, A., Castel, C., Favre, E., Dellacherie, E.: Physical alginate hydrogels based on hydrophobic or dual hydrophobic/ionic interactions: Bead formation, structure, and stability. J. Colloid Interface Sci. **273**(1), 131–139 (2004)
40. Francis Suh, J.-K., Matthew, H.W.: Application of chitosan-based polysaccharide biomaterials in cartilage tissue engineering: a review. Biomaterials **21**(24), 2589–2598 (2000)
41. Temenoff, J.S., Mikos, A.G.: Review: tissue engineering for regeneration of articular cartilage. Biomaterials **21**(5), 431–440 (2000)
42. Haag, R.: Supramolecular drug-delivery systems based on polymeric core-shell architectures. Angew. Chem. Int. Ed. **43**(3), 278–282 (2004)
43. LaVan, D.A., McGuire, T., Langer, R.: Small-scale systems for in vivo drug delivery. Nat. Biotechnol. **21**(10), 1184–1191 (2003)
44. Giller, K.E., Witter, E., Mcgrath, S.P.: Toxicity of heavy metals to microorganisms and microbial processes in agricultural soils: a review. Soil Biol. Biochem. **30**(10), 1389–1414 (1998)
45. Stohs, S., Bagchi, D.: Oxidative mechanisms in the toxicity of metal ions. Free Rad. Biol. Med. **18**(2), 321–336 (1995)
46. Pourjavadi, A., Amini-Fazl, M.S.: Optimized synthesis of carrageenan-graft-poly (sodium acrylate) superabsorbent hydrogel using the Taguchi method and investigation of its metal ion absorption. Polym. Int. **56**(2), 283–289 (2007)
47. Hirst, A.R., Escuder, B., Miravet, J.F., Smith, D.K.: High-tech applications of self-assembling supramolecular nanostructured gel-phase materials: from regenerative medicine to electronic devices. Angew. Chem. Int. Ed. **47**(42), 8002–8018 (2008)
48. Weng, W., Li, Z., Jamieson, A.M., Rowan, S.J.: Control of gel morphology and properties of a class of metallo-supramolecular polymers by good/poor solvent environments. Macromolecules **42**(1), 236–246 (2008)
49. Sackmann, E., Tanaka, M.: Supported membranes on soft polymer cushions: fabrication, characterization and applications. Trends Biotechnol. **18**(2), 58–64 (2000)
50. Zhang, J., Xu, S., Kumacheva, E.: Polymer microgels: reactors for semiconductor, metal, and magnetic nanoparticles. J. Am. Chem. Soc. **126**(25), 7908–7914 (2004)

51. Chen, Z., Higgins, D., Yu, A., Zhang, L., Zhang, J.: A review on non-precious metal electrocatalysts for PEM fuel cells. Energy Environ. Sci. **4**(9), 3167–3192 (2011)
52. Choudhury, N.A., Ma, J., Sahai, Y., Buchheit, R.G.: High performance polymer chemical hydrogel-based electrode binder materials for direct borohydride fuel cells. J. Power Sources **196**(14), 5817–5822 (2011)
53. George, M., Abraham, T.E.: Polyionic hydrocolloids for the intestinal delivery of protein drugs: alginate and chitosan—a review. J. Controlled Release **114**(1), 1–14 (2006)
54. Gombotz, W.R., Wee, S.: Protein release from alginate matrices. Adv. Drug Deliv. Rev. **31**(3), 267–285 (1998)
55. Smidsrød, O.: Alginate as immobilization matrix for cells. Trends Biotechnol. **8**, 71–78 (1990)
56. Djagny, K.B., Wang, Z., Xu, S.: Gelatin: a valuable protein for food and pharmaceutical industries: review. Crit. Rev. Food Sci. Nutr. **41**(6), 481–492 (2001)
57. Ishida, K., Kuroda, R., Miwa, M., Tabata, Y., Hokugo, A., Kawamoto, T., Sasaki, K., Doita, M., Kurosaka, M.: The regenerative effects of platelet-rich plasma on meniscal cells in vitro and its in vivo application with biodegradable gelatin hydrogel. Tissue Eng. **13**(5), 1103–1112 (2007)
58. Tabata, Y., Ikada, Y.: Protein release from gelatin matrices. Adv. Drug Deliv. Rev. **31**(3), 287–301 (1998)
59. Boucard, N., Viton, C., Agay, D., Mari, E., Roger, T., Chancerelle, Y., Domard, A.: The use of physical hydrogels of chitosan for skin regeneration following third-degree burns. Biomaterials **28**(24), 3478–3488 (2007)
60. Lee, K.Y., Mooney, D.J.: Hydrogels for tissue engineering. Chem. Rev. **101**(7), 1869–1880 (2001)
61. Ravi Kumar, M.N.: A review of chitin and chitosan applications. React. Funct. Polym. **46**(1), 1–27 (2000)
62. Dornish, M., Kaplan, D., Skaugrud, Ø.: Standards and guidelines for biopolymers in tissue-engineered medical products. Ann. N. Y. Acad. Sci. **944**(1), 388–397 (2001)
63. Lewen, G., Lindsay, S., Tao, N., Weidlich, T., Graham, R., Rupprecht, A.: A mechanism for the large anisotropic swelling of DNA films. Biopolymers **25**(5), 765–770 (1986)
64. Patel, P., Stripp, A., Fry, J.: Whipping test for the determination of foaming capacity of protein: a collaborative study. Int. J. Food Sci. Technol. **23**(1), 57–63 (1988)
65. Brandl, F., Sommer, F., Goepferich, A.: Rational design of hydrogels for tissue engineering: impact of physical factors on cell behavior. Biomaterials **28**(2), 134–146 (2007)
66. Gayet, J.-C., Fortier, G.: High water content BSA-PEG hydrogel for controlled release device: evaluation of the drug release properties. J. Controlled Release **38**(2), 177–184 (1996)
67. Liu Tsang, V., Bhatia, S.N.: Three-dimensional tissue fabrication. Adv. Drug Deliv. Rev. **56**(11), 1635–1647 (2004)
68. Garrett, Q., Chatelier, R.C., Griesser, H.J., Milthorpe, B.K.: Effect of charged groups on the adsorption and penetration of proteins onto and into carboxymethylated poly (HEMA) hydrogels. Biomaterials **19**(23), 2175–2186 (1998)
69. Montheard, J.-P., Chatzopoulos, M., Chappard, D.: 2-Hydroxyethyl methacrylate (HEMA): chemical properties and applications in biomedical fields. J. Macromol. Sci. Part C Polymer Rev. **32**(1), 1–34 (1992)
70. Xinming, L., Yingde, C., Lloyd, A.W., Mikhalovsky, S.V., Sandeman, S.R., Howel, C.A., Liewen, L.: Polymeric hydrogels for novel contact lens-based ophthalmic drug delivery systems: a review. Cont. Lens Anterior Eye **31**(2), 57–64 (2008)
71. Rossow, T., Heyman, J.A., Ehrlicher, A.J., Langhoff, A., Weitz, D.A., Haag, R., Seiffert, S.: Controlled synthesis of cell-laden microgels by radical-free gelation in droplet microfluidics. J. Am. Chem. Soc. **134**(10), 4983–4989 (2012)
72. Sisson, A.L., Haag, R.: Polyglycerol nanogels: highly functional scaffolds for biomedical applications. Soft Matter **6**(20), 4968–4975 (2010)
73. Sisson, A.L., Steinhilber, D., Rossow, T., Welker, P., Licha, K., Haag, R.: Biocompatible functionalized polyglycerol microgels with cell penetrating properties. Angew. Chem. Int. Ed. **48**(41), 7540–7545 (2009)

74. Chen, G., Jiang, M.: Cyclodextrin-based inclusion complexation bridging supramolecular chemistry and macromolecular self-assembly. Chem. Soc. Rev. **40**(5), 2254–2266 (2011)
75. Guo, M., Jiang, M., Pispas, S., Yu, W., Zhou, C.: Supramolecular hydrogels made of end-functionalized low-molecular-weight PEG and α-cyclodextrin and their hybridization with SiO_2 nanoparticles through host–guest interaction. Macromolecules **41**(24), 9744–9749 (2008)
76. Wang, C., Kopecek, J., Stewart, R.J.: Hybrid hydrogels cross-linked by genetically engineered coiled-coil block proteins. Biomacromolecules **2**(3), 912–920 (2001)
77. Steed, J.W., Atwood, J.L.: Supramolecular chemistry. Wiley, Hoboken (2009)
78. Chang, C., Zhang, L.: Cellulose-based hydrogels: present status and application prospects. Carbohydr. Polym. **84**(1), 40–53 (2011)
79. Klemm, D., Heublein, B., Fink, H.P., Bohn, A.: Cellulose: fascinating biopolymer and sustainable raw material. Angew. Chem. Int. Ed. **44**(22), 3358–3393 (2005)
80. Moon, R.J., Martini, A., Nairn, J., Simonsen, J., Youngblood, J.: Cellulose nanomaterials review: structure, properties and nanocomposites. Chem. Soc. Rev. **40**(7), 3941–3994 (2011)
81. Van Vlierberghe, S., Dubruel, P., Schacht, E.: Biopolymer-based hydrogels as scaffolds for tissue engineering applications: a review. Biomacromolecules **12**(5), 1387–1408 (2011)
82. Fatin-Rouge, N., Milon, A., Buffle, J., Goulet, R.R., Tessier, A.: Diffusion and partitioning of solutes in agarose hydrogels: the relative influence of electrostatic and specific interactions. J. Phys. Chem. B **107**(44), 12126–12137 (2003)
83. Bock, L.: Water-soluble cellulose ethers. Ind. Eng. Chem. **29**(9), 985–987 (1937)
84. Nishio, Y., Haratani, T., Takahashi, T., Manley, R.S.J.: Cellulose/poly (vinyl alcohol) blends: an estimation of thermodynamic polymer–polymer interaction by melting-point-depression analysis. Macromolecules **22**(5), 2547–2549 (1989)
85. Nishio, Y., Manley, R.J.: Cellulose-poly (vinyl alcohol) blends prepared from solutions in N,N-dimethylacetamide-lithium chloride. Macromolecules **21**(5), 1270–1277 (1988)
86. Dave, V., Tamagno, M., Focher, B., Marsano, E.: Hyaluronic acid-(hydroxypropyl) cellulose blends: a solution and solid state study. Macromolecules **28**(10), 3531–3539 (1995)
87. Gupta, D., Tator, C.H., Shoichet, M.S.: Fast-gelling injectable blend of hyaluronan and methylcellulose for intrathecal, localized delivery to the injured spinal cord. Biomaterials **27**(11), 2370–2379 (2006)
88. Tuan, T.-L., Nichter, L.S.: The molecular basis of keloid and hypertrophic scar formation. Mol. Med. Today **4**(1), 19–24 (1998)
89. Caicco, M.J., Zahir, T., Mothe, A.J., Ballios, B.G., Kihm, A.J., Tator, C.H., Shoichet, M.S.: Characterization of hyaluronan–methylcellulose hydrogels for cell delivery to the injured spinal cord. J. Biomed. Mater. Res. A **101A**(5), 1472–1477 (2013). doi:10.1002/jbm.a.34454
90. Wang, Y., Lapitsky, Y., Kang, C.E., Shoichet, M.S.: Accelerated release of a sparingly soluble drug from an injectable hyaluronan–methylcellulose hydrogel. J. Controlled Release **140**(3), 218–223 (2009)
91. Chang, C., Lue, A., Zhang, L.: Effects of crosslinking methods on structure and properties of cellulose/PVA hydrogels. Macromol. Chem. Phys. **209**(12), 1266–1273 (2008). doi:10.1002/macp.200800161
92. Dankers, P.Y.W., Hermans, T.M., Baughman, T.W., Kamikawa, Y., Kieltyka, R.E., Bastings, M.M.C., Janssen, H.M., Sommerdijk, N.A.J.M., Larsen, A., van Luyn, M.J.A., Bosman, A.W., Popa, E.R., Fytas, G., Meijer, E.W.: Hierarchical formation of supramolecular transient networks in water: a modular injectable delivery system. Adv. Mater. **24**(20), 2703–2709 (2012). doi:10.1002/adma.201104072
93. Dankers, P.Y.W., van Luyn, M.J.A., Huizinga-van der Vlag, A., van Gemert, G.M.L., Petersen, A.H., Meijer, E.W., Janssen, H.M., Bosman, A.W., Popa, E.R.: Development and in vivo characterization of supramolecular hydrogels for intrarenal drug delivery. Biomaterials **33**(20), 5144–5155 (2012). doi:10.1016/j.biomaterials.2012.03.052
94. Schubert, U.S., Winter, A., Newkome, G.R.: Chemistry and properties of terpyridine transition metal ion complexes. In: Terpyridine-based Materials, pp 65-127. Wiley-VCH Verlag GmbH & Co. KGaA (2011). doi:10.1002/9783527639625.ch3

95. Weng, W., Beck, J.B., Jamieson, A.M., Rowan, S.J.: Understanding the mechanism of gelation and stimuli-responsive nature of a class of metallo-supramolecular gels. J. Am. Chem. Soc. **128**(35), 11663–11672 (2006)
96. Zhang, J., Su, C.-Y.: Metal-organic gels: from discrete metallogelators to coordination polymers. Coord. Chem. Rev. **257**(7), 1373–1408 (2013)
97. Fiore, G.L., Klinkenberg, J.L., Pfister, A., Fraser, C.L.: Iron tris (bipyridine) PEG hydrogels with covalent and metal coordinate cross-links. Biomacromolecules **10**(1), 128–133 (2008)
98. Rossow, T., Bayer, S., Albrecht, R., Tzschucke, C.C., Seiffert, S.: Supramolecular hydrogel capsules based on PEG: a step toward degradable biomaterials with rational design. Macromol. Rapid Commun. (2013)
99. Fullenkamp, D.E., Rivera, J.G., Gong, Y.-k., Lau, K., He, L., Varshney, R., Messersmith, P.B.: Mussel-inspired silver-releasing antibacterial hydrogels. Biomaterials **33**(15), 3783–3791 (2012)
100. Guvendiren, M., Messersmith, P.B., Shull, K.R.: Self-assembly and adhesion of DOPA-modified methacrylic triblock hydrogels. Biomacromolecules **9**(1), 122–128 (2007)
101. Thompson, K.H., Orvig, C.: Boon and bane of metal ions in medicine. Science **300**(5621), 936–939 (2003)
102. Augst, A.D., Kong, H.J., Mooney, D.J.: Alginate hydrogels as biomaterials. Macromol. Biosci. **6**(8), 623–633 (2006)
103. Gibbs, B.F., Kermasha, S., Alli, I., Mulligan, C.N.: Encapsulation in the food industry: a review. Int. J. Food Sci. Nutr. **50**(3), 213–224 (1999)
104. Glicksman, M.: Utilization of natural polysaccharide gums in the food industry. Adv. Food Res. **11**, 109–200 (1962)
105. Glicksman, M.: Utilization of seaweed hydrocolloids in the food industry. Hydrobiologia **151–152**(1), 31–47 (1987). doi:10.1007/BF00046103
106. Matthew, I.R., Browne, R.M., Frame, J.W., Millar, B.G.: Subperiosteal behaviour of alginate and cellulose wound dressing materials. Biomaterials **16**(4), 275–278 (1995)
107. Ashley, M., McCullagh, A., Sweet, C.: Making a good impression: (a 'how to' paper on dental alginate). Dent Update **32**(3), 169 (2005)
108. Bratthall, G., Lindberg, P., Havemose-Poulsen, A., Holmstrup, P., Bay, L., Söderholm, G., Norderyd, O., Andersson, B., Rickardsson, B., Hallström, H., Kullendorff, B., Sköld Bell, H.: Comparison of ready-to-use EMDOGAIN®-gel and EMDOGAIN® in patients with chronic adult periodontitis. J. Clin. Periodontol. **28**(10), 923–929 (2001). doi:10.1034/j.1600-051x.2001.028010923.x
109. Tønnesen, H.H., Karlsen, J.: Alginate in drug delivery systems. Drug Dev. Ind. Pharm. **28**(6), 621–630 (2002)
110. Rowley, J.A., Madlambayan, G., Mooney, D.J.: Alginate hydrogels as synthetic extracellular matrix materials. Biomaterials **20**(1), 45–53 (1999)
111. Donati, I., Cesàro, A., Paoletti, S.: Specific interactions versus counterion condensation. 1. Nongelling ions/polyuronate systems. Biomacromolecules **7**(1), 281–287 (2006)
112. Topuz, F., Henke, A., Richtering, W., Groll, J.: Magnesium ions and alginate do form hydrogels: a rheological study. Soft Matter **8**(18), 4877–4881 (2012)
113. Milas, M., Rinaudo, M.: The gellan sol–gel transition. Carbohydr. Polym. **30**(2), 177–184 (1996)
114. Watase, M., Nishinari, K.: Effect of alkali metal ions on the viscoelasticity of concentrated kappa-carrageenan and agarose gels. Rheol. Acta **21**(3), 318–324 (1982)
115. Dalsin, J.L., Hu, B.-H., Lee, B.P., Messersmith, P.B.: Mussel adhesive protein mimetic polymers for the preparation of nonfouling surfaces. J. Am. Chem. Soc. **125**(14), 4253–4258 (2003)
116. Lee, H., Dellatore, S.M., Miller, W.M., Messersmith, P.B.: Mussel-inspired surface chemistry for multifunctional coatings. Science **318**(5849), 426–430 (2007)
117. Lee, H., Scherer, N.F., Messersmith, P.B.: Single-molecule mechanics of mussel adhesion. PNAS **103**(35), 12999–13003 (2006)

118. Lin, Q., Gourdon, D., Sun, C., Holten-Andersen, N., Anderson, T.H., Waite, J.H., Israelachvili, J.N.: Adhesion mechanisms of the mussel foot proteins mfp-1 and mfp-3. PNAS **104**(10), 3782–3786 (2007)
119. Taylor, S.W., Luther III, G.W., Waite, J.H.: Polarographic and spectrophotometric investigation of iron (III) complexation to 3,4-dihydroxyphenylalanine-containing peptides and proteins from *Mytilus edulis*. Inorg. Chem. **33**(25), 5819–5824 (1994)
120. Harrington, M.J., Masic, A., Holten-Andersen, N., Waite, J.H., Fratzl, P.: Iron-clad fibers: a metal-based biological strategy for hard flexible coatings. Science **328**(5975), 216–220 (2010)
121. Holten-Andersen, N., Harrington, M.J., Birkedal, H., Lee, B.P., Messersmith, P.B., Lee, K.Y.C., Waite, J.H.: pH-induced metal–ligand cross-links inspired by mussel yield self-healing polymer networks with near-covalent elastic moduli. PNAS **108**(7), 2651–2655 (2011)
122. Berger, J., Reist, M., Mayer, J., Felt, O., Gurny, R.: Structure and interactions in chitosan hydrogels formed by complexation or aggregation for biomedical applications. Eur. J. Pharm. Biopharm. **57**(1), 35–52 (2004)
123. Wu, J., Su, Z.-G., Ma, G.-H.: A thermo-and pH-sensitive hydrogel composed of quaternized chitosan/glycerophosphate. Int. J. Pharm. **315**(1), 1–11 (2006)
124. Zhang, R., Tang, M., Bowyer, A., Eisenthal, R., Hubble, J.: A novel pH- and ionic-strength-sensitive carboxy methyl dextran hydrogel. Biomaterials **26**(22), 4677–4683 (2005)
125. Pourjavadi, A., Sadeghi, M., Hosseinzadeh, H.: Modified carrageenan. 5. Preparation, swelling behavior, salt- and pH-sensitivity of partially hydrolyzed crosslinked carrageenan-graft-polymethacrylamide superabsorbent hydrogel. Polym. Adv. Technol. **15**(11), 645–653 (2004)
126. Bhattarai, N., Gunn, J., Zhang, M.: Chitosan-based hydrogels for controlled, localized drug delivery. Adv. Drug Deliv. Rev. **62**(1), 83–99 (2010)
127. Alonso, M.J., Sánchez, A.: The potential of chitosan in ocular drug delivery. J. Pharm. Pharmacol. **55**(11), 1451–1463 (2003)
128. Ishihara, M., Nakanishi, K., Ono, K., Sato, M., Kikuchi, M., Saito, Y., Yura, H., Matsui, T., Hattori, H., Uenoyama, M.: Photocrosslinkable chitosan as a dressing for wound occlusion and accelerator in healing process. Biomaterials **23**(3), 833–840 (2002)
129. Patel, M., Mao, L., Wu, B., VandeVord, P.J.: GDNF–chitosan blended nerve guides: a functional study. J. Tissue Eng. Regen. Med. **1**(5), 360–367 (2007)
130. Fujita, M., Ishihara, M., Simizu, M., Obara, K., Ishizuka, T., Saito, Y., Yura, H., Morimoto, Y., Takase, B., Matsui, T.: Vascularization in vivo caused by the controlled release of fibroblast growth factor-2 from an injectable chitosan/non-anticoagulant heparin hydrogel. Biomaterials **25**(4), 699–706 (2004)
131. Rosalam, S., England, R.: Review of xanthan gum production from unmodified starches by *Xanthomonas comprestris*. Enzyme Microb. Technol. **39**(2), 197–207 (2006)
132. Shimada, K., Fujikawa, K., Yahara, K., Nakamura, T.: Antioxidative properties of xanthan on the autoxidation of soybean oil in cyclodextrin emulsion. J. Agric. Food Chem. **40**(6), 945–948 (1992)
133. Taylor, K.C., Nasr-El-Din, H.A.: Water-soluble hydrophobically associating polymers for improved oil recovery: a literature review. J. Petrol. Sci. Eng. **19**(3), 265–280 (1998)
134. Katzbauer, B.: Properties and applications of xanthan gum. Polym. Degrad. Stab. **59**(1), 81–84 (1998)
135. Dumitriu, S., Magny, P., Montane, D., Vidal, P., Chornet, E.: Polyionic hydrogels obtained by complexation between xanthan and chitosan: their properties as supports for enzyme immobilization. J. Bioact. Compat. Polym. **9**(2), 184–209 (1994)
136. Chellat, F., Tabrizian, M., Dumitriu, S., Chornet, E., Magny, P., Rivard, C.H., Yahia, L.H.: In vitro and in vivo biocompatibility of chitosan–xanthan polyionic complex. J. Biomed. Mater. Res. **51**(1), 107–116 (2000)
137. Chellat, F., Tabrizian, M., Dumitriu, S., Chornet, E., Rivard, C.-H., Yahia, L.: Study of biodegradation behavior of chitosan–xanthan microspheres in simulated physiological media. J. Biomed. Mater. Res. **53**(5), 592–599 (2000)

138. Dumitriu, S., Chornet, E.: Immobilization of xylanase in chitosan–xanthan hydrogels. Biotechnol. Progr. **13**(5), 539–545 (1997)
139. Dumitriu, S., Chornet, E., Vidal, P. Polyionic insoluble hydrogels comprising xanthan and chitosan. US Patent 5,620,706, 1997
140. Dumitriu, S., Guttmann, H., Kahane, I.: Supported polyionic hydrogels. US Patent 5,858,392, 1999
141. Magnin, D., Lefebvre, J., Chornet, E., Dumitriu, S.: Physicochemical and structural characterization of a polyionic matrix of interest in biotechnology, in the pharmaceutical and biomedical fields. Carbohydr. Polym. **55**(4), 437–453 (2004)
142. Tsung, M., Burgess, D.J.: Preparation and stabilization of heparin/gelatin complex coacervate microcapsules. J. Pharm. Sci. **86**(5), 603–607 (1997)
143. Clark, A., Richardson, R., Ross-Murphy, S., Stubbs, J.: Structural and mechanical properties of agar/gelatin co-gels. Small-deformation studies. Macromolecules **16**(8), 1367–1374 (1983)
144. Clark, A.H., Gidley, M.J., Richardson, R.K., Ross-Murphy, S.B.: Rheological studies of aqueous amylose gels: the effect of chain length and concentration on gel modulus. Macromolecules **22**(1), 346–351 (1989)
145. Lange, R.F., Van Gurp, M., Meijer, E.: Hydrogen-bonded supramolecular polymer networks. J. Polym. Sci., Part A: Polym. Chem. **37**(19), 3657–3670 (1999)
146. Sijbesma, R.P., Beijer, F.H., Brunsveld, L., Folmer, B.J., Hirschberg, J.K., Lange, R.F., Lowe, J.K., Meijer, E.: Reversible polymers formed from self-complementary monomers using quadruple hydrogen bonding. Science **278**(5343), 1601–1604 (1997)
147. Tschoegl, N.W.: The phenomenological theory of linear viscoelastic behavior: an introduction. Springer, Berlin (1989)
148. Evans, G.R.: Challenges to nerve regeneration. In: Seminars in Surgical Oncology, vol. 3, pp. 312–318. Wiley Online Library (2000)
149. Belkas, J.S., Shoichet, M.S., Midha, R.: Peripheral nerve regeneration through guidance tubes. Neurol. Res. **26**(2), 151–160 (2004)
150. Meek, M., Coert, J.: Clinical use of nerve conduits in peripheral-nerve repair: review of the literature. J. Reconstr. Microsurg. **18**(02), 097–110 (2002)
151. Pfister, L.A., Papaloïzos, M., Merkle, H.P., Gander, B.: Hydrogel nerve conduits produced from alginate/chitosan complexes. J. Biomed. Mater. Res. A **80**(4), 932–937 (2007)
152. Armstrong, J., Wenby, R., Meiselman, H., Fisher, T.: The hydrodynamic radii of macromolecules and their effect on red blood cell aggregation. Biophys. J. **87**(6), 4259–4270 (2004)
153. Beel, J.A., Groswald, D.E., Luttges, M.W.: Alterations in the mechanical properties of peripheral nerve following crush injury. J. Biomech. **17**(3), 185–193 (1984)
154. Borschel, G.H., Kia, K.F., Kuzon Jr, W.M., Dennis, R.G.: Mechanical properties of acellular peripheral nerve. J. Surg. Res. **114**(2), 133–139 (2003)
155. Le Corre, D., Bras, J., Dufresne, A.: Starch nanoparticles: a review. Biomacromolecules **11**(5), 1139–1153 (2010)
156. Leach, H.W.: Gelatinization of starch. In: Whistler, R.L., Paschall Eugene, F. (eds.) Starch: Chemistry and Technology, pp. 289–307. Academic Press, New York (1965)
157. Kartha, K., Srivastava, H.: Reaction of epichlorhydrin with carbohydrate polymers. Part II. Starch reaction mechanism and physicochemical properties of modified starch. Starch-Stärke **37**(9), 297–306 (1985)
158. Kuniak, L., Marchessault, R.: Study of the crosslinking reaction between epichlorohydrin and starch. Starch-Stärke **24**(4), 110–116 (1972)
159. Prado, H.J., Matulewicz, M.C., Bonelli, P.R., Cukierman, A.L.: Preparation and characterization of a novel starch-based interpolyelectrolyte complex as matrix for controlled drug release. Carbohydr. Res. **344**(11), 1325–1331 (2009)
160. Capron, I., Yvon, M., Muller, G.: In vitro gastric stability of carrageenan. Food Hydrocolloids **10**(2), 239–244 (1996)

161. Li, J.-Y., Yeh, A.-I.: Relationships between thermal, rheological characteristics and swelling power for various starches. J. Food Eng. **50**(3), 141–148 (2001)
162. Dumitriu, S., Kahane, I., Guttmann, H.: Supported polyionic hydrogels containing biologically active material. US Patent 5,648,252, 1997

Hydrogels for Stem Cell Fate Control and Delivery in Regenerative Medicine

Wei Seong Toh, Yi-Chin Toh and Xian Jun Loh

Abstract The dynamic tissue environment presents spatial and temporal heterogeneity in the cellular and matrix composition. Oxidative stress and inflammation affect the mobilization of stem cells from the stem cell niche, survival and engraftment of exogenous stem cells, and are therefore important considerations when delivering cells in injectable hydrogels to the site of tissue injury. Strategies of anti-inflammation and/or anti-oxidative injury may be incorporated into multifunctional hydrogels to modify the tissue environment and help in the survival/engraftment of the transplanted cells. This could improve the outcome of the regenerative therapy by combined approaches utilizing hydrogels, microtechnologies and controlled release strategies. These advances in hydrogel design and related enabling technologies will continue to grow and aid in our future design of customized hydrogel delivery systems for healthy and injured/diseased tissues, and guide the development of future therapies.

W.S. Toh (✉)
Faculty of Dentistry, National University of Singapore, 11 Lower Kent Ridge Road, Singapore 119083, Singapore
e-mail: dentohws@nus.edu.sg

W.S. Toh
Tissue Engineering Program, Life Sciences Institute National University of Singapore, 27 Medical Drive, Singapore 117510, Singapore

Y.-C. Toh
Department of Biomedical Engineering, National University of Singapore, Singapore 119083, Singapore

X.J. Loh (✉)
Institute of Materials Research and Engineering (IMRE), A*STAR, 3 Research Link, Singapore 117602, Singapore
e-mail: lohxj@imre.a-star.edu.sg; XianJun_Loh@scholars.a-star.edu.sg

X.J. Loh
Department of Materials Science and Engineering, National University of Singapore, 9 Engineering Drive 1, Singapore 117576, Singapore

X.J. Loh
Singapore Eye Research Institute, 11 Third Hospital Avenue, Singapore 168751, Singapore

X.J. Loh (ed.), *In-Situ Gelling Polymers*, Series in BioEngineering,
DOI 10.1007/978-981-287-152-7_8

Keywords Hydrogels · Stem cells · Drug delivery · Tissue regeneration · Biomedical

1 Introduction

Stem cells represent an ideal cell source for applications in tissue engineering and regenerative medicine due to their ability to proliferate and differentiate to a wide variety of lineages for use in cellular therapies [1, 2]. Over the last decade, several advances have been made in isolation, expansion and differentiation of a variety of stem cell types. Immense efforts are ongoing to decipher the components of the 'stem cell niche' and the molecular mechanisms that regulate the self-renewal, proliferation, differentiation and migration of stem cells to become committed somatic cell types [3]. Undoubtedly, determining the specific niche components and deciphering the underlying mechanisms will allow researchers to better understand stem cell behavior and to unravel the full therapeutic potential of stem cells. When applying stem cells for tissue regeneration, it is becoming increasingly important to also consider the dynamic complexity of the tissue environment, either in healthy or diseased state, and how these may affect the stem cell fate and functions. The level of oxygenation, oxidative stress, inflammation, complexity of cell populations and signaling events present in the site of tissue injury are likely to influence the stem cell engraftment and survival.

Recent advances in the field of biomaterials have provided synthetic three-dimensional (3-D) extracellular matrices (ECM) with appropriate biophysical and biochemical signalling cues to probe changes in stem cell behaviours and functions. For instance, it is now becoming possible to study the changes in stem cell behaviour in a well-controlled microenvironment. Specific ECM components and morphogenetic factors may be introduced into the microenvironment to influence the stem cell fate and functions. Additional tissue elements such as hypoxia, oxidative stress and even inflammation may also be added to the microenvironment to interrogate the stem cell responses to these elements when they are being introduced into the tissue site of injury. Understanding the complex interactions of stem cells and the extracellular microenvironment would therefore provide important information for the design and engineering of the next-generation biomaterials for delivery of stem cells to the tissue site of injury.

Among the biomaterials, hydrogels are most commonly used as scaffolds and substrates for stem cell culture and as carrier systems for delivery of stem cells because of their tunable tissue-like properties, controllability of degradation and release behavior, and adaptability in a clinical setting for minimally invasive surgical procedures. Hydrogels may be made from natural and synthetic polymers. These highly-hydrated networks can be held together via physical or chemical crosslinks, can be made biodegradable, and responsive to specific stimuli such as pH and temperature, and can be engineered to deliver therapeutic stem cells and soluble factors in a sustained and controlled fashion.

Several advances have been made in the hydrogel chemistry and modifications, coupled with microtechnologies for enhanced control of stem cell fate and functions, and for improved stem cell delivery and therapeutic efficacy by augmenting stem cell functions and modulation of the tissue environment. This chapter will present an overview of stem cell characteristics, and how hydrogels aided with microtechnologies have advanced our understanding of stem cell biology towards application in cellular therapies. The second half of chapter presents some of the advanced multifunctional hydrogel systems for delivery of stem cells for tissue regeneration.

2 Stem Cells

Stem cells, defined by their capacities for self-renewal and for differentiation into a wide variety of cell lineages, hold great promise for applications in tissue engineering and regenerative medicine. The hallmarks of stem cell self-renewal and differentiation are controlled by both intrinsic gene regulatory machinery and extrinsic microenvironment or niche, which collectively influence the cell fate decisions. Gene expression profiling across various types of stem cells have advanced our understanding of the core gene regulatory networks that defined 'stemness' [4]. Extracellular matrix (ECM), soluble bioactive factors and neighboring support cells make up the stem cell microenvironment or niche [5] that controls stem cell self-renewal and differentiation. Stem cells can be derived from two major sources—multipotent adult stem cells isolated from various adult tissues [6] and pluripotent embryonic stem cells (ESCs) derived from inner cell mass of embryos [7].

2.1 Adult Stem Cells

Adult stem cells present in most tissues of mature organisms are multipotent and serve to repair and regenerate tissues. Mesenchymal stem cells (MSCs) are multipotent adult stem cells that are capable of differentiating to different lineages including chondrocytes [8, 9], osteoblasts [10] and adipocytes [11], and have been identified in bone marrow [6, 12] as well as in other tissues including adipose [12, 13], synovium [14, 15], and periosteum [16]. In recent years, MSCs and mesenchymal progenitor cells have been differentiated and derived from human pluripotent stem cells including embryonic stem cells (ESCs) [17] and induced pluripotent stem cells (iPSCs) [18] and demonstrated application potential in tissue engineering and regeneration [19]. Importantly, MSCs also potently modulate the immune and inflammatory responses, improve cell migration and angiogenesis, and prevent fibrosis by expression of specific trophic factors [20]. As such, the role of MSCs in regenerative medicine has extended from merely cell

differentiation to expression of bioactive factors that modulate tissue and immune responses, and facilitate overall tissue regeneration. Although adult MSCs have shown great promise for autologous and allogeneic transplantations, these cells have limited differentiation capability and suffer age-related loss of stem cell functions including proliferation and differentiation [21, 22].

2.2 Embryonic Stem Cells

Embryonic stem cells are pluripotent and can differentiate to cell lineages of all three germ layers (ectoderm, endoderm and mesoderm) [7]. To date, several diverse cell types have been derived from hESCs, including cardiomyocytes [23, 24], endothelial cells [25, 26], chondrocytes [27–30], osteoblasts [31, 32], neurons [33, 34], keratinocytes [35], and hepatocytes [36]. Recent advances in stem cell biology have also enabled the generation of induced pluripotent stem cells (iPS) from somatic cells by defined factors [37]. Much of the current focus of research on both ESCs and iPSCs is to better understand the developmental pathways and underlying the molecular mechanisms in directing stem cell differentiation to a particular lineage in a well-controlled manner for use in regenerative therapies [19, 38–41]. To shed light on mechanisms that control stem cell fate, synthetic stem cell microenvironments engineered by the use of biomaterials, in particular hydrogels were designed and engineered in vitro to model the stem cell niche in vivo [42–45].

3 Hydrogels

Hydrogels have become a biomaterial of choice for stem cell work and have been used as substrates, scaffolds and encapsulants for stem cells [46, 47]. Hydrogels are natural or synthetic polymer networks that have high water-absorbing capacity and closely mimic native extracellular matrices [46, 47].

3.1 Natural Hydrogels

3.1.1 Chemical and Physical Modifications of Natural Polymers

Many chitosan-based thermogelling systems have been previously reported. These include combinations of chitosan and glycerol-phosphate, poly(ethylene glycol)-grafted chitosan, poly(vinyl alcohol)/chitosan blended hydrogels [48–50]. Many different varieties of thermogels can be prepared, however, complicated multi-step reactions using organic solvents are not preferred as these materials may not be

very compatible for biomedical applications. Chitosan itself is also poorly water soluble under physiological conditions making it difficult to formulate for drug delivery applications. Simple mixing reactions or one-step chemical modification methods are ideal for clinical applications. For example, a chitosan-ammonium hydrogen phosphate (chitosan-AHP) blend was found to have thermogelling properties (Fig. 1) [51]. The preparation was simple as shown in the following. Chitosan was first dissolved in mild acetic acid solution. Following that, the chitosan solution was mixed with ammonium hydrogen phosphate solution to yield the thermogel.

Another simple formulation method relies on the modification of glycol chitosan. Glycol chitosan is water soluble under physiological conditions due to glycol residues. Its chitosan backbone is the reason behind the non-cytotoxic and biodegradable nature of the material. A glycol chitosan-based thermogelling polymer was recently prepared as a thermogelling polymer (Fig. 2) [52]. Here, selective N-acetylation of glycol chitosan was carried out in a mixed solvent of water and methanol. Acetic anhydride was added into the glycol chitosan solution for the acetylation of glycol chitosan. The polymer was treated with sodium hydroxide solution for the removal of the O-acetylated moieties and purified by dialysis.

Besides chitosan, naturally derived polymers such as hyaluronic acid can be chemically modified to form thermogels. For example, copolymers of NIPAAm and acrylic acid N-hydroxysuccinimide were first synthesized via free radical polymerization and then bonded to amine-functionalized hyaluronic acid (HA) to form a thermogelling polymer [53]. Other types of naturally derived polymers such as methyl cellulose have well-documented thermogelling effect as well [54].

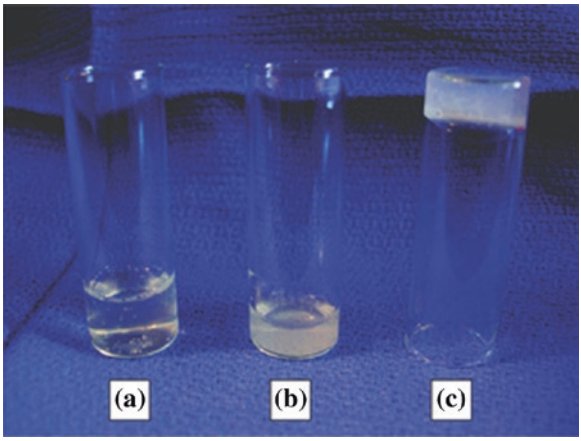

Fig. 1 Photograph showing the thermogelation of chitosan–AHP solution. **a** Chitosan solution in 0.5 % acetic acid. **b** Chitosan–AHP solution (0.075 g of AHP added to 5 mL of chitosan solution in an ice bath and stirred for 2 min followed by incubating at 37 °C for 4 min. **c** Thermogelled chitosan–AHP solution after incubating the chitosan–AHP solution at 37 °C for 11 min. Reproduced with permission [51]. Copyright 2007, American Chemical Society

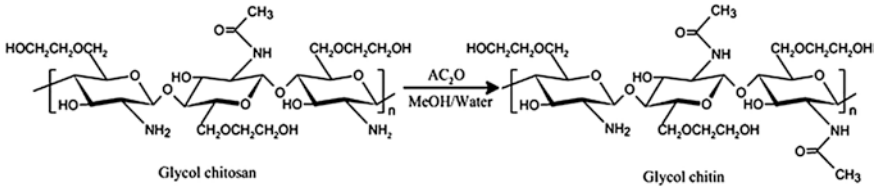

Fig. 2 Synthesis scheme of glycol chitin. Reproduced with permission [52]. Copyright 2013, Elsevier

3.2 Synthetic Hydrogels

3.2.1 Synthetic Gels Prepared by Ring-Opening Polymerization

Biodegradable polymers such as poly(ε-caprolactone) (PCL) and poly(lactic acid) (PLA) are typically synthetically prepared by ring-opening polymerization of lactones. The basic monomeric unit of PLA is lactic acid. In theory, the esterification of lactic acid forms PLA and the reaction can be expected to be straightforward. However, this is an equilibrium reaction and it is difficult to remove the water produced by the esterification process completely. The bonds formed are easily hydrolyzed by the water molecules and the maximum attainable molecular weight is thus limited. This problem is solved by using a cyclic lactide. This lactide undergoes a ring-opening polymerization to give PLA. As there is no water molecules produced in the course of the reaction, the molecular weights that can be attained are much higher than typical polycondensation reactions. Ring opening polymerization has been used by Jeong et al. to prepare thermogelling polymers. Using a telechelic dihydroxyl compound as the initiator, either a small molecule glycol or poly(ethylene glycol), many polyesters can be synthesized in this manner. In particular, polymers such as PCL, [55–59] PLGA, [59–67] and PLA [68, 69] have been reported. Poly(amino acids) have also been polymerized by ring-opening polymerization of N-carboxyanhydrides (NCA). To date, poly (l-Ala-co-L-Phe)-poly(propylene glycol)-poly (ethylene glycol)-poly(propylene glycol)-poly(L-Ala-co-L-Phe), poly(ethylene glycol)-poly(L-alanine-co-L-phenyl alanine), poly-(ethylene glycol)-poly(D-alanine-co-D-phenyl alanine), poly(ethylene glycol)-poly(L-alanine-co-L-phenyl alanine) grafted chitosan have been demonstrated to have a thermogelation effect [70–73].

3.2.2 Synthetic Gels Prepared by Radical Polymerization

Radical polymerization is the workhorse of many polymer chemists and has been used extensively to fabricate materials, which are easily scalable and also having multiple characteristics due to the different monomers in the polymer backbone. Typical monomers polymerized include N-isopropylacrylamide (NIPAAm) and

poly(acrylic acid) (PAA) [74, 75] Liu et al. reported the free radical polymerization of PNIPAAm grafted to methylcellulose (MC) using ammonium persulfate and N,N,N′,N′-tetramethyl ethylene diamine as an initiator [76]. The sol–gel transition of the thermogels occurs within a minute with tunable transition temperature based on the composition of the copolymer. Recently, controlled radical polymerization techniques such as atom transfer radical polymerization (ATRP) have allowed for new block architectures as well as modulation of the thermogel behavior. Recently, Kitazawa et al. reported the synthesis of a thermosensitive triblock copolymer, consisting of poly(benzyl methacrylate) as the terminal blocks and poly(methyl methacrylate) as the middle block, by ATRP [77]. This polymer exhibits a thermogelling effect in an ionic liquid and shows an extremely high gelation temperature of above 100 °C. Abandansari et al. reports the synthesis of a pentablock polymer of PNIPAAm-PCL-PEG-PCL-PNIPAAm, which was synthesized by combining ring-opening polymerization and ATRP [78]. Li et al. synthesized a class of thermogels for the delivery of cardiosphere-derived cells (CDCs) [79]. The hydrogels were based on a central polycaprolactone unit with flanking PNIPAAm, poly(2-hydroxyethyl methacrylate) and poly(dimethyl-γ-butyrolactone acrylate) (Fig. 3). Atom transfer radical polymerization was utilized for the fabrication of well-defined thermogelling polymers. These polymer solutions formed semi-solid gels within 5 s.

3.2.3 Synthetic Gels Prepared by the Formation of Poly(Urethane)S

The formation of multiblock copolymers with high molecular weights is the basis for the preparation of thermogelling copolymers with extremely low gelation concentrations. Typically, this is prepared by a one-pot reaction of poly(ethylene glycol) as the first block, poly(propylene glycol) as the second block, and a third block polymer of choice. Without the third block, the thermogelling effect is also observed [80]. However, based on the different requirements such as degradation stability, hydrophobicity of the block copolymer, and drug release profile of the thermogel, the third block can be used to tune the thermogel properties. Over the past 7 years, several blocks have been utilized including poly[(R)-3-hydroxybutyrate] (PHB) [81–83], PLA [84], PCL [85, 86] poly(ethylene butylene) [87, 88] and poly(trimethylene carbonate) [89]. Recently, Park et al. reported the synthesis of thermogelling polymers with functional groups in the backbone to allow for bio-functionalization to enhance cell–materials interactions [90]. Here, an amine-functionalized ABA block copolymer, poly(ethylene glycol)-poly(serinol hexamethylene urethane) (ESHU) with one free primary amine group on every repeating unit was synthesized. The polyurethane unit functions as the hydrophobic block and PEG acts as the hydrophilic block. Serinol is a serine derivative with two hydroxyl groups and one amine group; the hydroxyl groups allow for conjugation with the isocyanate groups to form the urethane linkages and the amino group can be used for further functionalization. The amino group was first protected during the urethane formation. This protected amino group was reacted to form a bio-functionalized ESHU with IKVAVS peptide which shows rapid thermogelling property.

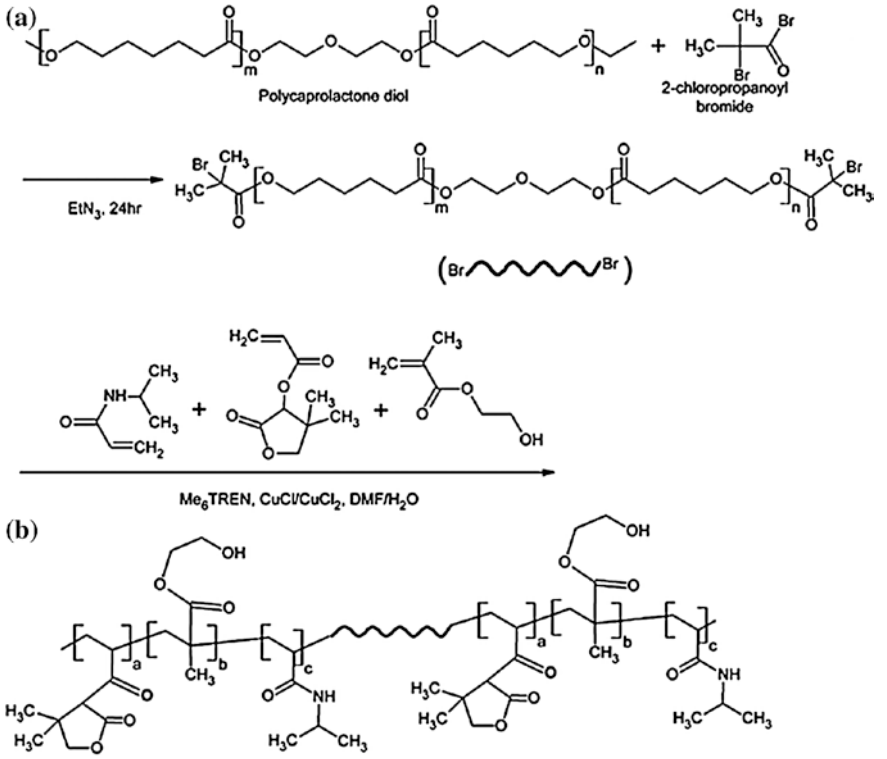

Fig. 3 Synthesis of **a** difunctional polycaprolactone initiator and **b** hydrogel polymers by ATRP. Reproduced with permission [78]. Copyright 2011 Elsevier

3.3 Composite Hydrogels and Hybrids

Organic–inorganic hybrid hydrogels may be defined as a water-swollen cross-linked polymer network impregnated with inorganic particles or nanostructures. While these materials have not been explored for stem cell culture, the presence of inorganic materials adds new properties to the hydrogel through different interactions when they are entrapped within the hydrogel network. Such nanocomposite structures have found applications in the areas of catalysis, stimuli-responsive drug release, biosensors, anti-bacterial, SERS, and many other technological areas [91]. The addition of these nanoparticles endow the one dimensional hydrogel with additional features for sensing and delivery applications.

Stimuli-responsive polymers undergo significant and reversible conformational changes in response to small changes in environmental conditions such as temperature, pH, light, ultrasound and magnetic fields. Hydrogels developed from those stimuli-responsive polymers can potentially be used in drug delivery since they are switchable and controllable in the transition from sol-gel states. This ‘switch’ can be applied as trigger for programming release of encapsulated biomolecules.

Heat can be generated by metal nanoparticles, this opens up a new approach for the development of new hybrid thermogelling systems with interesting properties as drug carriers. Metal nanoparticles also possess unique optical and electronic properties determined by their size, shape and composition. Gold, silver, copper or their alloys have attracted numerous attentions owing to their unique properties, such as size- and shape-dependent optical and electronic features, a high surface area to volume ratio, and surfaces that can be readily modified with ligands containing functional groups. The optical properties mainly relate to the interaction between light and the noble metallic nanoparticles, in such an interaction the coherent collective oscillation of electrons in the conduction band induces large surface electric fields which greatly enhance the radiative properties when they interact with the resonant radiation. Xia et al. prepared nanocages, via the galvanic replacement of silver nanocubes with gold. These gold nanocages can be applied in bio-systems for imaging, photothermal destruction and drug delivery [92, 93]. Recently, Han et al. reported the facile chemical synthesis method of well-defined gold nanocrosses through anisotropic growth along both ⟨110⟩ and ⟨001⟩ planes [94].

The multiple branching was achieved by breaking the face-centered-cubic lattice symmetry of gold through copper-induced formation of single or double twins (Fig. 4), and the resulting gold nanocrosses exhibited pronounced NIR absorption and were used for two photon luminescent imaging of cancer cells and photothermal destruction of cancer cells with very low power NIR laser irradiation. NIR light is very useful for biomedical applications since these wavelengths can penetrate biological tissues with relatively little attenuation or tissue damage. Programmed drug delivery was modulated by photothermal trigger through the combination of NIR-absorbing nanoparticles and thermally responsive polymers.

This smart system was first shown by Sershen et al. using NIPAAM-co-AAM (acrylamide) and gold-gold sulfide nanoparticles [95]. Light at 800 and 1200 nm was absorbed by the nanoparticles and converted to heat. Interestingly, the nanoshell-composite hydrogels showed enhanced drug release and the multiple bursts release effect of protein in response to repeated near-IR irradiation. In another work, Zhao et al. found that NIR at 980 nm can be used to induce sol-gel transition when loaded upconversion nanoparticles (UCNPs) into a photosensitive hybrid hydrogel. This novel system released large, inactive biomacromolecules such as protein and enzyme “on demand”, whereby the bioactivity was also preserved [96]. Unlike the plasmonic noble metals, some transitional metal nanoparticles, such as iron, cobalt and nickel, exhibit excellent magnetic properties. By adjusting the sizes of these nanoparticles, the magnetic properties can be tuned from ferromagnetic to superparamagnetic. When the shape of these nanoparticles is changed into nanorod, the coercivity will be increased. A number of iron, cobalt and nickel nanoparticles have been synthesized with different size and shapes. These nanoparticles have been used for magnetic field induced hyperthermia, drug delivery and as contrast agents in magnetic resonance imaging (MRI) based on their excellent response to the external magnetic fields. Iron oxide nanoparticles can be loaded into a hydrogel to create a remotely activated hydrogel by magnetic induction. Kohane et al. developed a ethyl cellulose-iron oxide composite

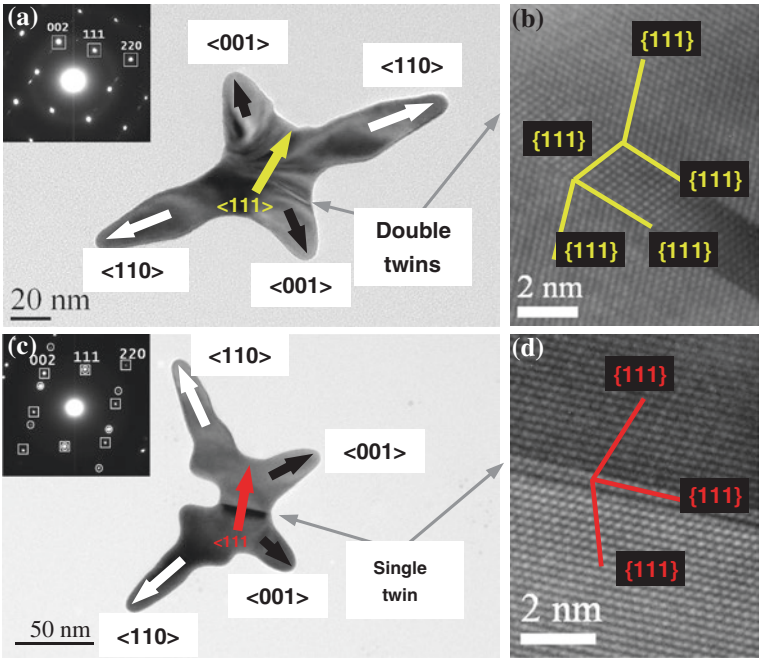

Fig. 4 Structural analysis of gold nanocrosses. **a** Low-magnification TEM and **b** HRTEM images of a doubly twinned gold nanocross with D_{2h} symmetry. The inset in **a** shows one set of SAED spots. **c** Low-magnification TEM and **d** HRTEM images of a singly twinned gold nanocross with C_{2v} symmetry. The inset in **c** shows two sets of SAED spots, labeled with *squares* and *circles*. This image is reproduced from [94] with permission

membrane based drug delivery system consisting of PNIPAAM hydrogel (Fig. 5) [97]. The engineered hybrid system was synthesized by co-evaporation to cause the entrapment of PNIPAAM and iron oxide nanoparticles to give a presumably disordered network. The obtained device enabled rapid, repeatable, and tunable drug delivery through the swelling and deswelling transition of PNIPAAM nanogel upon the application of an external oscillating magnetic field. Analysis with sodium flurorescein showed approximately 20-fold increase in flux when the device was turned "on" by exposure to an oscillating magnetic field, as well as consistent drug flux over four on-off cycles.

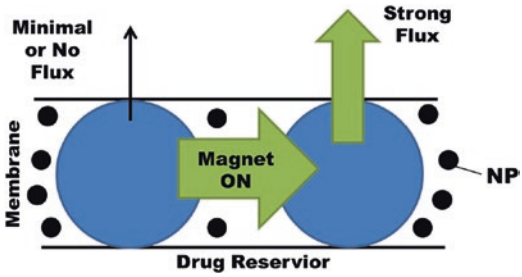

Fig. 5 Schematic illustration of drug delivery from magnetically triggered cellulose-iron oxide particle hybrid membrane consisting of PNIPAAM-based nanogels (this image is enhanced and reproduced from [97] with permission)

4 Hydrogel Microenvironments for Construction of Stem Cell Niche

Hydrogels serve as well-controlled 3-D microenvironment systems for incorporation of biochemical and biophysical cues for presentation to stem cells in a spatiotemporally controlled manner, which allows researchers to deconstruct components of the stem cell niche, and to decipher the underlying mechanisms that regulate stem cell proliferation, differentiation and migration [44, 45]. In recent years, new variables in hydrogel design, propelled by new tools and techniques, to incorporate the necessary cues and components to influence stem cell behavior, have greatly enhanced our understanding of the stem cell microenvironment, and its relevance for tissue regeneration [3].

4.1 Hydrogels as ECM-Mimetic

The native ECM is a 3-D network composed of matrix proteins (e.g. collagen, fibrin, laminin) that provides structural support framework for anchorage of cells and naturally sequesters soluble factors. Hydrogels are highly-hydrated networks of natural or synthetic polymers which resemble the naive ECM, and are therefore ideal biomaterial scaffold for culture of stem cells [44]. Hydrogels can be derived from natural materials including collagen [98, 99], gelatin [100–102], fibrin [103], dextran [104], hyaluronic acid (HA) [105–107] and keratin [108]. Since native tissue ECM is likely to compose of many types of matrix proteins, hydrogels made from decellularized tissue matrix represent an attractive alternative [109, 110]. However, the application of these natural hydrogels is often hampered by the batch variability and difficulty in the control of material properties including degradation, mechanics and bioactivity. These limitations may be overcome through synthetic modification of these natural materials [100, 105] or the use of purely synthetic materials such as PEG that allow decoration of ECM ligands to mimic the native ECM and to support cell adhesion [111, 112]. Among the various hydrogels, HA-based hydrogels are commonly used for stem cell culture, and have been shown to support self-renewal and differentiation of hESCs [107]. In the use of synthetic hydrogels such as the PEG for stem cell culture, integrin-specific adhesion ligands can be incorporated to the hydrogel network, and differential integrin activation was demonstrated to modulate ESC fate decisions [113, 114].

4.1.1 Matrix Architecture

Hydrogel network and matrix architecture is an important property that is required to ensure proper nutrient transport for optimal cell growth, and to allow space for cell movement and to generate cell-cell interactions [42, 44]. The native ECM is

composed of fibers that provide geometric and topographic signals to direct cell functions, cell-cell/matrix interactions, morphogenesis and structural organization in microscale. To this end, various approaches have been explored in the hydrogel design and engineering to influence stem cell fate and functions by tailoring the geometry, topography as well as porosity of the hydrogel.

It is well-known that cell shape and function are tightly-coupled [115, 116]. The change in cell shape is often accompanied not only by changes in the cytoskeleton assembly but also in cell functions through specific gene and protein expression. Apart from biochemical control of cell shape by the use of growth factors or actin-disrupting agents [117], biophysical strategies through stiffness control and micropatterning of hydrogel substrates have also proved efficacious in guiding stem cell differentiation [107, 118]. Using polyacrylamide hydrogels patterned by photolithography that approximate the mechanical properties of soft tissues, Lee and colleagues have shown that MSCs cultured in small circular islands show elevated expression of adipogenesis markers while cells that spread in anisotropic geometries tend to express elevated neurogenic markers [119].

When the hydrogel mesh size is smaller than the size of cell or protein, the cell movement and nutrient transport are likely to be affected, but may be overcome by material strategies including alterations in crosslinking density or tunable degradation. At a higher level of modification, electrospinning is the technique that has recently been adopted to fabricate hydrogel nanofibers to mimic the 3D nanofibrous structure of the native ECM and to control the biochemical and biomechanical properties [120, 121]. Hydrogel fibrous structure not only allows for improved cell movement and nutrient transport through increased porosity, but also exerts topographic control to influence cell fate, and presentation of anisotropic elasticity, which is important for certain tissues [122]. Other strategies to improve the porosity of hydrogels include the use of stimuli-responsive microspheres [123], microfibers [124] and gel systems [125] that may be dissolved in a controlled manner by specific changes in pH, temperature or exposure to enzymes. One example is the impregnation of cell-laden gelatin microspheres within the alginate hydrogel, which upon transfer to 37 °C, allowed the gelatin to be dissolved and released the cells into the spherical cavities created in the hydrogel bulk, creating space for further cell growth within the matrix [123]. Lau and colleagues observed enhanced cell survival and hepatogenesis of murine iPSCs encapsulated in such micro-cavitary hydrogel system [123].

4.1.2 Matrix Mechanics and Degradation

In their native tissue environment, cells experience a wide magnitude of matrix stiffness, from soft (brain ~0.1 kPa) to stiffer (bone ~80 kPa) tissues, which dictates several aspects of cellular functions [126]. The landmark study by Engler and colleagues [127] demonstrated that hMSCs cultured on 2-D polyacrylamide substrates of varying stiffness undergo lineage-specific differentiation to become cell types characteristic of tissues with the corresponding stiffness. A later study

showed that NSCs cultured on variable modulus substrates differentiate preferentially into neurons on softer substrates and astrocytes on stiffer materials [128]. In addition to differentiation, matrix elasticity can influence stem cell self-renewal. For instance, it was observed that 2-D soft substrates promote the ability of embryonic stem cells [129] and adult muscle stem cells [130] to self-renew in culture.

However, it is important to note that most studies of stem cell mechanotransduction have been performed with 2-D substrate systems [128–130], which lacked the 3-D complexity of the naive tissue environment. How stem cells sense and respond to the mechanics of their 2-D or 3-D microenvironments can be very different, resulting in changes in cell functions. This disparity in cell functions have been shown in studies, where cells showed increased spreading and motility on stiff 2-D matrix, but were confined to the 3-D matrix that it must degrade or deform [131]. One of the major challenges in understanding mechanosensitivity within 3-D microenvironments is the ability to decouple the effects of matrix mechanics from that caused by crosslinking density and porosity, since increased mechanics is often caused by increased crosslinking density that results in decreased mesh size and permeability.

While the matrix composition and mechanical structure determine the stem cell proliferation and differentiation, the matrix degradation rate influences the cell migration, matrix deposition, remodelling and tissue morphogenesis [131]. A variety of different systems have emerged to better control gel degradation. Hydrogels can be designed to undergo hydrolytic or enzymatic degradation where the latter allows for biomimetic control over local degradation dictated by the amount of cell enzyme secretion and the susceptibility of the cross-linker peptide sequence. The importance of cell-mediated gel degradation has been shown in studies to promote stem cell growth and differentiation as well as in neotissue formation where rate of gel degradation should match the rate of cell growth and matrix deposition in neotissue formation. Light may also be used to control hydrogel degradation, where photodegradable networks can be created that can undergo reverse gelation under cytocompatible conditions. These photodegradable hydrogels allow the greatest advantage of external control of degradation and in situ tuning of hydrogel mechanics. Seliktar and colleagues have used high-intensity pulsed laser light to photoablate guidance channels in transparent hydrogels to guide neural growth into the gel, which opens potential for treating nerve injuries [132].

4.2 Growth Factors and Biomolecules

Morphogens have been known to regulate cell fate and tissue morphogenesis during development [126] and represents the most potent and direct regulation of cell fate and function towards the lineage-of-interest [8, 133]. Many of these soluble factors are immobilized to the ECM framework via matrix-binding domains. The spatial distribution of factors with local and/or gradient concentrations, duration

and timing of exposure, and ligand presentation modulate the level of morphogen activity and cellular signaling to regulate cell fate and functions [126, 134].

Synthetic hydrogel systems enable delivery of morphogens in a spatiotemporally-controlled manner that affects signalling. Direct encapsulation is the conventional method of delivery in hydrogels, but limitations of this approach include poor control of release profiles. Often, there will a burst release profile, which may result in adverse cellular responses and tissue reactions [135]. One attractive approach to overcome this limitation is to incorporate into the hydrogels micro or nanoparticle delivery vehicles that may allow single or multiple growth factors to be released in a controlled and sustained fashion [101]. In order to further improve the growth factor stability and specificity, there are also efforts to identify the functional peptide domain sequences of growth factors, including those that bind to growth factor receptors and proteoglycans including heparin sulfate, as an alternative to the use of entire growth factor [136, 137].

In addition to the control of single or multiple growth factor release, spatial distribution of the growth factors within the 3-D hydrogel microenvironment could influence specific cellular processes. Wylie and colleagues used barnase-bastar and streptavidin-biotin binding pairs to immobilize sonic hedgehog (SHH) and ciliary neurotrophic factor (CNTF), respectively into modified agarose gel, thereby creating immobilized gradients of growth factors in distinct regions within the hydrogel microenvironment for guided cell migration and differentiation [138].

4.3 Support Cells

Support cells play important roles in regulating the self-renewal, mobilization and differentiation of stem cells. Support cells can interact with stem cells by direct contact through receptors and gap junctions, and by paracrine secretion of growth factors to influence cell fate and functions. In adult tissues, such as the adult brain, it has been shown that the adult hippocampal NSC proliferation occurs in a vascular niche where there is endothelial component of the vasculature, while NSC differentiation is promoted by contact with astrocytes [139]. The concept of support cells is perhaps best represented in vitro by the use of feeder cells [140] and feeder cell-derived matrices [141, 142] to support the self-renewal and pluripotency of hESCs.

In application of stem cells for tissue regeneration, support cells are often committed cell types that can be co-cultured with the stem cells to direct specific differentiation [143, 144]. In this instance, hydrogels serve as a platform to control the interactions between the stem and support cells [145] and as a delivery system to enable delivery of multiple cell types for regeneration of complex tissues [146]. It has been shown in several studies that co-delivery of stem cells and support cells have synergistic effects in tissue regeneration [146, 147].

5 Microfabricated Hydrogels

Microtechnologies including microfluidics and micropatterning are fast-evolving technologies that have become an integral part of constructing stem cell microenvironments using hydrogels. Besides modulating hydrogel micro-architecture (e.g. porosity) and composition by changing the polymer or cross-linking chemistry, hydrogels can be tuned by using microtechnologies to control their meso-scale structures. This allows one to reduce the feature size of the hydrogel structures being formed, which in turn translates to more precise control over the cell locality in 3-D space.

There are two general approaches to constructing a microfabricated cellular environment using hydrogels. A more simple approach is to first fabricate the hydrogel-based micro-structure before seeding cells onto it. For instance, hydrogel microwells are frequently constructed for the formation of ESC embryoid bodies (EBs) with controllable sizes [148]. 3D projection stereolithography as well as two-photon laser scanning photolithography (TPLSP) have been used to generate hydrogel scaffolds of defined architecture, porosity and interconnectivity [149, 150]. The advantage of decoupling hydrogel microfabrication from cell seeding is that we do not impose any restriction on the fabrication conditions (e.g. pH, temperature). However, control over the positioning of cells is much poorer since cells are stochastically located within the hydrogel micro-architecture.

The more commonly used approach to have more control over cell locality in 3D space is to generate cell-laded hydrogel micro-structures. Cells are suspended in the prepolymer before crosslinking is induced to "freeze" the cells in 3D space. UV polymerization of poly(ethylene glycol) diacrylate (PEGDA) is one of the most commonly used method. UV light can be spatially directed at submillimeter resolution onto a PEGDA solution impregnated with cells to induce crosslinking via photolithography [151] or TPLSP [152]. PEGDA-based hydrogels can be further modified to include bioactive active ligands, such as RGD peptides, to improve the bio-functionality or bio-compatibility of the hydrogels [151]. Photopolymerized hydrogels can also be used in conjunction with other microtechnologies to have an additional degree of control over the 3D multicellular construct. Albrecht et al. used dielectrophoresis (DEP) patterning to control the relative positions of two or more cell types before immobilizing them in 3D space by photopolymerized PEG hydrogel [153]. Photopatterned hydrogels are often used to immobilize cells within microfluidic systems [154, 155]. In another example, a 3D network of carbohydrate glass is printed within cell-laded PEG hydrogels to serve as a vascular network, which can be independently populated with endothelial cells [156]. Other than PEGDA, a myriad of photopolymerizable hydrogels have been developed. Typically, these hydrogels are the polymerizable variants of common hydrogels, such as hyaluronic acid (HA) [157], polyvinylalcohol (PVA) [158], and gelatin [159].

What are the biological implications of using microfabricated hydrogels to fine-tune the stem cell environment? Firstly, there is an overall improvement of mass transport to the cell-hydrogel construct due to a smaller diffusion distance [160]. Micropatterned hydrogels also offer protection from fluid shear stress in microfluidic perfusion culture systems that are meant to augment mass transport [161]. One can also achieve better control over heterotypic cell-cell interactions by being able to position two or more different cells types at defined locations. For instance, patterning stellate cells together with ESC can enhance their hepatic differentiation capacity [162]. In another configuration, tracks of cell-loaded fibrin hydrogels were patterned at different distances to investigate interactions between endothelial cells and MSCs in vasculogenesis [145].

One of the most notable biological effects enabled by microfabricated hydrogels is perhaps the spatial patterning of stem cell differentiation by creating juxtaposed differential 3D microenvironments. Qi et al., encapsulated mouse EBs in spatially asymmetrical hybrid hydrogel, where half of the EB was exposed to gelatin and the other half exposed to PEG. Owing to the differences of the different hydrogel microenvironments in directing vascular differentiation, they could spatially direct vasculogenesis in the EBs [163]. Khetan and Burdick employed a different strategy to create an asymmetrical 3D hydrogel microenvironments by performing UV photolithography on a primary HA hydrogel crosslinked by enzymatic reactions. Human MSCs could remodel and spread in areas that were not exposed to UV but remained rounded in UV exposed regions. This led to the spatially patterning of osteogenic-adipogenic differentiation fates of the hMSCs [164].

6 Complexity of Tissue Environment

The tissue environment is dynamic in nature and present spatial and temporal heterogeneity in the cellular and matrix composition, and this dynamics is highly impacted by the type and state of the tissue environment, whether in healthy or injured/diseased state [165]. The level of oxygenation and nutrient supply, oxidative stress and inflammation present in the injured/diseased tissue environment are likely to affect the mobilization of stem cells from the stem cell niche as well as the survival and engraftment of exogenous stem cells, and are therefore important considerations when applying hydrogels to recruit or deliver stem cells to the site of tissue injury [165]. In this aspect, modifying the tissue environment by strategies such as pre-conditioning, anti-inflammation and/or anti-oxidative injury may be helpful in the transplanted cell survival and engraftment. Modulating the cellular processes and guiding the development of the neotissue formation in parallel with the changes of the tissue environment would be pivotal in determining the outcome of the regenerative therapy.

7 Advanced Hydrogel Systems for Stem Cell Delivery

To better tailor stem cell therapies to the dynamic complexity of the tissue environment [165], whether in healthy or injured state, multi-phased and multi-functional hydrogel systems are being developed for stem cell delivery [43, 44, 47].

7.1 Multi-phased Hydrogels

The spatial organization of cells and biomolecules and the relative distribution in the hydrogel network are important in guiding the cellular processes including cell proliferation, differentiation and tissue morphogenesis towards the de novo formation of complex hierarchical tissue. Utilization of techniques including co-culture/co-encapsulation of different cells [147], photopatterning [166], and multi-phased/multi-layered hydrogel systems [167, 168] may aid in the spatially controlled organization of multiple cell types and bioactive molecules and facilitate the progress towards better organization and functionality of newly-generated complex tissue in vivo.

A notable study in this direction is the development of a three-layer PEG-based hydrogel to direct differentiation of single population of MSCs into multiple, spatially distinct phenotypes within the 3-D scaffold [167]. The three-layer PEG hydrogel with chondroitin sulfate and MMP-sensitive peptides in the top layer, chondroitin sulfate in the middle layer, and hyaluronic acid in the bottom layer, creates the zonal organization (superficial, transitional and deep zones) of the native-like articular cartilage. This study suggests the possibility of regenerating complex tissues from a single stem cell population by spatially varying the biomaterial composition to direct stem cell differentiation into multiple distinct phenotypes. Other studies utilize bilayered hydrogel matrices for co-culture of stem cells with committed somatic cells to direct stem cell differentiation [169, 170].

Towards this end, design of multi-phased hydrogel systems that allow directed stem cell differentiation to multiple lineages or co-culture/co-encapsulation of multiple cell types or biomolecules may improve the spatial organization of the newly generated tissue in vivo.

7.2 Multi-functional Hydrogels

During tissue injury, oxidative stress and inflammatory processes are always prevailing, making the tissue environment at the injury sites highly unfavorable for the introduction of therapeutic cells including stem cells. Oxidative stress is associated with increased production of oxidizing species including the production of

peroxides and free radicals that can damage all components of the cell, including proteins, lipids and DNA. Inflammation involves the production of cytokines including tumor necrosis factor-alpha (TNF-α) and interleukin-1α/β, and recruitment of inflammatory cells including monocytes and macrophages that are capable of secreting MMPs involved in matrix degradation. Both oxidative stress and inflammation can trigger cell death by mechanisms of apoptosis or necrosis, implicating these processes as important considerations when delivering cells in injectable hydrogels to the site of tissue injury.

In view of these considerations, various strategies by means of functionalization or loading of the hydrogel with anti-oxidants or anti-inflammatory agents and receptor blocking agents against oxidative stress and/or inflammation were developed [171–174]. A notable study in this direction is the development of thermosensitive chitosan hydrogel conjugated covalently with glutathione, a well-known anti-oxidant peptide molecule [171]. This functionalized hydrogel with anti-oxidant property are capable of scavenging reactive oxygen species (ROS) including oxygen radicals (superoxide and hydroxyl radicals) and was shown to enhance the survival of cardiomyocytes in the presence of hydrogen peroxide (H_2O_2) inducing oxidative stress [171]. Similarly, ferulic acid has been incorporated into the chitosan-gelatin-glycerophosphate hydrogel [172] or poly (anhydride-ester) nanogel [173] to improve the ROS scavenging capacity. Although H_2O_2 induces oxidative stress, it has been used as oxidant in the oxidative coupling reaction in the enzymatically cross-linked material systems such as HA-Tyr and Gtn-HPA, and it was found that the HRP-catalyzed cross-linking mechanism utilizing very low amount of H_2O_2 in the oxidative coupling reaction preconditioned the NSCs encapsulated in 3-D Gtn-HPA hydrogel and enhanced the oxidative stress resistance and survival of these cells, which might be potentially applied for neural regeneration [100]. Some biopolymers also possessed natural antioxidant capability. One example is the polymer pullulan, a carbohydrate glucan, known to exhibit potent antioxidant capabilities, and was recently demonstrated in a study that pullulan-based hydrogels were effective in delivery of MSCs and enhanced survival and engraftment in a high ROS environment in an ischemic excisional wound model in mouse [175].

Towards this end, the development of hydrogels that can modulate the tissue environment for enhanced survival and engraftment of the exogenous stem cells delivered, or even recruit endogenous adult stem cells to the tissue site of injury, is most likely to improve the outcome of the regenerative therapy.

8 Conclusions and Perspectives

Hydrogel-based culture platforms, coupled with advanced hydrogel designs and fast-evolving microtechnologies, have the greatest potential in constructing complex artificial stem cell microenvironments. Specific bioactive niche components may be incorporated into the microenvironment to modulate and manipulate stem

cell fate and function. Such components may be support cells and/or biomolecules and drugs that might affect stem cell fates (survival, self-renewal and differentiation). Notably, with the advances in hydrogel chemistries and micropatterning techniques, we can now control the spatial organization of cells and biomolecules and study the cell-cell and cell-matrix interactions over space and time in a well-controlled manner. Looking forward, defining the specific niche components present in the stem cell microenvironment and deciphering the underlying mechanisms will allow researchers to develop new therapeutics to enhance stem cell function and promote regeneration of injured or diseased tissues in vivo.

As mentioned, the tissue environment is dynamic in nature and present spatial and temporal heterogeneity in the cellular and matrix composition, and this dynamics is highly impacted by the type and state of the tissue environment, whether in healthy or injured/diseased state. Oxidative stress and inflammation present in the injured/diseased tissue environment are likely to affect the mobilization of stem cells from the stem cell niche as well as the survival and engraftment of exogenous stem cells, and are therefore important considerations when delivering cells in injectable hydrogels to the site of tissue injury. Looking forward, strategies of anti-inflammation and/or anti-oxidative injury may be incorporated into multifunctional hydrogels to modify the tissue environment and help in the survival/engraftment of the transplanted cells. Modulating the cellular processes and guiding the development of the neotissue formation in parallel with the changes of the tissue environment would be pivotal in determining the outcome of the regenerative therapy.

Looking into the future, combined approaches utilizing hydrogels, microtechnologies and controlled release strategies will provide new insights into the mechanistic regulation of stem cell fate. These advances in hydrogel design and related enabling technologies will continue to grow and aid in our future design of customized hydrogel delivery systems for healthy and injured/diseased tissues, and guide the development of future therapies.

Acknowledgement This work was supported by National University of Singapore, National University Healthcare System, Ministry of Education and A*STAR SERC Personal Care IAF.

Disclosure The author indicates no potential conflict of interest.

References

1. Caplan, A.I.: Adult mesenchymal stem cells for tissue engineering versus regenerative medicine. J. Cell. Physiol. **213**, 341–347 (2007)
2. Tabar, V., Studer, L.: Pluripotent stem cells in regenerative medicine: challenges and recent progress. Nat. Rev. Genet. **15**, 82–92 (2014)
3. Vazin, T., Schaffer, D.V.: Engineering strategies to emulate the stem cell niche. Trends Biotechnol. **28**, 117–124 (2010)
4. Boyer, L.A., Lee, T.I., Cole, M.F., Johnstone, S.E., Levine, S.S., Zucker, J.P., et al.: Core transcriptional regulatory circuitry in human embryonic stem cells. Cell **122**, 947–956 (2005)

5. Fuchs, E., Tumbar, T., Guasch, G.: Socializing with the neighbors: stem cells and their niche. Cell **116**, 769–778 (2004)
6. Pittenger, M.F., Mackay, A.M., Beck, S.C., Jaiswal, R.K., Douglas, R., Mosca, J.D., et al.: Multilineage potential of adult human mesenchymal stem cells. Science **284**, 143–147 (1999)
7. Thomson, J.A., Itskovitz-Eldor, J., Shapiro, S.S., Waknitz, M.A., Swiergiel, J.J., Marshall, V.S., et al.: Embryonic stem cell lines derived from human blastocysts. Science **282**, 1145–1147 (1998)
8. Toh, W.S., Liu, H., Heng, B.C., Rufaihah, A.J., Ye, C.P., Cao, T.: Combined effects of TGFβ1 and BMP2 in serum-free chondrogenic differentiation of mesenchymal stem cells induced hyaline-like cartilage formation. Growth Factors **23**, 313–321 (2005)
9. Mackay, A.M., Beck, S.C., Murphy, J.M., Barry, F.P., Chichester, C.O., Pittenger, M.F.: Chondrogenic differentiation of cultured human mesenchymal stem cells from marrow. Tissue Eng. **4**, 415–428 (1998)
10. Liu, H., Toh, W.S., Lu, K., MacAry, P.A., Kemeny, D.M., Cao, T.: A subpopulation of mesenchymal stromal cells with high osteogenic potential. J. Cell Mol. Med. **13**, 2436–2447 (2009)
11. Lu, Q., Liu, H., Cao, T.: Efficient Isolation of bone marrow adipocyte progenitors by silica microbeads incubation. Stem Cells Dev. **22**, 2520–2531 (2013)
12. Liu, T.M., Martina, M., Hutmacher, D.W., Hui, J.H.P., Lee, E.H., Lim, B.: Identification of common pathways mediating differentiation of bone marrow- and adipose tissue-derived human mesenchymal stem cells into three mesenchymal lineages. Stem Cells **25**, 750–760 (2007)
13. Gimble, J.M., Guilak, F.: Adipose-derived adult stem cells: isolation, characterization, and differentiation potential. Cytotherapy **5**, 362–369 (2003)
14. Jones, B.A., Pei, M.: Synovium-derived stem cells: a tissue-specific stem cell for cartilage engineering and regeneration. Tissue Eng. Part B. Rev. **18**, 301–311 (2012)
15. Fan, J., Varshney, R.R., Ren, L., Cai, D., Wang, D.-A.: Synovium-derived mesenchymal stem cells: a new cell source for musculoskeletal regeneration. Tissue Eng. Part B. Rev. **15**, 75–86 (2009)
16. Chang, H., Knothe Tate, M.L.: Concise review: the periosteum: tapping into a reservoir of clinically useful progenitor cells. Stem Cells Transl. Med. **1**, 480–491 (2012)
17. Lian, Q., Lye, E., Suan Yeo, K., Khia Way Tan, E., Salto-Tellez, M., Liu, T.M., et al.: Derivation of Clinically Compliant MSCs from CD105+ CD24− Differentiated Human ESCs. Stem Cells **25**, 425–436 (2007)
18. Lian, Q., Zhang, Y., Zhang, J., Zhang, H.K., Wu, X., Zhang, Y., et al.: Functional mesenchymal stem cells derived from human induced pluripotent stem cells attenuate limb ischemia in mice. Circulation **121**, 1113–1123 (2010)
19. Toh, W.S., Lee, E.H., Cao, T.: Potential of human embryonic stem cells in cartilage tissue engineering and regenerative medicine. Stem Cell Rev. **7**, 544–559 (2011)
20. da Silva, Meirelles L., Fontes, A.M., Covas, D.T., Caplan, A.I.: Mechanisms involved in the therapeutic properties of mesenchymal stem cells. Cytokine Growth Factor Rev. **20**, 419–427 (2009)
21. Stolzing, A., Jones, E., McGonagle, D., Scutt, A.: Age-related changes in human bone marrow-derived mesenchymal stem cells: Consequences for cell therapies. Mech. Ageing Dev. **129**, 163–173 (2008)
22. Payne, K.A., Didiano, D.M., Chu, C.R.: Donor sex and age influence the chondrogenic potential of human femoral bone marrow stem cells. Osteoarthritis Cartilage **18**, 705–713 (2010)
23. Shiba, Y., Fernandes, S., Zhu, W.-Z., Filice, D., Muskheli, V., Kim, J., et al.: Human ES-cell-derived cardiomyocytes electrically couple and suppress arrhythmias in injured hearts. Nature **489**, 322–325 (2012)
24. Zhang, J., Wilson, G.F., Soerens, A.G., Koonce, C.H., Yu, J., Palecek, S.P., et al.: Functional cardiomyocytes derived from human induced pluripotent stem cells. Circ. Res. **104**, e30–e41 (2009)

25. Rufaihah, A.J., Haider, H.K., Heng, B.C., Ye, L., Toh, W.S., Tian, X.F., et al.: Directing endothelial differentiation of human embryonic stem cells via transduction with an adenoviral vector expressing the VEGF165 gene. J. Gene Med. **9**, 452–461 (2007)
26. Rufaihah, A.J., Haider, H.K., Heng, B.C., Ye, L., Tan, R.S., Toh, W.S., et al.: Therapeutic angiogenesis by transplantation of human embryonic stem cell-derived CD133+ endothelial progenitor cells for cardiac repair. Regen. Med. **5**, 231–244 (2010)
27. Toh, W.S., Yang, Z., Liu, H., Heng, B.C., Lee, E.H., Cao, T.: Effects of culture conditions and bone morphogenetic protein 2 on extent of chondrogenesis from human embryonic stem cells. Stem Cells **25**, 950–960 (2007)
28. Toh, W.S., Guo, X.-M., Choo, A.B., Lu, K., Lee, E.H., Cao, T.: Differentiation and enrichment of expandable chondrogenic cells from human embryonic stem cells in vitro. J. Cell Mol. Med. **13**, 3570–3590 (2009)
29. Toh, W.S., Yang, Z., Heng, B.C., Cao, T.: Differentiation of human embryonic stem cells toward the chondrogenic lineage. Methods Mol. Biol. **407**, 333–349 (2007)
30. Toh, W.S., Lee, E.H., Richards, M., Cao, T.: In vitro derivation of chondrogenic cells from human embryonic stem cells. Methods Mol. Biol. **584**, 317–331 (2010)
31. Cao, T., Heng, B.C., Ye, C.P., Liu, H., Toh, W.S., Robson, P., et al.: Osteogenic differentiation within intact human embryoid bodies result in a marked increase in osteocalcin secretion after 12 days of in vitro culture, and formation of morphologically distinct nodule-like structures. Tissue Cell **37**, 325–334 (2005)
32. Heng, B.C., Toh, W.S., Pereira, B.P., Tan, B.L., Fu, X., Liu, H., et al.: An autologous cell lysate extract from human embryonic stem cell (hESC) derived osteoblasts can enhance osteogenesis of hESC. Tissue Cell **40**, 219–228 (2008)
33. Guloglu, M.O., Larsen, A., Brundin, P.: Adipocytes derived from PA6 cells reliably promote the differentiation of dopaminergic neurons from human embryonic stem cells. J. Neurosci. Res. **92**, 564–573 (2014)
34. Zhang, S.-C., Wernig, M., Duncan, I.D., Brustle, O., Thomson, J.A.: In vitro differentiation of transplantable neural precursors from human embryonic stem cells. Nat. Biotech. **19**, 1129–1133 (2001)
35. Kidwai, F.K., Liu, H., Toh, W.S., Fu, X., Jokhun, D.S., Movahednia, M.M., et al.: Differentiation of human embryonic stem cells into clinically amenable keratinocytes in an autogenic environment. J. Invest. Dermatol. **133**, 618–628 (2013)
36. Hay, D.C., Zhao, D., Fletcher, J., Hewitt, Z.A., McLean, D., Urruticoechea-Uriguen, A., et al.: Efficient differentiation of hepatocytes from human embryonic stem cells exhibiting markers recapitulating liver development in vivo. Stem Cells **26**, 894–902 (2008)
37. Takahashi, K., Tanabe, K., Ohnuki, M., Narita, M., Ichisaka, T., Tomoda, K., et al.: Induction of pluripotent stem cells from adult human fibroblasts by defined factors. Cell **131**, 861–872 (2007)
38. Heng, B., Cao, T., Haider, H., Wang, D., Sim, E.-W., Ng, S.: An overview and synopsis of techniques for directing stem cell differentiation in vitro. Cell Tissue Res. **315**, 291–303 (2004)
39. Heng, B.C., Cao, T., Lee, E.H.: Directing stem cell differentiation into the chondrogenic lineage in vitro. Stem Cells **22**, 1152–1167 (2004)
40. Heng, B.C., Cao, T., Stanton, L.W., Robson, P., Olsen, B.: Strategies for directing the differentiation of stem cells into the osteogenic lineage in vitro. J. Bone Miner. Res. **19**, 1379–1394 (2004)
41. Heng, B.C., Haider, H.K., Sim, E.K.-W., Cao, T., Ng, S.C.: Strategies for directing the differentiation of stem cells into the cardiomyogenic lineage in vitro. Cardiovasc. Res. **62**, 34–42 (2004)
42. Toh, W.S., Spector, M., Lee, E.H., Cao, T.: Biomaterial-mediated delivery of microenvironmental cues for repair and regeneration of articular cartilage. Mol. Pharm. **8**, 994–1001 (2011)
43. Lutolf, M.P., Hubbell, J.A.: Synthetic biomaterials as instructive extracellular microenvironments for morphogenesis in tissue engineering. Nat. Biotech. **23**, 47–55 (2005)
44. Guvendiren, M., Burdick, J.A.: Engineering synthetic hydrogel microenvironments to instruct stem cells. Curr. Opin. Biotechnol. **24**, 841–846 (2013)

45. Lutolf, M.P., Gilbert, P.M., Blau, H.M.: Designing materials to direct stem-cell fate. Nature **462**, 433–441 (2009)
46. Hoffman, A.S.: Hydrogels for biomedical applications. Adv. Drug Deliv. Rev. **54**, 3–12 (2002)
47. Fisher, O.Z., Khademhosseini, A., Langer, R., Peppas, N.A.: Bioinspired materials for controlling stem cell fate. Acc. Chem. Res. **43**, 419–428 (2009)
48. Bhattarai, N., Ramay, H.R., Gunn, J., Matsen, F.A., Zhang, M.Q.: PEG-grafted chitosan as an injectable thermosensitive hydrogel for sustained protein release. J. Controlled Release **103**, 609–624 (2005)
49. Chenite, A., Buschmann, M., Wang, D., Chaput, C., Kandani, N.: Rheological characterisation of thermogelling chitosan/glycerol-phosphate solutions. Carbohydr. Polym. **46**, 39–47 (2001)
50. Cao, Y.X., Zhang, C., Shen, W.B., Cheng, Z.H., Yu, L.L., Ping, Q.N.: Poly(N-isopropylacrylamide)-chitosan as thermosensitive in situ gel-forming system for ocular drug delivery. J. Controlled Release **120**, 186–194 (2007)
51. Nair, L.S., Starnes, T., Ko, J.W.K., Laurencin, C.T.: Development of injectable thermogelling chitosan-inorganic phosphate solutions for biomedical applications. Biomacromolecules **8**, 3779–3785 (2007)
52. Li, Z., Cho, S., Kwon, I.C., Janát-Amsbury, M.M., Huh, K.M.: Preparation and characterization of glycol chitin as a new thermogelling polymer for biomedical applications. Carbohydr. Polym. **92**, 2267–2275 (2013)
53. Mazumder, M.A.J., Fitzpatrick, S.D., Muirhead, B., Sheardown, H.: Cell-adhesive thermogelling PNIPAAm/hyaluronic acid cell delivery hydrogels for potential application as minimally invasive retinal therapeutics. J. Biomed. Mater. Res., Part A **100A**, 1877–1887 (2012)
54. Arvidson, S.A., Lott, J.R., McAllister, J.W., Zhang, J., Bates, F.S., Lodge, T.P., et al.: Interplay of phase separation and thermoreversible gelation in aqueous methylcellulose solutions. Macromolecules **46**, 300–309 (2012)
55. Hwang, M.J., Joo, M.K., Choi, B.G., Park, M.H., Hamley, I.W., Jeong, B.: Multiple sol-gel transitions of PEG-PCL-PEG triblock copolymer aqueous solution. Macromol. Rapid Commun. **31**, 2064–2069 (2010)
56. Hwang, M.J., Suh, J.M., Bae, Y.H., Kim, S.W., Jeong, B.: Caprolactonic poloxamer analog: PEG-PCL-PEG. Biomacromolecules **6**, 885–890 (2005)
57. Bae, S.J., Joo, M.K., Jeong, Y., Kim, S.W., Lee, W.K., Sohn, Y.S., et al.: Gelation behavior of poly(ethylene glycol) and polycaprolactone triblock and multiblock copolymer aqueous solutions. Macromolecules **39**, 4873–4879 (2006)
58. Bae, S.J., Suh, J.M., Sohn, Y.S., Bae, Y.H., Kim, S.W., Jeong, B.: Thermogelling poly(caprolactone-b-ethylene glycol-b-caprolactone) aqueous solutions. Macromolecules **38**, 5260–5265 (2005)
59. Chung, Y.M., Simmons, K.L., Gutowska, A., Jeong, B.: Sol-gel transition temperature of PLGA-g-PEG aqueous solutions. Biomacromolecules **3**, 511–516 (2002)
60. Jeong, B., Wang, L.Q., Gutowska, A.: Biodegradable thermoreversible gelling PLGA-g-PEG copolymers. Chem. Commun. **16**, 1516–1517 (2001)
61. Jeong, B., Windisch, C.F., Park, M.J., Sohn, Y.S., Gutowska, A., Char, K.: Phase transition of the PLGA-g-PEG copolymer aqueous solutions. J. Phys. Chem. B **107**, 10032–10039 (2003)
62. Tarasevich, B.J., Gutowska, A., Li, X.S., Jeong, B.M.: The effect of polymer composition on the gelation behavior of PLGA-g-PEG biodegradable thermoreversible gels. J. Biomed. Mater. Res., Part A **89A**, 248–254 (2009)
63. Jeong, B., Bae, Y.H., Kim, S.W.: Biodegradable thermosensitive micelles of PEG-PLGA-PEG triblock copolymers. Colloids Surf., B **16**, 185–193 (1999)
64. Jeong, B., Bae, Y.H., Kim, S.W.: Thermoreversible gelation of PEG-PLGA-PEG triblock copolymer aqueous solutions. Macromolecules **32**, 7064–7069 (1999)

65. Jeong, B., Bae, Y.H., Kim, S.W.: In situ gelation of PEG-PLGA-PEG triblock copolymer aqueous solutions and degradation thereof. J. Biomed. Mater. Res. **50**, 171–177 (2000)
66. Jeong, B., Bae, Y.H., Kim, S.W.: Drug release from biodegradable injectable thermosensitive hydrogel of PEG-PLGA-PEG triblock copolymers. J. Controlled Release **63**, 155–163 (2000)
67. Jeong, B., Kibbey, M.R., Birnbaum, J.C., Won, Y.Y., Gutowska, A.: Thermogelling biodegradable polymers with hydrophilic backbones: PEG-g-PLGA. Macromolecules **33**, 8317–8322 (2000)
68. Choi, S.W., Choi, S.Y., Jeong, B., Kim, S.W., Lee, D.S.: Thermoreversible gelation of poly(ethylene oxide) biodegradable polyester block copolymers. II. J. Poly. Sci., Part A. Poly. Chem. **37**, 2207–2218 (1999)
69. Joo, M.K., Sohn, Y.S., Jeong, B.: Stereoisomeric effect on reverse thermal gelation of poly(ethylene glycol)/poly(lactide) multiblock copolymer. Macromolecules **40**, 5111–5115 (2007)
70. Jeong, Y., Joo, M.K., Bahk, K.H., Choi, Y.Y., Kim, H.T., Kim, W.K., et al.: Enzymatically degradable temperature-sensitive polypeptide as a new in situ gelling biomaterial. J. Controlled Release **137**, 25–30 (2009)
71. Kang, E.Y., Yeon, B., Moon, H.J., Jeong, B.: PEG-L-PAF and PEG-D-PAF: Comparative Study on Thermogellation and Biodegradation. Macromolecules **45**, 2007–2013 (2012)
72. Kim, E.H., Joo, M.K., Bahk, K.H., Park, M.H., Chi, B., Lee, Y.M., et al.: Reverse thermal gelation of PAF-PLX-PAF block copolymer aqueous solution. Biomacromolecules **10**, 2476–2481 (2009)
73. Shinde, U.P., Joo, M.K., Moon, H.J., Jeong, B.: Sol-gel transition of PEG-PAF aqueous solution and its application for hGH sustained release. J. Mater. Chem. **22**, 6072–6079 (2012)
74 Ho, A.K., Bromberg, L.E., Huibers, P.D.T., O'Connor, A.J., Perera, J.M., Stevens, G.W., et al.: Hydrophobic domains in thermogelling solutions of polyether-modified poly(acrylic acid). Langmuir **18**, 3005–3013 (2002)
75. Cleary, J., Bromberg, L.E., Magner, E.: Diffusion and release of solutes in pluronic-g-poly(acrylic acid) hydrogels. Langmuir **19**, 9162–9172 (2003)
76. Liu, W.G., Zhang, B.Q., Lu, W.W., Li, X.W., Zhu, D.W., De Yao, K., et al.: A rapid temperature-responsive sol-gel reversible poly(N-isopropylacrylamide)-g-methylcellulose copolymer hydrogel. Biomaterials **25**, 3005–3012 (2004)
77. Kitazawa, Y., Ueki, T., Niitsuma, K., Imaizumi, S., Lodge, T.P., Watanabe, M.: Thermoreversible high-temperature gelation of an ionic liquid with poly(benzyl methacrylate-b-methyl methacrylate-b-benzyl methacrylate) triblock copolymer. Soft Matter **8**, 8067–8074 (2013)
78. Abandansari, H.S., Aghaghafari, E., Nabid, M.R., Niknejad, H.: Preparation of injectable and thermoresponsive hydrogel based on penta-block copolymer with improved sol stability and mechanical properties. Polymer **54**, 1329–1340 (2013)
79. Li, Z.Q., Guo, X.L., Matsushita, S., Guan, J.J.: Differentiation of cardiosphere-derived cells into a mature cardiac lineage using biodegradable poly(N-isopropylacrylamide) hydrogels. Biomaterials **32**, 3220–3232 (2011)
80. Loh, X.J., Cheng, L.W.I., Li, J.: Micellization and thermogelation of poly(ether urethane) s comprising poly(ethylene glycol) and poly(propylene glycol). Modern Trends Polym. Sci. **Epf 09**, 161–169 (2010)
81. Loh, X.J., Goh, S.H., Li, J.: New biodegradable thermogelling copolymers having very low gelation concentrations. Biomacromolecules **8**, 585–593 (2007)
82. Loh, X.J., Li, J.: Biodegradable thermosensitive copolymer hydrogels for drug delivery. Expert Opin. Ther. Pat. **17**, 965–977 (2007)
83. Loh, X.J., Wang, X., Li, H.Z., Li, X., Li, J.: Compositional study and cytotoxicity of biodegradable poly(ester urethane)s consisting of poly [(R)-3-hydroxybutyrate] and poly(ethylene glycol). Mater. Sci. Eng., C. Biomimetic Supramol. Syst. **27**, 267–273 (2007)

84. Loh, X.J., Tan, Y.X., Li, Z.Y., Teo, L.S., Goh, S.H., Li, J.: Biodegradable thermogelling poly(ester urethane)s consisting of poly(lactic acid)—Thermodynamics of micellization and hydrolytic degradation. Biomaterials **29**, 2164–2172 (2008)
85. Loh, X.J., Sng, K.B.C., Li, J.: Synthesis and water-swelling of thermo-responsive poly(ester urethane)s containing poly(epsilon-caprolactone), poly(ethylene glycol) and poly(propylene glycol). Biomaterials **29**, 3185–3194 (2008)
86. Loh, X.J., Yee, B.J.H., Chia, F.S.: Sustained delivery of paclitaxel using thermogelling poly(PEG/PPG/PCL urethane)s for enhanced toxicity against cancer cells. J. Biomed. Mater. Res., Part A **100A**, 2686–2694 (2012)
87. Loh, X.J., Vu, P.N.N., Kuo, N.Y., Li, J.: Encapsulation of basic fibroblast growth factor in thermogelling copolymers preserves its bioactivity. J. Mater. Chem. **21**, 2246–2254 (2011)
88. Nguyen, V.P.N., Kuo, N.Y., Loh, X.J.: New biocompatible thermogelling copolymers containing ethylene-butylene segments exhibiting very low gelation concentrations. Soft Matter **7**, 2150–2159 (2011)
89. Loh, X.J., Guerin, W., Guillaume, S.M.: Sustained delivery of doxorubicin from thermogelling poly(PEG/PPG/PTMC urethane)s for effective eradication of cancer cells. J. Mater. Chem. **22**, 21249–21256 (2012)
90. Park, D., Wu, W., Wang, Y.D.: A functionalizable reverse thermal gel based on a polyurethane/PEG block copolymer. Biomaterials **32**, 777–786 (2011)
91. Schexnailder, P., Schmidt, G.: Nanocomposite polymer hydrogels. Colloid Polym. Sci. **287**, 1–11 (2009)
92. Skrabalak, S.E., Chen, J., Au, L., Lu, X., Li, X., Xia, Y.: Gold nanocages for biomedical applications. Adv. Mater. **19**, 3177–3184 (2007)
93. Skrabalak, S.E., Chen, J., Sun, Y., Lu, X., Au, L., Cobley, C.M., et al.: Gold nanocages: synthesis, properties, and applications. Acc. Chem. Res. **41**, 1587–1595 (2008)
94. Ye, E., Win, K.Y., Tan, H.R., Lin, M., Teng, C.P., Mlayah, A., et al.: Plasmonic gold nanocrosses with multidirectional excitation and strong photothermal effect. J. Am. Chem. Soc. **133**, 8506–8509 (2011)
95. Sershen, S.R., Westcott, S.L., Halas, N.J., West, J.L.: Temperature-sensitive polymer–nanoshell composites for photothermally modulated drug delivery. J. Biomed. Mater. Res. **51**, 293–298 (2000)
96. Yan, B., Boyer, J.-C., Habault, D., Branda, N.R., Zhao, Y.: Near infrared light triggered release of biomacromolecules from hydrogels loaded with upconversion nanoparticles. J. Am. Chem. Soc. **134**, 16558–16561 (2012)
97. Hoare, T., Santamaria, J., Goya, G.F., Irusta, S., Lin, D., Lau, S., et al.: A Magnetically triggered composite membrane for on-demand drug delivery. Nano Lett. **9**, 3651–3657 (2009)
98. Macaya, D.J., Hayakawa, K., Arai, K., Spector, M.: Astrocyte infiltration into injectable collagen-based hydrogels containing FGF-2 to treat spinal cord injury. Biomaterials **34**, 3591–3602 (2013)
99. Jeng, L., Olsen, B.R., Spector, M.: Engineering endostatin-expressing cartilaginous constructs using injectable biopolymer hydrogels. Acta Biomater. **8**, 2203–2212 (2012)
100. Lim, T.C., Toh, W.S., Wang, L.-S., Kurisawa, M., Spector, M.: The effect of injectable gelatin-hydroxyphenylpropionic acid hydrogel matrices on the proliferation, migration, differentiation and oxidative stress resistance of adult neural stem cells. Biomaterials **33**, 3446–3455 (2012)
101. Lim, T.C., Rokkappanavar, S., Toh, W.S., Wang, L.-S., Kurisawa, M., Spector, M.: Chemotactic recruitment of adult neural progenitor cells into multifunctional hydrogels providing sustained SDF-1α release and compatible structural support. FASEB J. **27**, 1023–1033 (2013)
102. Wang, L.-S., Du, C., Toh, W.S., Wan, A.C.A., Gao, S.J., Kurisawa, M.: Modulation of chondrocyte functions and stiffness-dependent cartilage repair using an injectable enzymatically crosslinked hydrogel with tunable mechanical properties. Biomaterials **35**, 2207–2217 (2014)

103. Ho, S.T.B., Cool, S.M., Hui, J.H., Hutmacher, D.W.: The influence of fibrin based hydrogels on the chondrogenic differentiation of human bone marrow stromal cells. Biomaterials **31**, 38–47 (2010)
104. Sun, G., Zhang, X., Shen, Y.-I., Sebastian, R., Dickinson, L.E., Fox-Talbot, K., et al.: Dextran hydrogel scaffolds enhance angiogenic responses and promote complete skin regeneration during burn wound healing. Proc. Natl. Acad. Sci. **108**, 20976–20981 (2011)
105. Toh, W.S., Lim, T.C., Kurisawa, M., Spector, M.: Modulation of mesenchymal stem cell chondrogenesis in a tunable hyaluronic acid hydrogel microenvironment. Biomaterials **33**, 3835–3845 (2012)
106. Toh, W.S., Lee, E.H., Guo, X.-M., Chan, J.K.Y., Yeow, C.H., Choo, A.B., et al.: Cartilage repair using hyaluronan hydrogel-encapsulated human embryonic stem cell-derived chondrogenic cells. Biomaterials **31**, 6968–6980 (2010)
107. Gerecht, S., Burdick, J.A., Ferreira, L.S., Townsend, S.A., Langer, R., Vunjak-Novakovic, G.: Hyaluronic acid hydrogel for controlled self-renewal and differentiation of human embryonic stem cells. Proc. Natl. Acad. Sci. **104**, 11298–11303 (2007)
108. Wang, S., Taraballi, F., Tan, L., Ng, K.: Human keratin hydrogels support fibroblast attachment and proliferation in vitro. Cell Tissue Res. **347**, 795–802 (2012)
109. Sawkins, M.J., Bowen, W., Dhadda, P., Markides, H., Sidney, L.E., Taylor, A.J., et al.: Hydrogels derived from demineralized and decellularized bone extracellular matrix. Acta Biomater. **9**, 7865–7873 (2013)
110. Young, D.A., Ibrahim, D.O., Hu, D., Christman, K.L.: Injectable hydrogel scaffold from decellularized human lipoaspirate. Acta Biomater. **7**, 1040–1049 (2011)
111. Roberts, J.J., Elder, R.M., Neumann, A.J., Jayaraman, A., Bryant, S.J.: Interaction of hyaluronan binding peptides with glycosaminoglycans in poly(ethylene glycol) hydrogels. Biomacromolecules **15**(4), 1132–1141 (2014)
112. Roberts, J.J., Nicodemus, G.D., Giunta, S., Bryant, S.J.: Incorporation of biomimetic matrix molecules in PEG hydrogels enhances matrix deposition and reduces load-induced loss of chondrocyte-secreted matrix. J. Biomed. Mater. Res., Part A **97A**, 281–291 (2011)
113. Lee, S.T., Yun, J.I., van der Vlies, A.J., Kontos, S., Jang, M., Gong, S.P., et al.: Long-term maintenance of mouse embryonic stem cell pluripotency by manipulating integrin signaling within 3D scaffolds without active Stat3. Biomaterials **33**, 8934–8942 (2012)
114. Lee, S.T., Yun, J.I., Jo, Y.S., Mochizuki, M., van der Vlies, A.J., Kontos, S., et al.: Engineering integrin signaling for promoting embryonic stem cell self-renewal in a precisely defined niche. Biomaterials **31**, 1219–1226 (2010)
115. Folkman, J., Moscona, A.: Role of cell shape in growth control. Nature **273**, 345–349 (1978)
116. McWhorter, F.Y., Wang, T., Nguyen, P., Chung, T., Liu, W.F.: Modulation of macrophage phenotype by cell shape. Proc. Natl. Acad. Sci. **110**, 17253–17258 (2013)
117. Zhang, Z., Messana, J., Hwang, N.S.H., Elisseeff, J.H.: Reorganization of actin filaments enhances chondrogenic differentiation of cells derived from murine embryonic stem cells. Biochem. Biophys. Res. Commun. **348**, 421–427 (2006)
118. Wang, L.-S., Boulaire, J., Chan, P.P.Y., Chung, J.E., Kurisawa, M.: The role of stiffness of gelatin–hydroxyphenylpropionic acid hydrogels formed by enzyme-mediated crosslinking on the differentiation of human mesenchymal stem cell. Biomaterials **31**, 8608–8616 (2010)
119. Lee, J., Abdeen, A.A., Zhang, D., Kilian, K.A.: Directing stem cell fate on hydrogel substrates by controlling cell geometry, matrix mechanics and adhesion ligand composition. Biomaterials **34**, 8140–8148 (2013)
120. Loh, X.J., Peh, P., Liao, S., Sng, C., Li, J.: Controlled drug release from biodegradable thermoresponsive physical hydrogel nanofibers. J. Controlled Release **143**, 175–182 (2010)
121. Ji, Y., Ghosh, K., Li, B., Sokolov, J.C., Clark, R.A.F., Rafailovich, M.H.: Dual-syringe reactive electrospinning of cross-linked hyaluronic acid hydrogel nanofibers for tissue engineering applications. Macromol. Biosci. **6**, 811–817 (2006)
122. Yamada, M., Utoh, R., Ohashi, K., Tatsumi, K., Yamato, M., Okano, T., et al.: Controlled formation of heterotypic hepatic micro-organoids in anisotropic hydrogel microfibers for long-term preservation of liver-specific functions. Biomaterials **33**, 8304–8315 (2012)

123. Lau, T.T., Ho, L.W., Wang, D.-A.: Hepatogenesis of murine induced pluripotent stem cells in 3D micro-cavitary hydrogel system for liver regeneration. Biomaterials **34**, 6659–6669 (2013)
124. Bellan, L.M., Pearsall, M., Cropek, D.M., Langer, R.: A 3D interconnected microchannel network formed in gelatin by sacrificial shellac microfibers. Adv. Mater. **24**, 5187–5191 (2012)
125. Al-Abboodi, A., Fu, J., Doran, P.M., Tan, T.T.Y., Chan, P.P.Y.: Injectable 3D Hydrogel Scaffold with Tailorable Porosity Post-Implantation. Adv. Healthc. Mater. **3**(5), 725–736 (2013)
126. Discher, D.E., Mooney, D.J., Zandstra, P.W.: Growth factors, matrices, and forces combine and control stem cells. Science **324**, 1673–1677 (2009)
127. Engler, A.J., Sen, S., Sweeney, H.L., Discher, D.E.: Matrix elasticity directs stem cell lineage specification. Cell **126**, 677–689 (2006)
128. Leipzig, N.D., Shoichet, M.S.: The effect of substrate stiffness on adult neural stem cell behavior. Biomaterials **30**, 6867–6878 (2009)
129. Chowdhury, F., Li, Y., Poh, Y.-C., Yokohama-Tamaki, T., Wang, N., Tanaka, T.S.: Soft substrates promote homogeneous self-renewal of embryonic stem cells via downregulating cell-matrix tractions. PLoS ONE **5**, e15655 (2010)
130. Gilbert, P.M., Havenstrite, K.L., Magnusson, K.E.G., Sacco, A., Leonardi, N.A., Kraft, P., et al.: Substrate elasticity regulates skeletal muscle stem cell self-renewal in culture. Science **329**, 1078–1081 (2010)
131. Anderson, S.B., Lin, C.-C., Kuntzler, D.V., Anseth, K.S.: The performance of human mesenchymal stem cells encapsulated in cell-degradable polymer-peptide hydrogels. Biomaterials **32**, 3564–3574 (2011)
132. Sarig-Nadir, O., Livnat, N., Zajdman, R., Shoham, S., Seliktar, D.: Laser photoablation of guidance microchannels into hydrogels directs cell growth in three dimensions. Biophys. J. **96**, 4743–4752 (2009)
133. Lau, T.T., Wang, D.-A.: Bioresponsive hydrogel scaffolding systems for 3D constructions in tissue engineering and regenerative medicine. Nanomedicine **8**, 655–668 (2013)
134. Brizzi, M.F., Tarone, G., Defilippi, P.: Extracellular matrix, integrins, and growth factors as tailors of the stem cell niche. Curr. Opin. Cell Biol. **24**, 645–651 (2012)
135. Woo, E.: Adverse events after recombinant human bmp2 in nonspinal orthopaedic procedures. Clin. Orthop. Relat. Res. **471**, 1707–1711 (2013)
136. Bhakta, G., Rai, B., Lim, Z.X.H., Hui, J.H., Stein, G.S., van Wijnen, A.J., et al.: Hyaluronic acid-based hydrogels functionalized with heparin that support controlled release of bioactive BMP-2. Biomaterials **33**, 6113–6122 (2012)
137. Choi, Y.J., Lee, J.Y., Park, J.H., Park, J.B., Suh, J.S., Choi, Y.S., et al.: The identification of a heparin binding domain peptide from bone morphogenetic protein-4 and its role on osteogenesis. Biomaterials **31**, 7226–7238 (2010)
138. Wylie, R.G., Ahsan, S., Aizawa, Y., Maxwell, K.L., Morshead, C.M., Shoichet, M.S.: Spatially controlled simultaneous patterning of multiple growth factors in three-dimensional hydrogels. Nat. Mater. **10**, 799–806 (2011)
139. Song, H., Stevens, C.F., Gage, F.H.: Astroglia induce neurogenesis from adult neural stem cells. Nature **417**, 39–44 (2002)
140. Fu, X., Toh, W.S., Liu, H., Lu, K., Li, M., Hande, M.P., et al.: Autologous feeder cells from embryoid body outgrowth support the long-term growth of human embryonic stem cells more effectively than those from direct differentiation. Tissue Eng., Part C. Methods **16**, 719–733 (2009)
141. Fu, X., Toh, W.S., Liu, H., Lu, K., Li, M., Cao, T.: Establishment of clinically compliant human embryonic stem cells in an autologous feeder-free system. Tissue Eng., Part C. Methods **17**, 927–937 (2011)
142. Peng, Y., Bocker, M.T., Holm, J., Toh, W.S., Hughes, C.S., Kidwai, F., et al.: Human fibroblast matrices bio-assembled under macromolecular crowding support stable propagation of human embryonic stem cells. J. Tissue Eng. Regen. Med. **6**, e74–e86 (2012)

143. Bian, L., Zhai, D.Y., Mauck, R.L., Burdick, J.A.: Coculture of human mesenchymal stem cells and articular chondrocytes reduces hypertrophy and enhances functional properties of engineered cartilage. Tissue Eng. Part A **17**, 1137–1145 (2010)
144. Park, J.S., Yang, H.N., Woo, D.G., Kim, H., Na, K., Park, K.-H.: Multi-lineage differentiation of hMSCs encapsulated in thermo-reversible hydrogel using a co-culture system with differentiated cells. Biomaterials **31**, 7275–7287 (2010)
145. Trkov, S., Eng, G., Di Liddo, R., Parnigotto, P.P., Vunjak-Novakovic, G.: Micropatterned three-dimensional hydrogel system to study human endothelial–mesenchymal stem cell interactions. J. Tissue Eng. Regen. Med. **4**, 205–215 (2010)
146. Silva, N.A., Cooke, M.J., Tam, R.Y., Sousa, N., Salgado, A.J., Reis, R.L., et al.: The effects of peptide modified gellan gum and olfactory ensheathing glia cells on neural stem/progenitor cell fate. Biomaterials **33**, 6345–6354 (2012)
147. Chen, Y.-C., Lin, R.-Z., Qi, H., Yang, Y., Bae, H., Melero-Martin, J.M., et al.: Functional human vascular network generated in photocrosslinkable gelatin methacrylate hydrogels. Adv. Funct. Mater. **22**, 2027–2039 (2012)
148. Hwang, Y.-S., Chung, B.G., Ortmann, D., Hattori, N., Moeller, H.-C., Khademhosseini, A.: Microwell-mediated control of embryoid body size regulates embryonic stem cell fate via differential expression of WNT5a and WNT11. Proc. Natl. Acad. Sci. **106**, 16978–16983 (2009)
149. Hsieh, T.M., Benjamin Ng, C.W., Narayanan, K., Wan, A.C.A., Ying, J.Y.: Three-dimensional microstructured tissue scaffolds fabricated by two-photon laser scanning photolithography. Biomaterials **31**, 7648–7652 (2010)
150. Gauvin, R., Chen, Y.-C., Lee, J.W., Soman, P., Zorlutuna, P., Nichol, J.W., et al.: Microfabrication of complex porous tissue engineering scaffolds using 3D projection stereolithography. Biomaterials **33**, 3824–3834 (2012)
151. Tsang, V.L., Chen, A.A., Cho, L.M., Jadin, K.D., Sah, R.L., DeLong, S., et al.: Fabrication of 3D hepatic tissues by additive photopatterning of cellular hydrogels. FASEB J. **21**, 790–801 (2007)
152. Lee, S.-H., Moon, J.J., West, J.L.: Three-dimensional micropatterning of bioactive hydrogels via two-photon laser scanning photolithography for guided 3D cell migration. Biomaterials **29**, 2962–2968 (2008)
153. Albrecht, D.R., Underhill, G.H., Wassermann, T.B., Sah, R.L., Bhatia, S.N.: Probing the role of multicellular organization in three-dimensional microenvironments. Nat Meth. **3**, 369–375 (2006)
154. Ling, Y., Rubin, J., Deng, Y., Huang, C., Demirci, U., Karp, J.M., et al.: A cell-laden microfluidic hydrogel. Lab Chip **7**, 756–762 (2007)
155. Lii, J., Hsu, W.-J., Parsa, H., Das, A., Rouse, R., Sia, S.K.: Real-time microfluidic system for studying mammalian cells in 3D microenvironments. Anal. Chem. **80**, 3640–3647 (2008)
156. Miller, J.S., Stevens, K.R., Yang, M.T., Baker, B.M., Nguyen, D.-H.T., Cohen, D.M., et al.: Rapid casting of patterned vascular networks for perfusable engineered three-dimensional tissues. Nat. Mater. **11**, 768–774 (2012)
157. Park, Y.D., Tirelli, N., Hubbell, J.A.: Photopolymerized hyaluronic acid-based hydrogels and interpenetrating networks. Biomaterials **24**, 893–900 (2003)
158. Bryant, S.J., Davis-Arehart, K.A., Luo, N., Shoemaker, R.K., Arthur, J.A., Anseth, K.S.: Synthesis and characterization of photopolymerized multifunctional hydrogels: water-soluble poly(vinyl alcohol) and chondroitin sulfate macromers for chondrocyte encapsulation. Macromolecules **37**, 6726–6733 (2004)
159. Nichol, J.W., Koshy, S.T., Bae, H., Hwang, C.M., Yamanlar, S., Khademhosseini, A.: Cell-laden microengineered gelatin methacrylate hydrogels. Biomaterials **31**, 5536–5544 (2010)
160. Song, Y., Lin, R., Montesano, G., Durmus, N., Lee, G., Yoo, S.-S., et al.: Engineered 3D tissue models for cell-laden microfluidic channels. Anal. Bioanal. Chem. **395**, 185–193 (2009)
161. Figallo, E., Cannizzaro, C., Gerecht, S., Burdick, J.A., Langer, R., Elvassore, N., et al.: Micro-bioreactor array for controlling cellular microenvironments. Lab Chip **7**, 710–719 (2007)

162. Tuleuova, N., Lee, J.Y., Lee, J., Ramanculov, E., Zern, M.A., Revzin, A.: Using growth factor arrays and micropatterned co-cultures to induce hepatic differentiation of embryonic stem cells. Biomaterials **31**, 9221–9231 (2010)
163. Qi, H., Du, Y., Wang, L., Kaji, H., Bae, H., Khademhosseini, A.: Patterned differentiation of individual embryoid bodies in spatially organized 3D hybrid microgels. Adv. Mater. **22**, 5276–5281 (2010)
164. Khetan, S., Burdick, J.A.: Patterning network structure to spatially control cellular remodeling and stem cell fate within 3-dimensional hydrogels. Biomaterials **31**, 8228–8234 (2010)
165. Shastri, V.P.: In vivo engineering of tissues: biological considerations, challenges, strategies, and future directions. Adv. Mater. **21**, 3246–3254 (2009)
166. Mosiewicz, K.A., Kolb, L., van der Vlies, A.J., Martino, M.M., Lienemann, P.S., Hubbell, J.A., et al.: In situ cell manipulation through enzymatic hydrogel photopatterning. Nat. Mater. **12**, 1072–1078 (2013)
167. Nguyen, L.H., Kudva, A.K., Saxena, N.S., Roy, K.: Engineering articular cartilage with spatially-varying matrix composition and mechanical properties from a single stem cell population using a multi-layered hydrogel. Biomaterials **32**, 6946–6952 (2011)
168. Gillette, B.M., Rossen, N.S., Das, N., Leong, D., Wang, M., Dugar, A., et al.: Engineering extracellular matrix structure in 3D multiphase tissues. Biomaterials **32**, 8067–8076 (2011)
169. Lee, H.J., Yu, C., Chansakul, T., Varghese, S., Hwang, N.S., Elisseeff, J.H.: Enhanced chondrogenic differentiation of embryonic stem cells by coculture with hepatic cells. Stem Cells Dev. **17**, 555–564 (2008)
170. Natesan, S., Zhang, G., Baer, D.G., Walters, T.J., Christy, R.J., Suggs, L.J.: A bilayer construct controls adipose-derived stem cell differentiation into endothelial cells and pericytes without growth factor stimulation. Tissue Eng. Part A **17**, 941–953 (2010)
171. Li, J., Shu, Y., Hao, T., Wang, Y., Qian, Y., Duan, C., et al.: A chitosan–glutathione based injectable hydrogel for suppression of oxidative stress damage in cardiomyocytes. Biomaterials **34**, 9071–9081 (2013)
172. Cheng, Y.-H., Yang, S.-H., Liu, C.-C., Gefen, A., Lin, F.-H.: Thermosensitive hydrogel made of ferulic acid-gelatin and chitosan glycerophosphate. Carbohydr. Polym. **92**, 1512–1519 (2013)
173. Ouimet, M.A., Griffin, J., Carbone-Howell, A.L., Wu, W.-H., Stebbins, N.D., Di, R., et al.: Biodegradable ferulic acid-containing poly(anhydride-ester): degradation products with controlled release and sustained antioxidant activity. Biomacromolecules **14**, 854–861 (2013)
174. Su, J., Hu, B.-H., Lowe Jr, W.L., Kaufman, D.B., Messersmith, P.B.: Anti-inflammatory peptide-functionalized hydrogels for insulin-secreting cell encapsulation. Biomaterials **31**, 308–314 (2010)
175. Wong, V.W., Rustad, K.C., Glotzbach, J.P., Sorkin, M., Inayathullah, M., Major, M.R., et al.: Pullulan hydrogels improve mesenchymal stem cell delivery into high-oxidative-stress wounds. Macromol. Biosci. **11**, 1458–1466 (2011)

From Bench to Bedside—An Example of an In Situ Hydrogel in In Vivo Applications

Ankshita Prasad and Xian Jun Loh

Abstract The treatment of cancer requires several anticancer drugs targeting dissimilar cellular mechanisms. These therapies require balance with the associated toxicity of the administered drug. The ideal drug delivery system should sustain high local concentrations at the tumor site while minimizing systemic drug levels. Local cancer therapy depends on administration where targeted activity could possibly improve patient outcomes such as amplified local control and lowered metastatic potential. Combination anticancer treatments could also be improved with targeted therapies. OncoGel is a gel depot formulation of paclitaxel in ReGel. Oncogel has been studied in various in vitro setups. OncoGel has been shown to be able to physically target paclitaxel to the tumor site as well as reducing systemic circulation. OncoGel has also shown enhanced efficacy as a stand-alone treatment as well as synergistic activity in combination therapies. Clinical studies in superficially-palpable tumors and esophageal carcinoma confirmed local paclitaxel release from OncoGel in patients. OncoGel's ability to enhance present therapies for esophageal and brain cancers will be discussed.

Keywords Anti-cancer · Thermogel · Oncogel · In vivo · Clinical trials

1 Introduction

The need for drug delivery systems to improve safety, efficacy and patient compliance is well established. There exist various drug delivery systems such as microspheres, nano particles, as well as environmentally sensitive systems [1–3]. Thermosensitive polymers are a subset of environmentally sensitive polymers which undergo a phase transition (sol-gel) when subjected to a change in temperature.

A. Prasad · X.J. Loh (✉)
Institute of Materials Research and Engineering (IMRE), A*STAR, 3 Research Link, Singapore 117602, Singapore
e-mail: XianJun_Loh@scholars.a-star.edu.sg; lohxj@imre.a-star.edu.sg

X.J. Loh (ed.), *In-Situ Gelling Polymers*, Series in BioEngineering,
DOI 10.1007/978-981-287-152-7_9

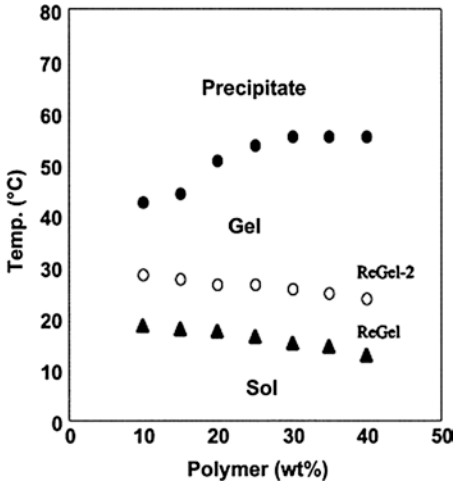

Fig. 1 ReGel phase diagram. Reproduced from Zentner et al. [4]

Regel™ copolymers are biocompatible and biodegradable polymers which exhibit such reverse thermal gelation properties [4]. These polymers are triblock copolymers consisting of A-blocks made up of poly(lactide-co-glycolide) and B-blocks made up of poly(ethylene glycol) arranged in an ABA or BAB sequence, with a defined molecular weight and hydrophobic/hydrophilic balance. Modification in the hydrophobic/hydrophilic ratio of the polymer constructs, results in Regel™ being water soluble below room temperature and a gel at body temperature [4]. As Regel™ is a physically formed hydrogel, the sol-gel transition occurs within seconds, without any chemical modification of the constituent co-polymers [5]. The reversible gelation behavior is presented in the phase diagram (Fig. 1), which illustrates the gelation behavior at physiologically relevant temperature (37 °C). This forms the basis of the biomedical application of Regel™ copolymers as a potential drug carrier. The polymer is hydrolytically degradable and degrades into lactic acid and glycolic acid components after a period of time. Another significant aspect to be noted is the water solubility of the residual polymer which enables its diffusion from the injection site and subsequent elimination through the kidneys.

Oncogel (ReGel™/Paclitaxel) is a formulation of the chemotherapeutic intratumorally injectable drug Paclitaxel, developed by MacroMed Inc. (Salt Lake City, Utah, USA) for local treatment of solid tumors [5]. Paclitaxel is an anti-microtubule agent which binds to tubulin-binding sites, causing mitotic arrest and apoptosis. Regel™ increases the solubility and stability of hydrophobic drugs such as paclitaxel, thus using the system (ReGel™/paclitaxel) ensures a sustained drug release for about 6 weeks. Oncogel is a drug delivery system which combines controlled release with physical targeting of the tumor site either via intra-lesional injection or direct placement into the tumor cavity after resection [6–8]. This poses an advantage over the systemic administration of paclitaxel as it provides continuous release of the therapeutic agent throughout the tumor irrespective of its vascular status. It is also established that Oncogel produces minimal on site toxicity, which enhances its possibility of being used as a component of combination

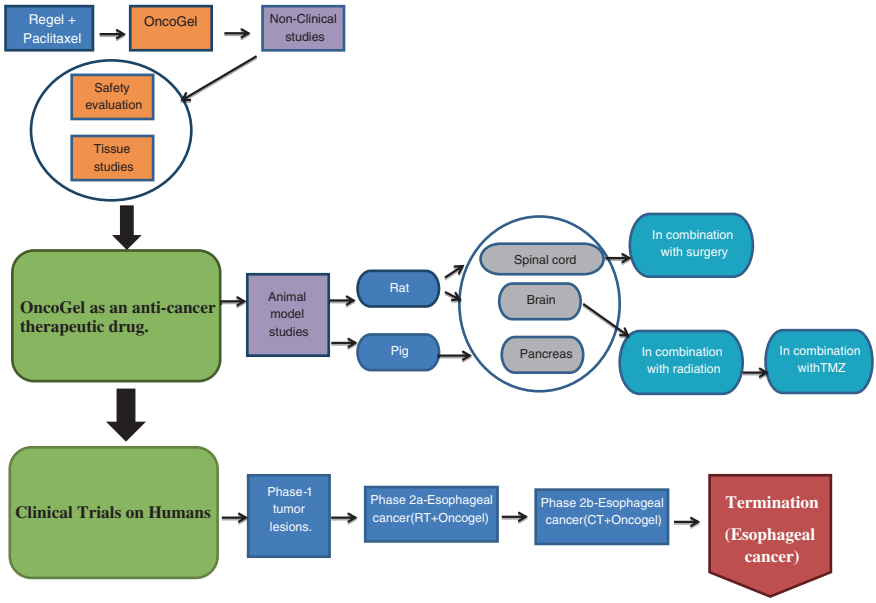

Scheme 1 Flowchart of the development of Oncogel

therapies. Thus complimentary cancer based cellular mechanisms can be targeted by combining Oncogel with systemic chemotherapy or surgeries. Moreover, paclitaxel's anti-neoplastic and radiosensitization activities can be exploited by combining Oncogel with radiotherapy to increase efficacy of the cancer therapy [9, 10]. The development of Oncogel is highlighted in Scheme 1.

2 Non-clinical Safety and Efficacy Evaluation

Several non-clinical studies were performed to explore Oncogel's anti-cancer activity and evaluate its biomedical applications. These included establishing its safety and tolerability Vis-a-Vis systemic administration of Paclitaxel and illustrating its localization within and around the tumor site. Emphasis was also laid on proving its efficacy as a standalone treatment and its tolerability in combination therapy [5].

2.1 Safety Studies

Before targeting the primary cancer cells with Oncogel, it was necessary to establish local tolerability of the system in normal tissue. Various studies were conducted on rats, dogs, pigs to evaluate the safety of Oncogel when delivered to the following tissues: skin (subcutaneous injection), central nervous system (CNS),

intracranial and spinal cord and the pancreas [4, 7, 8, 11, 12]. The focus of the studies in rats and dogs was to determine the no adverse event level (NOAEL) and the maximum tolerated dose in normal tissues. The outcome of these local tolerability studies established that the dose-limiting toxicities (DLTs) were local in nature, so the need to consider systemic toxicity was eliminated while considering the starting dose. These studies propelled the research towards the clinical dose escalation studies of Oncogel as an anti-cancer agent in humans.

2.2 Tissue Distribution Studies

After determining the DLT, it is necessary to carefully study the distribution of Paclitaxel following release from the Oncogel, in order to manage the potential additive toxicity and avoid further complications in the patient. An ADME (adsorption, distribution, metabolism, and excretion) study of paclitaxel was performed following OncoGel's intralesional administration to the MDA-MB-231 breast tumor xenograft in mice. The study examined the distribution of radioactively labeled paclitaxel over a span of 42 days. Paclitaxel was reported to be localized within the tumor with minimal levels (<0.2 %) detected in the blood, tissues or urine. The elimination route was via feces, similar to the paclitaxel elimination following systemic administration. The distribution and concentration of paclitaxel in the surrounding tissues, derived from these studies are essential criteria to be considered when selecting Oncogel injection sites and its placement into a tumor cavity after a surgery [5].

3 Development of Oncogel™ as a Potential Cancer Therapeutic Drug

After acquiring the preliminary information related to the distribution and safety of Oncogel™, it was necessary to evaluate its efficacy in animal models. Novel drug delivery methods were explored for efficient delivery of Oncogel™ to the tumor site. The feasibility of combining Oncogel™ with chemotherapy, radiation therapy and surgeries was also explored.

3.1 Rat Model Studies

3.1.1 Spinal Cord

Spinal column is the most common site of skeletal osseous metastases, with lung and breast lesions being the primary ones to metastasize [7]. As there are advances made in the diagnosis and treatment of the primary disease, the life span of a patient generally increases causing an increase in the frequency of treatment for symptomatic distant metastases.

Local chemotherapy could potentially provide a new option in the treatment of metastatic disease, and the efficacy of Oncogel™ in delaying paresis was tested on a spinal metastases rat model [7]. The pre-treatment hind limb function was evaluated using the BBB (Basso-Beattie-Bresnahan) locomotor rating scale. Animals were injected with Oncogel™ 3.0 % and Oncogel™ 6.0 %, and their locomotive function was re-evaluated. All surviving animals' demonstrated BBB locomotor scores of 21 in all limbs, postoperatively. On the 10th day, the average BBB scores for the control, Oncogel™ 3.0 %, and Oncogel™ 6.0 % animals was 9.00, 16.80, and 16.86, respectively. Though, the histological analysis showed no evidence of toxicity to the spinal cord in any animal, Oncogel™ 3.0 % groups experienced transient decreases in hind limb motor function and took about 3 days to recover. The cause for this was attributed to the surgical technique employed during the intravertebral injections. Oncogel™ was found to increase the life-span of the rats as well. The median survival time for the control, Oncogel™ 3.0 %, and Oncogel™ 6.0 % animals was 14, 18, and 18 days, respectively. However, there was no significant difference in the size of the tumor mass between the control and treatment groups at the time of histological analysis. Nevertheless, the delay in the onset of paresis led to the possibility of Oncogel™ increasing the quality of patient life.

The efficacy of Oncogel™ in a combination therapy along with surgery and radiotherapy was also evaluated in the spinal column metastases model, where Oncogel™ was injected into the tumor cavity during surgery. Surgery alone delayed the onset of paresis, but surgery + Oncogel™ resulted in a higher median BBB score (21 vs. 19, $P < 0.001$) [8]. Also, Oncogel™ was found to prolong the time to loss of ambulation by 20 %. Oncogel™ was also used as an adjuvant to radiation therapy and it was observed that further improved hind limb function also increased the time for the loss of ambulation from 17 to 19 days. However, certain factors need to be considered when analyzing the results of this study. This study determined the efficacy of a single dose of Oncogel™ injection *before* the onset of deficits by using *neurological assessment* and not direct animal imaging. This leaves scope for further clinical and laboratory studies comparing the effects of Oncogel™ after the onset of deficits in motor function. Following the encouraging results of Oncogel™ being a safe and effective gel depot-based delivery system, another study was conducted to evaluate the efficacy of the local delivery of Paclitaxel in the treatment of intramedullary spinal cord tumor (IMSCT) in rats challenged with a lethal dose of intramedullary 9L gliosarcoma [13]. The outcome indicated that Oncogel™ was safe for intramedullary injection in rats in doses up to 5 μl of 3.0 mg/ml of paclitaxel but a dose of 5 μl of 6.0 mg/ml caused rapid deterioration in BBB scores. Oncogel™ at concentrations of 1.5 and 3.0 mg/ml paclitaxel given on both Day 0 and 5 improved BBB scores and the median survival in comparison to the controls.

3.1.2 Glioma

Malignant gliomas are the most common type of primary brain tumor with relatively poor prognosis. The current treatment involves placement of Gliadel® wafers for the sustained release of carmustine [14]. The need to improve the efficacy of local drug

treatment by investigating new polymer carriers and pharmacological agents is well accentuated. Cellular proliferation inhibitors like paclitaxel are known to be effective against gliomas; however their systemic administration has been limited due to their poor penetration into the CNS. So, incorporating paclitaxel in a thermo-sensitive polymer depot delivery system can enhance its efficacy in cancer treatment. The safety and potential synergistic effects of Oncogel™ on rats challenged with intracranial 9L glioma was demonstrated in a study which combined Oncogel™ with radiotherapy [15]. Oncogel™ was intracranially implanted into 60 animals and divided into placebo (ReGel™), XRT, Oncogel™ 6.0 mg/m or Oncogel™ with single dose 20 Gy XRT. Animals treated with just Regel™ showed no increase in survival when compared to the controls but animals administered with Oncogel™ and XRT had a statistically significant increase in survival when compared to XRT alone ($P = 0.0182$). These results were further supported by another study which claimed the safety of 6.3 mg/ml of paclitaxel for intracranial injection in rats [16]. It was also established that combining Oncogel™ acts as a radiation sensitizer, thus, combining Oncogel™ treatment with radiation therapy is more effective than just the stand alone treatment.

Advancement in oncology research identified multiple signaling pathways to play a significant role in tumor progression. So, application of combination therapies which synergistically target different pathways could improve the efficacy of cancer therapies. Temozolomide (TMZ) is an alkylating agent shown to have improved survival in patients with glioblastoma [17]. Paclitaxel is a mitotic inhibitor which is effective against glioma in vitro and also makes the glioma cells sensitive to radiation therapy. As TMZ and paclitaxel have different mechanisms of action, it was hypothesized that the combination of TMZ (oral and local) and OncoGel™ might have a better synergistic effect in a rodent model of gliosarcoma. Oncogel™ + TMZ in general prolonged survival and no signs of systemic or neurological toxicity were observed. The combination of OncoGel™ with oral or local TMZ resulted in 57 and 100 % long term survivors, respectively, proving the local delivery of TMZ to be a better option of treatment. Since most of patients suffering from glioma undergo radiation therapy, the efficacy of Oncogel™ + TMZ + RT was also explored. The strong therapeutic effect of the treatment regimen involving this triple combination was indicated by the statistically longer survival ($P < 0.0001$) as compared to the combination of oral TMZ and XRT [18]. However, the ineffective correlation between animal model and human response was recognized and an attempt was made to increase the effectiveness of a drug delivery device by using computational models combining fluid transport and mass transport submodels [14]. The study attempted to bridge the gap between the rat model and the human tissue by using a simplified model to compare the paclitaxel distribution in the two systems. The therapeutic penetration distance from the injection site was found to be 1–2 mm (Fig. 2a). Though the rat and human brains have a similar penetration distances, the fraction of brain tissue exposed to therapeutic concentration of paclitaxel was reported to be higher in rats than humans.

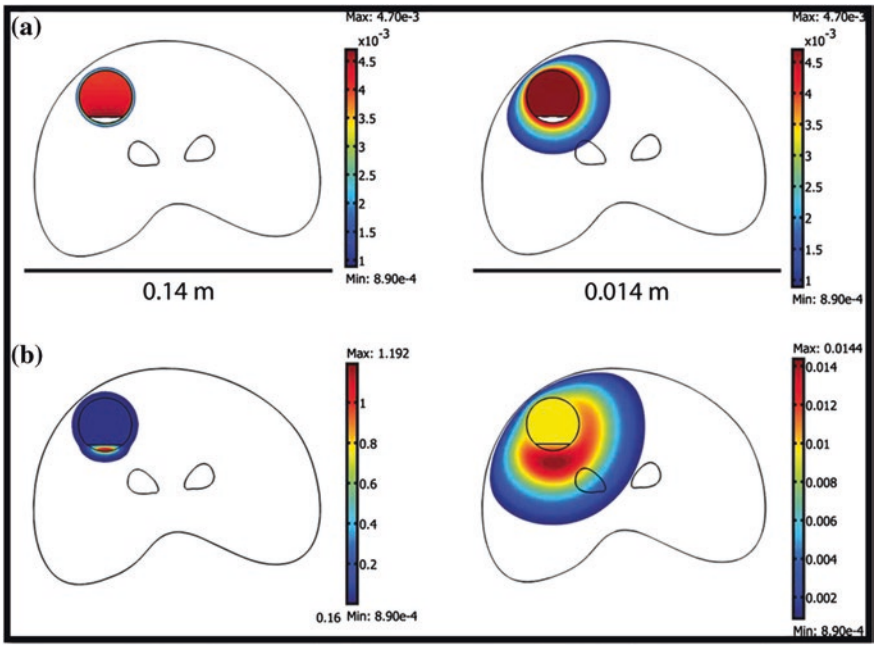

Fig. 2 Comparison of paclitaxel distribution between human and rat brain 30 days after implantation.**a** Paclitaxel distribution in rat (right panel) and human (left panel) brain obtained when the solubility of paclitaxel in water is taken as the limiting factor for drug release form the polymer matrix from a 7 % filled cavity. **b** Paclitaxel distribution in brain tissue assuming sink conditions in the brain from a 7 % filled cavity. Based on the assumptions used in the simulation drug penetration distances can differ in about one order of magnitude. Only concentrations above the minimum effective concentration have been displayed to visualize effective therapeutic distances. The convection term in the diffusion-reaction equation has been left out because the focus of this data is the amount of drug remaining in the polymer matrix due to the slow diffusion of paclitaxel and the difference in penetration scale between rat and human brains. Concentrations are given in mol/m^3. Reproduced from Torres et al. [14]

Though, simulations assuming sink conditions increases the effective therapeutic distances, it is inaccurate to assume sink conditions in the brain tissue (Fig. 2b). Nevertheless the study managed to establish that the penetration pattern of paclitaxel was similar to Gliadel® wafers, with paclitaxel maintaining effective concentrations for more than 30 days where as Gliadel® wafers could do so only for 4 days. They also reported that the convention in the brain tissue could prevent the formation of a stable drug concentration gradient.

An attempt was made to do the phase 1 and 2 dose escalation study clinical trials on subjects with recurrent glioma in a Protherics sponsored study in 2007. Though the predicted completion of study was 2010, it was terminated citing professional reasons.

3.2 Pig Model Studies

3.2.1 Pancreatic Cancer

Patients diagnosed with pancreatic cancer often suffer from local complications such as pain and biliary or intestinal obstruction. Though chemotherapy and radiation are the common treatments administered, the prognosis of the patients still remains poor. With the development of better drug delivery systems, sustainable release of chemotherapeutic drugs is possible. However, local delivery of drugs requires an easily accessible tumor where the drug can be placed. While superficial tumors of the skin, breasts, and cervical cancers provide an easy injection site, solid, deep seated tumors require specialized equipment for accurate placement of Oncogel. The feasibility of endoscopic ultrasound (EUS) a guided injection of Oncogel was evaluated in the porcine pig model. Oncogel was successfully injected into the tail of the pancreas using the EUS-guided fine needle [19] (Fig. 3). The procedure was also well tolerated and the blood samples indicated no presence of pancreatitis.

The gross and histological examination revealed a stable depot of Oncogel™ (Fig. 4), with no report of its extravasation out of the pancreas. The animals upon

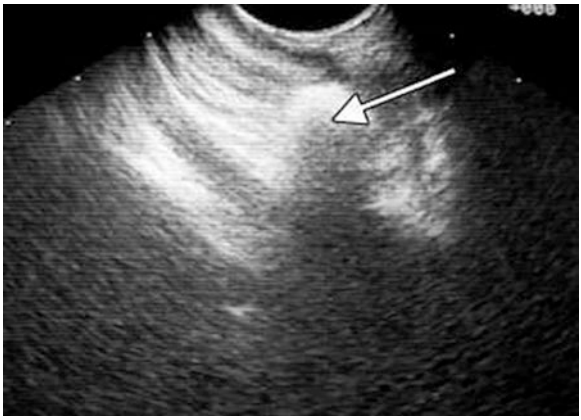

Fig. 3 Oncogel depot detected by ultrasound. Reproduced from Linghu et al. [19]

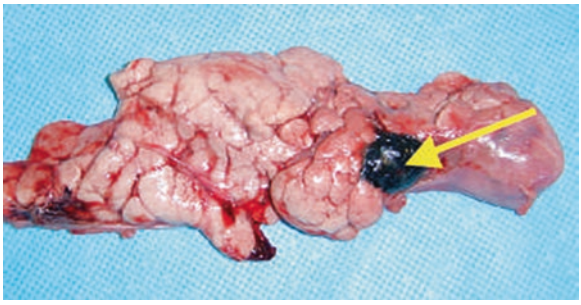

Fig. 4 Macroscopic view of the Oncogel depot. Reproduced from Linghu et al. [19]

which euthanasia was performed in 14 days showed localized fibrotic tissue changes and a decrease in inflammation.

Another study reported that the concentration of paclitaxel varied with the distance, with the high concentrations in the areas with the depot and low concentrations areas 10–30 mm from the injection site [11]. The study used a similar EUS guided injection of Oncogel™ and reported that the viscosity of the gel presented difficulties which could be overcome by using a threaded syringe and pressure tubing between the syringe and the EUS needle to increase the pressure. Though, the absence of pancreatitis, sclerotic or neurotic tissue formation indicates a good pancreatic tissue tolerability, further investigation is required to understand the possibility of long-term complications such as bone marrow suppression, neuropathy, cardiotoxicity.

3.3 Human-Clinical Trials

Pre-clinical studies of Oncogel™ established its cytotoxic potency and reported it to be localized within the injection site, thereby attenuating the systemic toxicities. As the research progressed beyond animal model studies, phase one clinical studies were designed to evaluate the efficacy of Oncogel™ when administered intralesionally to superficially accessible solid tumor lesions in patients who had not undergone any other curative therapy [20]. The blood chemistry and the hematology data was collected for 9 weeks following Oncogel™ injection. The tumor response was gauged from 3D images obtained from CT scan, ultrasound and MRI whereas caliper was used to obtain 2D measurements [5]. The main objective of this study was to identify the maximum tolerated dose (MTD) by observing the dose limiting toxicity (DLT) at various concentrations of Oncogel™. 16 patients receiving 0.06–2.0 mg paclitaxel/cm^3 tumor volume were under observation. Though Oncogel™ placement into the tumor was well tolerated at doses up to 2.0 mg paclitaxel/cm^3 tumor volume, 8 patients were observed with adverse local response to Oncogel™ administration such as injection site pain, muscle spasms and erythema. However, even at the highest dose of Oncogel™, no DLTs were reported, confirming the non-clinical studies data about the localization of the Oncogel™ depot.

Efficacy analysis was also performed on the patients according to the modified WHO criteria by comparing the change from baseline of the tumor volume every 4 weeks. 6 patients were reported to have a stable disease, and 8 patients were classified as having progressive disease. However, the significance of these results remains questionable due to the small sample size and varied tumor types (breast, lymphoma, malignant melanoma, etc.). On the other hand, the enrolled patients might have been previously exposed to paclitaxel or other therapeutic agents, which could cause them to be less sensitive to the Oncogel™. Thus, the results looked promising enough to continue with the clinical studies to achieve more reliable results.

Tumors are generally treated using combination therapies such as chemotherapy, radiation and surgery. Paclitaxel could be used as an adjuvant to any of these as discussed in the non-clinical studies, but it was reported that 18- to 24-h incubation with paclitaxel was needed to sensitize the cancer cells to radiation [21, 22]. Moreover, this sensitivity was only effective for a short period of time and declined rapidly after removal of paclitaxel [23]. Thus, Oncogel™ was found to meet this specification as it presented a sustained release of paclitaxel for a period of 6 weeks, which could increase the efficacy of radiotherapy.

3.3.1 Esophageal Cancer

The number of annual deaths caused by esophageal cancer is estimated to be about 300,000 [24]. The scenario is complicated by the fact that the 50 % of diagnosis is usually made when the disease is in its final stages. As the phase 1 studies illustrated the lack of any significant systemic circulation of paclitaxel, Oncogel™ was recognized as a potential alternative to the morbidity inducing treatment options like chemotherapy, radiotherapy and surgery. A multi-national US phase 2a dose escalation study was conducted to evaluate the efficacy of a dual therapy regimen (Oncogel™ + RT) on patients suffering from advanced esophageal disease without having undergone chemotherapy. Oncogel™ of varying concentrations (1.5, 3.1 and 6.3 mg/ml) was successfully injected using linear EUS guidance. Patients were subjected to 28 fractions of 1.8 Gy radiation 3 days after the injection. No dose limiting toxicities was observed and Oncogel™ did not add on to the risks of RT. The pharmacokinetics of paclitaxel was also uninfluenced by the presence of radiation. However, caution must be exercised while making the comparison since the study involved no cohort of patients undergoing only radiation therapy. The intratumoral concentration of Oncogel™ was reported to be 0.48, 1.0, and 2.0 mg paclitaxel per cm^3 of tumor [6, 12]. Peak plasma concentrations was related to the Oncogel™ concentration and ranged from 0.53 to 2.73 ng/ml. Oncogel™ was well tolerated in the body; 82 % of the patients (n = 11) were found to show an improvement in dysphagia over the study period. On a 5 point scale, 55 % had a two point improvement and three had a one point improvement. The efficacy results were positive; 2 patients were reported to have a progressive response, whereas 6 patients were classified as having a stable disease and two under progressive disease. The biopsies collected at the end of week 11 were negative for 4 patients and two patients with stage 3 disease showed significant improvements and were considered for resection. The phase 2b study has tumor response as the primary end point, whereas the safety, survival and pathological complete response (pCR) of the tumor was the secondary endpoints. It designed a control group comprising of patients receiving standard of care-(5-FU), cisplatin and RT (chemo radiotherapy) and the treatment group consisted of patients with Oncogel™ and chemo radiotherapy. Though the combination of Oncogel™ plus chemo radiotherapy increased the number of adverse events, overall the therapy was well tolerated. But the overall response of the Oncogel™ treatment group was

12.5 % whereas the standard of care group had 20 % response. A clearer differentiation between the two groups was provided by the pCR, where only 12.5 % of patients in the control arm experienced pCR as compared to 27.7 % response in the control group.

It is well established that systemic administration of paclitaxel increases the efficacy of chemo radiotherapy, thus the lack of significant improvement shown by this combined study was attributed to the localized delivery of paclitaxel in the form of an Oncogel™. Since Oncogel™ failed to show a significant improvement in the efficacy, it was terminated as a potential therapy for esophageal cancer in 2010 [25].

References

1. Park, M.H., Joo, M.K., Choi, B.G., Jeong, B.: Biodegradable thermogels. Acc. Chem. Res. **45**(3), 424–433 (2012). doi:10.1021/ar200162j
2. Jeong, B., Kim, S.W., Bae, Y.H.: Thermosensitive sol–gel reversible hydrogels. Adv. Drug Deliv. Rev. **64**, 154–162 (2012). doi:10.1016/j.addr.2012.09.012
3. Ko, D.Y., Shinde, U.P., Yeon, B., Jeong, B.: Recent progress of in situ formed gels for biomedical applications. Prog. Polym. Sci. **38**(3–4), 672–701 (2013). doi:10.1016/j.progpolymsci.2012.08.002
4. Zentner, G.M., Rathi, R., Shih, C., McRea, J.C., Seo, M.H., Oh, H., Rhee, B.G., Mestecky, J., Moldoveanu, Z., Morgan, M., Weitman, S.: Biodegradable block copolymers for delivery of proteins and water-insoluble drugs. J. Controlled Release **72**(1–3), 203–215 (2001). doi:10.1016/s0168-3659(01)00276-0
5. Elstad, N.L., Fowers, K.D.: OncoGel (ReGel/paclitaxel)—clinical applications for a novel paclitaxel delivery system. Adv. Drug Deliv. Rev. **61**(10), 785–794 (2009). doi:10.1016/j.addr.2009.04.010
6. DuValla, G.A., Tarabar, D., Seidela, R.H., Elstad, N.L., Fowers, K.D.: Phase 2: a dose-escalation study of OncoGel (ReGel/paclitaxel), a controlled-release formulation of paclitaxel, as adjunctive local therapy to external-beam radiation in patients with inoperable esophageal cancer. Anticancer Drugs **20**(2), 89–95 (2009). doi:10.1097/CAD.0b013e3283222c12
7. Bagley, C.A., Bookland, M.J., Pindrik, J.A., Ozmen, T., Gokaslan, Z.L., Witham, T.F.: Local delivery of OncoGel delays paresis in rat metastatic spinal tumor model. J. Neurosurg. Spine **7**(2), 194–198 (2007). doi:10.3171/spi-07/08/194
8. Gok, B., McGirt, M.J., Sciubba, D.M., Garces-Ambrossi, G., Nelson, C., Noggle, J., Bydon, A., Witham, T.F., Wolinsky, J.P., Gokaslan, Z.L.: Adjuvant treatment with locally delivered OncoGel delays the onset of paresis after surgical resection of experimental spinal column metastasis. Neurosurgery **65**(1), 193–200 (2009). doi:10.1227/01.neu.0000345948.54008.82
9. Ramalingam, S., Belani, C.P.: Basic treatment considerations: chemotherapy. Hematol. Oncol. Clin. North Am. **18**(1), 13–28 (2004). doi:10.1016/s0889-8588(03)00136-9
10. Safran, H., Akerman, P., Cioffi, W., Gaissert, H., Joseph, P., King, T., Hesketh, P.J., Wanebo, H.: Paclitaxel and concurrent radiation therapy for locally advanced adenocarcinomas of the pancreas, stomach, and gastroesophageal junction. Semin. Radiat. Oncol. **9**(2), 53–57 (1999)
11. Matthes, K., Mino-Kenudson, M., Sahani, D.V., Holalkere, N., Fowers, K.D., Rathi, R., Brugge, W.R.: EUS-guided injection of paclitaxel (OncoGel) provides therapeutic drug concentrations in the porcine pancreas (with video). Gastrointest. Endosc. **65**(3), 448–453 (2007). doi:10.1016/j.gie.2006.06.030
12. Duvall, A., Tarabar, D., Seidel, R.H., Doder, R., Elstad, N.L., Fowers, K.D.: Phase 2a dose escalation trial of OncoGel (R) (Regel (R)/Paclitaxel) as adjunctive local therapy to external

beam radiation in patients with inoperable esophageal cancer. Gastroenterology **132**(4), A417–A417 (2007)
13. Tyler, B.M., Hdeib, A., Caplan, J., Legnani, F.G., Fowers, K.D., Brem, H., Jallo, G., Pradilla, G.: Delayed onset of paresis in rats with experimental intramedullary spinal cord gliosarcoma following intratumoral administration of the paclitaxel delivery system OncoGel laboratory investigation. J. Neurosurg. Spine **16**(1), 93–101 (2012). doi:10.3171/2011.9.spine11435
14. Torres, A.J., Zhu, C., Shuler, M.L., Pannullo, S.: Paclitaxel delivery to brain tumors from hydrogels: a computational study. Biotechnol. Prog. **27**(5), 1478–1487 (2011). doi:10.1002/btpr.665
15. Tyler, B., Renard, V., Kaiser, S., Fowers, K., Brem, H.: 20 Gy radiotherapy with locally delivered OncoGel((R)) (6.0-mg/ml paclitaxel) significantly prolongs survival in an experimental rodent glioma model. J. Neurooncol. **87**(2), 243–244 (2008)
16. Tyler, B., Fowers, K.D., Li, K.W., Recinos, V.R., Caplan, J.M., Hdeib, A., Grossman, R., Basaldella, L., Bekelis, K., Pradilla, G., Legnani, F., Brem, H.: A thermal gel depot for local delivery of paclitaxel to treat experimental brain tumors in rats laboratory investigation. J. Neurosurg. **113**(2), 210–217 (2010). doi:10.3171/2009.11.jns08162
17. Appel, E.A., Rowland, M.J., Loh, X.J., Heywood, R.M., Watts, C., Scherman, O.A.: Enhanced stability and activity of temozolomide in primary glioblastoma multiforme cells with cucurbit[n]uril. Chem. Commun. **48**(79), 9843–9845 (2012). doi:10.1039/c2cc35131e
18. Vellimana, A.K., Recinos, V.R., Hwang, L., Fowers, K.D., Li, K.W., Zhang, Y.G., Okonma, S., Eberhart, C.G., Brem, H., Tyler, B.M.: Combination of paclitaxel thermal gel depot with temozolomide and radiotherapy significantly prolongs survival in an experimental rodent glioma model. J. Neurooncol. **111**(3), 229–236 (2013). doi:10.1007/s11060-012-1014-1
19. Linghu, E., Matthes, K., Mino-Kenudson, M., Brugge, W.R.: Feasibility of endoscopic ultrasound-guided OncoGel (ReGel/paclitaxel) injection into the pancreas in pigs. Endoscopy **37**(11), 1140–1142 (2005). doi:10.1055/s-870224
20. Vukelja, S.J., Anthony, S.P., Arseneau, J.C., Berman, B.S., Cunningham, C.C., Nemunaitis, J.J., Samlowski, W.E., Fowers, K.D.: Phase 1 study of escalating-dose OncoGel((R)) (ReGel((R))/paclitaxel) depot injection, a controlled-release formulation of paclitaxel, for local management of superficial solid tumor lesions. Anticancer Drugs **18**(3), 283–289 (2007). doi:10.1097/CAD.0b013e328011a51d
21. Tishler, R.B., Busse, P.M., Norris, C.M., Rossi, R., Poulin, M., Thornhill, L., Costello, R., Peters, E.S., Colevas, A.D., Posner, M.R.: An initial experience using concurrent paclitaxel and radiation in the treatment of head and neck malignancies. Int. J. Radiat. Oncol. Biol. Phys. **43**(5), 1001–1008 (1999). doi:10.1016/s0360-3016(98)00533-1
22. Tishler, R.B., Lamppu, D.M.: The interaction of taxol and vinblastine with radiation induction of p53 and p21(WAF1/CIP1). Br. J. Cancer **74**, S82–S85 (1996)
23. Zanelli, G.D., Quaia, M., Robieux, I., Bujor, L., Santarosa, M., Favaro, D., Spada, A., Caffau, C., Gobitti, C., Trovo, M.G.: Paclitaxel as a radiosensitiser: a proposed schedule of administration based on in vitro data and pharmacokinetic calculations. Eur. J. Cancer **33**(3), 486–492 (1997). doi:10.1016/s0959-8049(96)00478-9
24. Kamangar, F., Dores, G.M., Anderson, W.F.: Patterns of cancer incidence, mortality, and prevalence across five continents: defining priorities to reduce cancer disparities in different geographic regions of the world. J. Clin. Oncol. **24**(14), 2137–2150 (2006). doi:10.1200/jco.2005.05.2308
25. Williams, R.: Discontinued drugs in 2011: oncology drugs. Expert Opin. Investig. Drugs **22**(1), 9–34 (2013). doi:10.1517/13543784.2013.739605